ANALYSIS OF INLET FLOW
DISTORTION AND TURBULENCE EFFECTS
ON COMPRESSOR STABILITY

By

H. C. MELICK

31 March 1973

Distribution of this report is provided in the interest of
information exchange. Responsibility for the contents
resides in the author or organization that prepared it.

Prepared Under Contract No. ~~~~

By

VOUGHT SYSTEMS DIVISION
LTV AEROSPACE CORPORATION

For

National Aeronautics and Space Administration
Ames Research Center
Moffett Field, California

ANALYSIS OF INLET FLOW
DISTORTION AND TURBULENCE EFFECTS
ON COMPRESSOR STABILITY

By

H. C. MELICK

31 March 1973

Technical Report No. 2-57110/3R-3071

TABLE OF CONTENTS

SUMMARY

The effect of steady state circumferential total pressure distortion on the loss in compressor stall pressure ratio has been established by analytical techniques. Full scale engine and compressor/fan component test data were used to provide direct evaluation of the analysis. Favorable results of the comparison are considered verification of the fundamental hypothesis of this study. Specifically, since a circumferential total pressure distortion in an inlet system will result in unsteady flow in the coordinate system of the rotor blades, an analysis of this type distortion must be performed from an unsteady aerodynamic point of view. By application of the fundamental aerothermodynamic laws to the inlet/compressor system, parameters important in the design of such a system for compatible operation have been identified. A time constant, directly related to the compressor rotor chord, was found to be significant, indicating compressor sensitivity to circumferential distortion is directly dependent on the rotor chord.

As an initial step in the investigation of the effects of time dependent total pressure distortion on the compressor stability characteristics, an analytical model of turbulent flow typical of that found in aircraft inlets has also been developed. Due to the non-deterministic (random) nature of this type of flow distortion, the flow analysis requires use of statistical methods. These methods were combined with basic fluid dynamic concepts to provide a usable analysis technique. With this model, the power spectral density function and root mean square level of the time dependent total pressure take on considerable significance as indicators of the strength and extent of low pressure regions that are important in the compressor reaction to inlet flow disturbances. Spectra obtained from the model were compared with those obtained in tests of a Mach 3 mixed compression inlet to illustrate the technique of determining the mean size and strength of instantaneous low pressure regions by statistical techniques and to verify the turbulent flow model. Excellent agreement was obtained in the comparison verifying this fundamental approach.

Both the steady state distortion/compressor analysis and the turbulent flow model are considered developed to the point necessary to initiate the development program to achieve the long term program objective of combining these results to establish a fundamental relationship between both inlet steady state circumferential distortion and turbulence and loss in compressor stall margin.

INTRODUCTION

Inlet/engine system stability problems have grown to major proportions with the continuing press to improve performance and reduce system weight and volume. The need to solve such problems and to understand the effect of inlet total pressure distortion on engine compressor stability has become critical. To date, solutions to the problem of inlet/engine compatibility have had to come from experimental results since adequate stability analysis methods were not available. This has resulted in extensive inlet and engine test requirements. Notwithstanding, the important design variables for inlet/engine stability remained obscure.

An analytical approach that considers the fundamentals of the dynamic interaction between inlet flow and engine compressor is needed to augment the use of the traditional empirical distortion factors. The method needs to be sufficiently detailed to provide insight into the basic interaction and yield workable accuracy, yet not detailed to the point of being expensive and cumbersome to apply.

This program, initiated in April 1972, has been oriented toward developing basic relationships between inlet flow distortion and turbulence and the loss in compressor stall margin. A five task approach has been established. The initial two phases, which comprise the subject matter of this report, were designed to develop the fundamental techniques required for successful completion of the program. Future studies combine these fundamental analyses to relate inlet flow distortion and turbulence to the loss in compressor stall margin. These analyses can then be used with data from existing inlet/engine tests to establish procedures capable of predicting compressor stability margin during the design phase of a propulsion system.

The objective of Task I is to develop an analytical technique to relate inlet circumferential total pressure distortion to the loss in compressor stall margin. A steady state circumferential distortion appears as time variant in the rotor coordinate system. The developed analysis is unique since it considers the effects of this unsteady flow on the compressor stage characteristics. Secondly, the effects of flow distortion are established by consideration of only the stall margin changes caused by distortion, eliminating need for detailed construction of individual stage and compressor performance maps. Favorable comparison between results of the analysis and experimental data are considered to have verified this approach.

The objective of Task II is to develop a statistical model of inlet turbulent flow. This was accomplished by the combination of two engineering disciplines: fluid mechanics and statistical mathematics. Based on the fundamental hypothesis that the time dependent total pressure fluctuations are a direct result of streamline curvature rather than acoustic waves, it was assumed that these pressure fluctuations could be described by a random distribution of descrete vortices transported by the mean flow. The laws of fluid mechanics were used to describe the fluid dynamic characteristics of the vortices, while the statistical methods were used to handle the random properties of the flow. Results of the analysis were verified by test data. Through this model easily measured inlet flow properties such as total pressure RMS level and power spectral density function can be interpreted in a context meaningful to engine stability.

3

SYMBOLS

English

A	=	area
a	=	vortex core radius
B	=	vortex strength coefficient
C	=	coefficient
C	=	constant
c	=	chord
c_1	=	spring constant
c_2	=	damping factor
D	=	coefficient in transformed hyper-beta function
d	=	coefficient in transformed beta function
d( )	=	differential of ( )
E	=	energy
ERF	=	error function
ERFC	=	complementary error function
e	=	base of natural logarithm
F	=	force
f	=	frequency
f( )	=	function of ( )
$G_x(f)$	=	real one-sided power spectral density function
H	=	inlet duct height
h	=	enthalpy
h	=	probe location
i	=	$\sqrt{-1}$
k	=	beta density coefficient
k	=	reduced frequency = $\omega c/2U$
L	=	lift
M	=	Mach number
m	=	exponent in beta function
m	=	mass
N	=	frequency of occurence
N	=	rotor RPM
n	=	direction of vortex rotation (+,-)
n	=	exponent in beta and hyper-beta density function
n	=	harmonic number
P	=	pressure
q_o	=	dynamic pressure = $\frac{1}{2}\rho U_o^2$
R	=	ratio
RMS	=	root mean square
r	=	radius
S	=	LaPlacian variable

ΔSM	=	loss in stall margin
$S_x(f)$	=	complex power spectral density function
T	=	transfer function
t	=	time
U	=	axial velocity (vortex analysis)
U	=	relative velocity (compressor analysis)
u	=	perturbation velocity in x direction
V	=	vertical velocity (vortex analysis)
v	=	perturbation velocity in y direction
W	=	resultant velocity
X, Y	=	coordinates fixed to inlet probe
x, y	=	coordinates fixed to vortex
$\overline{(\ )}$	=	mean value of ( )
$\overline{(\ )}^2$	=	square of mean value of ( )
$\overline{(\ )^2}$	=	mean square value of ( )

Greek

α	=	angle of attack
α	=	flow angle
Γ	=	circulation
γ	=	ratio of specific heats = 1.4
Δ	=	difference
ϵ	=	small distance from probe
η	=	efficiency
η	=	total pressure recovery
θ	=	circumferential angle
ν	=	coefficient of kinematic viscosity
π	=	3.14159
ρ	=	density
σ	=	RMS value
τ	=	delay time
τ	=	nondimensional time = tU/c
$\tau_{(\ )}$	=	nondimensional time constant = time constant $t_{(\ )}U/c$

5

Ω = vorticity

ω = angular frequency = $2 \pi f$

English Script

$L[\ ]$ = Laplacian operator

$P(\ )$ = probability density function of ( )

$R_x(\tau)$ = autocorrelation function of x

Subscript

a = airflow

a = core size

avg = average

ax = axial

c = circulatory

c = compressor

eff = effective

g = general

inst = instantaneous

L = low pressure region

max = maximum

N.C. = non-circulatory

min = minimum

o = freestream (uniform conditions)

p = pressure

RTR = rotor

r = radial

T = total pressure

v = vortex strength

θ = tangential (circumferential) direction

o = steady-state

EFFECT OF STEADY STATE TOTAL PRESSURE DISTORTION ON COMPRESSOR STALL MARGIN

The objective of Task I is to relate inlet circumferential steady state total pressure distortion to loss in engine compressor stall margin. An analytical technique based on the fundamental aero-thermodynamic laws governing fluid flow and engine compressor operation has been developed. The general approach is outlined below and the details presented in subsequent sections.

Distorted inlet flow is composed of total pressure levels both above and below the average. These regions correspond to deviations in axial flow velocity from the mean. In the rotating coordinate system of the rotor, these deviations appear as fluctuations in the stream angle or angle of attack relative to the rotor blades. Therefore, the flow over the rotor blades is basically unsteady and hence steady state distortion, as well as unsteady, must be analyzed by unsteady aerodynamic techniques. Accordingly, as a basis for the study, the effects of a time varying angle of attack on the lifting characteristics of an isolated airfoil are established. The results are then applied to a compressor rotor blade and by relating the work done by the rotor to the lifting characteristics of the blades, the loss in compressor stall margin due to an arbitrary circumferential distortion pattern is established.

Isolated Airfoil Analysis

The primary objective of this specific item is to establish the effect of unsteady airflow on the lifting characteristics, and in particular on the maximum lift coefficient, of an isolated airfoil. This will include resolution of the effects for arbitrary transients in angle of attack. To accomplish this objective, it is first necessary to understand the flow phenomena involved in delaying the stall of an airfoil beyond its steady state characteristics when the airfoil is subjected to an unsteady angle of attack and then develop a mathematical representation of the process which can be solved for arbitrary, time dependent, angles of attack.

Effect of Unsteady Flow on Lift. - Lift on an airfoil is a consequence of unequal pressures acting on the upper and lower surfaces. In potential flow these pressures can be computed from the velocity field by use of the equations of motion. In the case of unsteady flow, the lift is dependent not only on the instantaneous angle of attack but also on the following two factors: (1) the inertia or acceleration of the mass of air in proximity of the airfoil and, (2) the shedding of the trailing edge vortex which acts as a dissipative force. The phenomena are analogous to the forces and acceleration of a damped mass/spring system which can be described by a linear second order differential equation. Similarly, the lift of an airfoil subjected to an unsteady flow can be described in the same manner. As an example, the lift per unit span due to an airfoil undergoing vertical oscillations at an angular frequency of   is:

$$L(t) = \left[\pi\rho\frac{c^2}{4} \right] \frac{d^2y}{dt^2} + \left[U\pi\rho c C(k) \right] \frac{dy}{dt} + \left[\rho U^2 c\pi \right] \alpha_0 \tag{1}$$

where: $\pi\rho\dfrac{c^2}{4}$ = virtual mass

$\pi\rho cC(k)$ = "dissipation constant"

$C(k)$ = function of reduced frequency, k

k = $\omega c/2U$

Similar expressions govern the response of airfoil lift to a wide variety of motions. The unsteady lift equations for the various classes of motions are summarized in Appendix A. Airfoil lift characteristics of an oscillating airfoil are shown in Figure 1 to illustrate the effects caused by the unsteady motion. Analytical results are shown compared with test data from Reference 3. The qualitative agreement verifies the classical potential flow analysis.

The effect of the unsteady motion, illustrated in Figure 1 are directly related to the reduced frequency, k, which is an extremely important parameter in the analysis of unsteady flow over airfoils. In this parameter the ratio of chord to airfoil velocity, c/U, is proportional to the time required for a disturbance to pass from the leading edge to the trailing edge of the airfoil. The time associated with the disturbance (in this case the oscillations) is proportional to $1/\omega$. The reduced frequency, k, can therefore be described as the ratio of the time associated with a disturbance $(1/\omega)$ to the time for the airfoil to react to the disturbance.
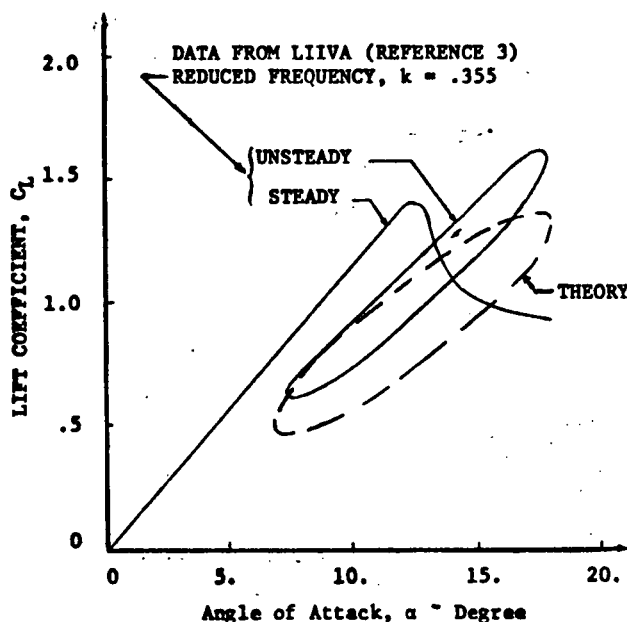

Figure 1. Unsteady Lift of Oscillating Airfoil

Unsteady Flow Model - The response of the airfoil to unsteady motions in unstalled flow forms the basis on which to develop the phenomenological model

8

of an isolated airfoil subjected to angle of attack excursions beyond the steady state stall limit. This is achieved by modeling the physical mechanisms involved with a stalling airfoil via the concept of an effective angle of attack.

When a airfoil is subjected to unsteady variations in angle of attack, the pressure distribution about the airfoil does not correspond to that associated with the steady state condition for the instantaneous value of angle of attack. This is due to the finite amount of time required for flow about an airfoil to adjust to the variations in angle of attack. Flow phenomena requiring adjustment include the external flow, shed vorticity, and the boundary layer. Initially the flow at the airfoil leading edge experiences the change in angle of incidence. At later times this new flow angle is felt at subsequent stations along the chord of the airfoil. Therefore an effective angle of attack, α eff, is hypothesized which lags the instantaneous angle. This angle accounts for the finite time required for airflow adjustment and boundary layer separation to occur and is modeled mathematically below to enable prediction of the stalling lift coefficient of an airfoil operating in unsteady flow.

In keeping with the findings of an unstalled airfoil, it is assumed that the physical mechanisms are governed by a linear second order differential equation. Thus, the relationship between the effective and instantaneous angle of attack can be written as:

$$\frac{d^2(\alpha_{eff} - \alpha_o)}{d\tau^2} + \left(\frac{1}{\tau_1} + \frac{1}{\tau_2}\right) \frac{d(\alpha_{eff} - \alpha_o)}{d\tau} + \frac{1}{\tau_1 \tau_2} (\alpha_{eff} - \alpha_o) = \frac{1}{\tau_1 \tau_2} (\alpha_{inst} - \alpha_o) \quad (2)$$

where: τ = non-dimensional time = $t(U/c)$

α_{inst} = actual (instantaneous) angle of attack at time, t

α_{eff} = effective angle of attack

α_o = angle of attack about which the perturbations occur.

The time constants, τ_1 and τ_2 are associated with the airfoil/airflow system and are to be established from test results. The equation can be solved by LaPlace transform techniques for instantaneous angles of attack that vary as simple functions of time. This method of solution and the solutions for a sine and ramp change are illustrated in Appendix B. The delay in the effective angle of attack resulting from a step increase in angle of attack is shown in Figure 2. The dependence of this delay on the respective time constants is evident.
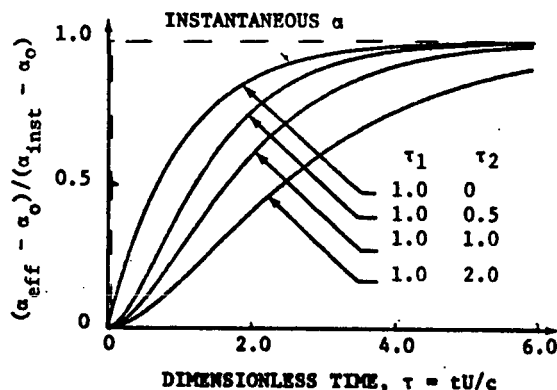
Figure 2. Response of Effective Angle of Attack to a Step Change

The reduction in amplitude and time lag of the effective angle resulting from an instantaneous angle of attack having a periodic sine variation with time is illustrated in the Figure 3. This is the type pattern that a compressor rotor blade might experience behind a 180 degree circumferential distortion pattern. The ratio of the maximum amplitude of the effective angle to the maximum instantaneous angle (Equation 3) is dependent only on the system reduced frequency and the two time constants and is designated, f(k).

$$\frac{(\alpha_{eff} - \alpha_o)_{max}}{(\alpha_{inst} - \alpha_o)_{max}} = f(k) = \frac{1}{\sqrt{(1 + 4k^2\tau_1^2)(1 + 4k^2\tau_2^2)}} \qquad (3)$$

Since only the ratio of the maximum angle is of interest the subscript "max" will be dropped. Henceforth, the function f(k) will be understood as representing this ratio. The function f(k), shown plotted in Figure 4 for various values of the respective time constants, is used along with a Fourier Series to establish the airfoil response to arbitrary variations in the instantaneous angle of attack.

Extension to Arbitrary Variations in Angle of Attack - To establish the rotor airfoil response characteristics to any type of circumferential distortion pattern, it is necessary to solve Equation 2 for the effective angle of attack given arbitrary variations in the instantaneous angle of attack. This will enable the compressor characteristics to be determined as a function of the circumferential distortion and the subsequent loss in stall margin estimated.

A periodic transient, α_{inst}, can be represented by a sum of sine and cosine waves, i.e. Fourier Series. Since the governing differential equation (Equation 2) is linear, solutions can be superimposed. Therefore, by representing the input transient as a Fourier Series and by the use of superposition, a solution for an arbitrary transient can be obtained.

10
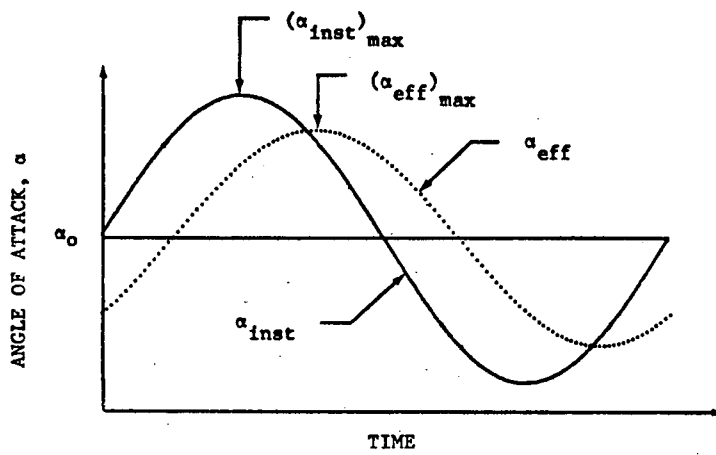
Figure 3. "Effective" Angle of Attack Resulting from
a Sine Variation of the Instantaneous Angle
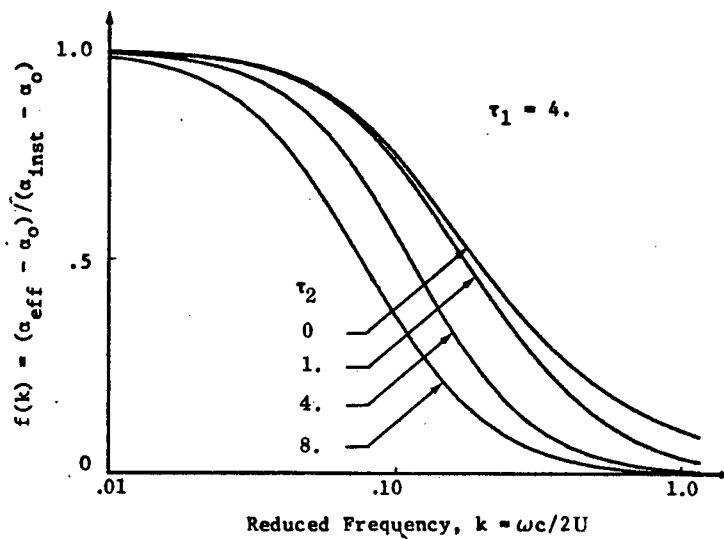
Figure 4. f(k) vs Reduced Frequency for Several Values of τ_2

The Fourier Series representation is as follows:

$$\alpha_{inst}(\theta) = \alpha_o + \sum_{n=1}^{\infty} a_n \cos(n\theta) + \sum_{n=1}^{\infty} b_n \sin(n\theta) \qquad (4)$$

Where: n = the harmonic number

   α_o = average angle of attack

   a_n, b_n = Fourier Coefficients

In practice, the number of harmonics required (n) is determined by the accuracy required in approximating the input signal. As an example the Fourier Series fit of one cycle of the periodic rectangular pattern is shown in Figure 5(a) for 10, 25 and 50 harmonics.

(b) Effective Angle of Attack

(a) Fourier Series Fit of Input Angle of Attack
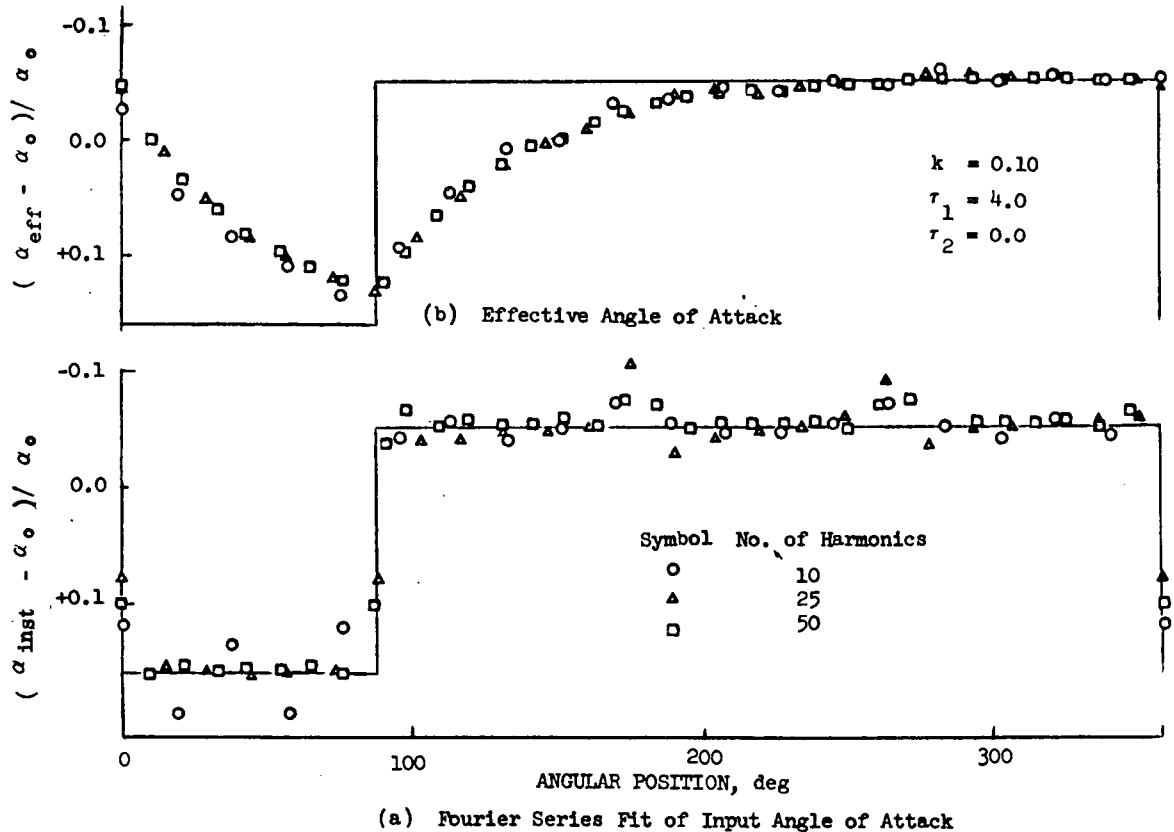
Figure 5. Fourier Series Fit of the Instantaneous and Computed Effective Angles of Attack.

The effective angle of attack is related to the instantaneous angle for each harmonic through Equation 3. If the variation in the instantaneous angle of attack has a frequency of f cycles/sec., the angular frequency of oscillation, ω, is $2\pi f$ and corresponds to the first harmonic in the Fourier Series.

12

The second harmonic will be twice $2\pi f$ or $4\pi f$. In general, the angular frequency of the nth harmonic will be $n(2\pi f)$. Equation 3 can now be applied to each harmonic as illustrated in Equation 5.

In general:

$$\left[\frac{\alpha_{eff} - \alpha_o}{\alpha_{inst} - \alpha_o}\right]_n = f(nk) \tag{5}$$

The effective angle of attack of the total input signal is found by adding the solutions for the individual harmonic as indicated by Equation 6.

$$\alpha_{eff}(\theta) - \alpha_0 = \sum_{n=1}^{\infty} f(nk) \, a_n \cos(n\theta + \Psi(nk)) + \sum_{n=1}^{\infty} f(nk) \, b_n \sin(n\theta + \Psi(nk))$$

$$\text{where} \quad \Psi(nk) = \tan^{-1}(2nk\tau_1) + \tan^{-1}(2nk\tau_2) \tag{6}$$

The results for the rectangular periodic pattern are shown in Figure 5(b) for an increasing number of harmonics. Although an accurate fit of the rectangular wave requires a large number of harmonics, the effective angle is relatively insensitive to this number.

Airfoil Dynamic Stall - Stall of an airfoil in unsteady flow occurs at higher instantaneous angles of attack than that obtained under steady state flow conditions. This is indicated schematically in Figure 6(a), where the point "D" represents the instantaneous stall point and "B" the steady state stall point. This concept results in a time lag in the airfoil response to the unsteady airflow and a reduction in the maximum effective angle of attack. Both of these items are due to the finite time required for the airflow about the airfoil to adjust. This lag in response is indicated in Figure 6(b) for a sinusoidal variation in angle of attack and superimposed on the airfoil characteristic in Figure 6(c). The relationship governing this effective angle of attack is given by Equation 6. It is hypothesized that when α_{eff} is equal to the steady state stall value, stall during unsteady flow will occur. Thus, in Figure 6(b) when α_{eff} reaches the steady state stall line (line B) the airfoil will stall. This stall condition, $\alpha_{eff} = \alpha_{sss}$ is represented for a sinusoidal oscillation by Equation 7.

$$\frac{\alpha_{sss} - \alpha_o}{\alpha_{inst} - \alpha_o} = f(k) \tag{7}$$

Solution of Equation 7 for the instantaneous angle of attack will yield the maximum allowable value for the specific, $f(k)$. Thus:

$$\alpha_{inst_{max}} - \alpha_o = (\alpha_{sss} - \alpha_o) / f(k) \tag{8}$$

13

(a) Typical Airfoil Lift Characteristic

(b) Hypothesized Effective Angle, α_{eff}

(c) Effect of Sinusoidal Oscillations on Airfoil Lift

O = steady state (or mean operating point)
B = steady state stall
C = maximum instantaneous excursion
D = "instantaneous" stall point
E = maximum effective angle
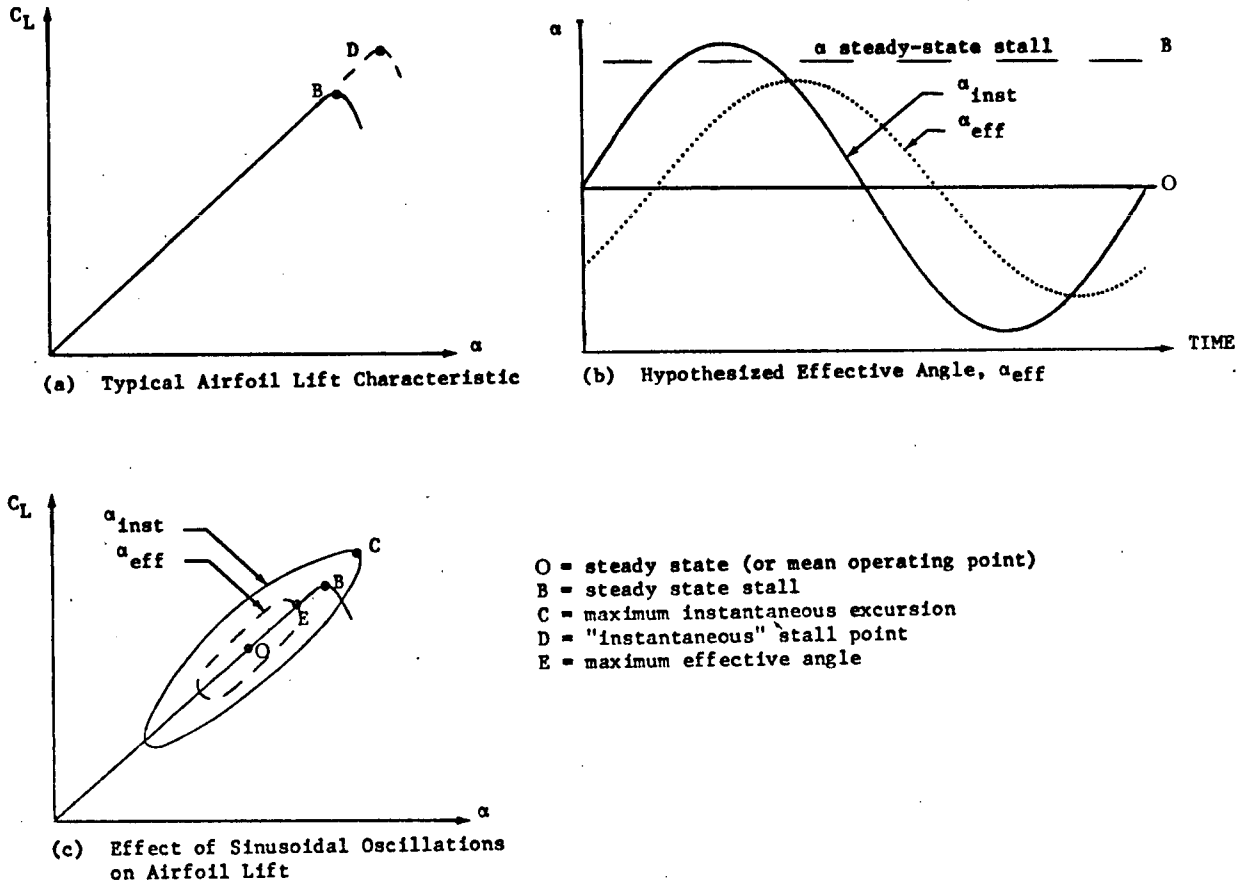
Figure 6. The Effect of Sinusoidal Oscillation on Airfoil Characteristics

The increase in maximum (stalling) angle of attack of an airfoil will therefore be:

$$\Delta\alpha_{max} = \alpha_{inst_{max}} - \alpha_{sss} = (\alpha_{sss} - \alpha_o)[\frac{1}{f(k)} - 1] \tag{9}$$

This will be the increase in the stalling value of α_{inst} as indicated by point D in Figure 6(a). The function $f(k)$ is dependent on the respective system time constants, τ_1 and τ_2, and the reduced frequency, k.

To establish an estimate of the time constants a limited literature survey

14

of the effect of unsteady flow on the maximum lift coefficient of an airfoil was conducted and is presented in Appendix C. Results indicate that the time constants are approximately equal and on the order of $3.5c/U$.

In summary, it was found that the response of a lifting airfoil to an unsteady change in angle of attack was in general governed by a second order linear differential equation. To represent this unsteady process which is a function of the time required for airflow accelerations, shedding of necessary trailing edge vortices, and the delay of boundary layer separation, an effective angle of attack was hypothesized. By means of this effective angle of attack a mathematical representation of the increase in stalling lift coefficient is established by solution of the governing differential equation. This is considered an important development since it enables the response characteristics of a rotor airfoil subjected to unsteady flow conditions to be determined. These characteristics can then be incorporated into a compressor analysis.

Compressor Analysis

The response of a compressor rotor to circumferential total pressure distortion will be established by first relating the change in rotor airfoil angle of attack caused by the distortion to the required change in compressor pressure ratio. This result will then be combined with the unsteady flow model for an isolated airfoil to relate the inlet pressure distortion to loss in compressor stall margin. Fundamental to this analysis is the assumption that the stage or stages that first cause breakdown or surge in the compressor operating in undistorted flow are the same limiting stages causing the compressor to stall when subjected to a distorted flow. This assumption enables the analysis to predict perturbations of the stall line due to distortion rather than an absolute stall margin level, which would require a stage by stage analysis.

Relate Distortion to Blade Lift Coefficient and Compressor Work. - The object of the following development is to relate the total pressure distortion at the compressor face to the required additional compressor pressure ratio and rotor blade lift coefficient. This is accomplished by means of the following approach.

The overall performance of a compressor is represented by a compressor map as shown schematically in Figure 7. To minimize weight, the engine is designed to operate at high stage loadings, near the stall line as shown. When the compressor is subjected to a distorted flow, the average work done by the compressor on the airflow remains constant, and corresponds to point 0 in Figure 7. However, that section of the compressor operating in the region of low inlet total pressure must operate at a higher pressure ratio (point 1 in Figure 7) to pump the flow to the uniform compressor exit pressure. The opposite condition holds for the high pressure regions, which correspond to point 2 in Figure 7. The low pressure regions are of prime interest since they tend to reduce the compressor stall margin. The additional work required in the low pressure regions is assumed to be evenly divided among the compressor

15

stages. For each stage, the relationship between the change in rotor work due to distortion and the change in rotor blade lift coefficient can be obtained by equating the change in work done on the air to the change in the rotor lift characteristics. This is developed in detail in Appendix D with the following result.

$$\left(\frac{d(\Delta h)}{\Delta h}\right)_{rotor} = \left(\frac{dC_L}{C_L}\right)_{rotor} = \left(\frac{d\alpha}{\alpha}\right)_{rotor} \tag{10}$$
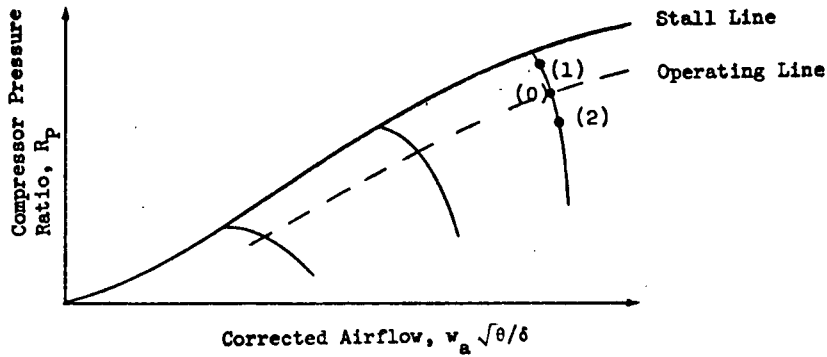
Figure 7. Schematic of the Compressor Map

In essence the fractional change in work done by each rotor on the airflow equals the fractional change in blade lift coefficient or angle of attack. Furthermore, the required work increase can be related to the required increase in compressor pressure ratio as indicated by Equation 11.

$$\frac{d(\Delta h)}{\Delta h} = \frac{\frac{\gamma - 1}{\gamma}}{1 - R_p^{\frac{1-\gamma}{\gamma}}} \frac{dR_p}{R_p} \tag{11}$$

where γ = ratio of specific heats = 1.4

   R_p = compressor pressure ratio

   Δh = rotor work increase

16

By combining equation (10) and (11) the increased blade lift coefficient and/or angle of attack is found to be:

$$\frac{d\alpha}{\alpha} = \frac{dC_L}{C_L} = \frac{\frac{\gamma-1}{\gamma}}{1 - R_p^{\frac{1-\gamma}{\gamma}}} \frac{dR_p}{R_p} \tag{12}$$

The increased pressure ratio required of the compressor is the negative of the change in inlet total pressure due to distortion, or

$$\tag{13}$$

$$dR_p/R_p = -dP_{T2}/P_{T2}$$

Combining this with Equation 12 produces the desired relationship between the change in rotor lift coefficient (dC_L), and angle of attack ($d\alpha$), and the inlet flow distortion (dP_{T2}).

$$\frac{dC_L}{C_L} = \frac{d\alpha}{\alpha} = -\frac{\frac{\gamma-1}{\gamma}}{1 - R_p^{(1-\gamma)/\gamma}} \frac{dP_{T2}}{P_{T2}} \tag{14}$$

This result can then be combined with the effects of unsteady flow on the stalling lift coefficient to establish the effect of distortion on the loss in compressor stall margin.

Relate Inlet Pressure Distortion to Loss in Compressor Stall Margin. - The procedure to establish the loss in stall margin is developed with the aid of Figure 8. The steady state and dynamic rotor airfoil characteristic are shown in Figure 8(a). The dynamic characteristics are typical of that produced by a circumferential distortion. The actual or instantaneous angle of attack on the rotor and resultant lift coefficient are shown as the outer ellipse. The maximum operating point is designated point C. The effective angle of attack as defined in the unsteady analysis lags the instantaneous angle and is shown as the inner ellipse with a maximum at point E.

17

$$\frac{dC_L}{C_L} = \frac{(\gamma-1)/\gamma}{1 - R_P^{(1-\gamma)/\gamma}} \frac{dR_P}{R_P}$$

8(a) Airfoil Characteristic   8(b) Compressor Map
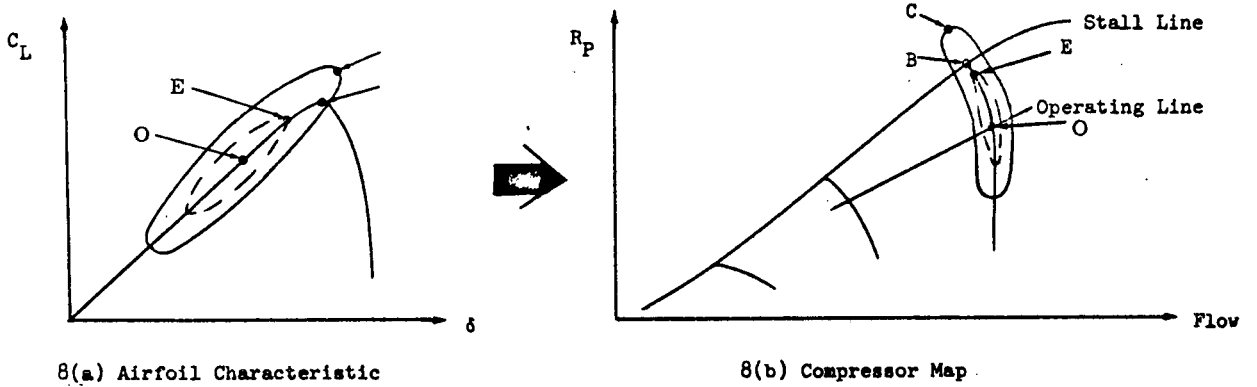
Figure 8. Transformation from Airfoil Characteristic to Compressor Characteristic

Equation 12 can be used to transform these changes in rotor character-istics of a single stage to the map characteristics of a multi-stage com-pressor. This relationship between the required change in compressor pres-sure ratio due to distortion and the change in rotor airfoil angle of attack is given by

$$\frac{d\alpha}{\alpha_0} = \frac{(\gamma-1)/\gamma}{1-R_P^{(1-\gamma)/\gamma}} \frac{dR_P}{R_P} = f(R_P) \frac{dR_P}{R_P} \tag{15}$$

On a finite basis, assuming small changes, the airfoil characteristics can be

converted to the compressor characteristics by use of Equation 15. The results are shown in Figure 8(b). The relationship between the effective and instantaneous pressure ratios is given by

$$\frac{(R_{P_{eff}} - R_{PO})}{(R_{P_{inst}} - R_{PO})} = \frac{f(R_P)\ (\alpha_{eff} - \alpha_0)}{f(R_P)\ (\alpha_{inst} - \alpha_0)} \tag{16}$$

The case of interest is where $R_{P_{inst}}$ is a maximum. This occurs at point "C", Figure 8. Thus, Equation 16 becomes:

$$\frac{R_{P_{eff}} - R_{PO}}{R_{P_{inst}} - R_{PO}} = \frac{R_{PE} - R_{PO}}{R_{PC} - R_{PO}} = \frac{\alpha_E - \alpha_0}{\alpha_c - \alpha_0} \tag{17}$$

Defining the compressor inlet and exit stations as station 2 and 3, respectively, R_{PC} can be established from the distortion level as follows:

$$R_{PC} = P_{T3}/P_{T2min} = (P_{T3}/\overline{P}_{T2})/(P_{Tmin}/\overline{P}_T)$$

$$R_{PC} = \frac{R_{PO}}{1 - \dfrac{\overline{P}_T - P_{Tmin}}{\overline{P}_T}} \tag{18a}$$

Defining the magnitude of distortion, Dist, as $(\overline{P}_T - P_{T_{min}}/\overline{P}_T)$, Equation 18(a) becomes

$$R_{PC} = \frac{R_{PO}}{1 - Dist} \tag{18b}$$

Referring to Figure 8(b), the stall margin (SM) with distortion will be:

$$(SM)_{DIST} = \frac{P_{PB} - P_{PE}}{R_{PO}} \tag{19a}$$

whereas stall margin with zero distortion is:

$$(SM)_{CLEAN} = \frac{R_{PB} - R_{PO}}{R_{PO}} \tag{19b}$$

19

Therefore, the <u>loss</u> in stall margin (Δ SM) due to distortion will be the difference of Equations 19(a) and 19(b) or

$$\Delta \text{SM} = \frac{R_{PB} - R_{PO}}{R_{PA}} - \frac{R_{PB} - R_{PE}}{R_{PA}}$$

$$= \frac{R_{PE} - R_{PO}}{R_{PO}}$$

(20a)

For a sinusoidal variation in angle of attack, the ratio of the maximum effective to maximum instantaneous angle of attack is equal to f(k) as defined in Equation 3. Therefore under these conditions Equation 17 can be written as

$$R_{PE} - R_{PO} = f(k)(R_{PC} - R_{PO})$$

This can be combined with Equation 20(a), resulting in the following:

$$\Delta \text{SM} = f(k) \left(\frac{R_{PC} - R_{PO}}{R_{PO}} \right)$$

The pressure ratio, R_{PC}, was related to distortion in Equation 18. Incorporating this expression into the above, the loss in stall margin becomes:

$$\Delta \text{SM} = f(k) \left[\frac{\dfrac{R_{PO}}{1-\text{Dist}}}{R_{PO}} - R_{PO} \right]$$

(20b)

$$\Delta \text{SM} = f(k) \left[\frac{1}{1-\text{Dist}} - 1 \right]$$

By a series expansion of $\dfrac{1}{1-\text{Dist}}$, Δ SM can be written

$$\Delta \text{SM} = f(k) \ (\text{Dist} + \text{Dist}^2 + \text{-----})$$

The second term is small for reasonable values of distortion and the relationship between the loss in compressor stall margin and distortion becomes simply:

$$\frac{\Delta \text{SM}}{\text{Dist}} = \frac{\Delta \text{SM}}{\left(P_T - P_{Tmin}\right)/P_T} = f(k)$$

(21)

The loss in compressor stall margin can be established by use of Equation 21 for a 180 degree sinusoidal circumferential distortion pattern. Results of this computation are shown in Figure 9 for $\tau_1 = \tau_2$ and for various values of the non-dimensional time constant. The abscissa has been modified to include the number of lobes, n, in the circumferential distortion pattern. The graph is thus generalized to enable the stall margin loss to be found for a compressor of reduced frequency, $k_c = \omega c/2U$ and for single or multiple lobe distortion patterns. This loss for several typical distortion patterns is shown in Figure 10 for three assumed compressors having reduced frequencies, k_c, of 0.05, 0.10 and 0.15, respectively, and time constants $\tau_1 = \tau_2 = 3.5$.
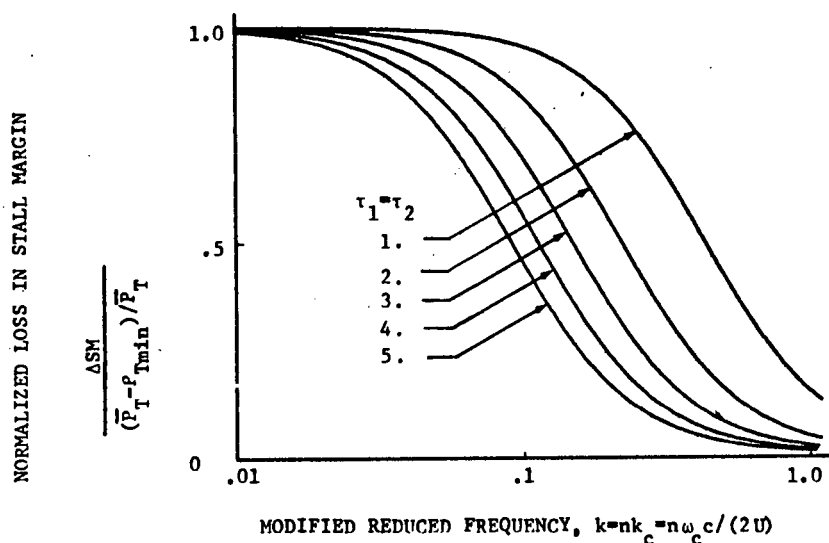
Figure 9 The Effect of Compressor Reduced Frequency
and System Time Constants on Loss in Normalized
Compressor Stall Margin
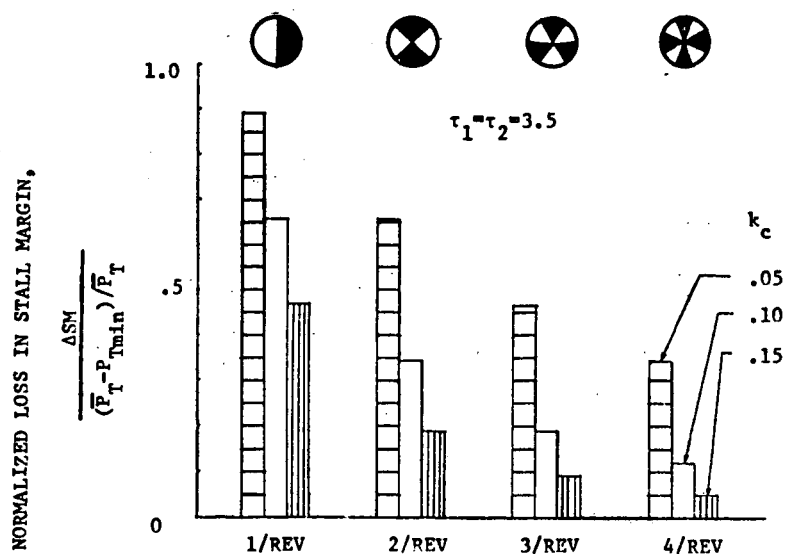
Figure 10 Tolerance to Sinusoidal Distortion for
Different Compressors

The difference in stall margin loss resulting from the assumption of first, second, third or fourth order systems (i.e., solutions to a first, second, third, and fourth order differential equations) is demonstrated in Figure 11. This knowledge will be used later in comparison of analytical predictions with actual compressor test results to obtain the proper time constants.
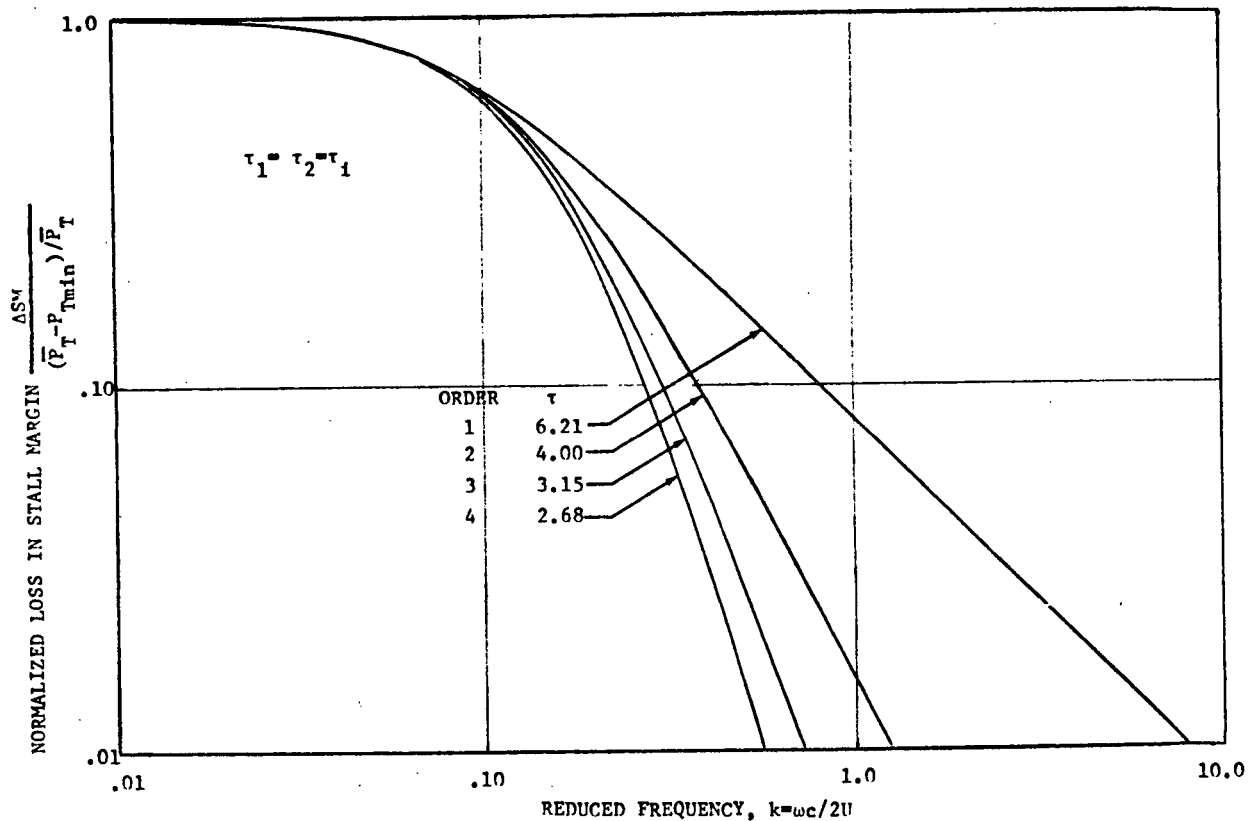
Figure 11 A Comparison of a First, Second, Third, and Fourth Order System
on Loss in Compressor Stall Margin

The loss in compressor stall pressure ratio resulting from arbitrary (non-sinusoidal) circumferential distortion patterns is determined by use of the Fourier Series techniques. A computer program has been developed to mechanize the calculation and is documented in Appendix E. Square and rectangular wave patterns can be evaluated by this technique. The loss in stall margin for a 180° square wave distortion pattern as opposed to a 180° sine wave pattern is shown in Figure 12. The results are shown in terms of a general

reduced frequency k_g which is equal to twice the product of the compressor reduced frequency, $\bar{k}_c$, the number of lobes in the distortion pattern, n, and the time constant τ. This type of presentation is valid only for the case where $\tau_1 = \tau_2 = \tau$. Results indicate that the square wave pattern will cause a greater loss in stall margin than the sine pattern. However, a rectangular pattern with a sharp edged profile cannot be realized with the mixing associated with non-uniform flow. An estimate of the effect of this mixing on the expected stall pressure ratio can be obtained by modifying the square profile as indicated in the insert of Figure 12 and computing the loss in stall margin caused by such a pattern. The effect of such modifications are also shown in Figure 12.
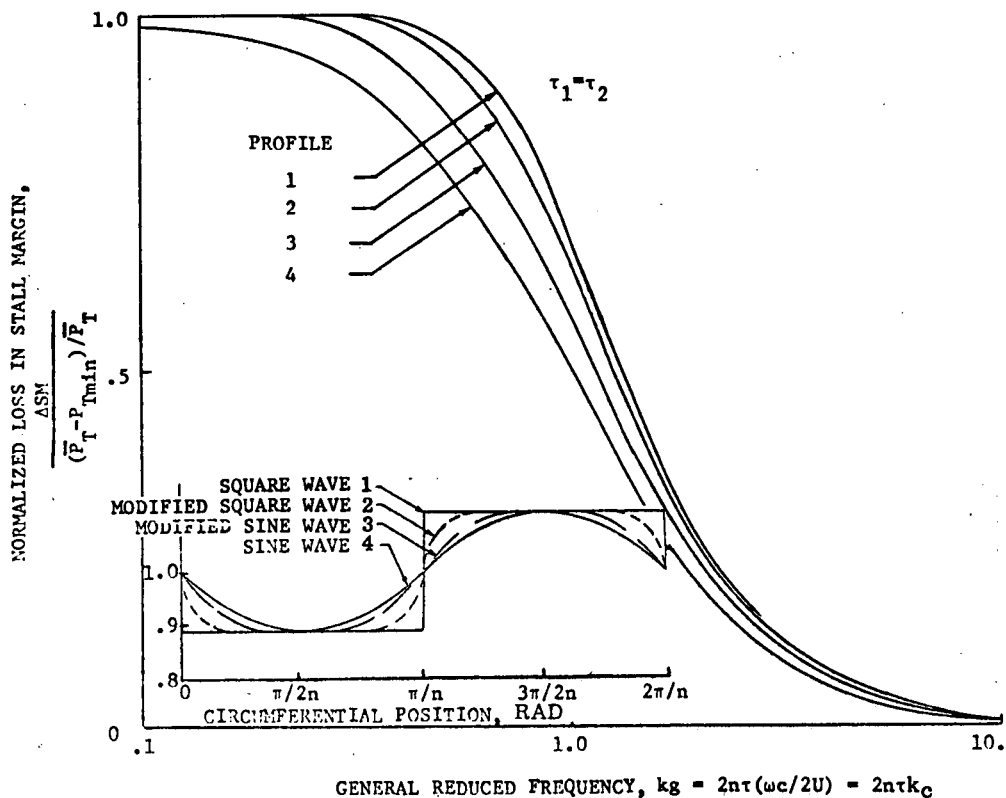
Figure 12 The Effect of Distortion Profile on Loss in Compressor Stall Margin

Although the analysis includes certain simplifying assumptions, it is based on fundamentals of fluid mechanics and aerodynamics, such as the compressor flow/work balance and the approximated lag functions which are known to characterize the airfoil and hence stage response to unsteady airflow. The analysis has shown that the stall margin loss is directly a function of the

distortion level $((\overline{P}_T - P_{T_{min}})/\overline{P}_T)$, the shape of the distortion pattern and of the compressor rotor reduced frequency, k_c.

Application and Generalized Curves

The technique relating arbitrary circumferential distortion patterns to the loss in compressor stall pressure ratio has been established. This analysis has been computerized. Documentation and instructions for use of this program is given in Appendix E. However, many inlet distortion patterns can be approximated by standard patterns of sine or rectangular wave shape. Furthermore, the loss in stall margin resulting from such distortion patterns is basically dependent upon only the extent of the low pressure region, Θ_L, the rotor time constant, τ, and the rotor reduced frequency, k_c. As a result, the loss in stall margin associated with these patterns can be presented as a function of these three variables, Θ_L, τ, and k_c. Therefore a set of generalized curves have been compiled that can be readily used to estimate the loss in compressor stall margin for these standard patterns.

The three basic distortion patterns utilized to compile the generalized curves are shown in Table III. Applicable definitions and nomenclature are presented in Table I as an aid in estimating the loss in stall pressure ratio for those patterns defined in Table III. A means to approximate the compressor reduced frequency is shown in Table II.

Table III is composed of two parts. The curves outlined in the first part are completely general and can be used with a non-dimensional time constant chosen by the user to establish, for example, the effect of different time constants on a comparison between the analysis and a specific set of compressor test data. The second part pertains to those generalized curves utilizing a fixed non-dimensional time constant with a value of $\tau = 3.5$. It will be shown in the Data/Analysis Comparison that this constant will produce a good match between test results and the analysis. The specific curve applicable to a given problem will depend on the distortion pattern and available information on the non-dimensional time constant. Table III is intended to give the required guidance for use of the specific curves, contained in Figures 13 through 16.

Comparison of Analysis with Test Data

A limited comparison between results of the analysis with test data was conducted to add credence to the analysis developed herein, which is based solely on theoretical grounds. A literature search was conducted and the data limited to that readily available in published sources. Much of this data lacks specific details and the reduced frequency of the respective turbomachinery has been estimated. A description of each test vehicle along with the source of information and the reduced frequency is given in Table IV.

The data comparison is made assuming a single non-dimensional time constant to be valid for all turbomachinery. In such a case the compressor

TABLE I

DEFINITIONS AND NOMENCLATURE

Distortion $= (\bar{P}_T - P_{Tmin})/\bar{P}_T$

SM $=$ Stall Margin

Δ SM $=$ Loss in SM along a line of constant corrected rotor speed

Δ SM $/((\bar{P}_T - P_{Tmin})/\bar{P}_T)$ $=$ Normalized Loss in Stall Margin

n $=$ number of lobes in distortion pattern (Refer to Table III)

k_c $=$ Compressor reduced frequency $= \omega c/2U$

ω $=$ Rotor angular frequency $= 2\pi N/60$

N $=$ Rotor RPM

c $=$ First stage rotor chord at the tip

U $=$ Velocity relative to the first stage rotor at the tip

k_g $=$ Generalized reduced frequency $= 2 k_c n$

τ $=$ Non-dimensional time constant*

D_{Tip} $=$ Rotor tip diameter

V_{ax} $=$ Axial velocity into the rotor

* It will be shown in the Data/Analysis comparison that a system having time constants $\tau_1 = \tau_2 = 3.5$ is a good approximation for all fan and compressor systems.

TABLE II

ESTIMATING COMPRESSOR REDUCED FREQUENCY

Compressor reduced frequency is defined as:

$$k_c = \omega \, c/2U = \pi Nc/60U$$

With lack of specific data this reduced frequency can be estimated by assuming axial inflow into the rotor. The reduced frequency is established by use of the velocity diagram, with the following result:

$$k_c = \frac{c}{D_{tip}} \left[1 - 1/2 \left(\frac{Vax}{U_{RTR}}\right)^2 + \frac{3}{8} \left(\frac{Vax}{U_{RTR}}\right)^4 - \text{----} \right]$$

High flow, high tip speed compressors will have a ratio of $(Vax/U_{RTR})^2$ on the order of 0.2. The approximate reduced frequency will then be as follows:
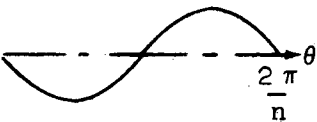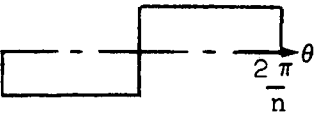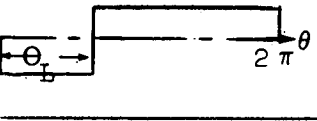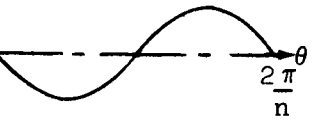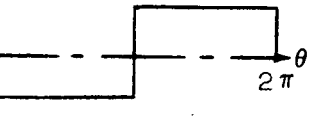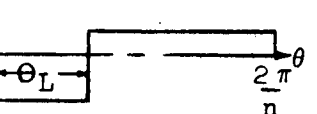
$$k_c = .9 \, c/D_{tip}$$

The range of this parameter normally lies between .05 and .15.

TABLE III

USE OF GENERALIZED CURVES TO ESTIMATE LOSS IN STALL PRESSURE RATIO

DISTORTION PATTERN DESCRIPTION	DISTORTION PATTERN SHAPE	NUMBER OF LOBES, n	LOW PRESSURE REGION WIDTH, θ_L	TIME CONSTANTS τ_1	τ_2	FIGURE NUMBER
Multi-lobe Sine Wave		n	180/n	τ	τ	13
Multi-lobe Square Wave		n	180/n	τ	τ	13
Single Lobe Square Wave		1	θ_L	τ	τ	14
Multi-lobe Sine Wave *		n	180/n	3.5	3.5	15
Multi-lobe Square Wave *		n	180/n	3.5	3.5	15
Single Lobe Square Wave *		1	θ_L	3.5	3.5	16

* This data incorporates the preliminary estimate of a universal non-dimensional time constant.

NORMALIZED LOSS IN STALL MARGIN, $\dfrac{\Delta SM}{(\bar{P}_T - P_{T_{Min}}) / \bar{P}_T}$

GENERAL REDUCED FREQUENCY, $k_g = 2k_c n \mathcal{T}$

square wave

sine wave

$\mathcal{T}_1 = \mathcal{T}_2$
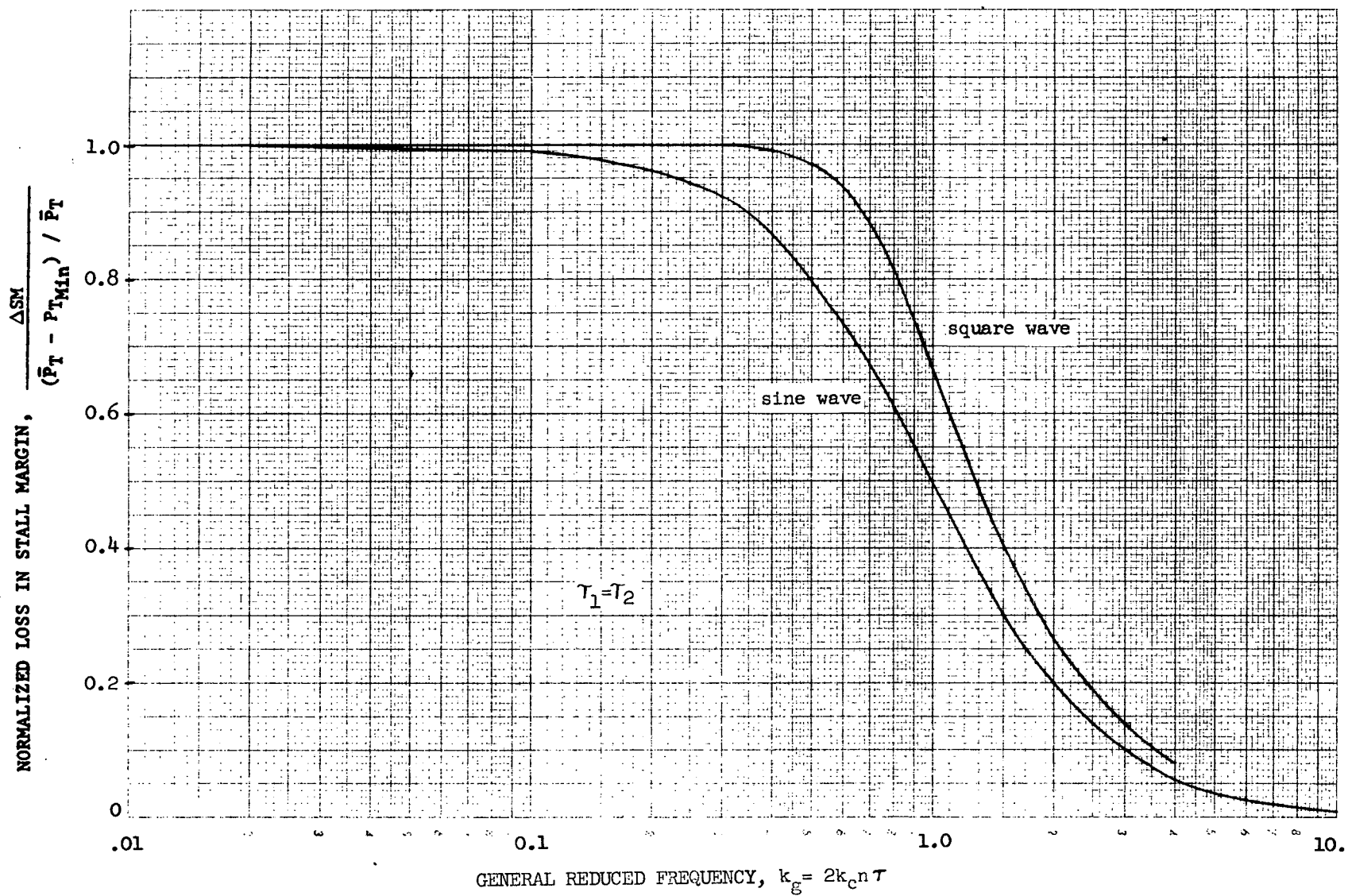
Figure 13. The Effect of the General Reduced Frequency on the Loss in Stall Margin for Sine and Square Wave Patterns.

28
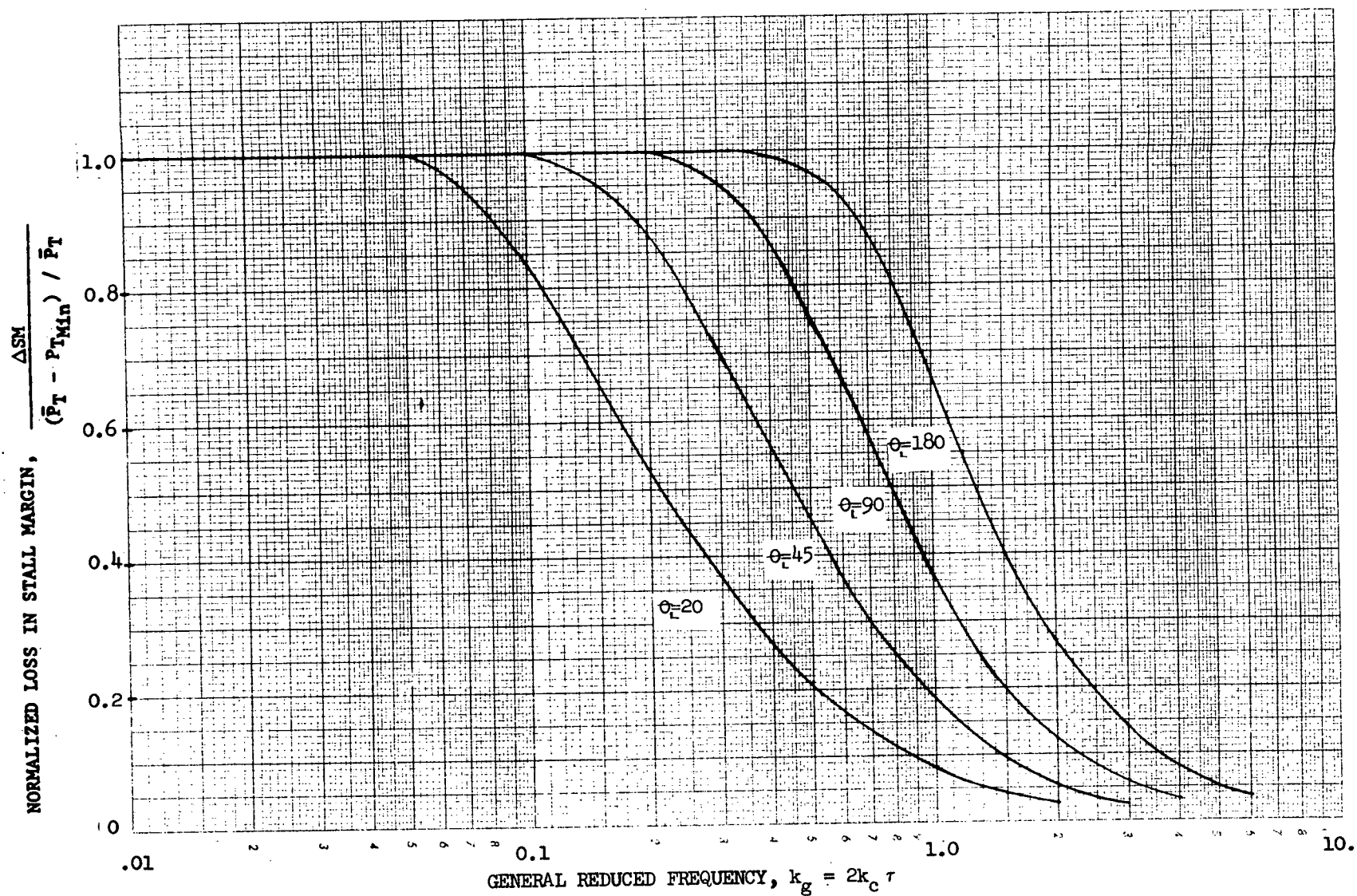
Figure 14. The Effect of the General Reduced Frequency on the Loss in Stall Margin for the Single-Lobe Square Wave Patterns.
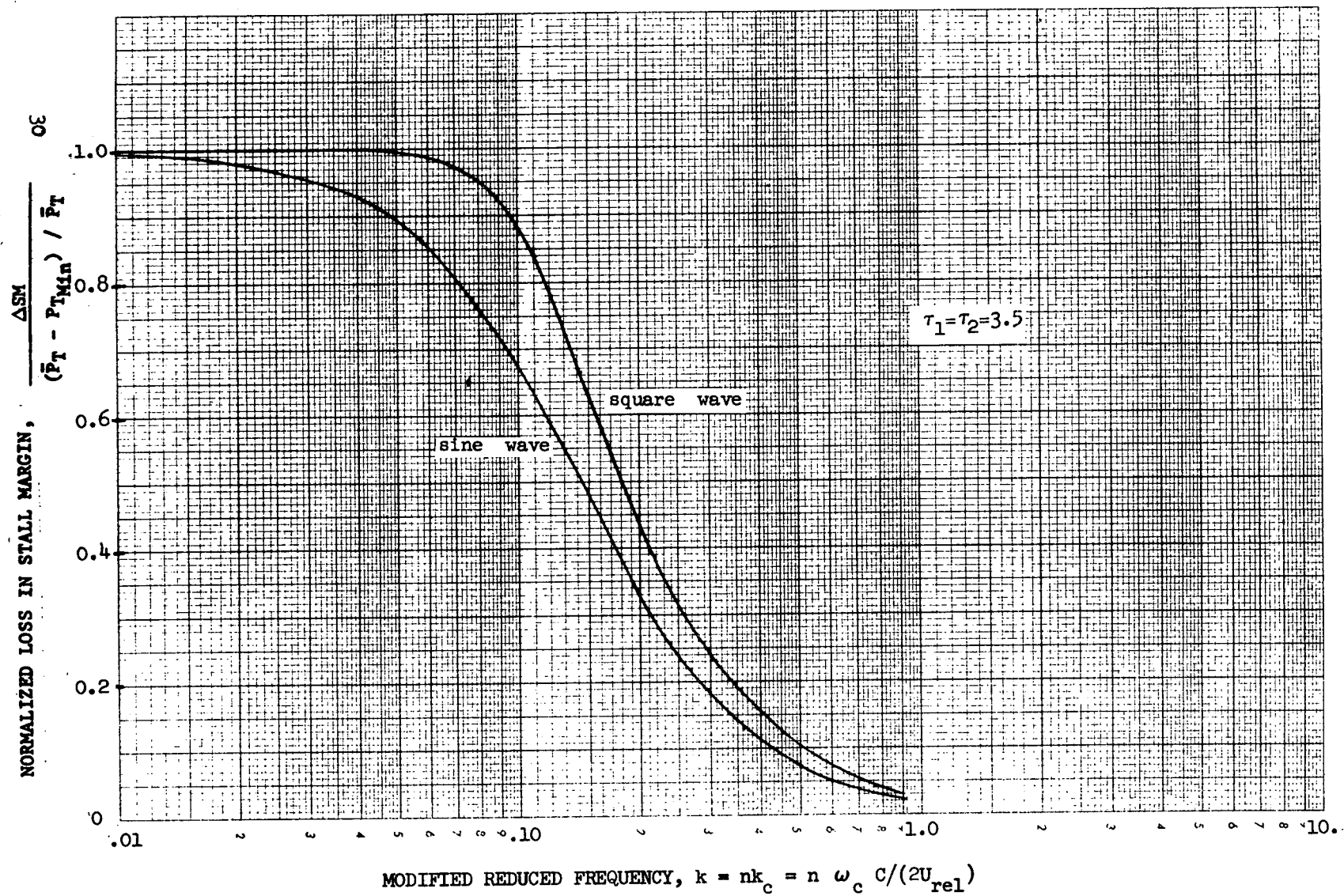
Figure 15. The Effect of the Compressor Reduced Frequency on the Loss in Stall Margin for Sine and Square Wave Patterns.
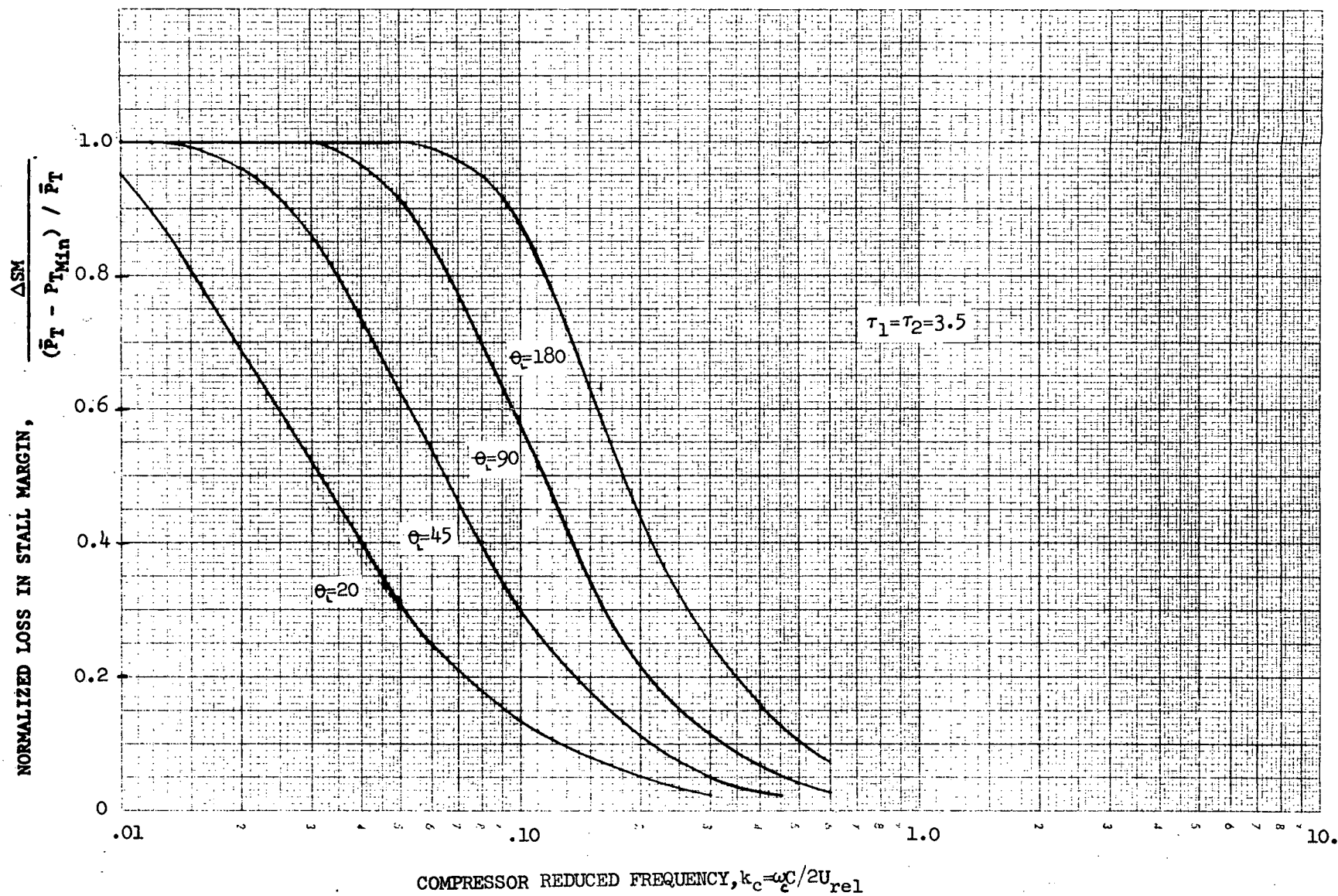
Figure 16. The Effect of the Compressor Reduced Frequency on the Loss in Stall Margin for Single-Lobe Rectangular Patterns.

TABLE IV
SOURCE OF TEST INFORMATION

Description of Test Vehicle	Type of Distortion Pattern	Designation	Source Reference No.	First Stage Rotor Reduced Frequency, $k_{c_{tip}}$	Figure No.
General Electric Compressor Component Test	Sine Profile	GE4 Block I	4	.089*	17
General Electric Compressor Component Test	Sine Profile	GE4 Block II	5	.059*	17
General Electric Turbojet Engine	Rectangular Profile	J85-13	6	.087*	18
General Electric/ NASA High Speed Single Stage Research Compressor	Rectangular Profile		7	.082	18
Pratt and Whitney Aircraft Fan-Low Compressor Rig Test	Rectangular Profile		8	.10 *	19
Pratt and Whitney Aircraft 3 Stage Low Speed Research Compressor Rig	Sine Profile		1	.0325 .065 .130	20
Rolls Royce 6 Stage Compressor Component	Rectangular Profile		9	.067*	21

* Estimated

Figure 17. Comparison of Analysis With General Electric Full Scale
Compressor Test Data
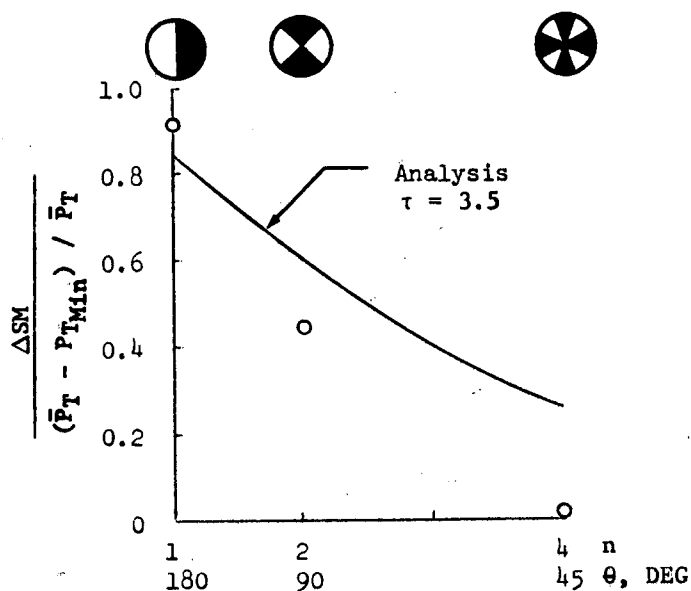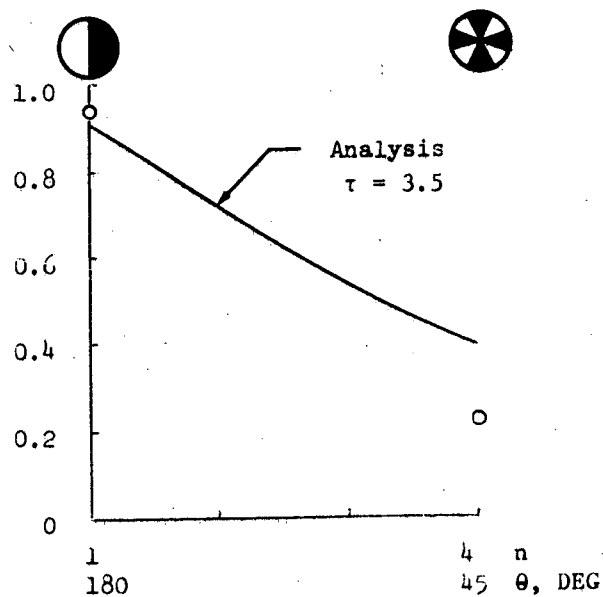
(a) GE4 - Block I (Reference 4)   (b) GE4 - Block II (Reference 5)
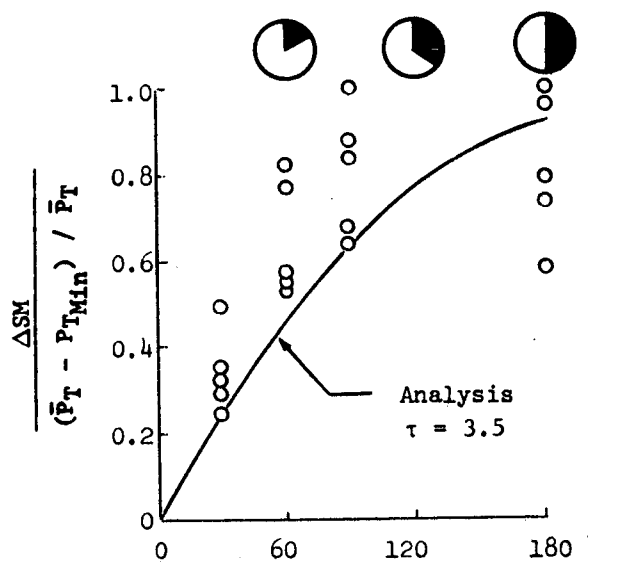
(a) J-85 Engine (Reference 6)   (b) NASA Single Stage Rotor (Reference 7)
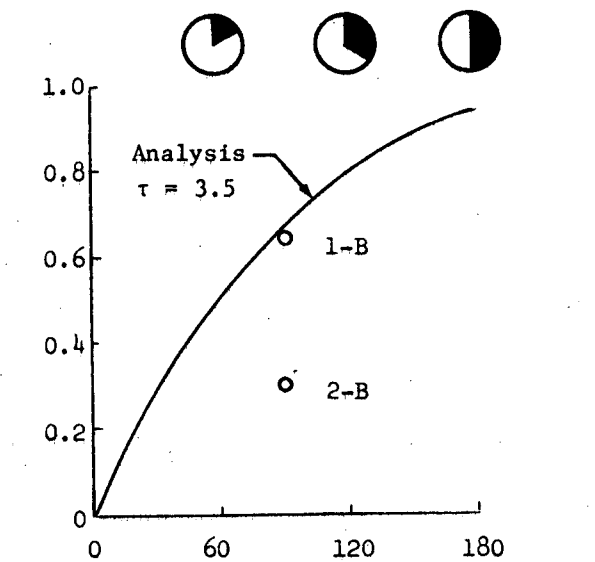
Figure 18. Comparison of Analysis with Test Data
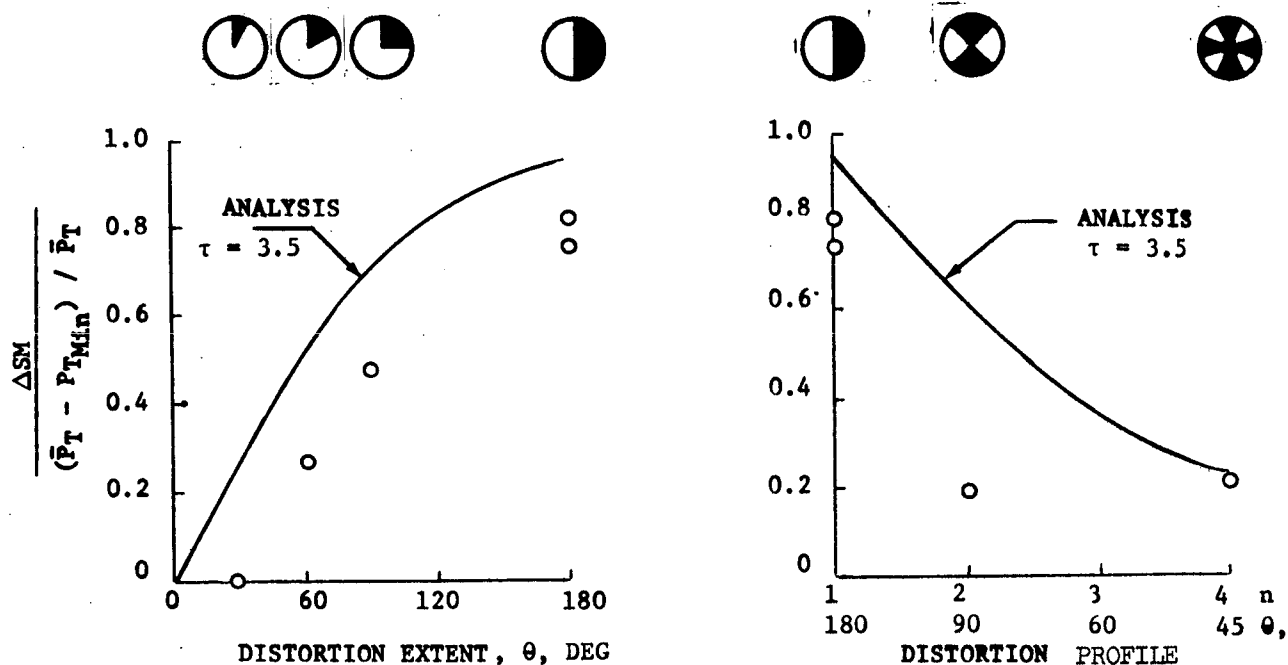
Figure 19. Comparison of Analysis with Pratt and Whitney Fan/Low Compressor Component (Reference 8)
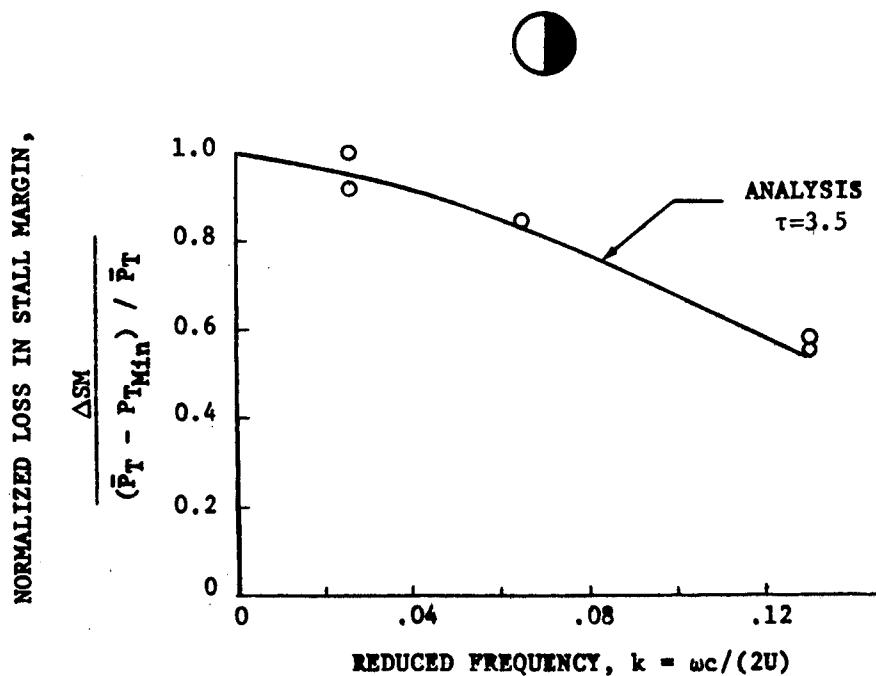
Figure 20: Comparison of Analysis with Test Results of the Pratt and Whitney Aircraft Low Speed 3 Stage Research Compressor (Reference 1)

34
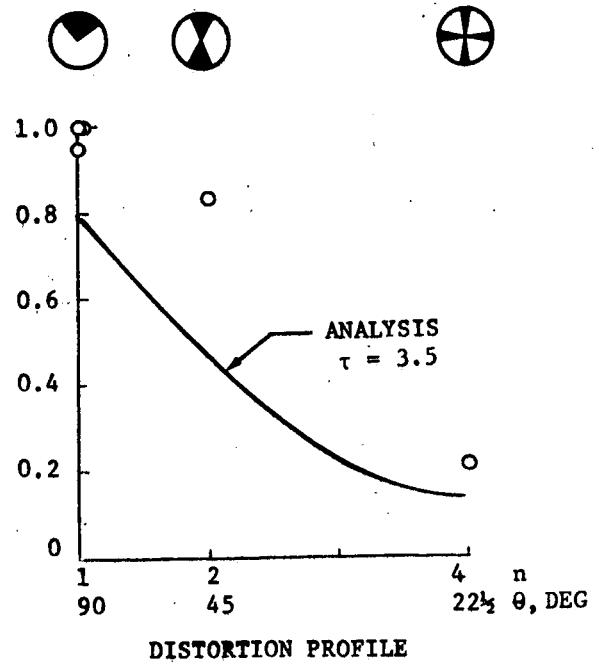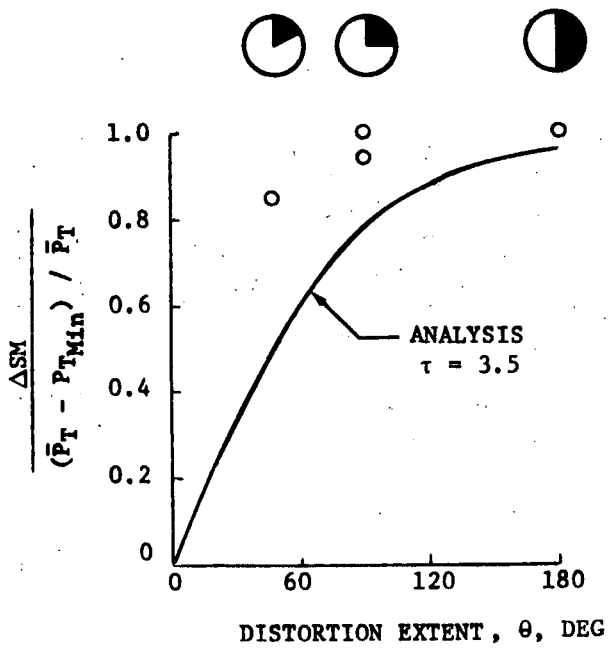
Figure 21. Comparison of Analysis with Test Results of the Rolls Royce 6 Stage Scale Model Compressor (Reference 9)
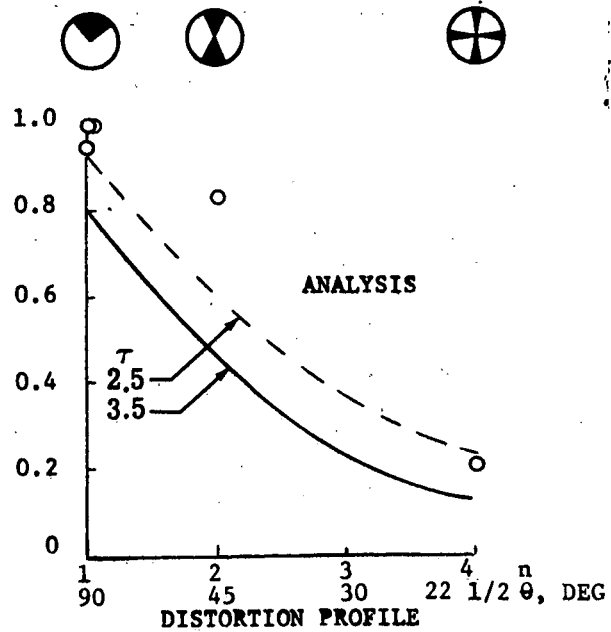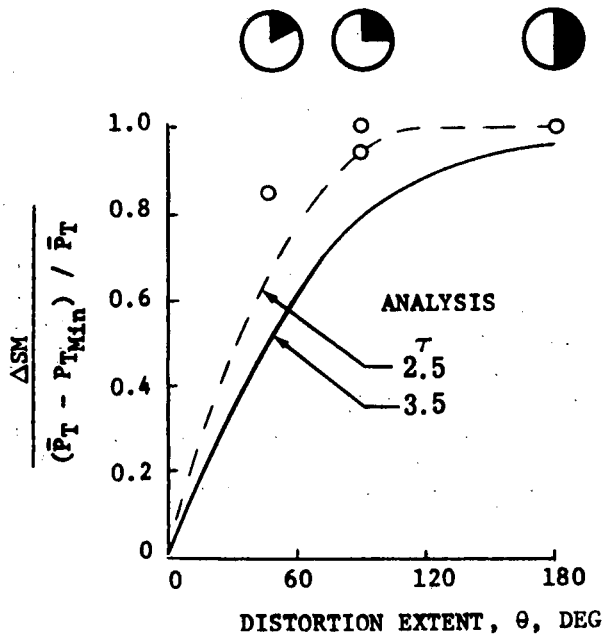
Figure 22: Comparison of Analysis with Test Results of the Rolls Royce 6 Stage Scale Model Compressor (Reference 9)

sensitivity to distortion is dependent only on the rotor reduced frequency as shown earlier (Effect of Inlet Pressure Distortion on Loss in Stall Pressure Ratio). The comparison is presented in terms of the normalized loss in stall pressure ratio in Figures 17 through 21 for the constant non-dimensional time constant of 3.5. Without exception, the trends predicted by use of the analysis are in very good agreement with results of the tests, and in many cases, good quantitative agreement is obtained. (See for example Figure 20)

The non-dimensional time constant of 3.5 was assumed universally applicable in the above comparison. As shown it produces reasonable agreement with data and as a result is recommended for use during the development phase of an inlet/engine program. However, the analysis also provides the mechanism to improve data/analysis comparison once test data of production type hardware is available. For example, the prediction shown in Figure 21 for τ = 3.5 can be modified by assuming a time constant, τ = 2.5, bringing the analysis in exceptionally close agreement with the test results as shown in Figure 22. This further demonstrates the validity of the basic approach.

In conclusion, the impact of this inlet flow distortion analysis in the area of inlet/engine compatibility could be substantial. A means is now available to carry-on compatibility studies prior to engine test. The analysis identifies those inlet flow and compressor design variables most important in the interaction of the inlet flow and the compressor. These are specifically the inlet distortion profile and magnitude, and the compressor reduced frequency. This latter parameter is directly dependent on the rotor chord which emerges as a strong factor in the design of hardware for compatibility. Therefore this approach can help to insure inlet/engine compatibility prior to hardware commitment. Furthermore, the successful treatment of the problem by fundamental aero-thermodynamic relationships can also put into perspective and tie together the number of empirical distortion indices currently in use.

The favorable results of the data/analysis comparison are considered verification of the fundamental hypothesis of the analysis; specifically that distortion must be analyzed from an unsteady point of view. The accuracy is also considered sufficient to justify the simplifying assumptions incorporated in the analysis including the use of the overall compressor work balance rather than a detailed stage-by-stage analysis. Additional comparisons with a few test programs are recommended for refining the steady state analysis. The programs should provide information such as the detailed distortion patterns, compressor geometry and compressor operating conditions. However, the compressor model has been developed to the point necessary for conducting the phase of study designed to analyze the compressor reaction to unsteady turbulent flow.

TASK II
FLUID DYNAMIC MODEL OF TURBULENT INLET FLOW

Turbulent flow produced in an aircraft inlet system can result in momentary total pressure distortion levels of a magnitude and duration sufficient to cause engine compressor stall. The first attempt to identify such instantaneous distortion levels was in terms of the Root Mean Square (RMS) level and the Power Spectral Density (PSD) function of the total pressure fluctuations. These statistical averages are relatively inexpensive to obtain. However, no physical interpretation could be given such quantities and as a result were of little value in the correlation of unsteady flow and compressor stall. Presently, it is common practice to measure an instantaneous distortion pattern at each instant of time by use of high response, highly (time) correlated total pressure instrumentation. This requires complex and expensive data measurement systems. While these instantaneous patterns graphically demonstrate the existence of unsteady flow, only limited empirical correlations of unsteady flow and compressor stall have been shown. The high cost of data reduction severely restricts the quantity of data analysis that can be made to substantiate any correlation. In addition, an empirical approach is inherently weak since it does not provide physical understanding of the basic flow phenomena. An analysis relating turbulent flow phenomena in the inlet to compressor stall is required.

A fluid dynamic model of turbulent flow is developed herein as a means of understanding turbulent inlet flow and as a practical tool for evaluating flow properties through the use of the total pressure RMS level and PSD functions. By use of this flow model, which is based on a combination of basic fluid dynamic concepts and statistical analyses, a better understanding of the mechanics of the flow is obtained. Consequently, the loss in compressor stall margin may ultimately be related to the statistical characteristics of turbulence.

The approach used to analyze this turbulent flow is outlined below and presented in detail in the subsequent sections of the report. Turbulence, normally measured in terms of velocity or total pressure, implies pressure gradients exist in the flow. It is a fundamental of fluid mechanics that pressure gradients can be supported by only two means: (1) pressure waves traveling at (or above) the local sound speed and (2) by streamline curvature. Since turbulence is produced by viscous phenomena, it is proposed that the pressure fluctuations measured in an inlet are primarily supported by streamline curvature. To realistically model the flow, it is hypothesized that the streamline curvature and resultant pressure fluctuations are caused by a random distribution of discrete vortices being convected downstream by the mean flow. This is illustrated schematically in Figure 23.

To obtain a mathematical representation of this flow model, a coordinate system moving downstream with the mean flow is used and enables the individual vortices to be analyzed in a steady frame of reference. Steady state flow equations can then be applied to describe the flow field about an isolated vortex. Analytical construction of the total pressure signature of this

isolated vortex is accomplished through the superposition of the vortex flow and the transport velocity. Consistent with the basic hypothesis, the turbulent nature of the flow is assumed to result from a distribution of these vortices having random size, strength, location, and direction of rotation. The total pressure root mean square level and power spectral density function resulting from this random flow field are found by use of statistical methods as applied to the analysis of this stochastic process. This development is followed by sensitivity studies to determine the impact of certain assumptions on the results. In addition, results of the analysis are compared with test data.
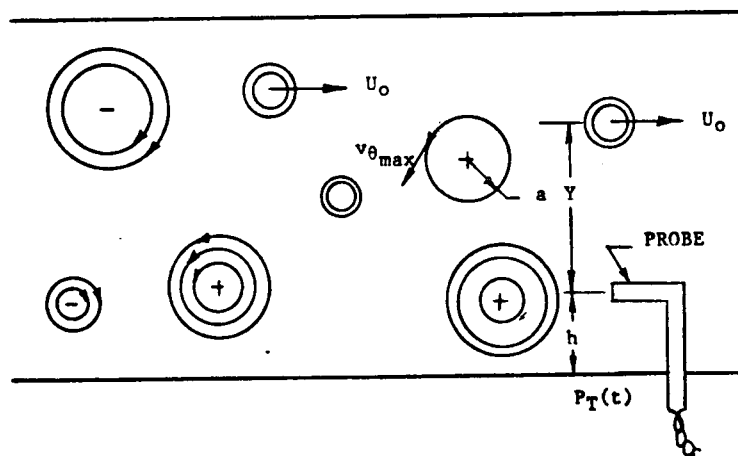
Figure 23. Hypothesized Turbulent Flow Composed of Random Vortices.

Isolated Vortex

The definition of the flow field associated with an isolated vortex is the first step in the development of this turbulent flow model. The description is based on a time dependent solution of the Navier-Stokes Equations. This vortex and associated properties are used in the subsequent development of the fluid flow model.

Solutions of the Navier-Stokes Equations of Motion. - Depending upon the initial and boundary conditions, several vortex flow fields are found to be

38

solutions of the Navier-Stokes Equations. The details and the characteristics of these solutions are presented in Appendix F. It was found that all steady state solutions have singularities (infinite velocities) at either the vortex center or outer extremity and therefore do not represent real flows. Therefore, the time dependent solutions, each representing different vortex boundary conditions, were examined. For a realistic flow, the solution must satisfy the following boundary conditions: (1) the vortex must have a tangential velocity of zero at both the center and at an infinite radius, (2) the velocity must be continuous for all radii, and (3) the influence of the vortex must move outward with time. The solution of the two-dimensional time dependent Navier-Stokes Equations that fits these assumed boundary conditions is a vortex formed by an impulsive start in an undisturbed flow. The normalized velocity field associated with this vortex is given in Equation 22.

$$\frac{v_\Theta}{v_{\Theta max}} = n\frac{r}{a} \left\{ e^{-\frac{1}{2}\left[\left(\frac{r}{a}\right)^2 - 1\right]} \right\} \tag{22}$$

where v_Θ = velocity in the Θ direction (cylindrical coordinate system)

$v_{\Theta max}$ = maximum velocity of the given vortex at a given time

a = radius at which $v_\Theta = v_{\Theta max}$

n = specifies direction of rotation, = 1 for counter-clockwise and -1 for clockwise

The radius $r = a$ at which the velocity is a maximum is considered the vortex core radius. This core radius varies with time and as a result, the influence of this vortex increases in the radial direction with time.

A complete development of this vortex is presented in Appendix H and includes a description of the angular momentum, vorticity, circulation and a discussion on the time of origin and decay of the vortex.

Vortex Description in Cartesian Coordinates. - In order to describe the properties of the vortex in terms of a coordinate system fixed with respect to the inlet it is first necessary to express the vortex properties in terms of a Cartesian coordinate system fixed to the center of the vortex (x, y) as opposed to the cylindrical coordinate system (r, Θ) used for solutions of the Navier-Stokes Equations. A description of the coordinate system used is shown in Figure 24(a).

As developed in Appendix H the circumferential velocity is a function of the radius and time and is given by Equation 23.

$$v_\theta = \frac{Br}{t^2} e^{-\frac{r^2}{4\nu t}} \tag{23}$$

39
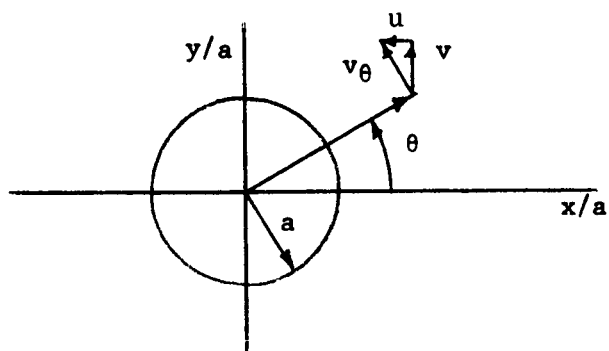
(a). Vortex Model Cartesian Coordinate System
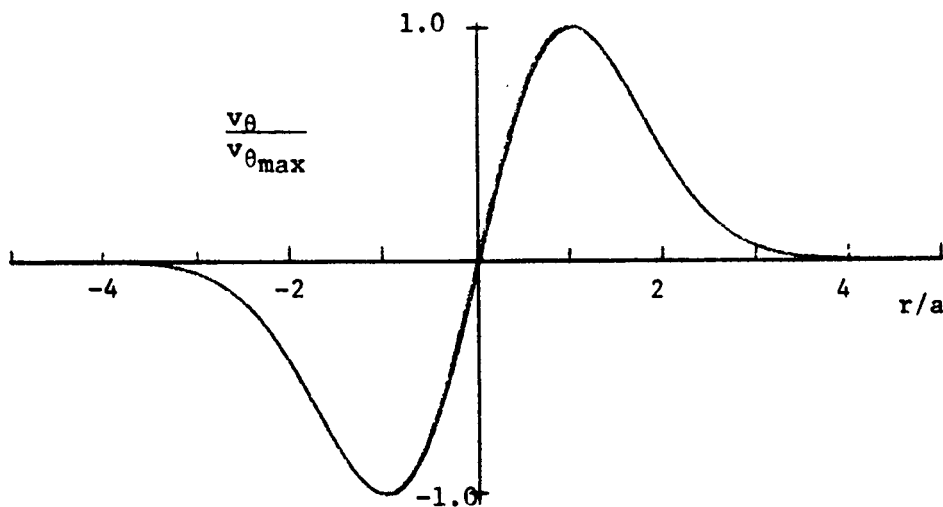
(b). Vortex Velocity Distribution
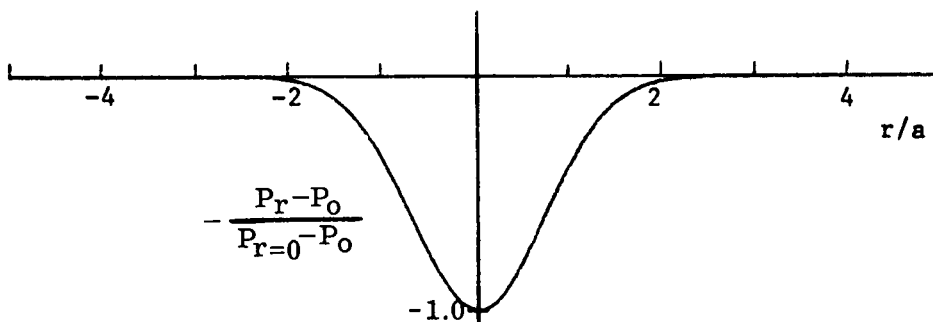
(c). Vortex Static Pressure Distribution

Figure 24. Isolated Vortex Flow Field

where: B = constant depending on the vortex strength

ν = kinematic viscosity

t = time since the vortex started.

However, due to the short period of time the vortex is in the field of interest (the inlet duct) and the very slow rate of growth of the vortex, the time is assumed constant. The vortex tangential velocity normalized by the maximum velocity, which occurs at r = a, was given by Equation 22 and repeated below. The variation of v_θ with r is shown in Figure 24(b).

$$\frac{v_\theta}{v_{\theta max}} = n(r/a) \; e^{-\frac{1}{2}[(r/a)^2 - 1]} \tag{22}$$

The horizontal (u) and vertical (v) velocity components of the vortex velocity are obtained by use of the description and definitions of the coordinate systems of Figure 24(a). These are:

$$u = -v_{\theta_{max}} n(Y/a) \; e^{-\frac{1}{2}[(x/a)^2 + (y/a)^2 - 1]} \tag{24}$$

$$v = v_{\theta_{max}} n(x/a) \; e^{-\frac{1}{2}[(x/a)^2 + (y/a)^2 - 1]} \tag{25}$$

The local flow angle is dependent on the velocity components, and is given by Equation 26.

$$\alpha = \arctan(v/u) = \arctan\left(\frac{-1}{\tan \theta}\right) \tag{26}$$

The static pressure variation with radius as determined in Appendix I is given by Equation 27 and shown in Figure 24(c).

$$P_r - P_o = \frac{-\rho}{2} v_{\theta_{max}}^2 \; e^{-[(x/a)^2 + (y/a)^2 - 1]} \tag{27}$$

where: P_r = static pressure at radius r

P_o = static pressure beyond the vortex influence, r >> a

ρ = density

The total pressure in the vortex flow field, based on a coordinate system fixed to the vortex center, is equal to the sum of static and dynamic pressures or

$$P_T = P_r + \frac{\rho}{2} v_\theta^2 \tag{28}$$

In terms of the cartesian coordinate system, the total pressure is obtained by combining Equations 22, 27, and 28 and is given by Equation 29.

$$P_T - P_o = \frac{\rho}{2} \left[(x/a)^2 + (y/a)^2 - 1 \right] v_{\theta_{max}}^2 \ e^{\ -\ [(x/a)^2 + (y/a)^2 - 1]} \tag{29}$$

Transformation of the Vortex Flow Field to the Inlet Coordinate System. - The vortex flow field has been described in the coordinate system fixed to the vortex center. The vortex, however, is moving downstream at the local average flow velocity. To determine the total pressure as it would be measured at the engine face, it is necessary to transform the vortex velocity field into the coordinate system fixed to the inlet.

Allowing the vortex to move downstream at the local velocity, U_o, as shown in Figure 25, the local instantaneous velocity components as would be measured in a coordinate system fixed at the probe becomes:

$$U = U_o + v_{\theta_{max}} (Y/a) \ e^{\ -\ \frac{1}{2}[(X/a)^2 + (Y/a)^2 - 1]} \tag{30}$$

$$V = -v_{\theta_{max}} (X/a) \ e^{\ -\ \frac{1}{2}[(X/a)^2 + (Y/a)^2 - 1]} \tag{31}$$

Here, the upper case (X, Y) represent the position of the vortex center relative to the origin of the fixed coordinate system located on the probe. In essence, U and V are the velocity components at the probe due to a vortex located at (X, Y). In this case, the transformation between the moving and fixed coordinate systems is simply

$$X = -x$$
$$Y = -y \tag{32}$$

The static pressure in the fixed coordinate system is

$$P_r - P_o = -\frac{\rho}{2} v_{\theta_{max}}^2 \ e^{\ -\ [(X/a)^2 + (Y/a)^2 - 1]} \tag{33}$$

42
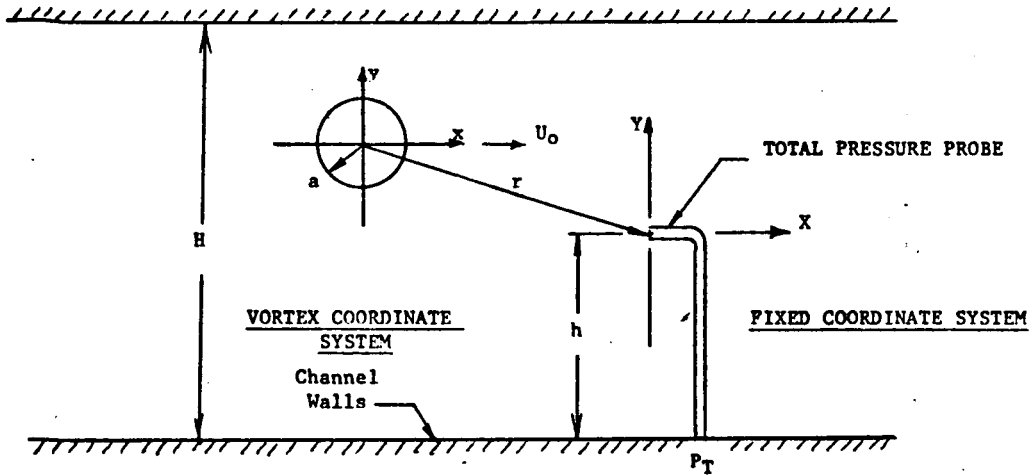
Figure 25. Transformation of Coordinate Systems.

To account for the fact that the local flow angle at the total pressure probe is not aligned with the probe, the total pressure as expressed in Equation 34 is assumed to be the local static pressure plus a corrected dynamic pressure.

$$P_T = P_r + \eta_R(\alpha)\frac{\rho}{2}W^2 \tag{34}$$

where: P_r = static pressure (which is independent of coordinate system)

W = the resultant velocity vector, $(U^2 + V^2)^{1/2}$

η_R = probe total pressure recovery

α = local flow angle

Since the vortex is moving downstream at velocity U_0, the position, X, of the vortex center with respect to the fixed (probe) coordinate system is a function of the velocity, U_0, and time, t. Thus:

$$X = U_0 t \tag{35}$$

This implies that the origin of time must be chosen such that X = 0 when t = 0.

The total pressure recovery is assumed to vary directly by the square of the cosine of the flow angle, α , at the probe.

$$\eta_R = \cos^2\alpha = \left(\frac{U}{W}\right)^2 \tag{36}$$

43

Using the transformation of Equation 35, the total pressure recovery, and the definition of static pressure (Equation 33) and velocity (Equation 30 and 31), the total pressure expressed by Equation 34 becomes:

$$P_T - P_{T_o} = n \rho U_o v_{\theta max} (\tfrac{Y}{a}) e^{-\tfrac{1}{2}[(\tfrac{U_o t}{a})^2 + (\tfrac{Y}{a})^2 - 1]} \qquad (37)$$

$$+ n^2 \tfrac{\rho}{2} v_{\theta max}^2 \left[(Y/a)^2 - 1 \right] e^{-[(\tfrac{U_o t}{a})^2 + (\tfrac{Y}{a})^2 - 1]}$$

where P_{T_o} is the total pressure of the undisturbed flow and equal to $P_o + \tfrac{1}{2}\rho U_o^2$

Defining this delta pressure as ΔP_T and normalizing by the dynamic pressure,

$$q_o = \tfrac{\rho}{2} U_o^2 \qquad (38)$$

the total pressure becomes:

$$\frac{\Delta P_T}{q_o} = 2n(\frac{v_{\theta max}}{U_o}) \; (Y/a) \; e^{-\tfrac{1}{2}[(U_o t/a)^2 + (Y/a)^2 - 1]} \qquad (39)$$

$$+ n^2 (\frac{v_{\theta max}}{U_o})^2 \left[(Y/a)^2 - 1 \right] e^{-[(U_o t/a)^2 + (Y/a)^2 - 1]}$$

The resultant total pressure is a function of the time, t, the mean velocity, U_o, the strength of the vortex $v_{\theta max}$, the core size of the vortex a, and direction of rotation, n. Detailed development of these relationships are given in Appendix I.

Although these relations have been developed for a single vortex, they are applicable to a series of vortices. These vortices can assume random values of size, strength, location and direction. In such a case the vortex properties, a, $v_{\theta max}$, y, and n, become random variables. The techniques required to treat these properties as random variables are developed in Appendix J. These tools are then used in conjunction with Equation 39 to establish the statistical characteristics (RMS and PSD) of the proposed flow field.

Statistical Flow Model

The model of turbulent inlet flow is hypothesized as being composed of a random distribution of vortices, each having a specific size, strength, direction of rotation, and location as shown in Figure 23. The total pressure

44

fluctuation created by each vortex is given in Equation 39. For a specific vortex having a given set of properties, a, $v_{\Theta max}$, y, and n, Equation 39 signifies a single time function. However, each vortex has a different set of properties; consequently, the flow field is composed of a family of time functions. This family is called a stochastic process.

The autocorrelation function and its Fourier Transform, the power spectral density function resulting from this process, are found in functional form by statistical methods as applied to a general stochastic process in Appendix J. These developments are applied to the vortex flow field to obtain the total pressure autocorrelation and power spectral density functions of the turbulence. The fluctuations in total pressure are also related to the fluctuations in velocity by use of the flow model, providing an analytical means to relate, hot wire anemometer velocity measurements and total pressure measurements.

Autocorrelation Function. - The autocorrelation function of the stochastic process composed of the random vortices flowing downstream with the flux of N per second can be summarized as follows.

The general total pressure wave described by Equation 39 can be represented by the following functional notation.

$$\Delta P_T = \Delta P_T \ (a,v,Y,n,t) \tag{40}$$

The autocorrelation function of this discrete total pressure wave is found by means of the definition of the autocorrelation function and is given by

$$R_{\Delta P_T}(a,v,Y,n,t) = \int_{-\infty}^{\infty} \Delta P_T(a,v,Y,n,t) \, \Delta P_T(a,v,Y,n,t+t)dt \tag{41}$$

To establish the autocorrelation function of the entire family of waves, a weighted sum of the function $R_{\Delta P_T}(a, v, Y, n, \tau)$ is performed over all possible values of a, v, Y, and n. The weighting functions are the percentage of vortices having a specific core size between a and a $+ \Delta a$, specific strength between $v_{\Theta max}$ and $v_{\Theta max} + \Delta v_{\Theta max}$, a specific location between y and y $+\Delta y$ and a direction of rotation (n = +1 or -1). These weighting functions are assumed independent of each other, are simply the probability density functions of a, v, Y, and n, respectively, and are designated by the notation, $P(\ )$. The autocorrelation function of the resultant total pressure wave (Equation 42) is therefore the weighted sum of the general autocorrelation function.

$$R_{\Delta P_T}(\tau) = N \iiiint_{a \ v \ Y \ n} R_{\Delta P_T}(a,v,Y,n,\tau)P(a)P(v)P(Y)P(n)dndYdvda \tag{42}$$

The autocorrelation function of the vortex flow field, as measured at the total pressure probe, is found by incorporating the total pressure wave (Equation 40), the definition of the autocorrelation for a discrete wave

$(\overline{v}_{\theta max}/U_o) = 0.25$

$m_V = 4$

$n_V = 14$

$U_o P(v_{\theta max}) = k_V \left(\dfrac{v_{\theta max}}{U_o}\right)^{m_V} \left(1 - \dfrac{v_{\theta max}}{U_o}\right)^{n_V}$

(a). Vortex Maximum Velocity

$HP(y) = 1$

(c). Vortex Lateral Location

$(\overline{a}/H) = 0.1$

$m_a = 2$

$n_a = 26$

$HP(a) = k_a \left(\dfrac{a}{H}\right)^{m_a} \left(1 - \dfrac{a}{H}\right)^{n_a}$
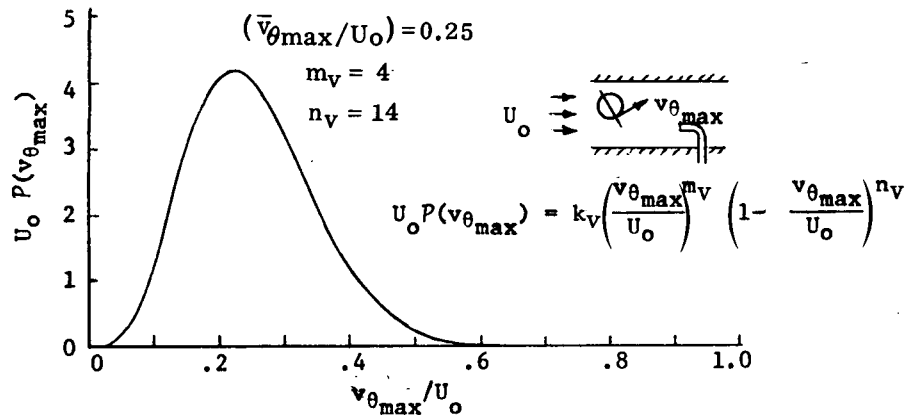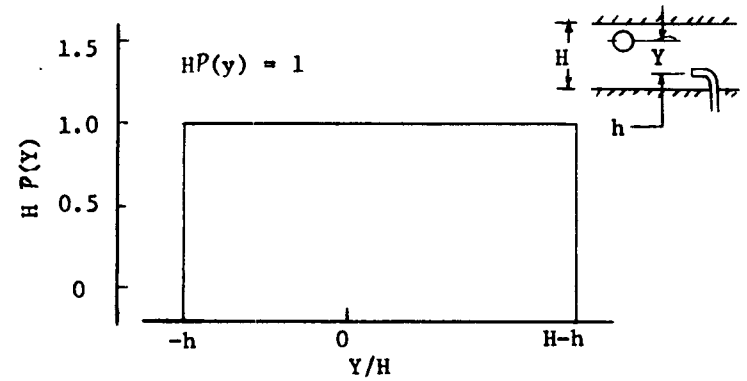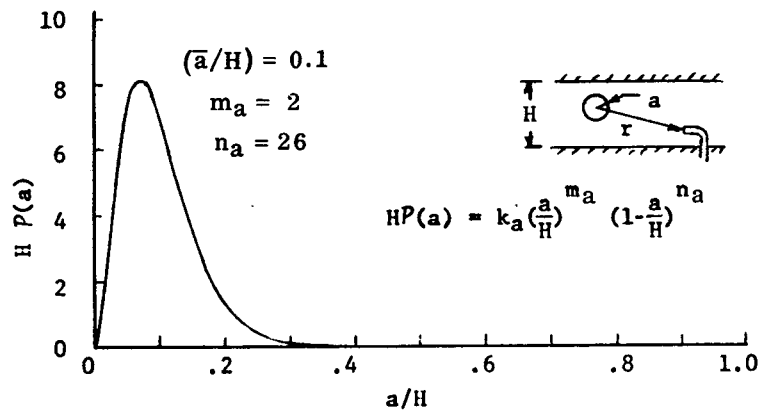
(b). Vortex Core Size
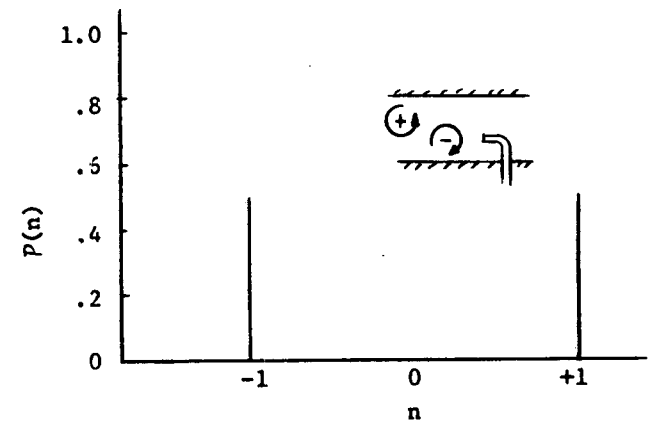
(d). Vortex Spin Direction

Figure 26. Probability Density Functions of the Vortex Random Properties.

(Equation 41), and appropriate probability density functions into Equation 42. This substitution is accomplished in Appendix J and the resulting integral equation is solved by numerical techniques. The particular probability density functions used in this analysis are discussed in detail in Appendix K and outlined in Figure 26.

A computer program was written to evaluate the integral and the resulting normalized autocorrelation function is shown in Figure 27. Although an absolute autocorrelation function is directly dependent on the probability density functions of the mean core size, $\bar{a}$, and the mean vortex strength, $\bar{v}_{\theta max}$, it will be shown in the sensitivity studies this normalized function shown in Figure 27 is relatively insensitive to the probability density functions used.

RMS Total Pressure Fluctuations: The mean square total pressure fluctuation is identical to the autocorrelation function at a time delay, τ, equal to zero. Thus,

$$\sigma^2 = \overline{\Delta P_T{}^2} = R_{\Delta P_T} (0) \tag{43}$$

For this case and using the assumed probability density functions (Figure 26) with h = (1/2)H (probe at center of the duct) and $\bar{a}/H \ll 1$ Equation 42 can be integrated in closed form to give

$$\frac{\overline{\Delta P_T{}^2}}{q_0{}^2} = \pi e n^2 \left(\frac{NH}{U_0}\right) \left(\frac{\bar{a}}{H}\right) \left(\frac{\bar{v}_{\theta max}}{U_0}\right) \frac{(m_a+2)}{(m_a+n_a+3)} \left[\frac{2(m_V+2)}{(m_V+n_V+3)}\right. \tag{44}$$

$$\left. + \frac{11e}{32} \frac{(m_V+2)}{(m_V+n_V+3)} \frac{(m_V+3)}{(m_V+n_V+4)} \frac{(m_V+4)}{(m_V+n_V+5)}\right]$$

The mean square level is later used to normalize the power spectral density function and utilized below to relate the velocity and total pressure fluctuations.

Relationship Between Velocity and Pressure Fluctuations: The flow model also provides a base from which other quantitative relationships can be developed. By application of the statistical techniques developed herein, the fluctuating velocity components defined by the isolated vortex, the auto and cross correlations of the unsteady velocity terms ($\overline{u^2}$, $\overline{v^2}$, $\overline{uv}$) can be obtained. The detailed development of these correlations are presented in Appendix L. Briefly, the mean square axial perturbation velocity in the center of the duct is:

$$\frac{\overline{u^2}}{U_0{}^2} = \frac{e\pi n^2}{2} \left(\frac{NH}{U_0}\right) \left(\frac{\bar{a}}{H}\right) \left(\frac{\bar{v}_{\theta max}}{U_0}\right) \frac{(m_a+2)}{(m_a+n_a+3)} \frac{(m_V+2)}{(m_V+n_V+3)} \tag{45}$$

47

NOTE: The probability density functions are given in Figure 26.
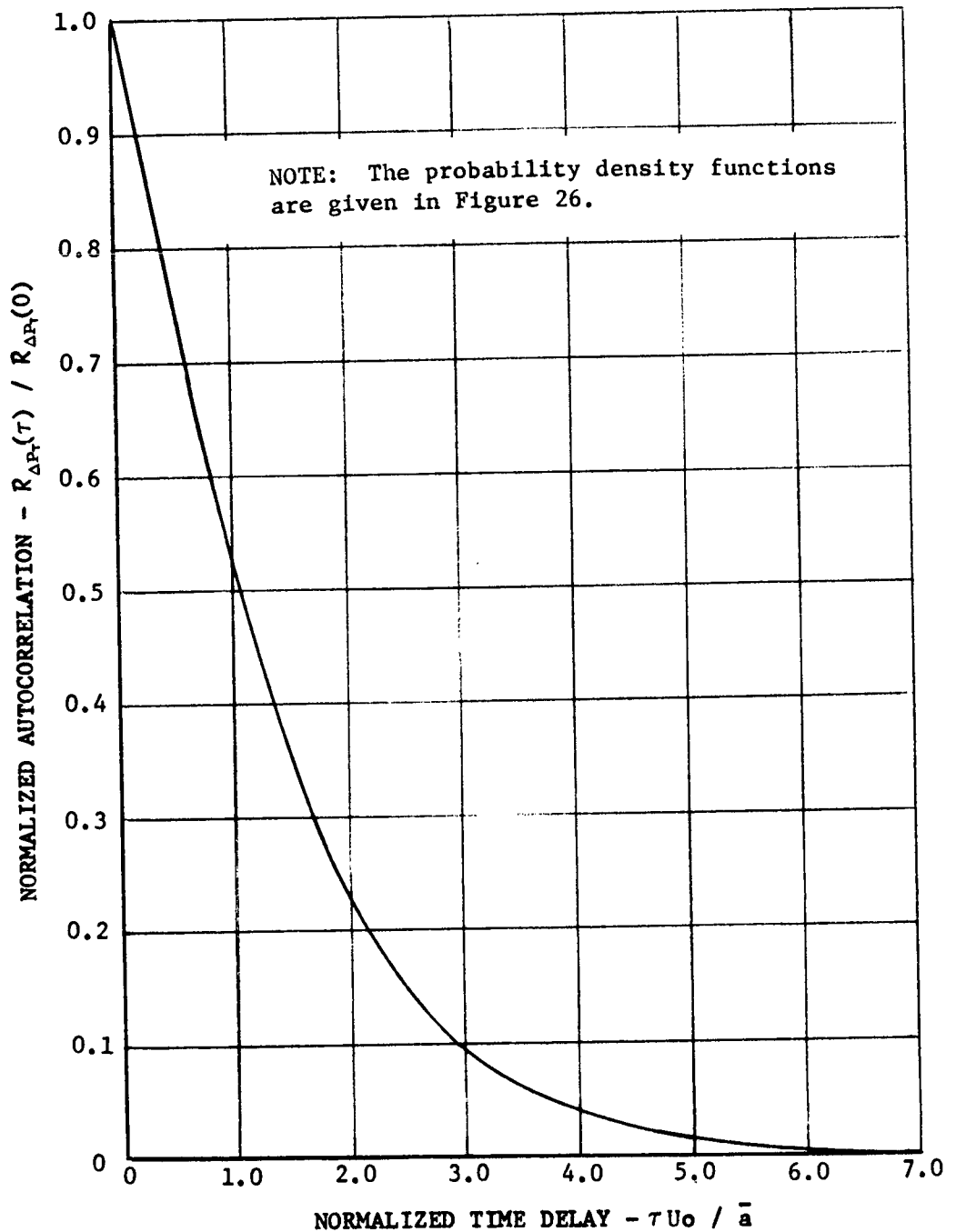
Figure 27. Autocorrelation Function Computed From The Turbulent Flow Model.

48

The relationship between the velocity fluctuations and the total pressure fluctuations in a turbulent flow field is obtained by combination of Equations 44 and 45. This is:

$$\frac{\overline{u^2}/U_0^2}{\overline{\Delta P_T^2}/q_0^2} = \frac{1}{4 + \frac{11e}{16} \frac{(m_V+3)}{(m_V+n_V+4)} \frac{(m_V+4)}{(m_V+n_V+5)}} \tag{46}$$

For the velocity probability density function having the exponents $m_V = 4$ and $n_V = 14$ (Refer to Figure 26 for the density functions) the ratio has a value of

$$\frac{\overline{u^2}/U_0^2}{\overline{\Delta P_T^2}/q_0^2} = 0.238 \tag{47}$$

It should be noted that for reasonable values of m_V and n_V, the numerical value of Equation 46 is weakly dependent upon these variables.

Equation 47 can be written in terms of the mean Mach number, M_0, and total pressure, $\overline{P}_T$, as follows and is shown graphically in Figure 28.

$$\frac{\overline{u^2}}{U_0^2} = 0.238 \frac{\overline{\Delta P_T^2}}{\overline{P_T}^2} \frac{2(1 + \frac{\gamma-1}{2} M^2)^{\frac{\gamma}{\gamma-1}}}{\gamma M^2}$$

This result, in itself, is significant. For the first time a relationship has been developed which will relate the fluctuating velocity as measured by hot wire anemometry with the total pressure fluctuations. Previously, the relationship was developed by assuming either sonic waves or a quasi-steady analysis with a constant static pressure, neither of which represented the physical process.

Power Spectral Density Function. - The power spectral density function is the Fourier Transform of the autocorrelation. Thus:

$$S_{\Delta P_T}(f) = \int_{-\infty}^{\infty} R_{\Delta P_T}(\tau) e^{-j 2\pi f \tau} d\tau \tag{48}$$

where: $S_{\Delta P_T}(f)$ = the complex power spectral density function,

$R_{\Delta P_T}(\tau)$ = the autocorrelation function.

49
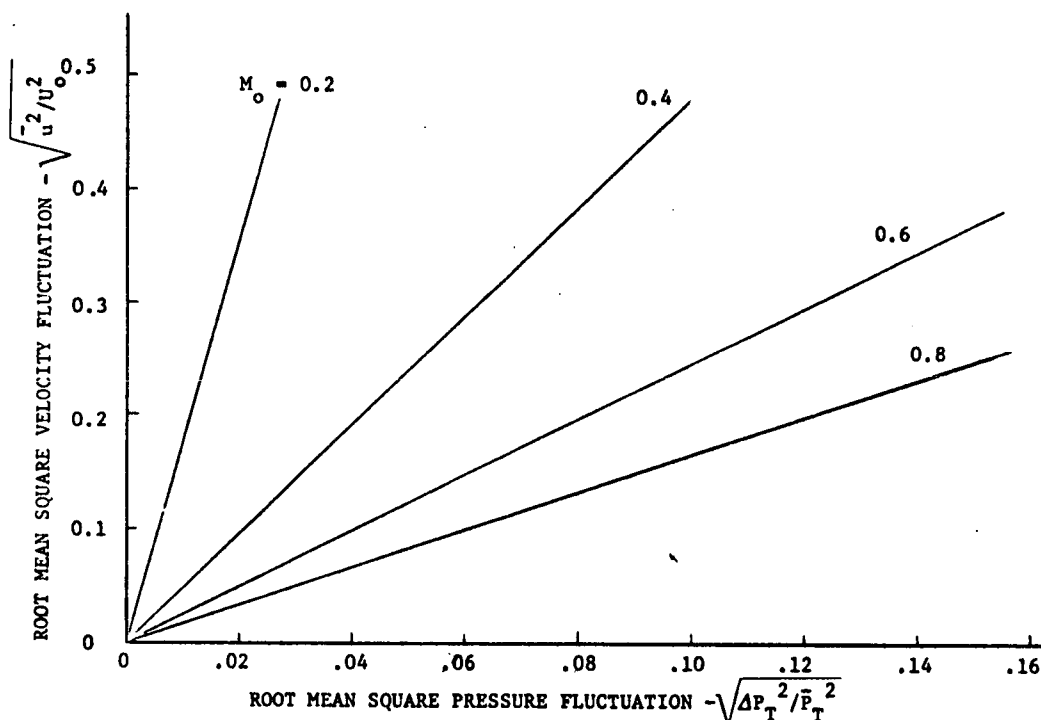
Figure 28. Relation Between Velocity and Pressure Turbulence.

Of immediate interest is the real part which is the physically realizable one-sided power spectral density function as normally obtained from test data. This function G (f) is defined (see, for example, Reference 11) as:

$$G_{\Delta P_T}(f) = 4 \int_0^\infty R_{\Delta P_T}(\tau)\cos(2\pi f\tau)d\tau \tag{49}$$

The normalized power spectral density function obtained from the autocorrelation function illustrated in Figure 27 is shown in Figure 29. The spectrum is normalized by the mean square total pressure fluctuations, σ^2, and the mean vortex core size, $\bar{a}$.

Sensitivity Studies

The effect of the assumed statistical distributions on the resultant autocorrelation and power spectral density functions must be determined since these distributions, in effect, describe the mean core size and mean strength. The level and frequency content of the power spectral density function is directly related to the mean vortex strength as measured by $\overline{V_{\Theta max}}/U_o$, the mean core size, $\bar{a}/H$, and the shape of their respective probability density curves. However, the normalized spectrum may not be sensitive to these variables, since it is normalized by the mean square of the pressure fluctuations and the mean core size. If this is the case, a great simplification in application will result. It is the specific objective of this section to establish this sensitivity.

While it was felt that the power spectral density function is primarily dependent on the strength and size of the vortices, the effects of spin direction, n, and probe location, Y/H, were also investigated. The effects of these variables on the power spectrum were found to be negligible.

50

10.0

NORMALIZED POWER SPECTRAL DENSITY - $\frac{G_{\Delta P_L}(f)}{\sigma^2}(\bar{a}/U_o)$

1.0

NOTE: The probability density functions
are given in Figure 26.

0.1

0.01

.001   0.01   0.1   1.0   10.0

NORMALIZED FREQUENCY - $f\ \bar{a}/U_o$
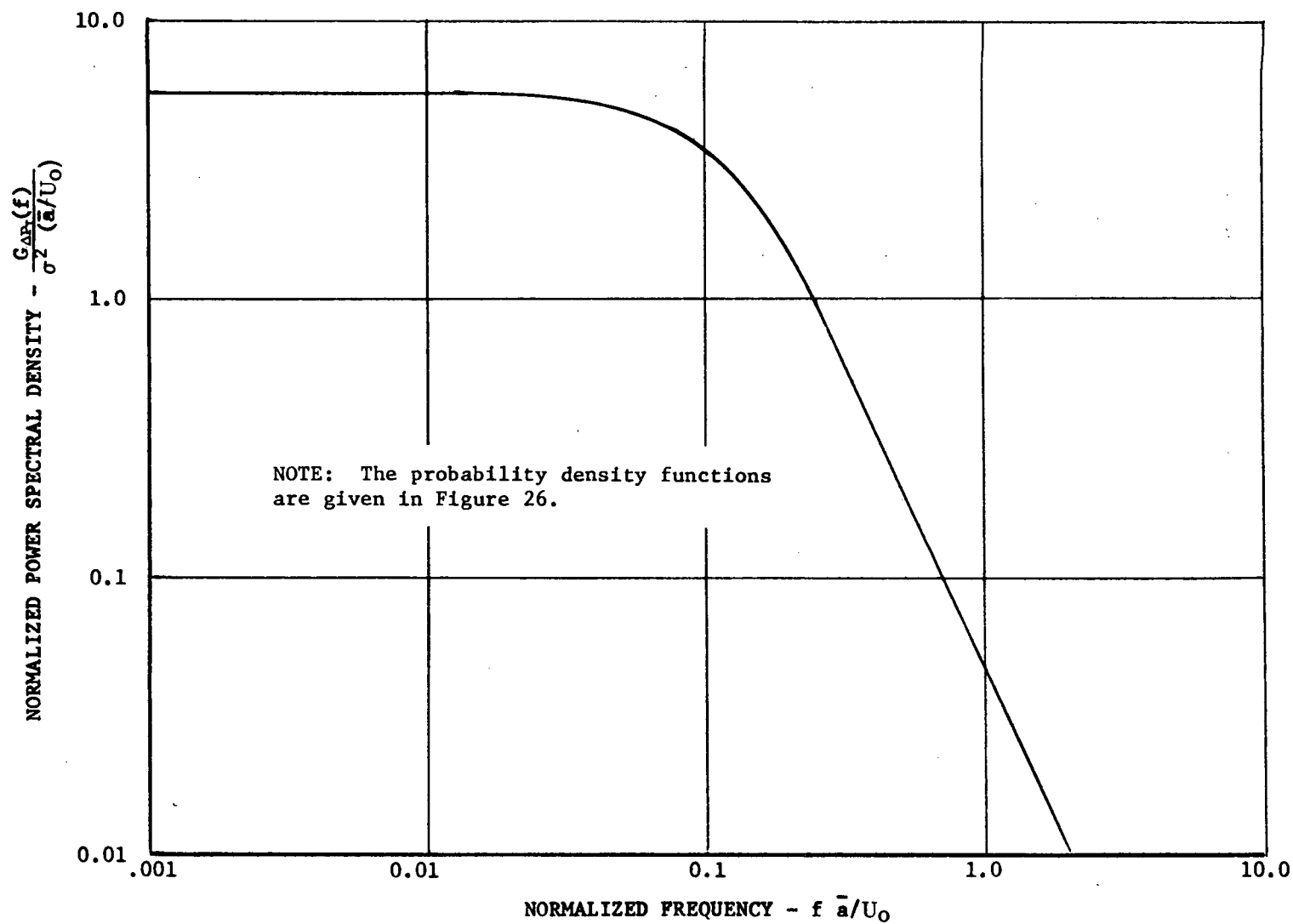
Figure 29. Normalized Power Spectral Density.

In the turbulent flow model, the vortex strength is represented by the maximum tangential velocity. The distribution of vortices having various strengths is governed by a Beta probability density function given in Equation 50:

$$P(v_{\theta_{max}}) = \frac{k_v}{U_o} \left(\frac{v_{\theta_{max}}}{U_o} \right)^{m_v} \left(1 - \frac{v_{\theta_{max}}}{U_o} \right)^{n_v} \tag{50}$$

where

$$\frac{\overline{v_{\theta_{max}}}}{U_o} = \frac{m_v + 1}{m_v + n_v + 2} \quad \text{and} \quad K_v = \frac{\Gamma(m_v + n_v + 2)}{\Gamma(m_v + 1)\ \Gamma(n_v + 1)}$$

The shape of this density function can be altered by changing the constants m_v and n_v as illustrated in Figure 30. The effect of such changes serve only to modify the mean square value of the fluctuating pressures and do not affect the shape of the normalized autocorrelation or power spectral density function as shown in Figure 31.
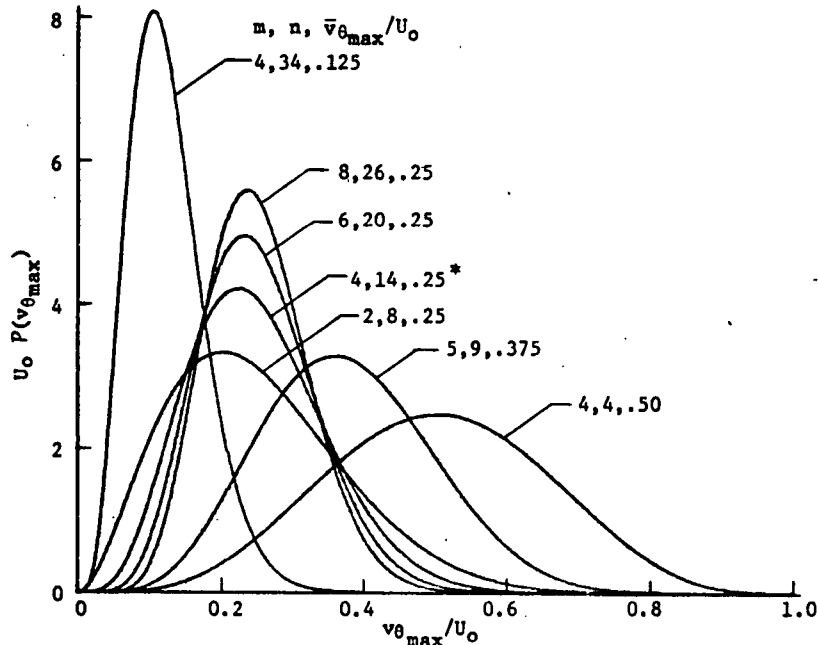
Figure 30. **Probability Density Function of Vortex Strength.**

The distribution of vortices having various core sizes is also described by a Beta probability density function as given by Equation 51:

$$P(a) = \frac{k_a}{H} \left(\frac{a}{H} \right)^{m_a} \left(1 - \frac{a}{H} \right)^{n_a} \tag{51}$$

where

$$\frac{\overline{a}}{H} = \frac{m_a + 1}{m_a + n_a + 2} \qquad K_a = \frac{\Gamma(m_a + n_a + 2)}{\Gamma(m_a + 1)\ \Gamma(n_a + 1)}$$
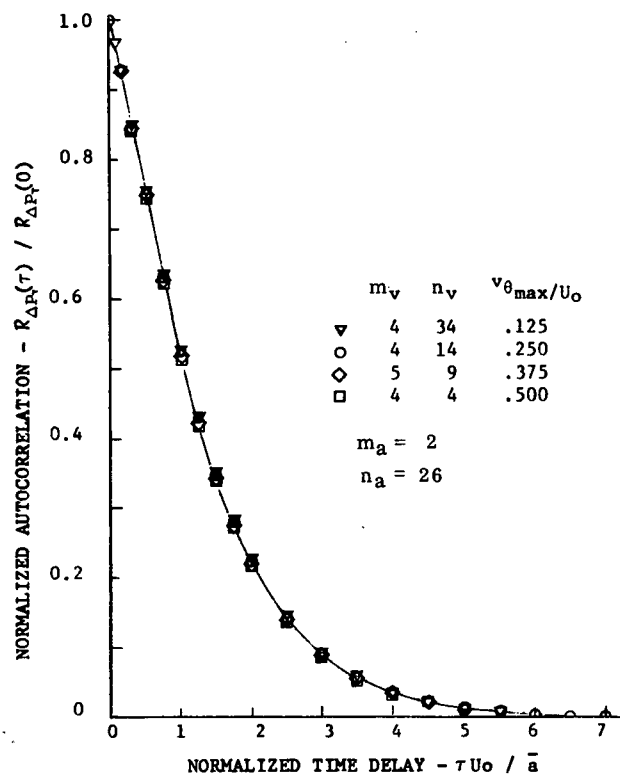
Figure 31 (a). The Effect of Velocity Density Function on the Autocovariance Function
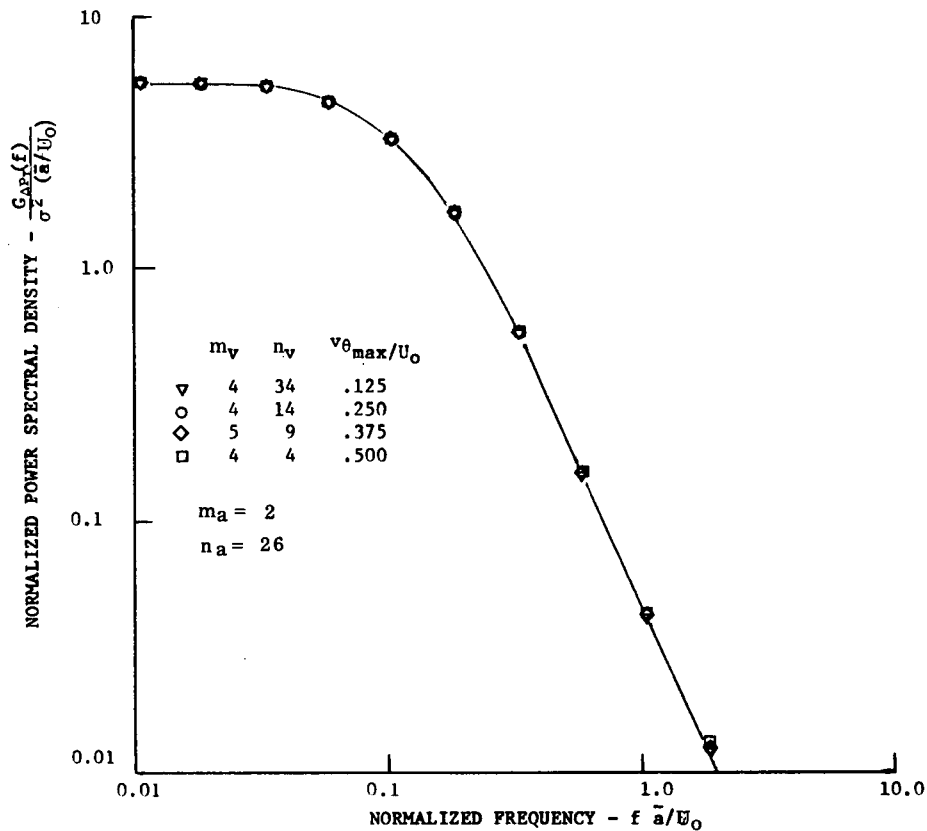
Figure 31 (b). The Effect of Vortex Velocity Density Function on the Normalized Power Spectrum.

Variations in shape of this function have some impact on both the amplitude of turbulence and the autocorrelations and power spectral density functions. Several variations used in the sensitivity study are shown in Figure 32. An example of the effect of these variations on the autocorrelation and power spectral density function is shown in Figure 33.
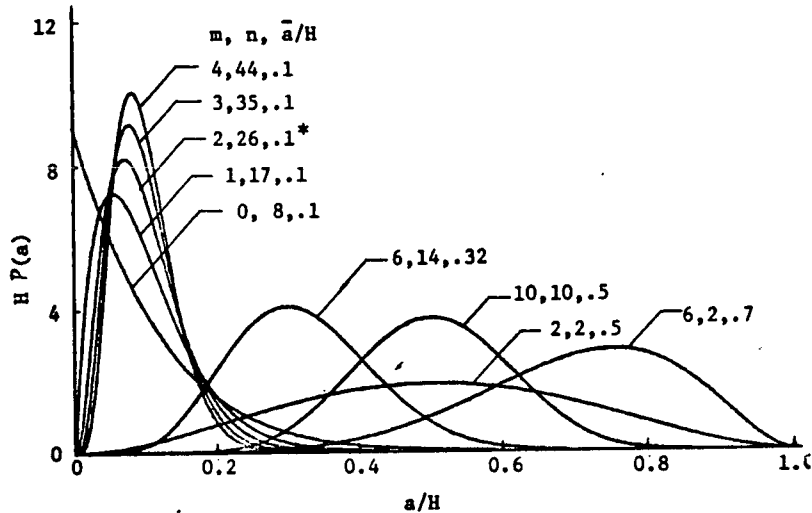
Figure 32.·Probability Density Function of Core Size.

As illustrated in Figures 31(b) and 33(b), the normalized power spectral density function is independent of the mean value of the vortex strength $v_{\theta max}$ and the shape of its probability density function and only weakly dependent upon the mean vortex core size $\bar{a}$ and its probability density function. If these latter variations are ignored for the moment, it is apparent that this normalized spectrum along with particular values of the mean core size $\bar{a}$ and the mean square of the pressure fluctuations σ^2 can be used to calculate an absolute PSD function $(G_{\Delta \bar{P}_T}(f)$ as a function of f).Furthermore, if the power spectrum is normalized by σ^2, the resulting absolute spectrum is only a function of $\bar{a}$.

The importance of this result lies in the fact that the analytical spectrum can be easily matched to experimental data using only the normalized spectrum and the mean core size $\bar{a}$. As an example of this concept the analytical model was matched to the turbulence data from an axisymmetric mixed compression inlet presented in Reference 12. The procedure for determining the mean core size associated with this particular spectrum is given below and illustrated in Figure 34.

1) Normalize the measured power spectral density function by the mean square of the turbulence (σ^2).

2) Compute an absolute spectra $(G_{\Delta \bar{P}_T}(f)/\sigma^2)$ from the normalized spectrum obtained from the analysis by assuming various values of the mean core size, $\bar{a}$, and using the local velocity, U_o.
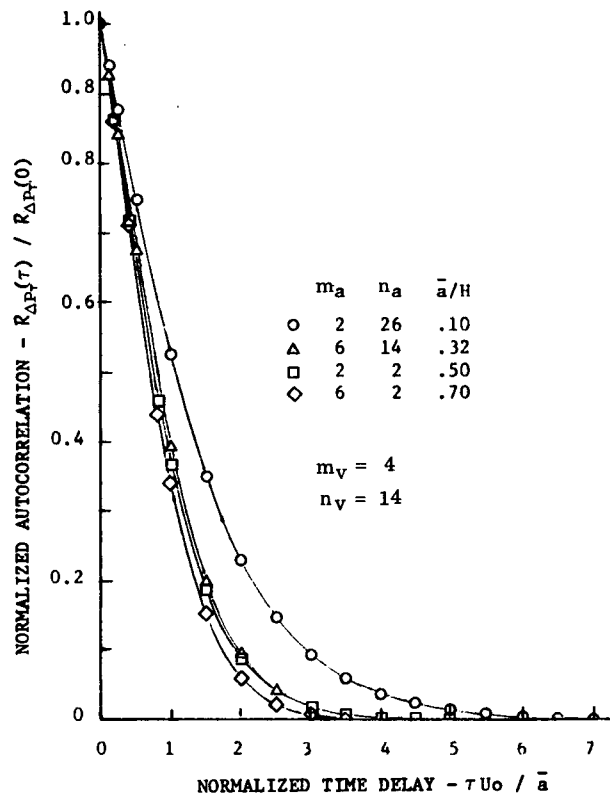
Figure 33(a). The Effect of Vortex Core Size Density Function on the Auto-covariance Function.
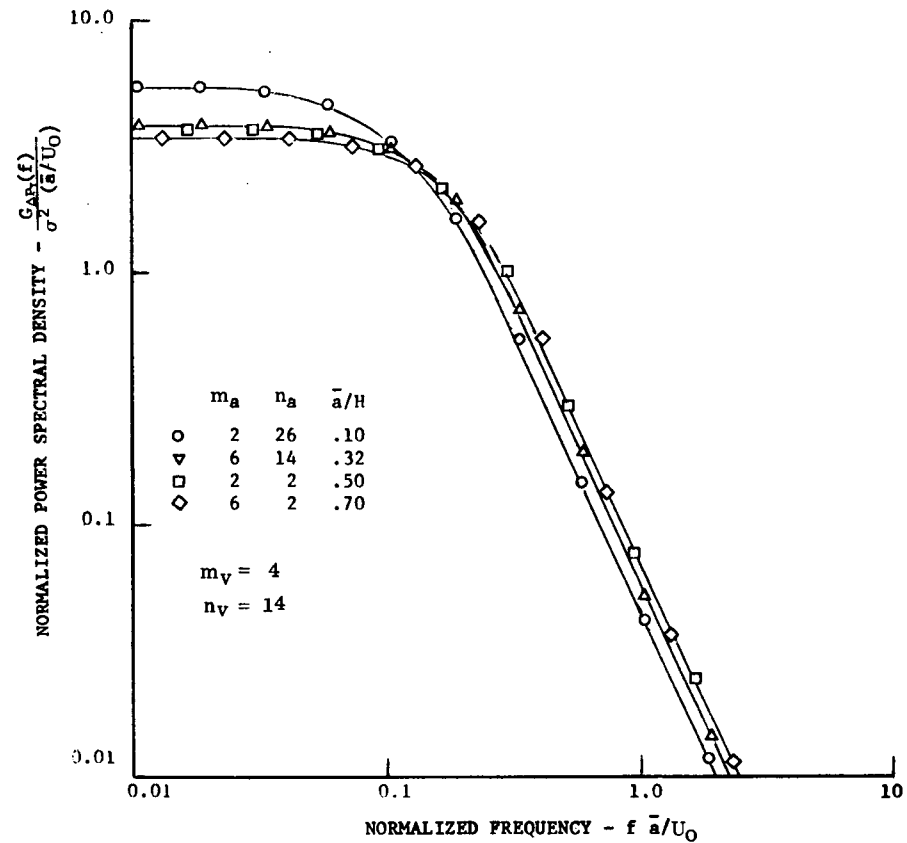
Figure 33(b). The Effect of Vortex Core Size Density Function on the Normalized Power Spectrum.

3) Compare the computed spectra with that obtained experimentally. The mean core size producing the best fit with the data corresponds the characteristic mean core size for the particular flow conditions.

As shown in Figure 34, the mean vortex core size producing the best fit under the constraints of both the shape of the spectrum and the area under the spectrum (σ^2) is 2.1 centimeters. The comparison shown yields excellent agreement. Additional examples of test/analysis comparison will be discussed in the "Data/Analysis Comparison" section.

As previously indicated and illustrated in Figure 33(b) the mean core size and shape of its probability density function have a small effect on the normalized power spectral density function. Therefore, depending upon the particular spectrum used, this frequency shift in the normalized spectrum will result in variations in the mean core size, $\bar{a}$, obtained from the analytical model when it is matched to experimental data. As a measure of the sensitivity of the computed mean core size to the assumed probability density function, the computations summarized in Table V were made. It was assumed that the test data was represented by the normalized power spectrum with the core size and maximum velocity probability density functions corresponding to $m_a = 2$, $n_a = 26$, and $m_v = 4$, $n_v = 14$, respectively. This result is indicated by the asterisk in Table V and shown in Figure 32. The frequency shift of the other normalized spectra, caused by other assumed density functions, will thus cause a false indication in actual mean core size. This error is given in Table V as $\Delta\bar{a}/\bar{a}^*$. As shown the maximum error is 25% and occurs for assumed probability density functions yielding large values of $\bar{a}/H$. For data indicating mean core sizes greater than 30% it may be necessary to choose coefficients that give consistent values of core size. This would require iteration. However, it is felt that typical values of core size will be less than 30%, in which case the error will be small and hence iterations will not be necessary.

Results of this sensitivity study indicate that for turbulent flow with $\bar{a}/H < 0.30$ the probability density functions of core size and maximum velocity have only small impact on the overall turbulent flow model itself. This is important to the use of the model eliminating two degrees of freedom that might ordinarily have to be taken into account.
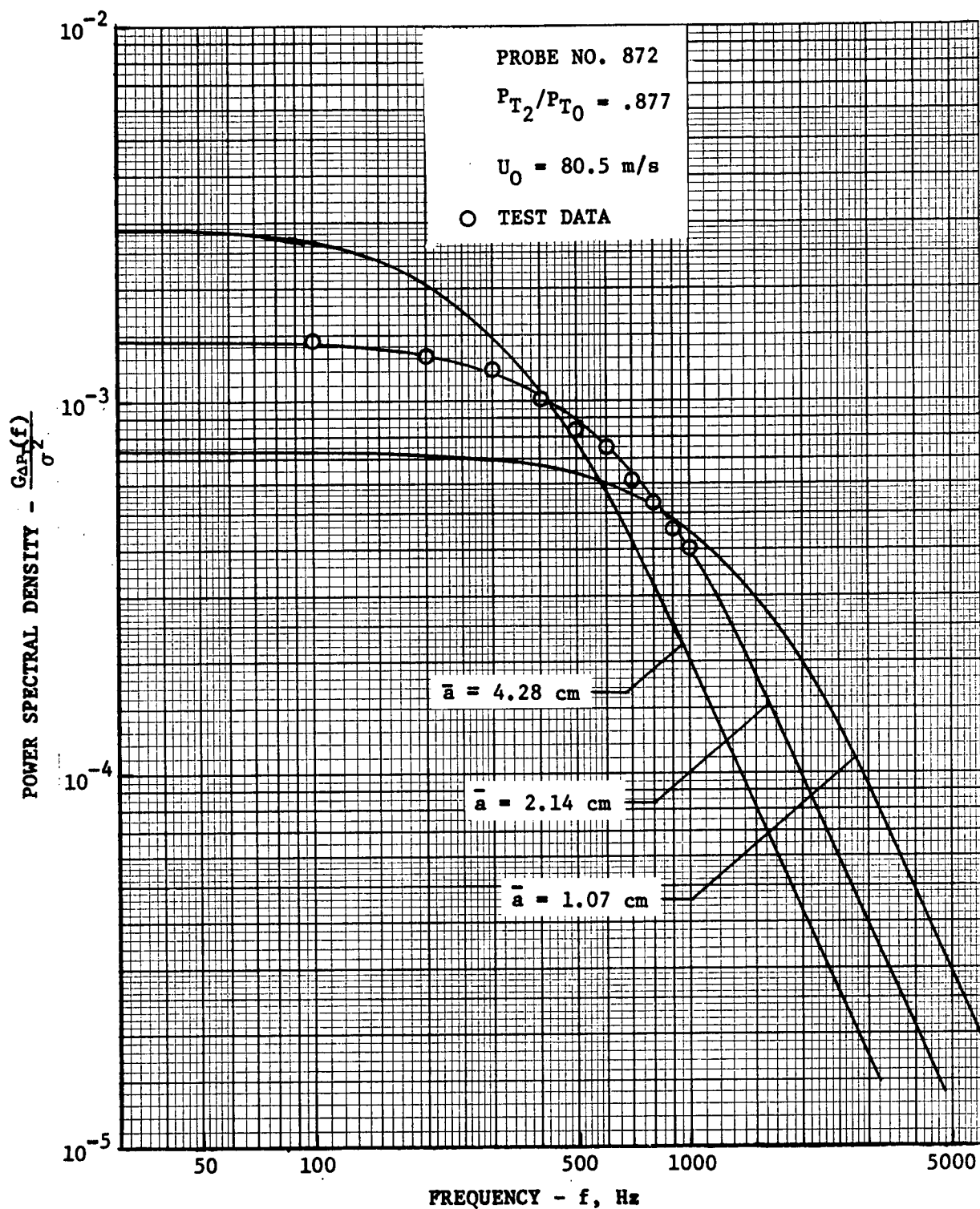
Figure 34. Comparison of Spectra Computed from the Flow Model with Inlet Test Data of Martin (Reference 12).

TABLE V
IMPACT OF ASSUMED DISTRIBUTIONS ON POWER SPECTRUM

m_a	n_a	$\bar{a}/H$	m_v	n_v	$\bar{v}_{\theta\,max}/U_o$	$\Delta\bar{a}/\bar{a}*$
2	26	.100	2	8	.250	0
2	26	.100	6	20	.250	0
2	26	.100	8	26	.250	0
0	8	.100	4	14	.250	-.14
1	17	.100	4	14	.250	-.06
*2	26	.100	4	14	.250	0
3	35	.100	4	14	.250	.025
4	44	.100	4	14	.250	.055
2	2	.500	4	14	.250	.245
6	2	.700	4	14	.250	.173
6	14	.318	4	14	.250	.145
2	26	.100	4	34	.125	-.003
2	26	.100	5	9	.375	.021
2	26	.100	4	4	.500	.056
10	10	.500	4	14	.250	.146
20	20	.500	4	14	.250	.145

Scaling Law For Turbulent Flow

Inlet development universally begins with subscale testing. These test results are then extrapolated to full scale to establish the expected inlet performance. The technique to scale turbulence has, however, not yet been defined, although dimensional analyses suggest that the power spectrum will shift in frequency in inverse proportion to the actual scale size.

The scaling techniques have not been defined because of the complex nature of random, unsteady flow. "Ever since the derivation of the momentum equation, the fundamental problem of the analysis of turbulent flow has been that of closing the system of governing equations. This is caused by the fact that even in its simplest form the turbulent flow momentum equation contains a "Reynolds stress" term made up of a correlation of the fluctuating components of the turbulent velocity field which acts as an apparent stress. Since the momentum equation is the governing equation for the mean velocity field, the presence of this apparent stress term introduces additional unknowns into the problem, and any equation derived without further assumptions to characterize these unknown quantities will in turn introduce other unknown quantities. One method of closing the system of equations is to formulate models for the turbulent shear stress in terms of already known (or knowable) quantities" (Reference 20). This formulation of models has classically been handled in one of two ways--either some model can be postulated for the turbulent shear stress itself, or, in analogy to a laminar flow, the turbulent shear stress can be assumed to be given by some effective viscosity multiplied by a local velocity gradient.

An attempt to develop a third, perhaps more fundamental model, was made by use of the fluid dynamic model of turbulent flow developed in this program. The model was used to define the "Reynolds stresses" in terms of the mean turbulent flow properties, providing a third model for the shear stress.

This development is outlined in Part A below. The resultant set of Equations could not, however, be solved for an arbitrary inlet flow profile within the scope of the planned effort. Nonetheless, a specialized case is given in Part B which may give some indication of the method of scaling the turbulence power spectrum.

A. General Development: The longitudinal velocity is assumed to be dominant in the following development and the flow velocity and static pressure is defined in terms of a fixed value plus the perturbation value as indicated below:

$$U = U_0 + \bar{u}$$
$$V = 0 + \bar{v}$$
$$P = p_0 + \overline{\Delta p}$$

(52)

The initial velocity distribution in the x-direction serves as a boundary condition. This distribution is shown sketched below:
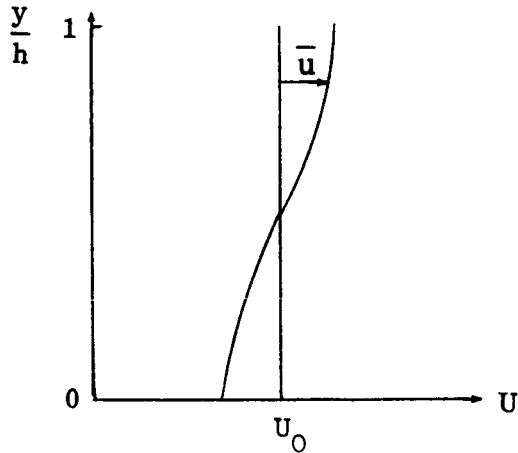
Utilizing the notation defined above the following ten Equations can be identified.

Momentum:

$$U_0 \frac{\partial \overline{u}}{\partial x} + \overline{v} \frac{\partial \overline{u}}{\partial y} = \frac{-1}{\rho} \frac{\partial \overline{\Delta p}}{\partial x} - \frac{\partial \overline{u^2}}{\partial x} - \frac{\partial \overline{uv}}{\partial y} \tag{53}$$

$$U_0 \frac{\partial \overline{v}}{\partial x} + \overline{v} \frac{\partial \overline{v}}{\partial y} = \frac{-1}{\rho} \frac{\partial \overline{\Delta p}}{\partial y} - \frac{\partial \overline{uv}}{\partial x} - \frac{\partial \overline{v^2}}{\partial y} \tag{54}$$

Continuity:

$$\frac{\partial \overline{u}}{\partial x} + \frac{\partial \overline{v}}{\partial y} = 0 \tag{55}$$

Crocco's Theorem: As applied to a velocity change caused by an entropy gradient in total pressure, Crocco's Theorem (See for example Reference 21, page 281) relates the total vorticity, $N\Gamma$, to the velocity gradient ΔU . This is: is:

$$N\Gamma = \int_h U du = \frac{U_{h2}^2 - U_{h1}^2}{2} \cong U_0 \Delta U \tag{56}$$

Fluid Flow Model: The remaining six equations are defined by use of the fluid flow model developed in this program. The alternative Equation numbers refer to their explicit definition as established elsewhere in this report.

60

$$\overline{u^2} = f(N, \overline{a}, \overline{v_{\theta_{max}}}) \tag{57}$$

$$\overline{v^2} = f(N, \overline{a}, \overline{v_{\theta_{max}}}) \tag{58}$$

$$\overline{uv} = f(N, \overline{a}, \overline{v_{\theta_{max}}}) \tag{59}$$

$$\overline{u} = f(n, N, \overline{a}, \overline{v_{\theta_{max}}}) \tag{60}$$

$$\overline{v} = f(n, N, \overline{a}, \overline{v_{\theta_{max}}}) \tag{61}$$

$$\Delta p = f(N, \overline{a}, \overline{v_{\theta_{max}}}) \tag{62}$$

Similarly, the following ten unknowns are identified:

$$\overline{u}, \overline{v}, \overline{\Delta p}, \overline{u^2}, \overline{v^2}, \overline{uv}, N, n, \overline{a}, \overline{v_{\theta_{max}}} \tag{63}$$

By solution of these ten equations, the unknowns $\overline{u^2}$ and $\overline{a}$ can be obtained as a function of the initial velocity (distortion) profile. These quantities are directly related to the total pressure RMS level and power spectrum as established by Equation 46 and the techniques leading to the spectrum of Figure 29. If it can be assumed that the inlet velocity (or total pressure) profile can be scaled, the techniques for scaling RMS level and power spectral density function will result.

Solution of these equations for an arbitrary distortion profile was beyond the scope of the planned program. However, some insight can be gained into scaling of the power spectrum by application to a specialized case.

B. Specialized Velocity Profile: Consider flow in a two dimensional duct that has a non-uniform total pressure and hence velocity profile. As established from fluid flow model, a gradient in velocity will occur if the vortices have a non-uniform distribution of direction of rotation, e.g., more vortices having a positive spin than negative spin. The general expression for this gradient is given by Equation L-13 in Appendix L.

$$\frac{\bar{u}}{U_0} = n \left(\frac{NH}{U_0}\right) (2\pi e)^{1/2} \frac{(m_v + 1)}{(m_v + n_v + 2)} \int_0^1 [e^{-\frac{1}{2}\left(\frac{h}{a}\right)^2} - e^{-\frac{1}{2}\left(\frac{H-h}{a}\right)^2}]$$

$$[K_a \left(\frac{a}{H}\right)^{m_a + 2} (1 - \frac{a}{H})^{n_a}] \, d\left(\frac{a}{H}\right) \qquad \text{L-13}$$

Equation L-13 can be integrated in closed form at the duct walls, h = 0 and h = H, by assuming $\bar{a}/H \ll 1$. This results in

$$\left.\frac{\bar{u}}{U_0}\right|_{h=H} = -n \left(\frac{NH}{U_0}\right) (2\pi e)^{1/2} \left(\frac{\overline{v_{\theta_{max}}}}{U_0}\right) \left(\frac{\bar{a}}{H}\right)^2 \qquad (64)$$

$$\left.\frac{\bar{u}}{U_0}\right|_{h=0} \quad n \left(\frac{NH}{U_0}\right) (2\pi e)^{1/2} \left(\frac{\overline{v_{\theta_{max}}}}{U_0}\right) \left(\frac{\bar{a}}{H}\right)^2 \qquad (65)$$

This will enable the maximum difference in velocity across the duct to be established. The total vorticity flux is dependent only on this difference and hence for the purposes of this example it is not nexessary to obtain the velocity profile between h = 0 and H, which would require numerical integration of Equation L-13. However, it is for this special case of interest that the scaling technique will be defined which is valid only for the velocity profile implied in Equation L-13.

The absolute value of vorticity passing between h = 0 and H can be computed by use of the flow model as in Appendix H. This flux of vorticity becomes:

$$N\Gamma = n \, 8\pi \, NH \, U_0 \, e^{-1/2} \left(\frac{\bar{a}}{H}\right) \left(\frac{\overline{v_{\theta_{max}}}}{U_0}\right) \qquad (66)$$

However, this flux is related to the change in velocity across the duct by Crocco's Theorem, Equation 56, which in turn is obtained by combining Equations 64, 65, and 66. By so doing it is found that $\bar{a}/H$ is a constant (within the confines of the velocity profile described by Equation L-13).

Since the power spectral density function is directly related to the mean vortex core size, this result specifies that increasing inlet size would shift the spectrum in inverse proportion to the inlet scale. This result would verify the present practice of scaling the frequency content of the turbulence power spectrum inversely with the inlet scale size. Again, this applies only to the specialized case.

Data/Analysis Comparison

The power spectral density functions of turbulent flow computed from this turbulent flow model were compared with data obtained from Reference 12 for a test of a .55 meter diameter, Mach 3 mixed compression axisymmetric inlet. The comparisons were performed to illustrate the technique of determining the mean turbulence scale size, verify the assumptions incorporated in the turbulent flow model, and to gain insight into production of turbulence by interpretation of test data through use of the model.

The experimentally determined power spectra used in the comparisons are shown in Figures 35 and 38. The mean core size of the turbulent flow was computed for these spectra by assuming a mean core size and comparing the test data with results of the turbulent flow model. These comparisons are shown in Figures 36 and 37 and Figures 39 through 44. Excellent agreement is obtained indicating the turbulent flow model accurately represents the real case and that the flow can be modeled by the assumption of random vortices with the indicated mean core size.

Data from probe number 900 (Figure 36), which is in the inlet duct extension, approximately 3-1/2 diameters downstream of the inlet diffuser exit (Figure 36) shows some disagreement with the analysis at the higher frequencies. However, if it is assumed that this scatter is created by turbulence from two separate sources each having a different mean core size, a composite spectrum can be constructed incorporating the two different mean core sizes. This composite spectrum is shown compared with data in Figure 45. Excellent agreement is obtained. This not only adds credence to the turbulent flow model but allows concrete interpretation of the power spectra. For example, it can be postulated that the source of the turbulence having the scale size of approximately $\bar{a} = 2.0$ cm. at the compressor face probe 872 may be produced by shock boundary layer interaction. This turbulence carries through to the inlet duct extension (probe 900) but is reduced in size to approximately $\bar{a} = 0.8$ cm., as indicated in the composite of Figure 45. However, a new source is identified by introducing of turbulence having the scale size of 2.9 cm. which may be attributed to the wakes generated by the centerbody support struts.

As a second, perhaps more significant example, consider the data of Figure 39 (Probe 872) in which case the total pressure recovery was 88% and the mean core size of the turbulent flow 2.14 cm. As the inlet is operated at increased supercritical margins (increased terminal shock strength) the power spectrum changes as shown by the data in Figure 44 for a recovery of 57%. A composite spectrum for this supercritical case was computed from the turbulent flow model and is shown in Figure 46. It indicates the flow is composed of eddies having a mean core size of 1.9 cm plus additional turbulence having a mean core size of 5.0 cm. This may be indicating large scale separation is occurring and the turbulence is not only increasing in strength but in size as well.

Comparison between the power spectrum as established from the analytical model and that obtained from test data shows exceptional agreement giving considerable credence to the development outlined herein. With this model the total pressure power spectrum and root mean square level of the total pressure

fluctuations take on considerable significance. It is specifically the strength and size of these low pressure regions, derived by application of the model, that are important in the inlet flow/engine interactions.
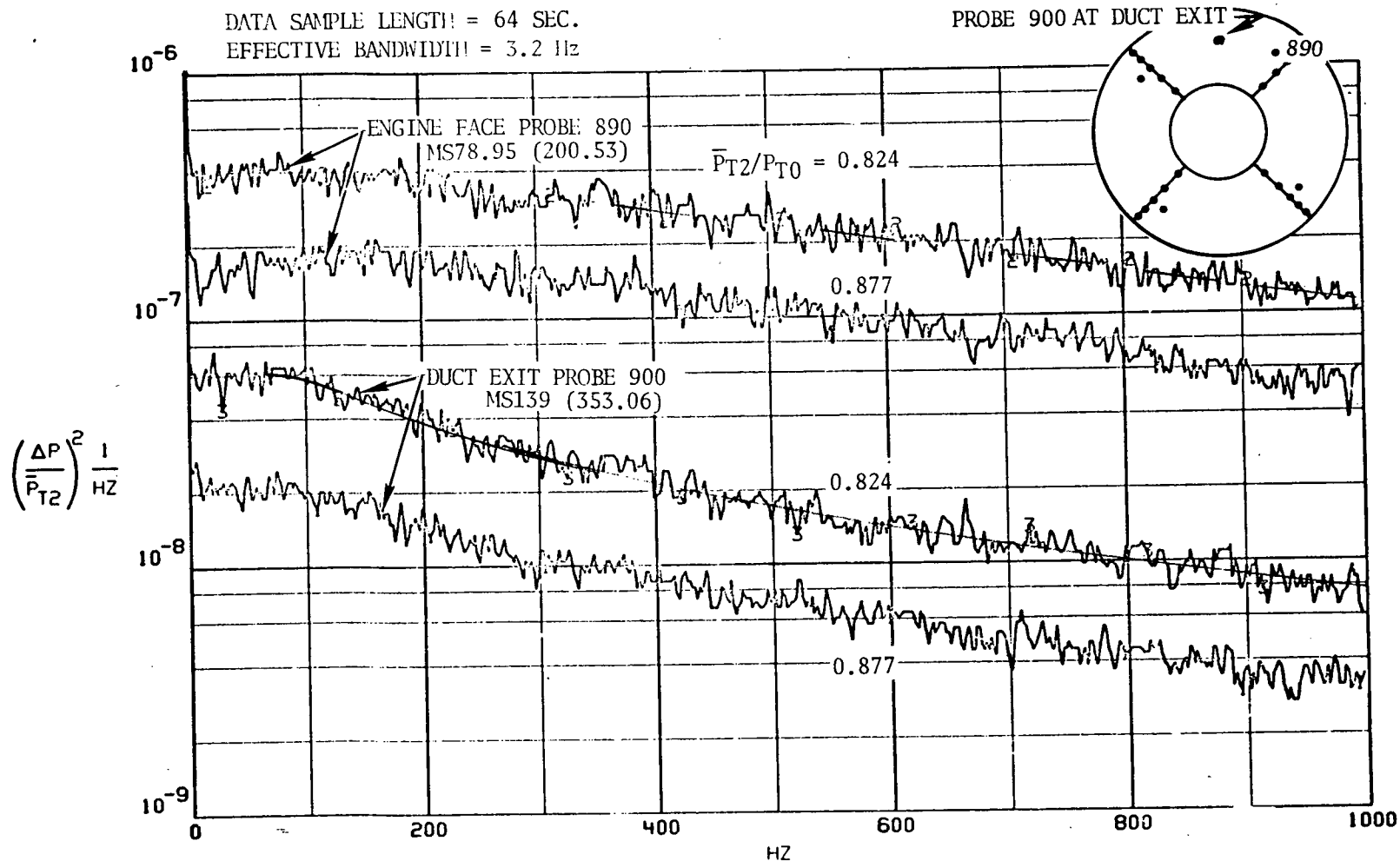
Figure 35 - Comparison of engine face and duct exit total pressure power spectral densities, $M_0 = 3.0$. (Reference 12)
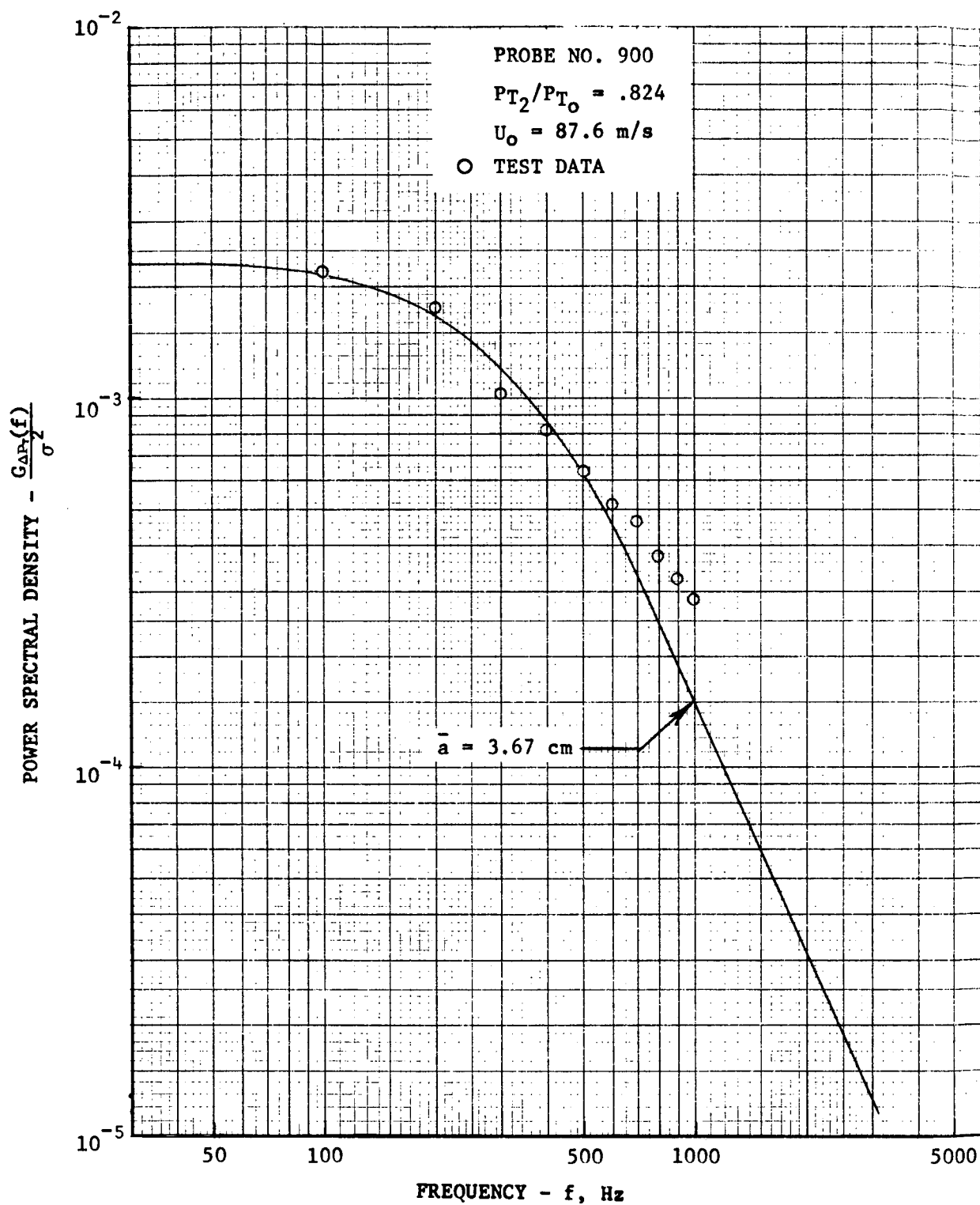
Figure 36.   Comparison of Spectra Computed from the Flow Model with
             Inlet Test Data of Martin (Reference 12).
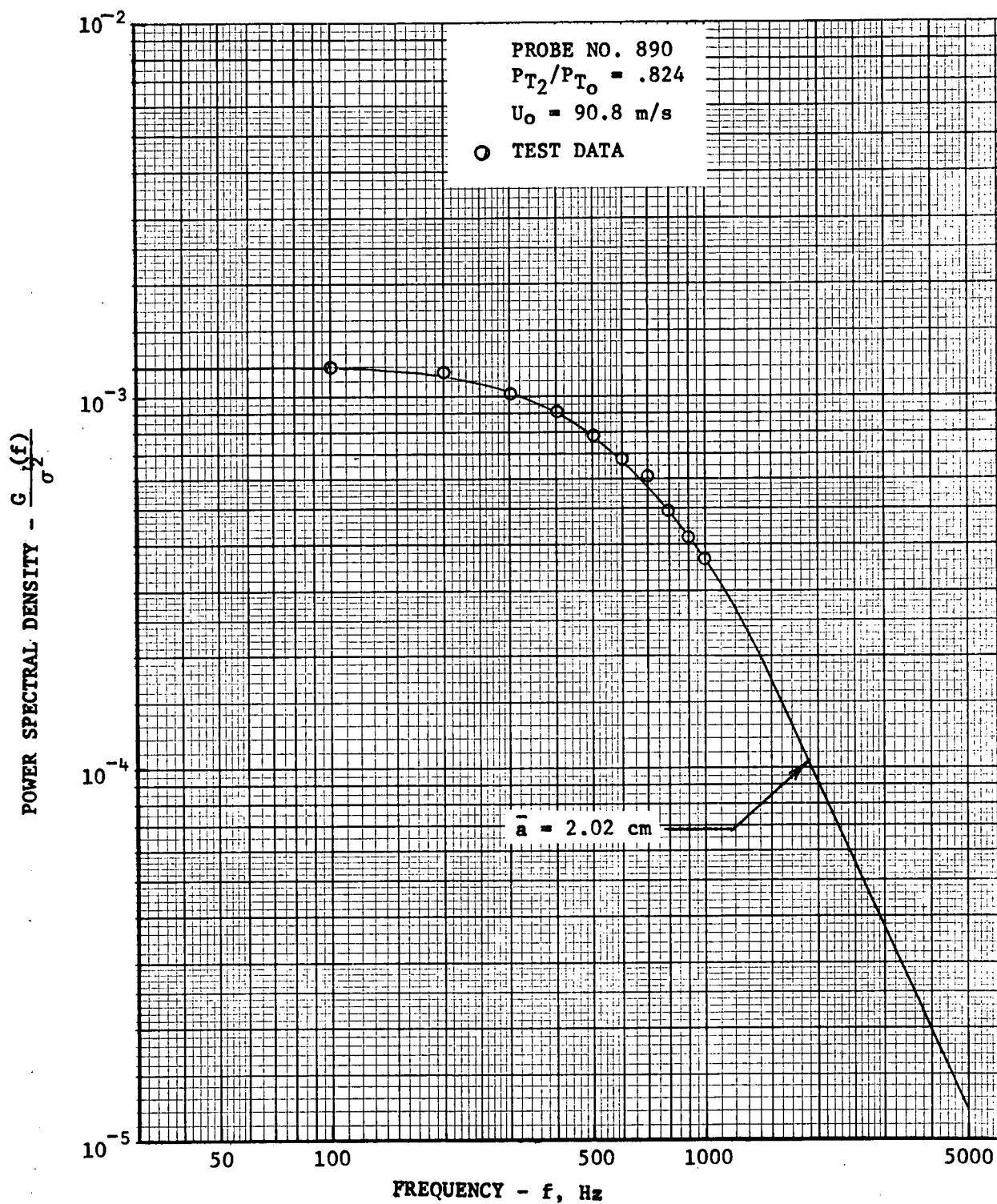
Figure 37. Comparison of Spectra Computed from the Flow Model with Inlet Test Data of Martin (Reference 12).

67
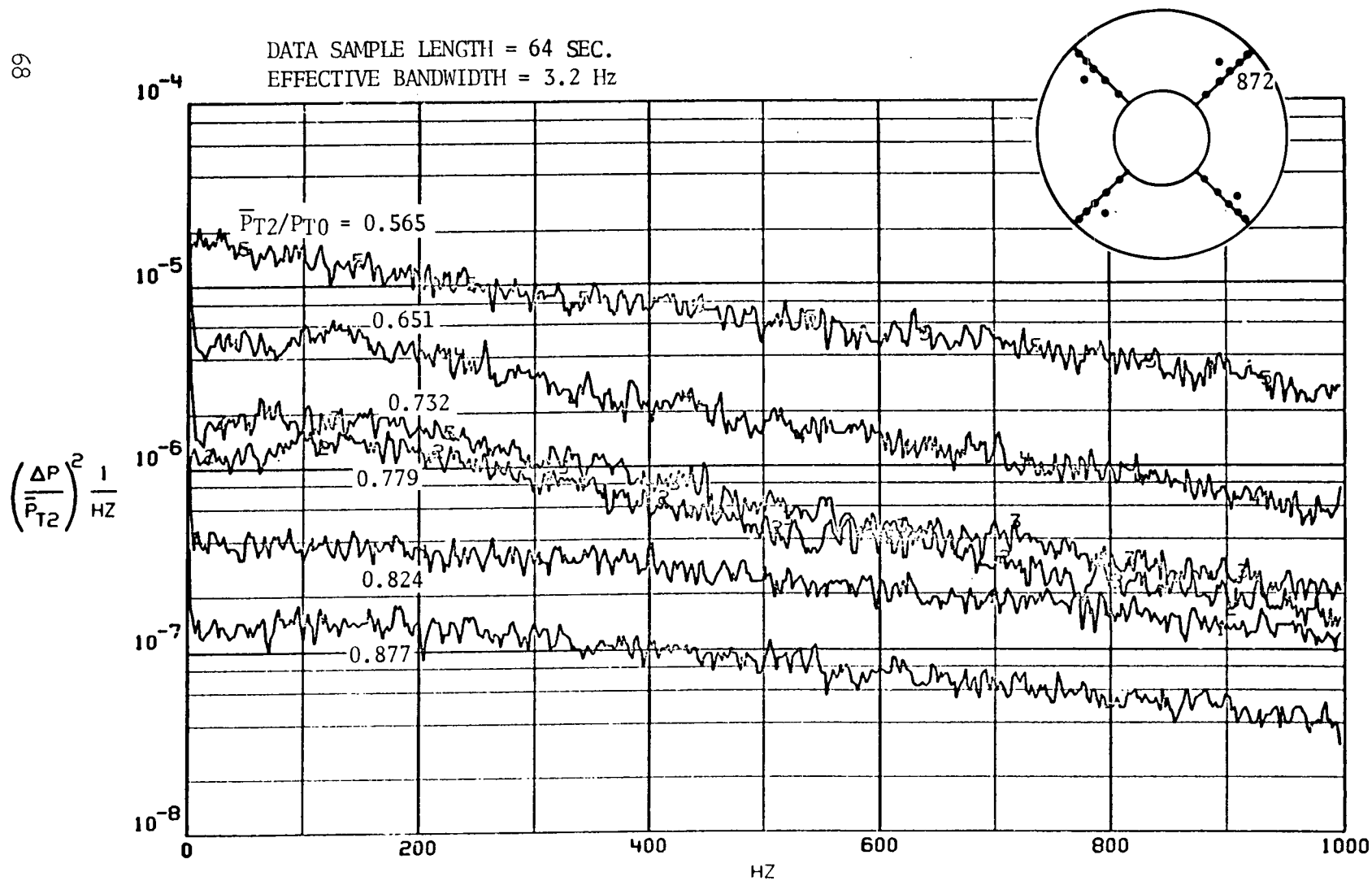
Figure 38. - Engine face total pressure power spectral density variation with recovery, probe 872, $M_O = 3.0.$ (Reference 12)
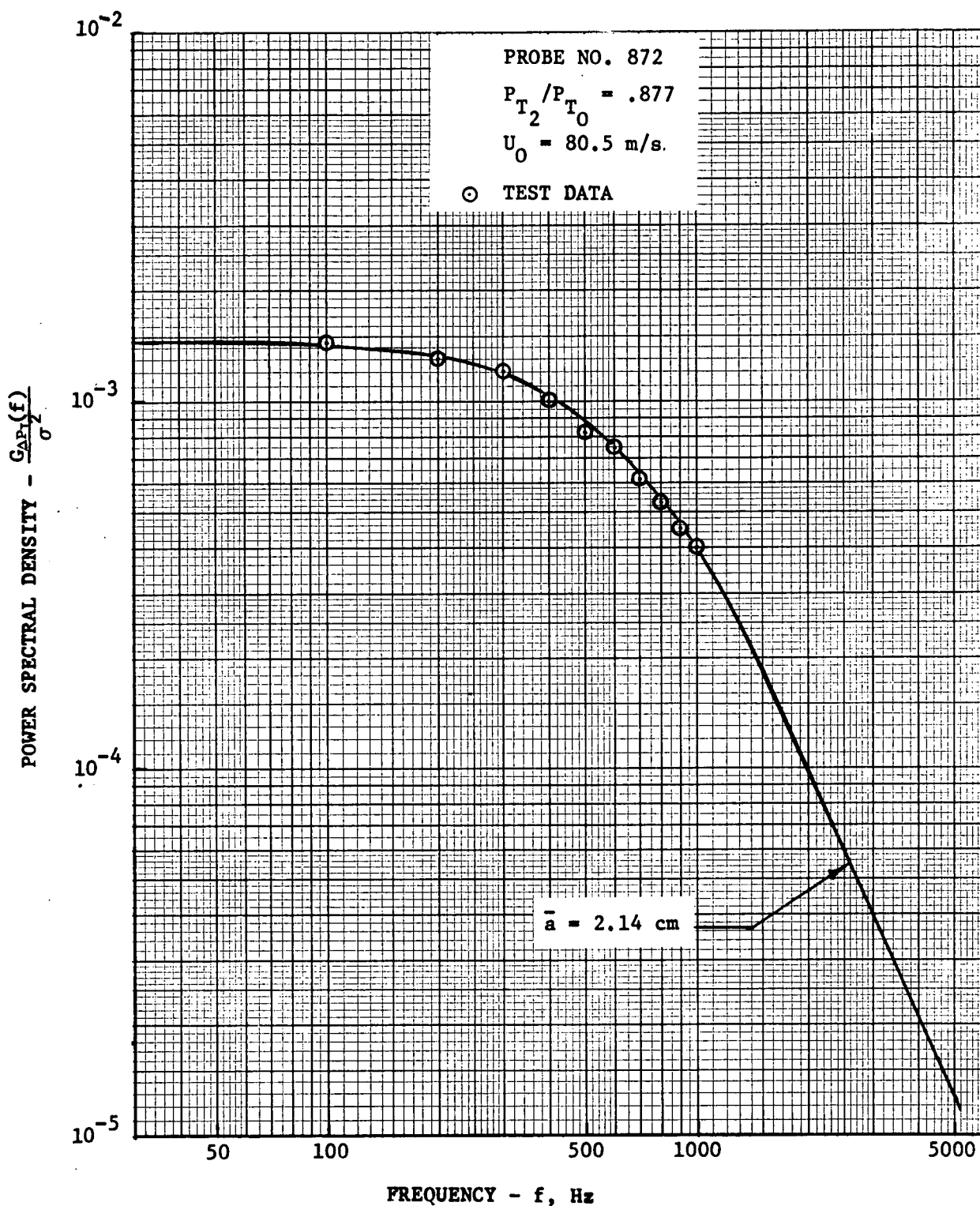
Figure 39. Comparison of Spectra Computed from the Flow Model with Inlet Test Data of Martin (Reference 12).

69
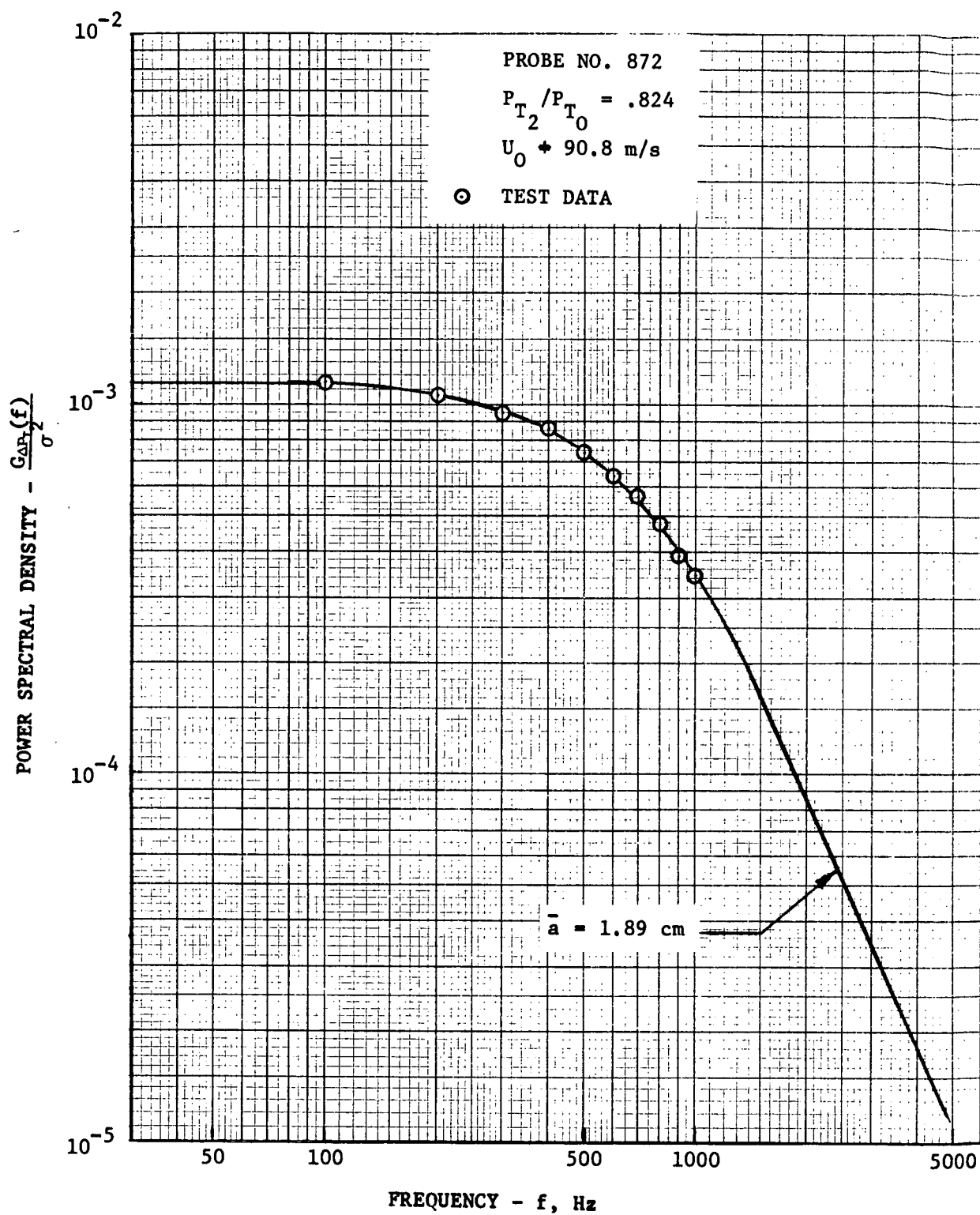
Figure 40. Comparison of Spectra Computed from the Flow Model with Inlet Test Data of Martin (Reference 12).
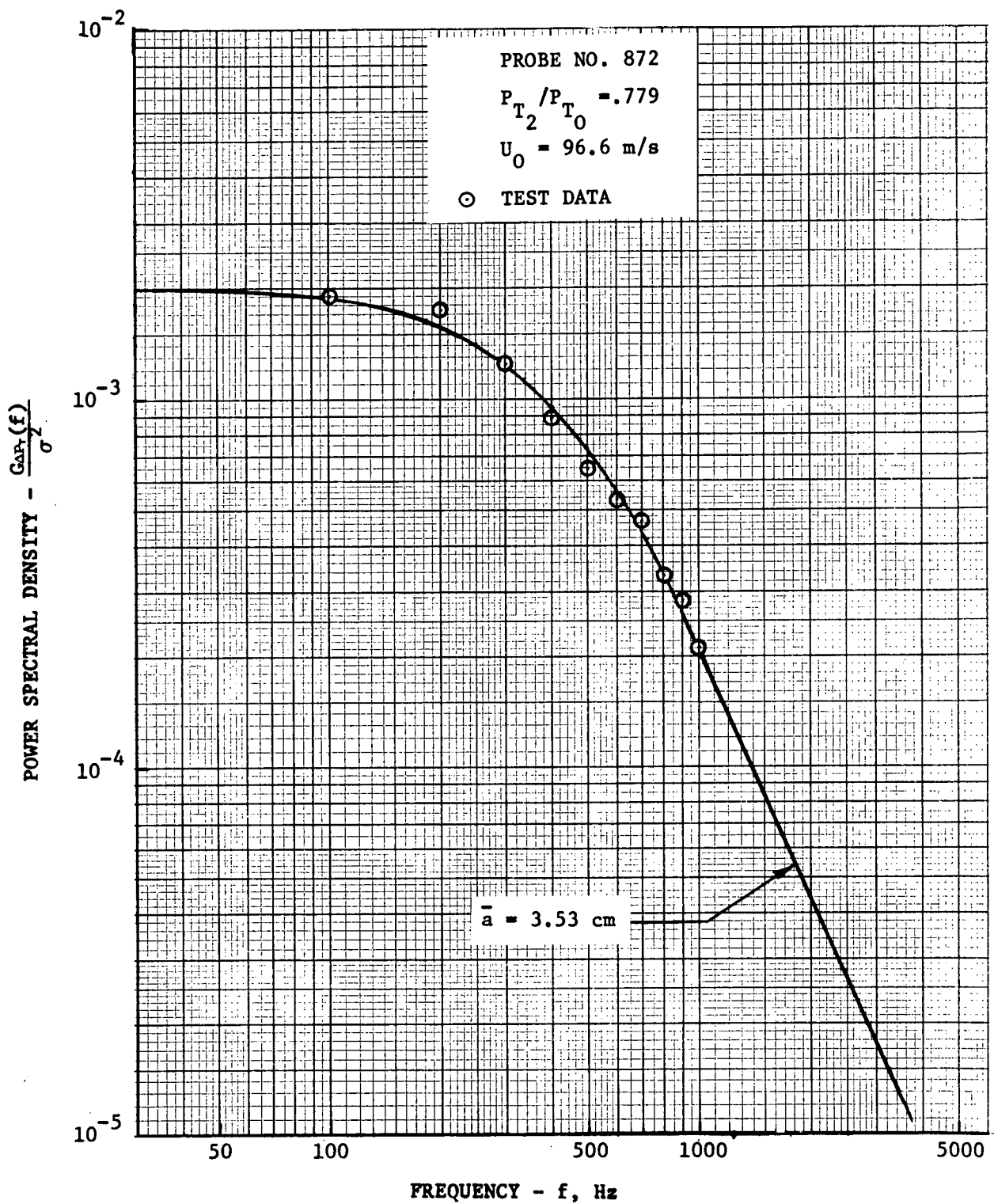
Figure 41. Comparison of Spectra Computed from the Flow Model with Inlet Test Data of Martin (Reference 12).

71
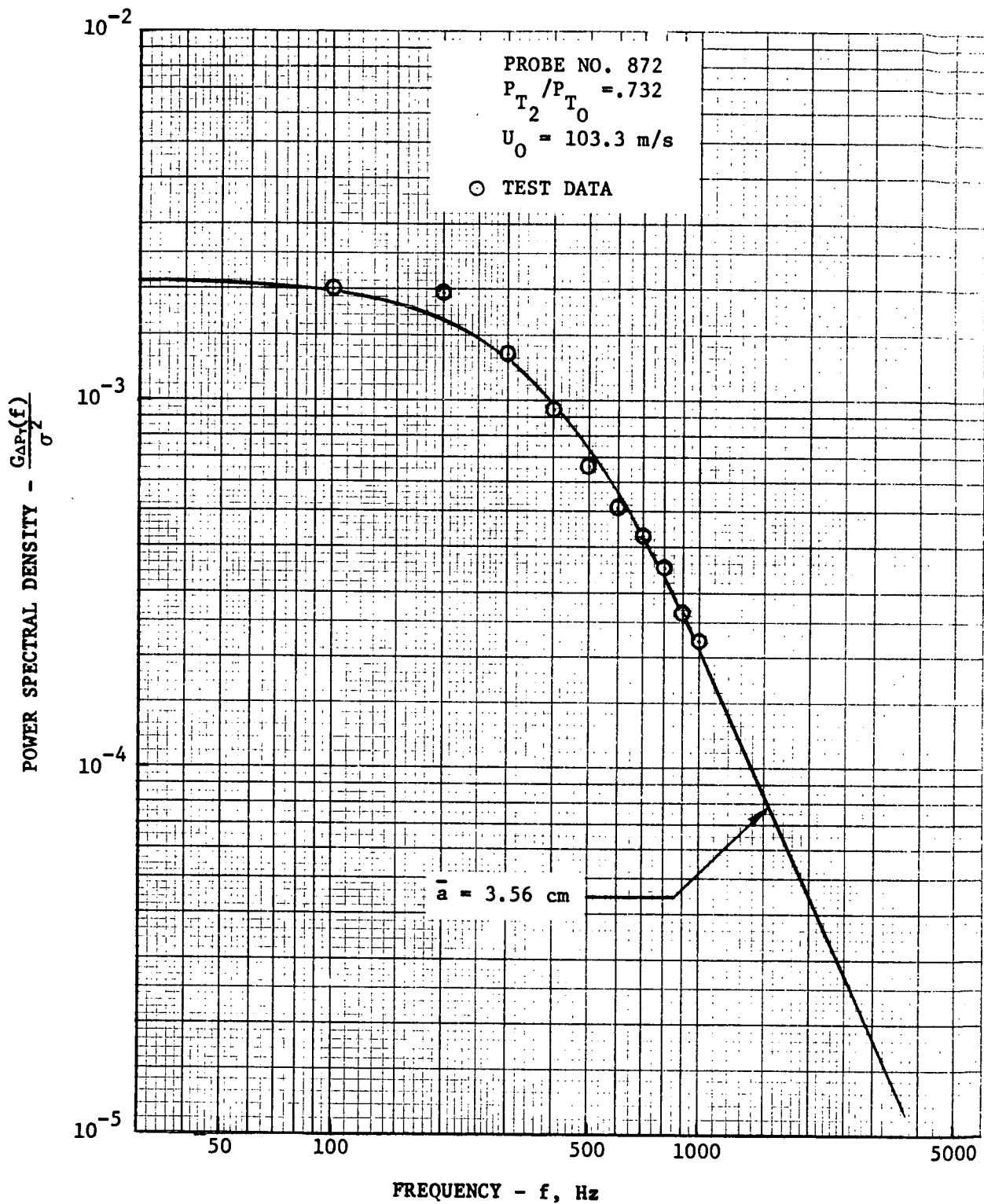
Figure 42. Comparison of Spectra Computed from the Flow Model with Inlet Test Data of Martin (Reference 12).
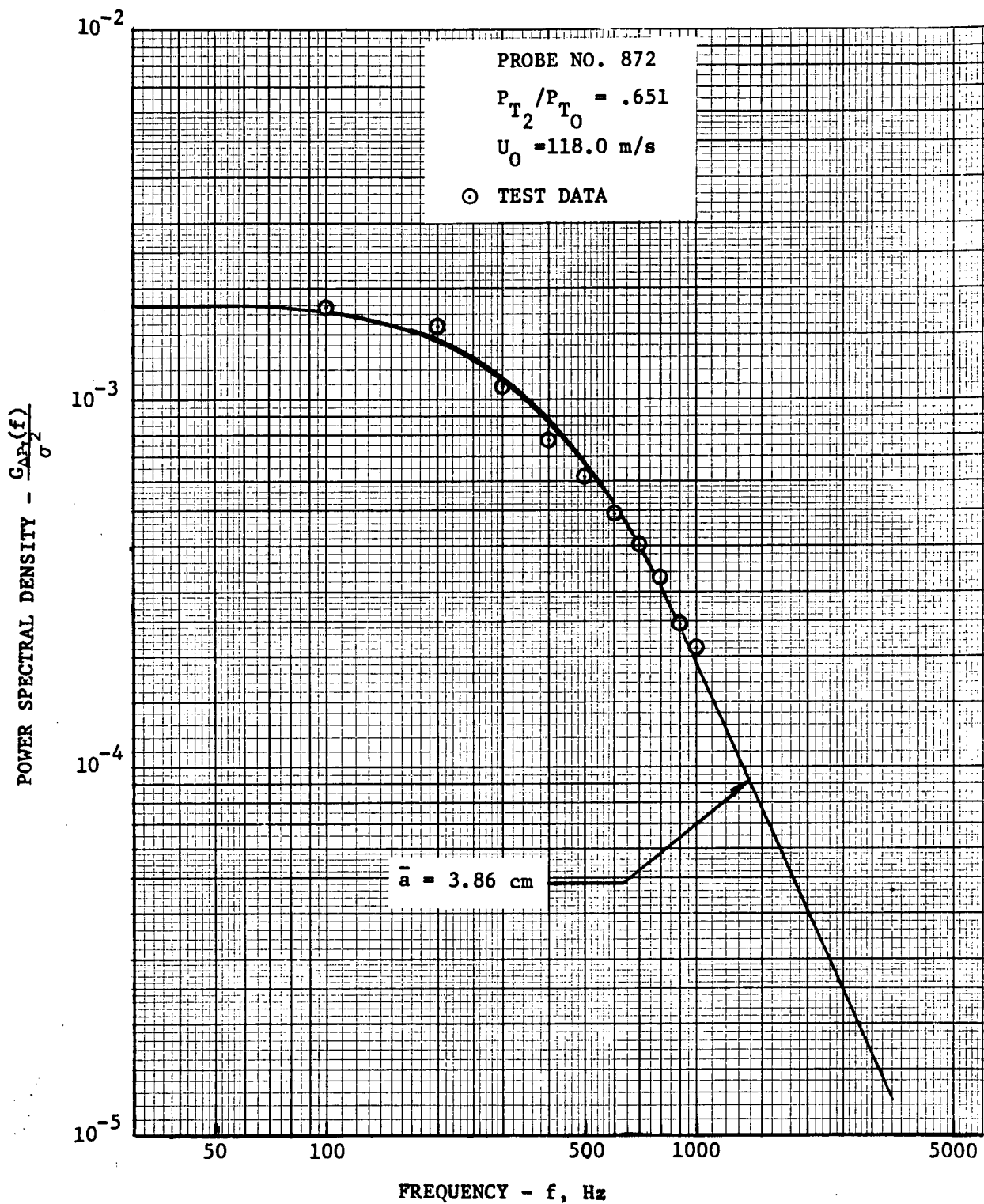
Figure 43. Comparison of Spectra Computed from the Flow Model with Inlet Test Data of Martin (Reference 12).
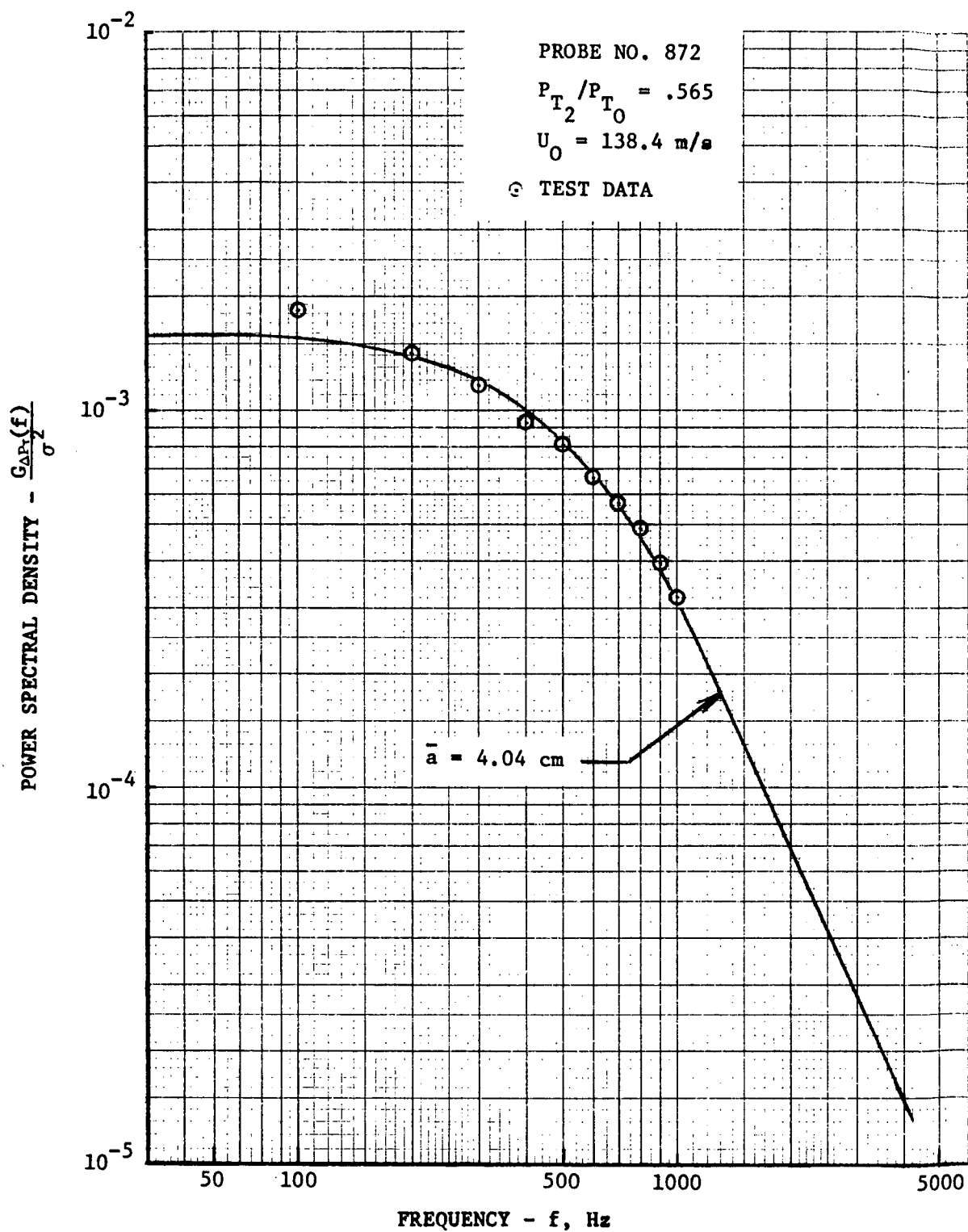
Figure 44. Comparison of Spectra Computed from the Flow Model with
Inlet Test Data of Martin (Reference 12).
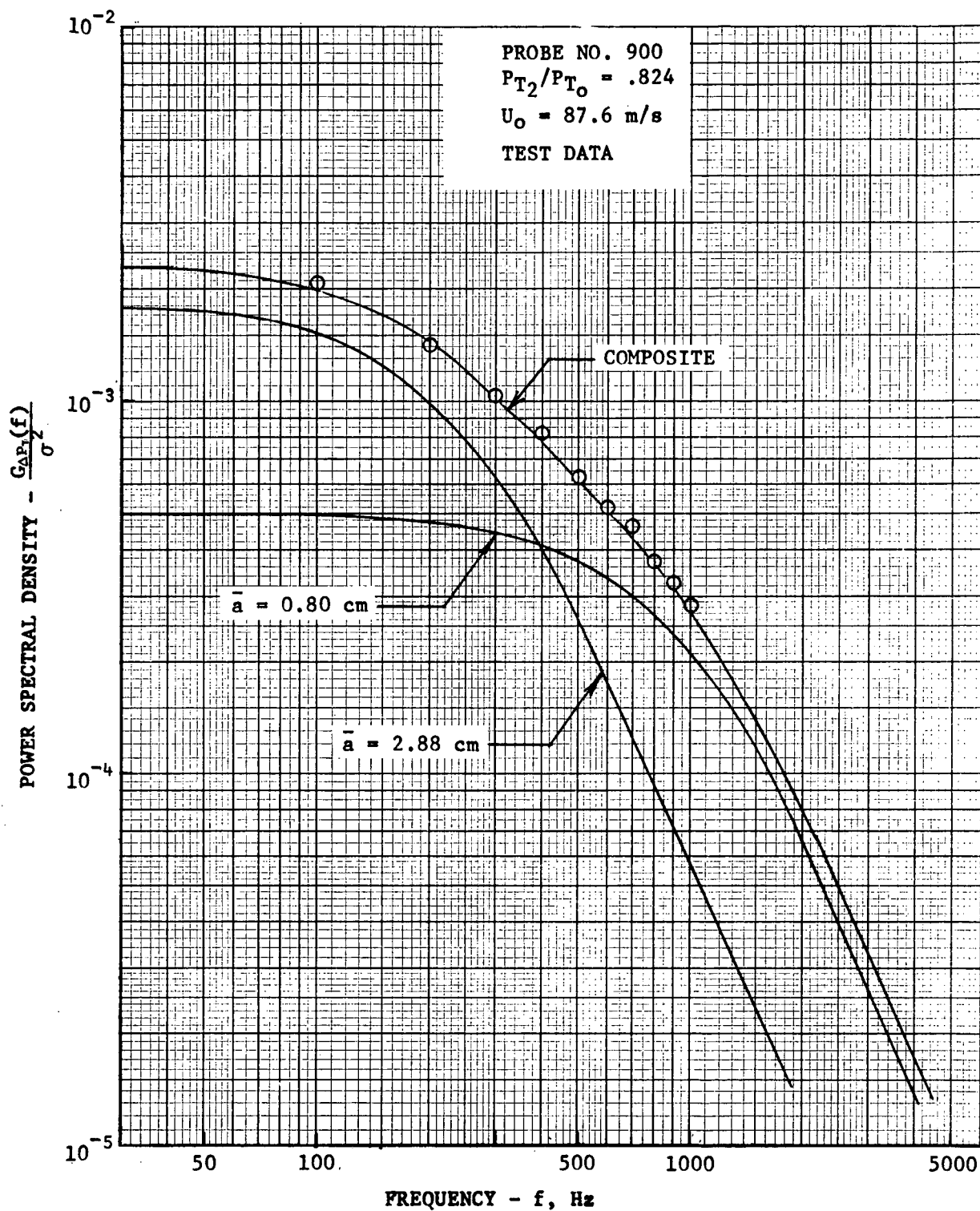
Figure 45.   Construction of the Composite Spectrum and Comparison
with Data from Probe 900 (Downstream)
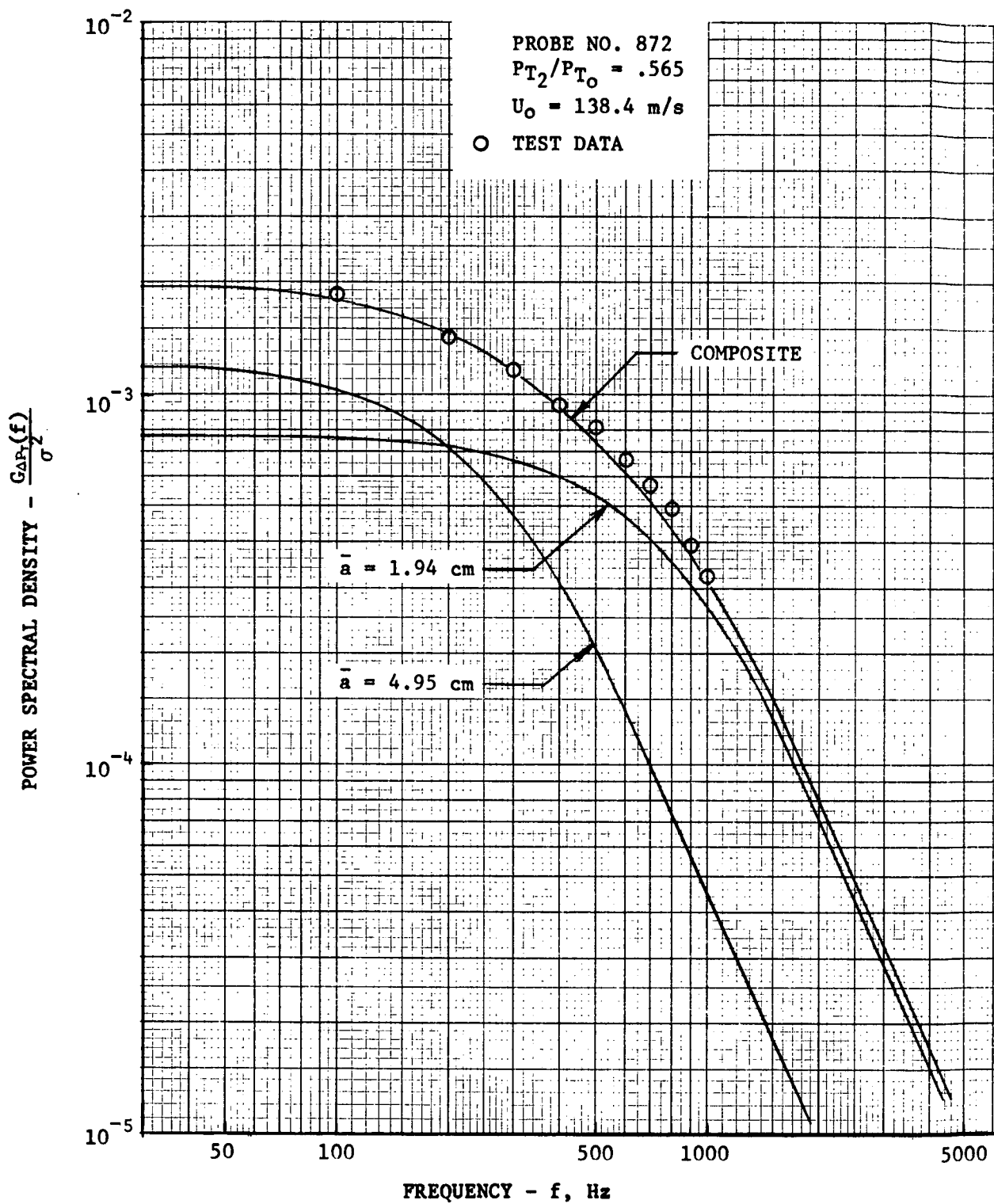
Figure 46. Construction of the Composite Spectrum and Comparison
with Data from Probe 872 (Diffuser Exit) at Low Recovery

CONCLUSIONS AND RECOMMENDATIONS

The analytical developments reported herein provide a fundamental approach to the problem of inlet/engine compatibility. With further development, this approach will provide a method of evaluating inlet tests and engine designs early in the propulsion system development cycle. Ultimately, it shows promise as a method for predicting and evaluating the effects of distortion and turbulence on engine stall characteristics, prior to system test.

The following are the more significant conclusions arising from the work to date and suggestions for continued activity to achieve the basic program goal: establishing the fundamental relationship between inlet distortion and turbulence and loss in compressor stall margin.

Conclusions

(1) The effect of circumferential total pressure distortion on the loss in compressor stall margin has been established analytically. The analysis has shown that the stall margin loss is directly a function of the distortion pattern, the distortion level $((\overline{P}_t - P_{t_{min}})/\overline{P}_t)$, and of the compressor rotor reduced frequency, $k = \omega c/2U$.

(2) The rotor chord is the principal design variable in the reduced frequency, k, and therefore emerges as a significant engine parameter in design for compatibility.

(3) Favorable comparison of distortion and engine stall data with analysis results is considered verification of the fundamental hypothesis of the analysis. Specifically, a circumferential total pressure distortion will result in an unsteady flow over the rotor blades requiring these unsteady aerodynamic effects to be included in the stage characteristics.

(4) The accuracy of the stall prediction technique is sufficient to justify the simplified approach which considers an overall compressor work balance rather than a detailed stage-by-stage development.

(5) A phenomenological model of turbulent flow typical of that found in aircraft inlets has been developed by combining statistical techniques with the basic laws governing fluid dynamics. The power spectral density function and root mean square level of the fluctuating total pressure take on considerable significance as a consequence of the model resulting in a means of determining the strength and extent of time variant low pressure regions.

(6) Favorable comparison of spectra obtained from the analytical model with test data of a Mach 3 mixed compression inlet verify the Turbulent Flow Model.

(7) The agreement with test data for both the Compressor Analysis and Turbulent Flow Model strongly suggest that compatibility problems, heretofore only attacked by empirical methods, are amenable to analysis.

Recommendations

(1) Both the Compressor Analysis and Turbulent Flow Model are considered developed to the point necessary to initiate the program to achieve the long term goal of establishing a fundamental relationship between both inlet distortion and turbulence and compressor stall margin loss.

(2) Further comparisons of the compressor analysis with test data are recommended for refining the method. The data used should provide the detailed distortion patterns, compressor geometry and compressor operating conditions.

(3) Additional analysis of turbulence data from a well documented inlet test program should be conducted to demonstrate the use of the turbulent flow model in isolating the source of turbulence and establishing turbulence decay characteristics.

(4) Finally, the developed relationships between distortion, turbulence and loss in compressor stall margin should be compared with data from an aircraft flight test program to verify the analysis.

78

APPENDIX A

Analysis of Unsteady Potential Flow on an Airfoil

This appendix contains a detailed discussion of the physical mechanisms effecting the interaction between an airfoil and the surrounding unsteady flow. The effects of unsteady airflow or airflow motion on an airfoil below the stalling angle of attack are explained in terms of the physical mechanism in part A and then related quantitatively with the governing mathematical relationships in part B.

A. The Governing Physical Mechanisms. - Lift on an airfoil is a consequence of the unequal pressures acting on the upper and lower surfaces. In potential flow these pressures along the surface of an airfoil can be computed from the velocity field by use of the equations of motion. The result of a potential flow solution, with zero circulation, about a flat plate of length, "c", and inclined to the stream at an angle, α, would yield stream lines similar to those sketched in Figure A1.
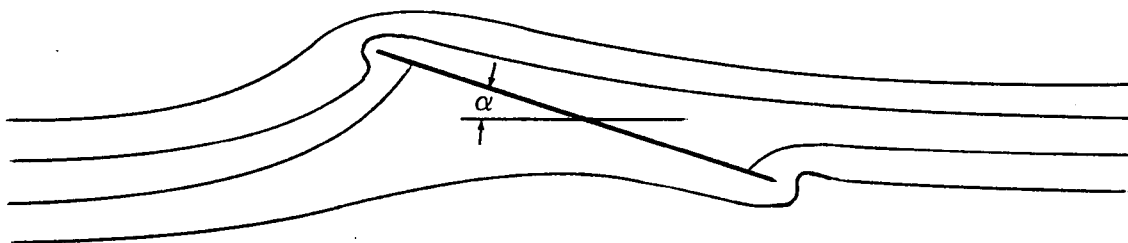
**Figure A1:   Potential Streamlines Around an
Airfoil with no Circulation**

The required boundary condition is that of zero flow through the plate. This is equivalent to the plate being a streamline which by definition implies zero cross flow. The lift on the airfoil is given by Equation A-1 and is designated as the non-circulatory lift, L_{NC}. Although the lift component is zero for steady flow, it can be non-zero under non-steady conditions.

$$L_{NC} = - \int_{0}^{c} (P_U - P_L) \, dx \qquad \qquad (A-1)$$

To bring this mathematical model into agreement with experience it is necessary to move the rear stagnation point aft to the airfoil trailing edge (Kutta condition). This can be accomplished by imposing a circulatory flow around the airfoil as shown in Figure A2.

NON-CIRCULATORY FLOW   PURE CIRCULATORY FLOW   COMBINED FLOW
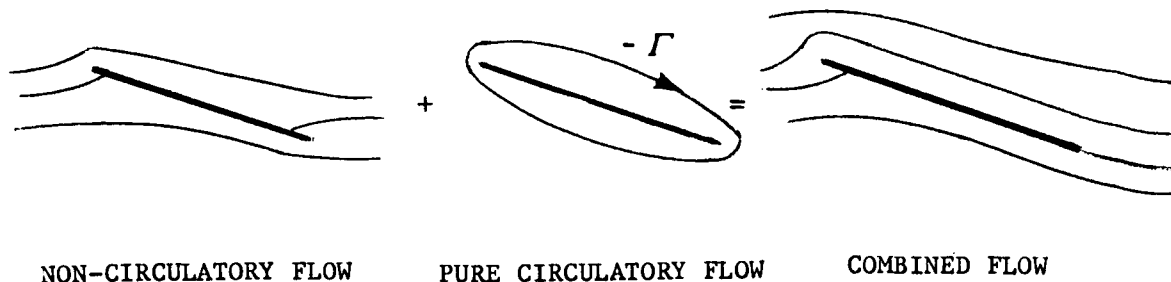
Figure A-2. Flow About an Airfoil with Circulation.

By so doing an equal circulation of opposite sign is shed from the airfoil such that the sum of the two is zero. The circulation about the airfoil imparts an additional velocity field around the airfoil and must be accounted for in obtaining the total lift. This additional lift is directly proportional to the amount of circulation Γ required to move the stagnation point aft to the trailing edge and is given by Equation A-2.

$$L_C = \rho U \Gamma \tag{A-2}$$

This in turn is related to the angle of attack, α, of the airfoil by

$$L_C = \rho U_o \Gamma = 2\pi\alpha(\tfrac{1}{2}\rho U_o{}^2)c \tag{A-3}$$

where $\Gamma = \pi U_o c\alpha$

$$\tag{A-4}$$

Total lift is therefore composed of two terms each caused by imposing a boundary condition:

$$L = L_{NC} + L_C \tag{A-5}$$

where L_{NC} is of non-circulatory (potential) origin and is a consequence of the requirement for zero flow through the plate

and L_C results from the circulation required (Kutta condition) to move the rear stagnation point to the trailing edge.

In steady flow and as indicated by the symmetry of Figure A-1, the lift due to non-circulatory flow is zero. Thus, in steady flow the total lift is approximated by the circulatory term,

$$L = L_C = (\tfrac{1}{2}\rho U^2)c\ 2\pi\alpha \tag{A-6}$$

For unsteady airfoil motion, however, inertial forces due to the finite mass of fluid that is forced to adjust cause the non-circulatory lift to be non-zero. As an example, consider the resultant lift due to oscillatory vertical translation and pitching motion (about the mid chord) of an airfoil:

$$L_{NC} = \pi\rho \frac{c^2}{4}[\ddot{y} + U\dot{\alpha}] \tag{A-7}$$

where $\pi\rho \frac{c^2}{4}$ is termed the virtual mass per unit span associated with the vertical acceleration $\ddot{y}$ and/or $U\dot{\alpha}$. It is equivalent to the mass of a cylinder of fluid with a diameter equal to the airfoil chord.

In addition, for any change in motion of the airfoil a trailing edge vortex must be shed to force the stagnation point to remain at the trailing edge. This adjustment requires a finite time and it too contributes to the resultant airfoil lift. The vortex shed is non-recoverable and might be considered as a dissipative or damping force. For the case mentioned above the lift of circulatory origin is:

$$L_C = \pi\rho UcC(k) \left[\dot{y} + U\alpha + \frac{c}{4}\dot{\alpha} \right] \tag{A-8}$$

Combining equations A-7 and A-8 the total lift for an airfoil undergoing oscillations in the vertical direction and along the pitch axis is as follows

$$L = \pi\rho \frac{c^2}{4}[\ddot{y} + U\dot{\alpha}] + \pi\rho UcC(k) \left[\dot{y} + U\alpha + \frac{c}{4}\dot{\alpha} \right] \tag{A-9}$$

For a general treatment of non-steady airfoil/airflow refer to References 18 and 19.
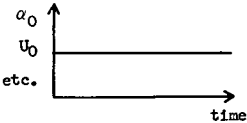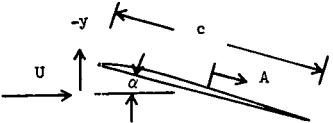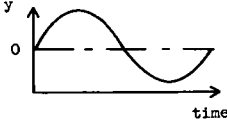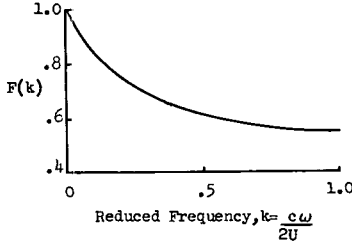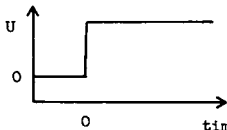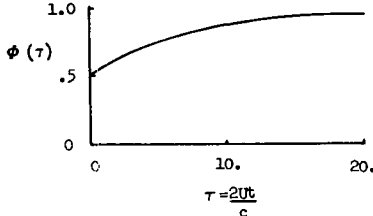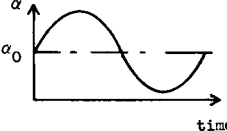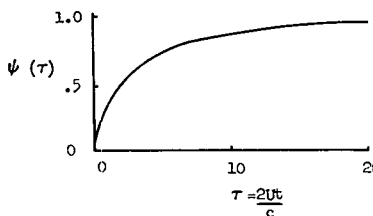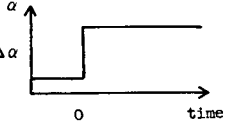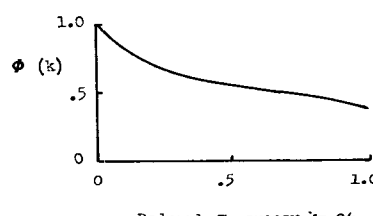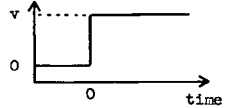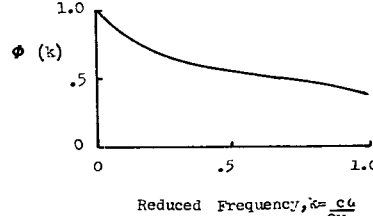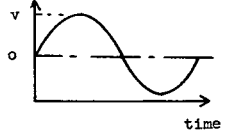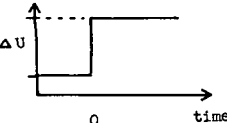
B. The Governing Equations. - The pressure forces due to unsteady flow acting on the isolated airflow discussed in Part A will be quantitatively described below. This will be important in developing the effects of unsteady flow on the stalling airfoil lift coefficients in subsequent sections.

Airfoil lift in unsteady airflow is dependent upon three prime factors:

1. The type of motion occurring. This can be classified by the following:

    (a) Airfoil unsteady - freestream airflow steady
        (i) Airfoil undergoing vertical translation
        (ii) Airfoil undergoing horizontal translation
        (iii) Airfoil exhibiting pitch oscillation
    (b) Free stream airflow unsteady - airfoil steady
        (i) Airflow with vertical gust
        (ii) Airflow with horizontal gust

2. The type of input, e.g., sinusoidal, step, arbitrary, etc.

3. The times associated with the disturbance compared with the airfoil "time constant".

Unsteady lift equations for the various classes of motions are summarized in Table A-1.

TABLE A1 UNSTEADY LIFT EQUATIONS

MOTION	SKETCH OF INPUT	COMPONENT OF LIFT DUE TO NON-CIRCULATORY (POTENTIAL) FLOW-INERTIA	COMPONENT OF LIFT DUE TO CIRCULATORY FLOW (VORTEX SHEDDING)	DEFINITION OF TERMS
(0) Steady State	α_0, U_0, etc.	0	$2\pi\alpha_o$	
(a) Airfoil Unsteady – Freestream Airflow Steady				
i. Sinusoidal Vertical Translation		$\frac{1}{4}\,\pi\rho c^2 \ddot{y}$	$\pi\rho U c F(k)\dot{y}$	
ii. Horizontal Change in Motion		------------	$\pi\rho U^2 c\alpha_o \phi(\tau)$	
iii. (a) Sinusoidal Change in Angle of Attack		$\frac{1}{4}\,\pi c^2 \rho (U\dot{\alpha} - \frac{c}{2}A\ddot{\alpha})$	$\pi\rho c U^2 F(k)[\alpha + \frac{c\dot{\alpha}}{2U}(\frac{1}{2} - A)]$	
(b) Step Change in Angle of Attack		$\frac{1}{4}\,\pi\rho c^2 U\Delta\alpha\delta(0)$	$\pi\rho c U^2 \Delta\alpha\phi(\tau)$	
(b) Free Stream Airflow Unsteady – Airfoil Steady				
i. (a) Step Vertical Gust		------------	$\pi\rho c U^2\, \frac{v}{U}\, \psi(\frac{2Ut}{c})$	
(b) Sinusoidal Vertical Gust		------------	$\pi\rho c U^2\, \frac{v}{U}\, \phi(k)$	
ii. Horizontal Gust	ΔU			

As indicated by the response functions in Table A-1, the change in lift characteristics is delayed in response to instantaneous change in airfoil angle of attack or flow velocity. The two physical mechanisms causing delay are found to be:

1. inertia of the mass of air requiring adjustment and

2. the finite time for the trailing edge vortices to be shed and cause adjustment with the flow field leading to a damping of the unsteadiness.

These phenomena are analogous to a damped mass/spring system which can be described by a second order differential equation, such as:

$$m \frac{d^2x}{dt^2} + c \frac{dx}{dt} + c_2 x = f(t) \tag{A-10}$$

where: m = mass

c_1 = damping factor

c_2 = spring constant

An unsteady flow field about an airfoil will most likely be composed of a combination of several of the above motions. Nevertheless, each of the above motions can be approximated by a second order differential equation and the composite flow field modeled by a general second order equation. This response of the airfoil to these motions in unstalled flow will form the basis upon which to develop the phenomenological model of an isolated airfoil subjected to angle of attack excursions beyond the steady state stall limit, and ultimately to represent the phenomenological model in usable, mathematical terms.

Solution of the Differential Equation for the
Effective Angle of Attack

    The effective angle is related to the instantaneous angle of attack through a second order linear differential equation. The differential equation is solved below for step, ramp, and sinusoidal changes in the instantaneous angle of attack. LaPlace transform techniques are utilized in the solutions.

    In terms of dimensional time, t, and dimensional time constants, t_1 and t_2, the governing equation is

$$\frac{d^2}{dt^2}(\alpha_{eff} - \alpha_o) + \left(\frac{1}{t_1} + \frac{1}{t_2}\right)\frac{d}{dt}(\alpha_{eff} - \alpha_o) + \frac{1}{t_1 t_2}(\alpha_{eff} - \alpha_o)$$

$$= \frac{1}{t_1 t_2}(\alpha_{inst} - \alpha_o) \qquad \text{(B-1)}$$

It is convenient to non-dimensionalize this equation by the airfoil velocity, U, and chord c. A non-dimensional time and time constants are defined below:

$$\tau = tU/c$$

$$\tau_1 = t_1 U/c$$

$$\tau_2 = t_2 U/c$$

Employing these definitions Equation B-1 becomes:

$$\frac{d^2}{d\tau^2}(\alpha_{eff} - \alpha_o) + \left(\frac{1}{\tau_1} + \frac{1}{\tau_2}\right)\frac{d}{d\tau}(\alpha_{eff} - \alpha_o) + \frac{1}{\tau_1 \tau_2}(\alpha_{eff} - \alpha_o)$$

$$= \frac{1}{\tau_1 \tau_2}(\alpha_{inst} - \alpha_o) \qquad \text{(B-2)}$$

This is identical to Equation 2 in the main text. Equation B-2 is a linear second order differential equation, is conveniently solved by LaPlace Transform techniques and is represented in the LaPlace domain as:

$$\frac{L(\alpha_{eff} - \alpha_o)}{L(\alpha_{inst} - \alpha_o)} = \left(\frac{1}{\tau_1 s + 1}\right)\left(\frac{1}{\tau_2 s + 1}\right) = T(s) \qquad \text{(B-3)}$$

    where $T(s)$ = transfer function

    and s = LaPlace dummy variable

The effective angle of attack can be obtained for simple changes in the instantaneous angle of attack, $\alpha_{inst} - \alpha_o$, by the method outlined below:

$$\alpha_{eff} - \alpha_o = L^{-1}\{L(\alpha_{eff} - \alpha_o)\} = L^{-1}\{(\alpha_{inst} - \alpha_o) \times T(s)\} \quad (B\text{-}4)$$

For example, assume that the instantaneous angle of attack, α_{inst}, increases as a step function of time as shown in Figure B-1.

$$L(\alpha_{inst} - \alpha_o) = \frac{1}{s}$$

$$\alpha_{eff} - \alpha_o = L^{-1}\left\{ \frac{1}{s(s\tau_1 + 1)(s\tau_2 + 1)} \right\}$$

$$\frac{\alpha_{eff} - \alpha_o}{\alpha_{inst} - \alpha_o} = 1 + \frac{1}{\tau_2 - \tau_1}[\tau_1 e^{-\tau/\tau_1} - \tau_2 e^{-\tau/\tau_2}] \quad (B\text{-}5)$$

The effective angle lags the instantaneous angle as shown below.
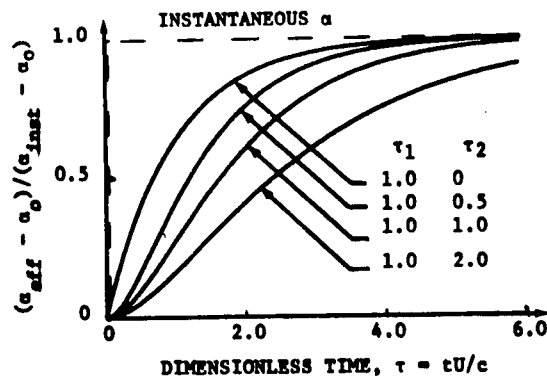
Figure B-1 Response of Effective Angle of Attack to a Step Change

The actual shape of the α_{eff} curve will depend on the system time constants, τ_1 and τ_2, as indicated in (B-5).

As another example the effective angle is found for a ramp input in α_{inst}, with a ramp rate of increase, $\frac{d\alpha}{dt} = $ constant $= c_1$.

85

$$L \left(\alpha_{inst} - \alpha_o \right) = c_1 / s^2$$

$$\alpha_{eff} - \alpha_o = L^{-1} \left\{ \frac{c_1}{s^2 (s\tau_1 + 1)(s\tau_2 + 1)} \right\}$$

$$\alpha_{eff} - \alpha_o = c_1 \left\{ \frac{\tau_2^2}{\tau_2 - \tau_1} e^{-\tau/\tau_2} - \frac{\tau_1^2}{\tau_2 - \tau_1} e^{-\tau/\tau_1} + \tau - \tau_2 - \tau_1 \right\} \quad (B-6)$$

An arbitrary variation in the instantaneous angle of attack can be represented by a Fourier Series as discussed in the section "Extension to Arbitrary Variations in Angle of Attack." A Fourier series utilizes the sum of sine and/or cosine waves to approximate the variation. Solution of the differential equation (Equation B-2) for a sine wave will therefore allow solution for arbitrary instantaneous angles of attack. This solution follows:

$$\alpha_{inst} - \alpha_o = \Delta \alpha_{inst} \sin(\omega t)$$

$$L \left(\alpha_{inst} - \alpha_o \right) = \frac{\omega}{s^2 + \omega^2}$$

$$\alpha_{eff} - \alpha_o = L^{-1} \left\{ \frac{\omega}{(s\tau_1 + 1)(s\tau_2 + 1)(s^2 + \omega^2)} \right\}$$

$$\frac{\alpha_{eff} - \alpha_o}{\Delta \alpha_{inst}} = \frac{2k}{\tau_1 \tau_2} \left\{ \frac{e^{-\tau/\tau_1}}{\left(\frac{1}{\tau_2} - \frac{1}{\tau_1} \right)\left(\frac{1}{\tau_1^2} + 4k^2 \right)} + \frac{e^{-\tau/\tau_2}}{\left(\frac{1}{\tau_1} - \frac{1}{\tau_2} \right)\left(\frac{1}{\tau_2^2} + 4k^2 \right)} \right.$$

$$\left. + \frac{\sin(2k\tau - \phi)}{2k \sqrt{ 4k^2 \left(\frac{1}{\tau_1} + \frac{1}{\tau_2} \right)^2 + \left(\frac{1}{\tau_1 \tau_2} - 4k^2 \right)^2 }} \right\} \quad (B-7)$$

$$\text{where } k = \omega / 2$$

86

The exponential decaying terms are neglected for periodic motion, simplifying the amplitude of the sine wave results in

$$\frac{\alpha_{eff} - \alpha_o}{\Delta\alpha_{inst}} = \frac{\sin(2k\tau - \phi)}{(1 + 4k^2\tau_1^2)(1 + 4k^2\tau_2^2)} = f(k)\sin(2k\tau - \phi) \qquad (B-8)$$

The amplitude of the sine wave is noted as $f(k)$ for convenience and shown in Figure B2. The phase shift is

$$\phi = \tan^{-1}(2k\tau_1) + \tan^{-1}(2k\tau_2) \qquad (B-9)$$
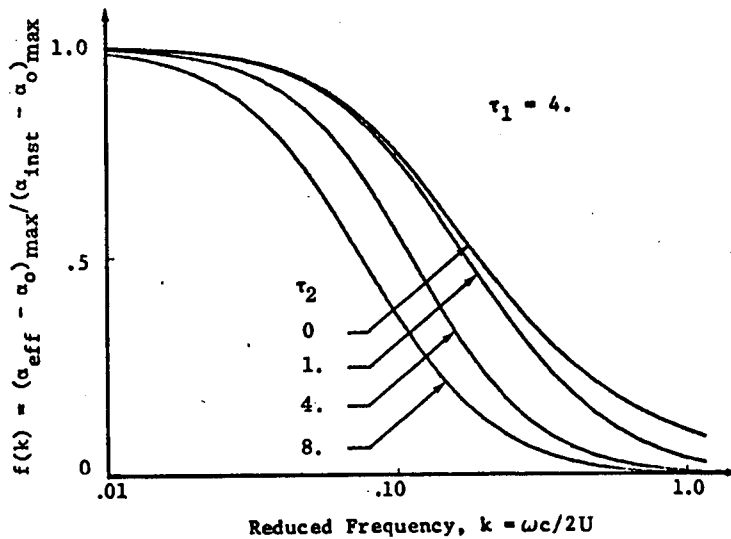
Figure B2. $f(k)$ vs Reduced Frequency for Several Values of τ_2.

APPENDIX C

Increase in Airfoil Maximum Lift Coefficient for
Unsteady Flow Test Data

A limited literature survey of the effect of unsteady flow on the maximum lift coefficient of an airfoil was conducted to establish an estimate of the time constants associated with airfoil stall in unsteady flow.

Available data were for a ramp rate of increase in angle of attack defined as an increase in angle of attack at a rate = $d\alpha/dt$ = constant. The lift coefficient achieved at stall with this type of unsteady motion was found to be greater than that achieved with steady flow. This increase, $\Delta C_{L_{max}}$, is shown in Figure C-1 as compiled from several sources.

Solution to the governing differential equation, Equation 2, for the ramp rate of increase was given in Appendix B. The analysis is dependent on the non-dimensional time constants τ_1 and τ_2. Based on a comparison between compressor component data and the analysis it was established that by setting the two time constants equal, $\tau_1 = \tau_2$, the best match between data and analysis could be achieved. For this reason, analytical results are shown compared with the data in Figure C-1 for values of $\tau_1 = \tau_2 = \tau = 2.0$ and 3.5. The comparison indicates time constants on the order of $3c/u$ are representative of the interaction between the unsteady flow and stall.

The chart shows STALL LIFT COEFFICIENT INCREASE, $\Delta C_{L_{stall}}$ on the vertical axis (0 to 1.0) versus DIMENSIONLESS PITCH RATE, $\frac{c}{U}\frac{\partial\alpha}{\partial t}$ ~radians on the horizontal axis (0 to .03).

symbol	airfoil	$N_{re}\times10^{-6}$	Reference
✧	NACA 2301x	<1.3	20
✩	$^{\omega}$66,2-(1.8)(15.2)	.6-13.4	21
	$^{\omega}$66,1-(1.8)(12)		
○	Gö 398	.36	19
◇	Gö 398,459	.12-.48	19
▽	NACA 2R$_1$	.1-.3	19
△	-	-	19
◇	NASA 65,213	1.3-2.8	22
△	NASA 65,209	2.8	23
▷	-	.4-1.1	24

ANALYSIS

$\tau_1 = \tau_2 = 3.5$

$\tau_1 = \tau_2 = 2.0$
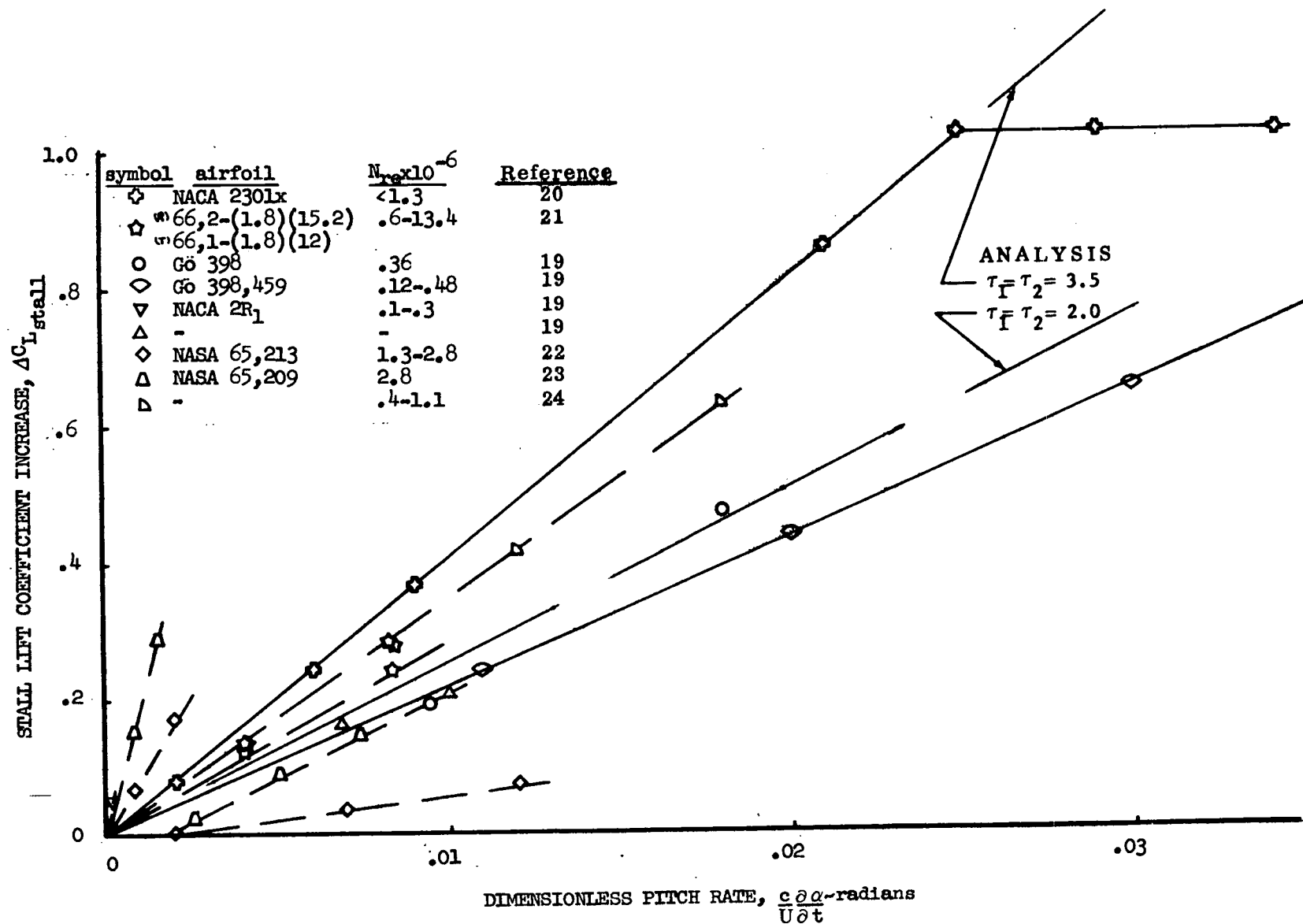
FIGURE C-1   Increase in Stall Lift Coefficient vs Dimensionless Pitch Rates for Several Airfoil Tests

APPENDIX D

Relating Inlet Distortion to Rotor Blade Lift Coefficient

The objective of this Appendix is to develop the relationship between the change in rotor blade lift coefficient required to perform the increased compressor work and the inlet distortion. Since a multistage compressor is built of individual stages having similar characteristics, the effect of a change in maximum angle of attack of one stage will therefore be similar to the response of the next stage and derivatives or influence factors should be similar. The procedure will be to equate the change in work (due to distortion) done on the airflow to the change in work done by the rotor blade. From this equality will come the relationship between C_L and pressure ratio which can be evaluated in terms of the operating point and the total pressure distortion.

Change of Work Done on the Air. - The compressor work per unit time done on the airflow is:

$$\Delta \dot{E} = w_a \Delta h = \rho A_x U \Delta h \tag{D-1}$$

where W_a = airflow = $\rho A_x U$

Δh = ideal compressor total enthalpy increase

$(\Delta \dot{E})'$ = increase in energy of the air per unit time.

A_x = flow area normal to the axial direction

U = axial velocity

Consistent with the parallel compressor model which is based on a uniform compressor exit pressure, inlet total pressure distortion will require a change in work done on the air to maintain this uniform exit pressure. The change in work can be written:

$$\frac{d(\Delta \dot{E})'}{\Delta \dot{E}'} = \frac{d\rho}{\rho} + \frac{dA_x}{A_x} + \frac{dU}{U} + \frac{d(\Delta h)}{\Delta h} \tag{D-2}$$

This change of work done on the air must be balanced by the change in work done by the rotor.

Change of Work Done by the Rotor. - The rotor work is as follows:

$$\dot{E}_{RTR} = \frac{1}{2} \rho V_R^2 A_{RTR} U_{RTR} C_L \tag{D-3}$$

where $\dot{E}_{RTR}$ = work per unit time done by the rotor

V_R = air velocity relative to the rotor

A_{RTR} = rotor area = chord X unit span

U_{RTR} = compressor blade velocity

C_L = rotor lift coefficient

The useful work done on the air by the rotor will be somewhat less due to the finite efficiency. Thus:

$$\dot{E}_R{}' = \eta \dot{E}_R$$

$$\dot{E}_R{}' = \frac{1}{2} \rho V_R{}^2 A_{RTR} U_{RTR} C_L \eta \tag{D-4}$$

The change in useful rotor work required by distortion is therefore:

$$\frac{d(\dot{E}_R)'}{\dot{E}_R{}'} = \frac{d\rho}{\rho} + \frac{2dV_R}{V_R} + \frac{dA_{RTR}}{A_{RTR}} + \frac{dU_{RTR}}{U_{RTR}} + \frac{dC_L}{C_L} + \frac{d\eta}{\eta} \tag{D-5}$$

Equating the Change in Work. - Since the useful work done by the rotor must be equal to the work done on the air equations (D-2) and (D-5) can be equated:

$$\frac{d\rho}{\rho} + \frac{dA_x}{A_x} + \frac{dU}{U} + \frac{d\Delta h}{\Delta h} = \frac{d\rho}{\rho} + \frac{2dV_R}{V_R} + \frac{dA_{RTR}}{A_{RTR}} + \frac{dU_{RTR}}{U_{RTR}} + \frac{dC_L}{C_L} + \frac{d\eta}{\eta}$$

Since the rotor area, the axial flow area, and speed remain constant, and assuming the change in efficiency due to distortion is strictly a secondary effect and therefore negligible, the equality reduces to the following:

$$\frac{dU}{U} + \frac{d\Delta h}{\Delta h} = \frac{2dV_R}{V_R} + \frac{dC_L}{C_L} \tag{D-6}$$

It remains to find a relationship between dC_L, dU, and dV_R. This can be established from the typical stage velocity diagram.

92

<u>Velocity Diagram.</u> - In the compressor mid stages, the stage stator exit angle will be to a first order independent of distortion around the circumference. Making this assumption the velocity into the following rotor will be as below:

Stage n-1 stator row

Stage n rotor cascade
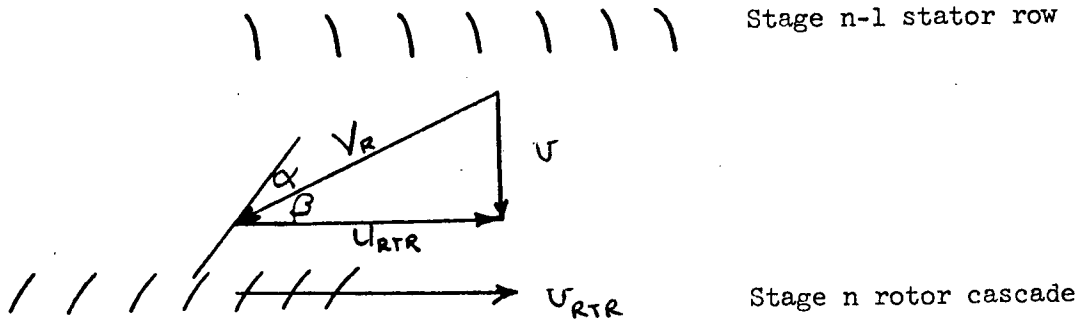
$$\Gamma = \alpha + \beta = \text{constant}$$

$$\tan \beta = \tan (\Gamma - \alpha) = U/U_{RTR}$$

$$\therefore U = U_{RTR} \tan (\Gamma - \alpha)$$

Taking the derivative of U

$$dU = -U_{RTR} (1 + \tan^2 (\Gamma - \alpha)) \, d\alpha$$

and

$$\frac{dU}{U} = \left(\frac{-\alpha}{\tan (\Gamma - \alpha)} - \frac{\alpha \tan (\Gamma - \alpha)}{1} \right) \frac{d\alpha}{\alpha} \qquad (D\text{-}7)$$

Similarly:

$$V_R = U_{RTR} (\cos (\Gamma - \alpha))^{-1}$$

$$dV_R = - U_{RTR} \left(\cos (\Gamma - \alpha)^{-2} \sin (\Gamma - \alpha) \right) d\alpha$$

$$\frac{dV_R}{V_R} = - \alpha \tan (\Gamma - \alpha) \frac{d\alpha}{\alpha} \qquad (D\text{-}8)$$

Recall:

$$C_L = 2\pi\alpha$$

and

$$\frac{dC_L}{C_L} = \frac{d\alpha}{\alpha}$$

Using these relationships equation (D-6) becomes:

$$\left[\frac{-\alpha}{\tan(\Gamma-\alpha)} - \alpha\tan(\Gamma-\alpha)\right]\frac{d\alpha}{\alpha} + \frac{d\Delta h}{\Delta h} = -2\alpha\tan(\Gamma-\alpha)\frac{d\alpha}{\alpha} + \frac{d\alpha}{\alpha}$$

Combining terms:

$$\frac{d\alpha}{\alpha}\left[\frac{-\alpha}{\tan(\Gamma-\alpha)} + \alpha\tan(\Gamma-\alpha)\right]-1 \quad + \frac{d\Delta h}{\Delta h} = 0$$

Typical flow angles $(\Gamma-\alpha)$ are 35 degrees (Reference 13) and angle of attack of 12 degrees.

$$\tan 35° = .7$$

$$\alpha = 12° = .21 \text{ radians}$$

$$\frac{d\alpha}{\alpha}\left[-.15 - 1\right] = -\frac{d\Delta h}{\Delta h}$$

In essence

$$\frac{dU}{U} - 2\frac{dV_R}{V_R} \cong 0$$

$$\frac{d\Delta h}{\Delta h} \cong \frac{d\alpha}{\alpha} = \frac{dC_L}{C_L} \tag{D-9}$$

The additional required work comes from an increase in blade angle of attack (or lift coefficient). This additional work must be related to the inlet flow distortion.

Compressor Work and Inlet Distortion. - The average work done by the compressor on the airflow remains constant. However, that section of the compressor operating in the region of low inlet total pressure must increase the pressure ratio to pump the flow to the uniform compressor exit pressure. It is assumed that this additional work is divided evenly among the compressor stages and the stage work, " $\Delta(\Delta h_i)$," can be related to the required increase

in overall pressure ratio as shown below:

$$\Delta h_i = C_p \left(T_{T_i} - T_{T_{i-1}}\right) \qquad \text{(D-10)}$$

where Δh_i = $i\underline{^{th}}$ stage work

T_{T_i} = total temperature at the exit of the $i\underline{^{th}}$ compressor stage

$T_{T_{i-1}}$ = total temperature at the inlet to the $i\underline{^{th}}$ stage
(exit of $((i - 1)th)$ stage)

and

$$\frac{d\Delta h_i}{\Delta h_i} = \frac{C_p d T_{T_i}}{C_p \left(T_{T_i} - T_{T_{i-1}}\right)}$$

The change in overall work is therefore given by Equation D-11.

$$\frac{d(\Delta h)}{\Delta h} = \frac{\sum\limits_{i=1}^{n} d(\Delta h_i)}{\sum\limits_{i=1}^{n} \Delta h_i} = \frac{\sum\limits_{i=1}^{n} \dfrac{d(\Delta h_i)}{\Delta h_i} \Delta h_i}{\sum\limits_{i=1}^{n} \Delta h_i} \qquad \text{(D-11)}$$

Since $\dfrac{d\Delta h_i}{\Delta h_i} \cong \dfrac{dC_L}{C_L}$ Equation (D-11) becomes:

$$\frac{d(\Delta h)}{\Delta h} = \frac{\sum\limits_{i=1}^{n} \dfrac{d_{CL}}{C_L} \Delta h_i}{\sum\limits_{i=1}^{n} \Delta h_i} \quad \frac{n \; \Delta h_i \; dC_L/C_L}{n \; \Delta h_i} \qquad \text{(D-12)}$$

and therefore

$$\frac{d \; \Delta h}{\Delta h}\bigg|_{overall} = \frac{dC_L}{C_L}\bigg|_{stage} \qquad \text{(D-13)}$$

Thus it is shown that the overall increase in compressor work is related directly to the increase in airfoil lift coefficient of a single typical stage. By assuming this additional required work is divided evenly among the compressor stages the required increased work can be equated to the required increased pressure ratio as developed below. The overall compressor work, assuming an efficiency of 100%, is given by:

$$\Delta h = C_p (T_{T_3} - T_{T_2}) = C_p T_{T_2} (\frac{T_{T_3}}{T_{T_2}} - 1)$$

$$= C_p T_{T_2} \left[\left(\frac{P_{T_3}}{P_{T_2}} \right)^{\frac{\gamma-1}{\gamma}} - 1 \right]$$

Taking the derivative the following results

$$\frac{d(\Delta h)}{dR_p} = C_p T_{T_2} \left(\frac{\gamma-1}{\gamma} \right) R_p^{\frac{\gamma-1}{\gamma} - 1} \qquad (D-14)$$

Therefore

$$\frac{d(\Delta h)}{\Delta h} = \frac{\left(\frac{\gamma-1}{\gamma} \right)}{1 - \left(R_p \right)^{\frac{\gamma-1}{\gamma}}} \frac{dR_p}{R_p} \qquad (D-15)$$

where R_p = overall compressor pressure ratio = P_{T_3}/P_{T_2}

By combining equation (D-13) with this result the relationship between the increased pressure ratio and required blade lift coefficient is derived.

$$\frac{dC_L}{C_L} = \frac{d\Delta h}{\Delta h} = \frac{\frac{\gamma-1}{\gamma}}{1 - R_p^{\frac{\gamma-1}{\gamma}}} \frac{dR_p}{R_p} \qquad (D-16)$$

Realizing that the increased pressure ratio required of the compressor is the negative of the change in inlet total pressure, (distortion)

$$\frac{dR_p}{R_p} = - \frac{dP_{T_2}}{P_{T_2}} \qquad (D-17)$$

equation (D-16) produces the relationship between the stage lift coefficient (dC_L) and the distortion (dP_{T_2}) as given by Equation D-18.

$$\frac{d\alpha}{\alpha} = \frac{dC_L}{C_L} = - \frac{\frac{\gamma-1}{\gamma}}{1 - R_p^{(1-\gamma)/\gamma}} \quad \frac{dP_{T_2}}{P_{T_2}} \tag{D-18}$$

This result is combined with the effects of unsteady flow on the stalling lift coefficient to establish the effect of distortion on the compressor stall margin.

C-2

APPENDIX E

Computation of the Loss in Compressor Stall Margin

Computer Program Description

I. ABSTRACT

A computer program has been written to calculate the loss in compressor stall margin due to inlet steady-state circumferential total pressure distortion. The program is written in Fortran IV and is operational on the LTVAC CDC 3300 computer. The mechanics of the program are discussed below, and a program listing included. Input instructions and examples of the input and output are given.

The program input is the circumferential total pressure profile which can be of arbitrary shape. A Fourier Series is then fit to this profile and the coefficients are modified by a transfer function to account for the delay in dynamic airfoil stall of the rotors. The loss in stall pressure ratio is then calculated as an output.

II. FORMULATION

A. Mathematical Description

1. Distortion Amplitude

The distortion amplitude is defined from the input total pressure field as the difference between the average and the minimum pressure divided by the average pressure $(\bar{P}_t - P_t min)/\bar{P}_t$. The distortion amplitude is used to normalize the calculated loss in stall margin.

2. Fourier Series

The technique of predicting stall pressure ratio loss for arbitrary distortion profiles utilizes Fourier series fit of the profile as indicated below.

$$P_T(\theta) = a_o + \sum_{n=1}^{\infty} a_n \cos(n\theta) + \sum_{n=1}^{\infty} b_n \sin(n\theta) \qquad (E-1)$$

where

$P_t(\theta)$ = total pressure as a function of circumferential position,

n = harmonic number

$$a_0 = \overline{P}_T = \frac{1}{2\pi} \int_{-\pi}^{\pi} P_T(\theta)d\theta$$

$$a_n = \frac{1}{\pi} \int_{-\pi}^{\pi} P_T(\theta) \cos(n\theta)\, d\theta \qquad\qquad \text{(E-2)}$$

$$b_n = \frac{1}{\pi} \int_{-\pi}^{\pi} P_T(\theta) \sin(n\theta)\, d\theta$$

The Fourier series can also be represented by sine terms. This will facilitate calculation of the loss in stall margin as will be shown later.

Let

$$a_n = c_n \sin(\phi n)$$

$$b_n = c_n \cos(\phi n)$$

$$c_n = \sqrt{a_n^2 + b_n^2}$$

$$\phi_n = \tan^{-1}(a_n/b_n)$$
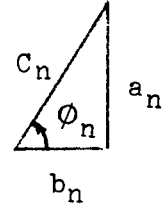
Then

$$a_n \cos(n\theta) + b_n \sin(n\theta) = c_n \sin(n\theta + \phi n)$$

The series is thus written as

$$\frac{P_T(\theta)}{\overline{P}_T} = 1 - \sum_{n=1}^{\infty} \frac{c_n}{\overline{P}_T} \sin(n\theta + \phi n) \qquad\qquad \text{(E-3)}$$

where the minus sign is the result of a change in the limits of integration from, $-\pi$ to π, to 0 to 2π.

3. Compressor Loss in Stall Pressure Ratio for Arbitrary Distortion Profiles

The technique to establish the loss in compressor stall margin is fully described in the section of the main text entitled "Compressor Analysis." Briefly, loss in stall margin is defined with the aid of the following figure which represents the process on a steady state compressor map.
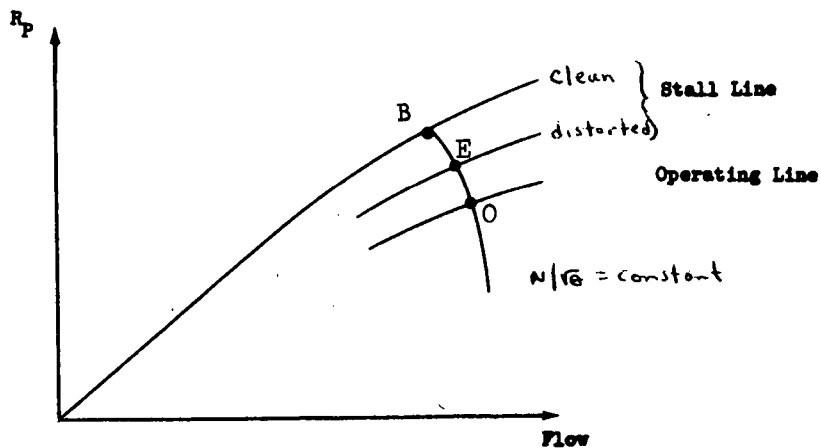
The "clean" stall margin is defined as

$$SM = \frac{R_{P_B} - R_{P_O}}{R_{P_O}}$$

(E-4)

101

The stall margin with distortion is defined as

$$SM_{Dist} = \frac{R_{P_E} - R_{P_O}}{R_{P_O}} \tag{E-5}$$

The loss in stall margin is thus the difference between these two equations:

$$\Delta SM = \frac{R_{P_{E'}} - R_{P_O}}{R_{P_O}} \tag{E-6}$$

This loss in stall margin is normalized by the distortion level as defined in Equation E7

$$Dist = (\overline{P}_T - P_{T_{min}})/\overline{P}_T \tag{E-7}$$

resulting in a normalized loss in stall margin, Equation E-8.

$$\frac{\Delta SM}{(\overline{P}_T - P_{T_{min}})/\overline{P}_T} \tag{E-8}$$

The technique to compute this normalized loss in stall margin due to an arbitrary inlet distortion profile is briefly as follows:

(1) The input distortion profile is represented by a Fourier series.

(2) The response of the compressor to this pattern is equal to the sum of the response to each of the components of the Fourier series. This is computed by the program.

(3) The highest compressor stall pressure ratio, during a complete revolution of the rotor, is used to compute the loss in stall margin.

B. Program Input

1. The program is designed to compute the normalized loss in stall margin assuming a second order response with the non-dimensional time constants, $\tau_1 = \tau_2 = 3.5$. This is the recommended mode of operation. In such a case

the only required input is the distortion pattern and the compressor reduced frequency, k.

However, if it is desired to change the non-dimensional time constant and/or the "order of response" the program is designed to accept these as input items on Card 1 (Refer to Figure E-1).

2. An arbitrary number of total pressure values are input into the program in order of increasing circumferential position up to a maximum of 144. The corresponding circumferential positions, which are arbitrary, are required. As an option it is possible to use the sine input subroutine to generate single or multiple harmonic sine waves of a specified amplitude in percent. Three sample cases are given which demonstrate the use of both types of input.

Multiple cases are run by repeating all cards except the initial card which gives the number of cases to be run.

3. The number of harmonics used in the Fourier series can be changed by changing the value of the parameter KN in the main program. KN = 72 is recommended for complex patterns where five degree resolution is adequate. If, for example, 2 1/2 degree resolution is required, set KN equal to 144. More harmonics will increase the accuracy of representing the input wave at the expense of more computing time; the effect on the calculated loss in stall margin is usually small.

4. The input data arrangement is illustrated in Figure E-1. The data on the first card is used to signal the number of cases to be executed during the run. All control parameters are input for each case. The input data for the arbitrary distortion profile and the sine wave distortion profile are different; and are illustrated in Figures E-1(b) and E-1(c), respectively. A detailed description of each input parameter follows. Parameters input in I format (see Figure E-1) are right adjusted.

JJ   - Number of cases to be executed during run, input only once.

NORD   - Order of system response.

KREF   - Compressor reduced frequency.

τ_1 - First time constant; if zero input, τ_1 defaults to 3.5.

τ_2 - Second time constant; if zero input, τ_2 defaults to 3.5.

LSPR   - Key for long print out; LSPR $\neq$ 2, long printout
                              LSPR = 2, short printout

KKKK   - Key for sine or arbitrary distortion profile
                  KKKK = 1, sine input follows
                  KKKK $\neq$ 1, arbitrary input follows

K   - Number of data points in arbitrary distortion profile definition $1 \leq K \leq 149$.

.. AND SO ON THROUGH CASE "JJ".

CASE 2

CASE 1

FORMAT
PARAMETER
```
I6
JJ
```

Figure E-1(a). General Input Data Deck Arrangement.

| F10.5 | F10.5 | F10.5 | F10.5 | F10.5 | F10.5 | F10.5 | F10.5 |
| T (1) | T (2) | " | " | " | T (K) | | |

| F10.5 | F10.5 | F10.5 | F10.5 | F10.5 | F10.5 | F10.5 | F10.5 |
| PT (1) | PT (2) | " | " | " | PT(K) | | |

| I6 |
| K |

BLANK CARD

FORMAT
PARAMETER

| I6 | F10.5 | F10.5 | F10.5 | I5 |
| NORD | KREF | τ_1 | τ_2 | LSPR |

Figure E-1(b). Arbitrary Distortion Profile Input Data Deck Arrangement.

| I6 | F10.5 |
| MMM | AMPL |

| I6 |
| KKKK |

FORMAT
PARAMETER

| I6 | F10.5 | F10.5 | F10.5 | I5 |
| NORD | KREF | τ_1 | τ_2 | LSPR |

Figure E-1(c). Sine Wave Distortion Profile Input Data Deck Arrangement.

104

PT(I)   -   Total pressure distortion profile; arbitrary units, either ratio of local to freestream or avg, or absolute dimensions (PSIA, PSFA, N/M^2, etc.).

T(I)   -   Circumferential location (degrees) to describe distortion profile, must be input in ascending order.

MMM   -   Sine wave input distortion, number of cycles per revolution.

AMPL   -   Sine wave distortion maximum amplitude.

     5.   Most of the output data are labeled. The printed data include a summary of the input data, a short or long output data format, and a printer plot of the instantaneous and effective pressure ratios.

     For the short printout, the output data include:

SYS ORDR   -   System order, input parameter NORD

KC   -   Compressor reduced frequency, input parameter KREF

TAU_1 -   System time constant one, τ_1

TAU_2 -   System time constant two, τ_2

SINE WAVE INPUT

     a.   AMPLITUDE   -   Sine wave distortion profile maximum amplitude, input parameter AMPL

     b.   MULTIPLE/REV NO.   -   Number of sine wave cycles per revolution, input parameter MMM

     or

INPUT PT THETA - list of arbitrary distortion profile total pressure and angle pairs; these are PT(I) and T(I) input parameters, from I = 1 to K.

PT AVG   -   Average total pressure of the input distortion profile.

LOSS IN STALL MARGIN - This is the loss in stall margin.

NORMALIZED LOSS - Loss in stall margin divided by distortion, where distortion is $(\bar{P}_T - P_{Tmin})/\bar{P}_T$.

The printer plot is composed of:

     1.   the input instantaneous total pressure ratios

     2.   and the effective total pressure ratios versus circumferential location, in degrees.

The long printout also includes

PT/PTAVG   - linearly interpolated total pressures divided by the average; computed from the input profile.

THETA   - Circumferential location, radians.

A(I)/AVE   - Fourier coefficients, a, for harmonics 1 to 18, divided by average total pressure.

B(I)/AVE   - Fourier coefficients, b, for harmonics 1 to 18, divided by average total pressure.

C(I)/AVE   - Fourier coefficients, c, for harmonics 1 to 18, divided by average total pressure.

PHI(I)   - See Equation (E-3), radians

PHASE ANGLE   - Transfer function phase shift for harmonics 1 to 18, radians

AMPLITUDE RATIO - Transfer function amplitude ratio for harmonics 1 to 18

PT_2 INST   - Instantaneous total pressure computed from Fourier fit

THETA   - Circumferential angle, radians

THETA   - Circumferential angle, degrees

PT_2 INST   - Instantaneous total pressure ratio computed from Fourier fit and normalized by average total pressure.

PT_2 EFF   - The computed effective total pressure ratio, normalized by the average.

SPR LOSS   - The loss in stall pressure ratio.

INPUT RPI/RPO   - Defined by Equation (18) in main text.

RP(EFF)/RPO   - See Equation (17) and Figure 8, in main text, for definition.

C. Subroutine Descriptions

    1. Subroutine LINR

        Subroutine LINR accepts the input total pressure and angle data. The angles (and corresponding pressures) are input in increasing order and may be unevenly spaced. The subroutine linearly interpolates the data to generate total pressures every five degrees (KN = 72).

2. Subroutine ALF

Subroutine ALF accounts for the dynamics of the rotor stall process. The subroutine accepts (1) the number of harmonics to be used, (2) the order of the response, (3) the compressor reduced frequency, and (4) two time constants. The output is the phase angle and amplitude for each of the harmonics.

3. Subroutine Sine

The sine subroutine may be used to generate sinusoidal input data. When the sine subroutine is used, no pressure or angle data are input. The subroutine accepts the amplitude, and the number of sine waves per 360 degrees.

4. Subroutine Plot

The PLOT subroutine generates a printer plot of the interpolated input total pressure ratio, and the calculated effective total pressure ratio. The plot is suppressed when the output circumferential spacing is other than five degrees (i.e., $KN \neq 72$).

D. Program Limitation

The dimension statements allow for a maximum value of $KN = 144$ which corresponds to 36 harmonics, and 144 circumferential spaced total pressures. The plot limits are fixed; the upper limit is 1.25 and the lower limit is 0.75. If the order of response is other than two, the two input time constants have to be equal.

IV   PROGRAM LISTING

A listing of the main program and the four subroutines are given below:

```
          PROGRAM D4815(INPUT,OUTPUT,TAPE5=INPUT,TAPE6=OUTPUT)
          REAL K,N,KREF
          DIMENSION A(50), B(50), C(50), PHI(50), PT(150), T(150), TT(150),
         1PTA(150), PTC(150), PP(150), TTT(150), THA(150),RPI(150),RPEF(150)
   5      DIMENSION PHE(50), COFK(50), PTCC(150), DSM(150)
          READ (5,170) JJ
          WRITE(6,320)
          DO 160 II=1,JJ
        C CALCULATION OF NORMALIZED STALL PR RAT LOSS FOR ARBITRARY TOTAL
  10    C PRESSURE INPUTS
        C CALCULATION OF FOURIER SERIES FOR ARBITRARY PATTERNS
        C INPUT ANGLE ONLY ONCE
        C KN = NO OF INTERPOLATED PROBES
        C PHE= PHASE ANGLE FROM TRANSFER FUNCTION
  15    C PTCC= INSTANTANEOUS PT ON COMPRESSOR MAP,ANGLE= EFFECTIVE ANGLE
        C INPUT IS INTERPOLATED TO 72 PARTS FOR 5 DEG RESOLUTION..
        C DETERMINATION OF MAX NO OF HARMONICS AND MIN STEP SIZE
        C 360/(MAX NO OF HARMONICS)= THETA CYCLIC
        C THETA CYCLIC/4.= MIN DELTA THETA
  20    C EX. 18 HARMONICS FOR MIN DELTA THETA OF 5. DEG I.E. KN=72.
        C JJ=NO OF CASES,  TH= ANGLE,PT(I)=TOTAL PRESSURE,K=NO OF RAKES
        C NORD=ORDER OF SYSTEM RESPONSE,KREF=COMPRESSOR REDUCED FREQUENCY,T1
        C    AND T2 ARE TIME CONSTANTS,LSPR=2 FOR SHORT PRINT OUT
          KN=72
  25      KNM=KN+1
          MM=KN/2
          KNN=KN
          QQ=KN
          EE=0.0
  30      READ(5,172) NORD,KREF,T1,T2,LSPR
          IF(T1.EQ.0.) T1=3.5
          IF(T2.EQ.0.) T2=3.5
          WRITE(6,174)
          WRITE(6,172) NORD,KREF,T1,T2,LSPR
  35      READ(5,170) KKKK
        C KKKK=1 FOR SIN NTHETA , MMM=NO./REV
          IF(KKKK-1) 4,2,4
        2 READ(5,195)MMM,AMPL
          WRITE(6,196) KKKK,MMM,AMPL
  40      CALL SINE(AMPL,MMM,KN,EE,TTT)
        4 CONTINUE
          IF (KKKK-1) 8,35,8
        8 CONTINUE
          READ (5,180) K
  45      L=K
          KK=K
        C INPUT FIRST ANGLE AT ZERO DEGREES
          WRITE(6,310)
          WRITE(6,192)
  50      READ (5,190) (PT(I),I=1,L)
          WRITE(6,310)
          READ (5,190) (T(I),I=1,L)
          WRITE (6,190) (PT(I),T(I),I=1,L)
          DPT1=50.
  55      DO 20 I4=1,L
```

```
              IF (PT(I4)-DPT1) 10,21,27
        10 DPT1=PT(I4)
        20 CONTINUE
              DO 30 I6=1,KK
  60         T(I6)=T(I6)/57.2957795
        30 CONTINUE
              CALL LINR (PT,T,KK,KN,PP,TTT)
        35 CONTINUE
              DO 40 I9=1,MM
  65         J1=2*I9-1
              J2=J1+1
              J3=J2+1
              EE=EE+PP(J1)+4.0*PP(J2)+PP(J3)
        40 CONTINUE
  70         OTH=6.2831853/QQ
              AVE=EE*OTH/6.2831853/3.0
              WRITE(6,310)
              WRITE(6,208)
              WRITE (6,210)
  75         WRITE (6,220) AVE
              WRITE(6,310)
              IF(KKKK.NE.1) GO TO 49
              DPT1=200000.
              DO 48  KI=1,KNM
  80         IF(PP(KI)-DPT1)  44,48,48
        44 DPT1=PP(KI)
        48 CONTINUE
        49 CONTINUE
              DPT1=DPT1/AVE
  85         DPT1=1.0-DPT1
              DO 50 LM=1,KNM
              PT(LM)=PP(LM)/AVE
              T(LM)=TTT(LM)
        50 CONTINUE
  90         IF(LSPR-2)51,52,51
        51 CONTINUE
              WRITE(6,198)
              WRITE (6,200) (LP,PT(LP),T(LP),LP=1,KNM)
        52 CONTINUE
  95  C    IT TAKES 4. DATA POINTS FOR CORRECT INTEGRATION
              MML=MM/2
              DO 70 M=1,MML
              N=M
              AA=0.0
 100         BB=0.0
              DO 60 I2=1,MM
              J4=2*I2-1
              J5=J4+1
              J6=J5+1
 105         ANG1=N*T(J4)
              ANG2=N*T(J5)
              ANG3=N*T(J6)
              AA=AA+PT(J4)*COS(ANG1)+4.*PT(J5)*COS(ANG2)+PT(J6)*COS(ANG3)
              BB=BB+PT(J4)*SIN(ANG1)+4.*PT(J5)*SIN(ANG2)+PT(J6)*SIN(ANG3)
 110      60 CONTINUE
```

```
        C     CALCULATION OF FOURIER COEFFICIENTS
              A(M)=AA*DTH/3.1415926536/3.0
              B(M)=BB*DTH/3.1415926536/3.0
              C(M)=SQRT(A(M)*A(M)+B(M)*B(M))
115           D=A(M)/B(M)
              PHI(M)=ATAN(D)
           70 CONTINUE
              IF(LSPR-2) 71,72,71
           71 CONTINUE
120           WRITE(6,310)
              WRITE(6,232)
              WRITE (6,230)
              WRITE (6,240) (M,A(M),B(M),C(M),PHI(M),M=1,MML)
           72 CONTINUE
125     C     CALCULATION OF PT(I)
              BCMAX=0.0
              BCMAX=AMAX1(B)
              IF(BCMAX.EQ.0.0) BCMAX=-1.0
              SIGN=BCMAX/ABS(BCMAX)
130           DO 150 LK=1,1
              IF(T1-0.0) 76,74,76
           74 CONTINUE
        C     T1=T2 IF N NOT =2
              IF(T2-0.0)76,75,76
135        75 CONTINUE
              T1=3.5
              T2=3.5
           76 CONTINUE
              CALL ALF   (MML,NORD,KREF,T1,T2,PHE,COFK)
140           IF(LSPR-2)77,78,77
           77 CONTINUE
              WRITE (6,250)
              WRITE (6,260) (LL,PHE(LL),COFK(LL),LL=1,MML)
           78 CONTINUE
145     C     18 HARMONICS ARE CALCULATED        FOR KN=72
              THETA=0.0
              DO 80 KJJ=1,KNM
              THA(KJJ)=THETA
              THETA=THETA+DTH
150        80 CONTINUE
        C     OUTPUT DATA ARE CALCULATED AT  5 DEG INCREMENTS
              DO 100 I4=1,KNM
              FTEF=0.0
              PTT=0.0
155           DO 90 I5=1,MML
              N=I5
              ANG=N*THA(I4)+PHI(I5)
              ANGE=ANG-PHE(I5)
              BA=C(I5)*SIN(ANG)
160           PTT=PTT+BA
        C     PTT IS THE LOCAL DISTORTION =CN*SIN(NTH + PHI)
              PTEF=PTEF+COFK(I5)*SIN(ANGE)*C(I5)
           90 CONTINUE
        C     AVE - PTT IF THETA ZERO =0.0
165           PTC(I4)=1.0+ SIGN*PTT
```

```
                        PTA(I4)=PTC(I4)*AVE
                        TT(I4)=THA(I4)*57.2957795
            C           PTCC(I4) IS THE EFFECTIVE PRESSURE
                        PTCC(I4)=1.0+ SIGN*PTEF
       170              RPI(I4)=2.0 -PT(I4)
                        REEF(I4)=1.0 - SIGN*PTEF
                        DSM(I4)=PTEF
            100 CONTINUE
                        DSMAX=0.0
       175              DO 120 I4=1,KNM
                        IF (DSM(I4)-DSMAX) 120,110,110
            110 DSMAX=DSM(I4)
            120 CONTINUE
                        DSMN=DSMAX/DPT1
       180              IF (DSMN-1.0) 140,140,130
            130 DSMN=1.0
            140 CONTINUE
                        WRITE(6,310)
                        WRITE (6,270)
       185              WRITE (6,280) DSMAX,DSMN
                        IF(LSFR-2) 141,142,141
            141 CONTINUE
                        WRITE(6,310)
                        WRITE (6,290)
       190              WRITE (6,300) (I4,PTA(I4),THA(I4),TT(I4),PTC(I4),PTCC(I4),DSM(I4),
                       1I4=1,KNM)
            142 CONTINUE
                        WRITE (6,310)
            150 CONTINUE
       195              CALL PLOT(KNM,RPI,REFF,LSFR)
                        WRITE(6,320)
            160 CONTINUE
                        STOP
            C
       200  170 FORMAT (1X,I5)
            172 FORMAT(1X,I5,3F10.5,I5)
            174 FORMAT(1X,60HSYS OPDP    KC        TAU1        TAU2        LONG/SHORT PR
                       1INT OUT)
            180 FORMAT (1X,F10.5)
       205  190 FORMAT (8F10.5)
            192 FORMAT(1X,15HINPUT PT   THETA)
            195 FORMAT(1X,I5,F10.5)
            196 FORMAT(1X,2I5,F10.5)
            198 FORMAT(9X,15HPT/PTAVG   THETA)
       210  200 FORMAT (1X,I5,2F10.5)
            208 FORMAT(1X,11HOUTPUT DATA)
            210 FORMAT(1X,6HPT AVG)
            220 FORMAT (1X,F10.5)
            230 FORMAT (52HI     A(I)/AVE  B(I)/AVE  C(I)/AVE  PHI(I)            )
       215  232 FORMAT(1X,20HFOURIER COEFFICIENTS)
            240 FORMAT (1X,I5,4F10.5)
            250 FORMAT (4X,42HHARMONIC NO  PHASE ANGLE  AMPLITUDE  RATIO)
            260 FORMAT(9X,I5,F10.5,5X,F10.5)
            270 FORMAT(1X,45HLOSS IN STALL MARGIN          NORMALIZED LOSS)
       220  280 FORMAT(1X,F10.5,20X,F10.5)
```

```
       290 FORMAT (9X,6BHPT2 INST   THETA     THETA     PT2INST   PT2 EFF    SP
           1R LOSS  )
       300 FORMAT (1X,I5,6F10.5)
       310 FORMAT (1X,/)
   225 320 FORMAT(1H1)
           END
```

```
          SUBROUTINE LINR (PT,T,N,KN,PP,TT)
          DIMENSION PT(150), T(150), PP(150), TT(150)
          A=KN
          KNM=KN+1
 5        DTH=6.2831853/A
          NM=N+1
          PT(NM)=PT(1)
          T(NM)=6.2831853
          TH=0.0
 10       J=0
          B=0.0
          DO 60 I=1,N
          BB=B+DTH
          IF (BB-T(I+1)) 10,10,60
 15    10 CONTINUE
       20 J=J+1
          IF (J-KNM) 30,30,60
       30 CONTINUE
          IF (J-1) 40,40,50
 20    40 PP(J)=PT(1)
          TT(J)=0.0
          GO TO 20
       50 TH=TH+DTH
          B=TH
 25       PINTC=PT(I)
          PSLOP=(PT(I+1)-PT(I))/(T(I+1)-T(I))
          PP(J)=PINTC+PSLOP*(TH-T(I))
          TT(J)=TH
          BB=B+DTH
 30       IF (BB-T(I+1)) 10,10,50
       60 CONTINUE
          PP(KN+1)=PT(1)
          TT(KN+1)=6.2831853
          RETURN
 35       END
```

```
            SUBROUTINE ALF (M,NORD,KREF,T1,T2,PHI,COFK)
      C     H=HARMONIC NO,COFK=F(K)
            REAL MAGD,MAG,K,KREF
            DIMENSION PHI(50), COFK(50), MAG(50)
  5   C     A AND B ARE RECIPOCALS OF NONDIMENSIONAL TIME CONSTANTS
      C     A AND B DETERMINE THE STALL FILTER CHARACTERISTICS
            ORD=NORD
            A=1./T1
            B=1./T2
 10         WRITE(6,160)
            WRITE (6,140)
            WRITE (6,150) T1,T2,KREF
            IF(T1-T2)25,15,25
         15 CONTINUE
 15         IF (NORD-2) 17,25,17
         17 CONTINUE
            DO 20 J=1,M
            H=J
            K=KREF*H
 20         ARG=2.*K*T1
            PHI(J)=ORD*ATAN(ARG)
            MAGD=(1.+4.*K*K*T1*T1)
            EXP=ORD/2.
            MAG(J)=1./(MAGD**EXP)
 25         COFK(J)=MAG(J)
         20 CONTINUE
            GO TO 135
         25 CONTINUE
            DO 130 J=1,M
 30         H=J
            K=KREF*H
            A3=2.*K/A
            A4=2.*K/B
            PHI(J)=ATAN(A3)+ATAN(A4)
 35         MAGD=SQRT((1.0-4.*K*K/(A*B))*(1.-4.*K*K/(A*B))+4.*K*K*(A+B)*(A+B)/
           1(A*B*A*B))
            MAG(J)=1.0/MAGD
            COFK(J)=MAG(J)
        130 CONTINUE
 40     135 CONTINUE
            WRITE (6,160)
            RETURN
      C
        140 FORMAT(8X,20HTAU1     TAU2        KC)
 45     150 FORMAT (1X,3F10.5)
        160 FORMAT (1X,/)
            END
```

```
              SUBROUTINE SINE(AMPL,MMM,KN,PP,TTT)
              DIMENSION PP(150),TTT(150)
              A=KN
              KNM=KN+1
    5         DTH= 6.2831853/A
              PMM=MMM
              WRITE(6,66)
              WRITE(6,65)
              WRITE(6,62)
   10      62 FORMAT(1X,26HAMPLITUDE  MULTIPLE/REV NO.)
              WRITE(6,63)  AMPL,PMM
           63 FORMAT(1X,2F10.5)
              TH=0.0
              DO 60 I=1,KNM
   15         TTT(I)=TH
              ANGL=PMM*TH
              PP(I)= 1.0 - AMPL*SIN(ANGL)
              TH=TH+DTH
           60 CONTINUE
   20      65 FORMAT(1X,15HSINE WAVE INPUT)
           66 FORMAT(1X,/)
              RETURN
              END
```

```
            SUBROUTINE PLOT (KNM,PT,RPE,LSPR)
            DIMENSION FT(150),RFE(150),NN(21,144),LN(120)
            DATA(NB=1H ),(NI=1HI),(NO=1HE)
            IF(KNM-73) 183,9,183
    5     9 CONTINUE
            IF (LSPR-2) 11,13,11
         11 CONTINUE
            WRITE(6,10)
         10 FORMAT(1X,27HINPUT RPI/RP0    RP(EFF)/RP0)
   10       WRITE(6,12)(FT(I),RFE(I),I=1,KNM)
         12 FORMAT(1X,F10.5,10X,F10.5)
            WRITE(6,85)
         13 CONTINUE
            PTH=1.275
   15       WRITE(6,78)
            WRITE(6,16)
         16 FORMAT(40X,16HRPI/RP0 =INPUT=I)
            WRITE(6,17)
         17 FORMAT(40X,20HRF(EFF)/RP0=OUTPUT=E)
   20       WRITE(6,78)
            DO 20 J=1,21
            DO 18 I=1,KNM
            NN(J,I)=0
         18 CONTINUE
   25    20 CONTINUE
            DO 40 J=1,21
            FTH=FTH-.025
            PTL=PTH-0.025
            DO 30 I=1,KNM
   30       IF(FT(I).GT.FTH) GO TO 25
            IF(PT(I).LE.PTL) GO TO 25
            NN(J,I)=1
         25 IF(RPE(I).GT.PTH) GO TO 29
            IF(RPE(I).LE.PTL) GO TO 29
   35       NN(J,I)=2
            GO TO 30
         29 CONTINUE
            IF(NN(J,I)-1) 32,34,32
         32 NN(J,I)=0
   40    34 CONTINUE
         30 CONTINUE
         40 CONTINUE
            DO 76 J=1,21
            DO 60 I=1,KNM
   45       IF(NN(J,I)-1) 45,50,55
         45 LN(I)=NB
            GO TO 60
         50 LN(I)=NI
            GO TO 60
   50    55 LN(I)=NO
         60 CONTINUE
            D=J
            D1=D/1.
            D2=D/11.
   55       D3=D/21.
```

```
              IF(D1-1.)64,61,64
          61  WRITE(6,63)(LN(I),I=1,KNM)
          63  FORMAT ( 5X,8H1.25   1 ,73A1)
              GO TO 76
          64  CONTINUE
              IF(D2-1.)67,65,67
          65  WRITE(6,66)(LN(I),I=1,KNM)
              GO TO 76
          66  FORMAT(5X,8H1.00   1 ,73A1)
          67  CONTINUE
              IF(D3-1.)70,68,70
          68  WRITE(6,69)(LN(I),I=1,KNM)
          69  FORMAT( 5X,8H0.75   1 ,73A1)
              GO TO 76
          70  CONTINUE
              WRITE(6,72)(LN(I),I=1,KNM)
          72  FORMAT(12X,1H1,73A1)
          76  CONTINUE
              WRITE(6,78)
          78  FORMAT(1X,/)
              WRITE(6,80)
          80  FORMAT(11X,3H0.0,32X,4H180.,32X,4H350.)
              WRITE(6,78)
              WRITE(6,82)
          82  FORMAT(35X,34HCIRCUMFERENTIAL POSITION , DEGREES)
          85  FORMAT(1H1)
         103  CONTINUE
              RETURN
              END
```

118

65

70

75

80

V. SAMPLE PROBLEM

A. Input Data Description

```
                              SAMPLE INPUT DATA    PAGE   1

                                   CARD COLUMN                        CARD NUMBER
          1         2         3         4         5         6         7         8
 1234567890123456789012345678901234567890123456789012345678901234567890123456789 0

     3                                                                              1
 2   .10   3.5       3.5                                                            2
                                                                                    3
   6.                                                                               4
 1.5      0.9       0.9       1.0       1.2       1.2                               5
 0.5      1.0       89.0      90.       91.       359.                              6
 2   .1   3.5       3.5       2                                                     7
 1                                                                                  8
 2  0.2                                                                             9
 2   .1   3.5       3.5       2                                                    10
                                                                                   11
                                                                                   12
   6.0                                                                             13
 1.5      0.9       1.5       1.05      1.20      1.05                              14
 0.5      90.0      180.      265.      270.      275.
          1         2         3         4         5         6         7         8
 1234567890123456789012345678901234567890123456789012345678901234567890123456789 0
```

B. Output Description

Pages 120 through 125 present the long output for the arbitrary distortion profile input. A two per revolution sine wave short output is presented on page 126. A final short output for a complex distortion profile input is presented on page 127.

119

SYS ORDR	KC	TAU1	TAU2	LONG/SHORT PRINT OUT
2	.10000	3.50000	3.50000	0

INPUT PT   THETA

1.00000	0	.90000	1.00000	.90000	89.00000	1.00000	90.00000
1.20000	91.00000	1.20000	359.00000				

OUTPUT DATA
PT AVG
   1.12407

	PT/PTAVG	THETA
1	.88962	0
2	.80066	.08727
3	.80066	.17453
4	.80066	.26180
5	.80066	.34907
6	.80066	.43633
7	.80066	.52360
8	.80066	.61087
9	.80066	.69813
10	.80066	.78540
11	.80066	.87266
12	.80066	.95993
13	.80066	1.04720
14	.80066	1.13446
15	.80066	1.22173
16	.80066	1.30900
17	.80066	1.39626
18	.80066	1.48353
19	.88962	1.57080
20	1.06755	1.65806
21	1.06755	1.74533
22	1.06755	1.83260
23	1.06755	1.91986
24	1.06755	2.00713
25	1.06755	2.09440
26	1.06755	2.18166
27	1.06755	2.26893
28	1.06755	2.35619
29	1.06755	2.44346
30	1.06755	2.53073
31	1.06755	2.61799
32	1.06755	2.70526
33	1.06755	2.79253
34	1.06755	2.87979
35	1.06755	2.96706
36	1.06755	3.05433
37	1.06755	3.14159
38	1.06755	3.22886
39	1.06755	3.31613
40	1.06755	3.40339
41	1.06755	3.49066
42	1.06755	3.57792
43	1.06755	3.66519
44	1.06755	3.75246

45	1.06755	3.83972
46	1.06755	3.92699
47	1.06755	4.01426
48	1.06755	4.10152
49	1.06755	4.18879
50	1.06755	4.27606
51	1.06755	4.36332
52	1.06755	4.45059
53	1.06755	4.53786
54	1.06755	4.62512
55	1.06755	4.71239
56	1.06755	4.79966
57	1.06755	4.88692
58	1.06755	4.97419
59	1.06755	5.06145
60	1.06755	5.14872
61	1.06755	5.23599
62	1.06755	5.32325
63	1.06755	5.41052
64	1.06755	5.49779
65	1.06755	5.58505
66	1.06755	5.67232
67	1.06755	5.75959
68	1.06755	5.84685
69	1.06755	5.93412
70	1.06755	6.02139
71	1.06755	6.10865
72	1.06755	6.19592
73	.88962	6.28319

OUPIER COEFFICIENTS

I	$A(I)/AVE$	$B(I)/AVE$	$C(I)/AVE$	$PHI(I)$
1	-0.08578	-0.08578	.12131	.78540
2	-0.00000	-0.08495	.08495	.00000
3	.02749	-0.02749	.03888	-0.78540
4	-0.00165	.00000	.00165	-1.57080
5	-0.01782	-0.01782	.02520	.78540
6	-0.00000	-0.02833	.02833	.00000
7	.01132	-0.01132	.01601	-0.78540
8	-0.00165	.00000	.00165	-1.57080
9	-0.01028	-0.01028	.01454	.78540
10	-0.00000	-0.01705	.01705	.00000
11	.00694	-0.00694	.00981	-0.78540
12	-0.00165	.00000	.00165	-1.57080
13	-0.00743	-0.00743	.01051	.78540
14	-0.00000	-0.01232	.01232	.00000
15	.00496	-0.00496	.00701	-0.78540
16	-0.00165	.00000	.00165	-1.57080
17	-0.00600	-0.00600	.00849	.78540
18	-0.00000	-0.00988	.00988	.00000

TAU1	TAU2	KC
3.50000	3.50000	.10000

HARMONIC NO	PHASE ANGLE	AMPLITUDE RATIO
1	1.22145	.67114
2	1.90109	.33784
3	2.25275	.18484
4	2.45554	.11312

5	2.58499	.07547
6	2.67411	.05365
7	2.73896	.03998
8	2.78817	.03090
9	2.82676	.02458
10	2.85780	.02000
11	2.88330	.01659
12	2.90461	.01397
13	2.92269	.01193
14	2.93821	.01031
15	2.95169	.00899
16	2.96349	.00791
17	2.97392	.00701
18	2.98319	.00626

LOSS IN STALL PRESS RATIO   NORMALIZED LOSS
  .11709   .58737

	PT2 INST	THETA	THETA	PT2INST	PT2 EFF	SPR LOSS
1	1.04538	0	0	.92999	1.06483	-0.06483
2	.91047	.08727	5.00000	.80997	1.06299	-0.06299
3	.87420	.17453	10.00000	.77771	1.05816	-0.05816
4	.90089	.26180	15.00000	.80145	1.05061	-0.05061
5	.90916	.34907	20.00000	.80881	1.04128	-0.04128
6	.89362	.43633	25.00000	.79498	1.03079	-0.03079
7	.89282	.52360	30.00000	.79427	1.01940	-0.01940
8	.90316	.61087	35.00000	.80347	1.00744	-0.00744
9	.89977	.69813	40.00000	.80045	.99530	.00470
10	.89302	.78540	45.00000	.79445	.98315	.01685
11	.89977	.87266	50.00000	.80045	.97111	.02889
12	.90316	.95993	55.00000	.80347	.95939	.04061
13	.89282	1.04720	60.00000	.79427	.94809	.05191
14	.89362	1.13446	65.00000	.79498	.93718	.06282
15	.90916	1.22173	70.00000	.80881	.92674	.07326
16	.90089	1.30900	75.00000	.80145	.91697	.08303
17	.87420	1.39626	80.00000	.77771	.90773	.09227
18	.91047	1.48353	85.00000	.80997	.89881	.10119
19	1.04538	1.57080	90.00000	.92999	.89077	.10923
20	1.18589	1.65806	95.00000	1.05499	.88509	.11491
21	1.22771	1.74533	100.00000	1.09220	.88291	.11709
22	1.19522	1.83260	105.00000	1.06329	.88401	.11599
23	1.18125	1.91986	110.00000	1.05087	.88734	.11266
24	1.20303	2.00713	115.00000	1.07024	.89223	.10777
25	1.20985	2.09440	120.00000	1.07631	.89847	.10153
26	1.19257	2.18166	125.00000	1.06094	.90575	.09425
27	1.18934	2.26893	130.00000	1.05806	.91356	.08644
28	1.20415	2.35619	135.00000	1.07124	.92166	.07834
29	1.20505	2.44346	140.00000	1.07204	.93002	.06998
30	1.19171	2.53073	145.00000	1.06017	.93846	.06154
31	1.19263	2.61799	150.00000	1.06099	.94673	.05327
32	1.20523	2.70526	155.00000	1.07219	.95475	.04525
33	1.20258	2.79253	160.00000	1.06984	.96261	.03739
34	1.18966	2.87979	165.00000	1.05834	.97019	.02981
35	1.19461	2.96706	170.00000	1.06275	.97732	.02268
36	1.21369	3.05433	175.00000	1.07972	.98408	.01592
37	1.21758	3.14159	180.00000	1.08319	.99064	.00936
38	1.20387	3.22886	185.00000	1.07099	.99701	.00299
39	1.19607	3.31613	190.00000	1.06405	1.00299	-0.00299
40	1.19943	3.40339	195.00000	1.06703	1.00850	-0.00850
41	1.19960	3.49066	200.00000	1.06719	1.01360	-0.01360

122

42	1.19556	3.57792	205.00000	1.06359	1.01830	-0.01830
43	1.19729	3.66519	210.00000	1.06514	1.02259	-0.02259
44	1.20120	3.75246	215.00000	1.06862	1.02653	-0.02653
45	1.19843	3.83972	220.00000	1.06615	1.03016	-0.03016
46	1.19497	3.92699	225.00000	1.06307	1.03349	-0.03349
47	1.19843	4.01426	230.00000	1.06615	1.03650	-0.03650
48	1.20120	4.10152	235.00000	1.06862	1.03925	-0.03925
49	1.19729	4.18879	240.00000	1.06514	1.04179	-0.04179
50	1.19556	4.27606	245.00000	1.06359	1.04409	-0.04409
51	1.19960	4.36332	250.00000	1.06719	1.04616	-0.04616
52	1.19943	4.45059	255.00000	1.06703	1.04805	-0.04805
53	1.19607	4.53786	260.00000	1.06405	1.04979	-0.04979
54	1.20387	4.62512	265.00000	1.07099	1.05135	-0.05135
55	1.21758	4.71239	270.00000	1.08319	1.05284	-0.05284
56	1.21369	4.79966	275.00000	1.07972	1.05441	-0.05441
57	1.19461	4.88692	280.00000	1.06275	1.05596	-0.05596
58	1.18966	4.97419	285.00000	1.05834	1.05727	-0.05727
59	1.20258	5.06145	290.00000	1.06984	1.05832	-0.05832
60	1.20523	5.14872	295.00000	1.07219	1.05930	-0.05930
61	1.19263	5.23599	300.00000	1.06099	1.06021	-0.06021
62	1.19171	5.32325	305.00000	1.06017	1.06095	-0.06095
63	1.20505	5.41052	310.00000	1.07204	1.06153	-0.06153
64	1.20415	5.49779	315.00000	1.07124	1.06212	-0.06212
65	1.18934	5.58505	320.00000	1.05806	1.06268	-0.06268
66	1.19257	5.67232	325.00000	1.06094	1.06307	-0.06307
67	1.20985	5.75959	330.00000	1.07631	1.06337	-0.06337
68	1.20303	5.84685	335.00000	1.07024	1.06375	-0.06375
69	1.18125	5.93412	340.00000	1.05087	1.06411	-0.06411
70	1.19522	6.02139	345.00000	1.06329	1.06426	-0.06426
71	1.22771	6.10865	350.00000	1.09220	1.06438	-0.06438
72	1.18589	6.19592	355.00000	1.05499	1.06479	-0.06479
73	1.04538	6.28319	360.00000	.92999	1.06483	-0.06483

INPUT RPI/RP0	RP(FFF)/RP0
1.11038	.93517
1.19934	.93701
1.19934	.94184
1.19934	.94939
1.19934	.95872
1.19934	.96921
1.19934	.98060
1.19934	.99256
1.19934	1.00470
1.19934	1.01685
1.19934	1.02889
1.19934	1.04061
1.19934	1.05191
1.19934	1.06282
1.19934	1.07326
1.19934	1.08303
1.19934	1.09227
1.19934	1.10119
1.11038	1.10923
.93245	1.11491
.93245	1.11709
.93245	1.11599
.93245	1.11266
.93245	1.10777
.93245	1.10153
.93245	1.09425
.93245	1.08644

.93245	1.07834
.93245	1.06998
.93245	1.06154
.93245	1.05327
.93245	1.04525
.93245	1.03739
.93245	1.02981
.93245	1.02268
.93245	1.01592
.93245	1.00936
.93245	1.00299
.93245	.99701
.93245	.99150
.93245	.98640
.93245	.98170
.93245	.97741
.93245	.97347
.93245	.96984
.93245	.96651
.93245	.96350
.93245	.96075
.93245	.95821
.93245	.95591
.93245	.95384
.93245	.95195
.93245	.95021
.93245	.94865
.93245	.94716
.93245	.94559
.93245	.94414
.93245	.94273
.93245	.94168
.93245	.94070
.93245	.93979
.93245	.93905
.93245	.93847
.93245	.93788
.93245	.93732
.93245	.93693
.93245	.93663
.93245	.93625
.93245	.93589
.93245	.93574
.93245	.93562
.93245	.93521
1.11038	.93517
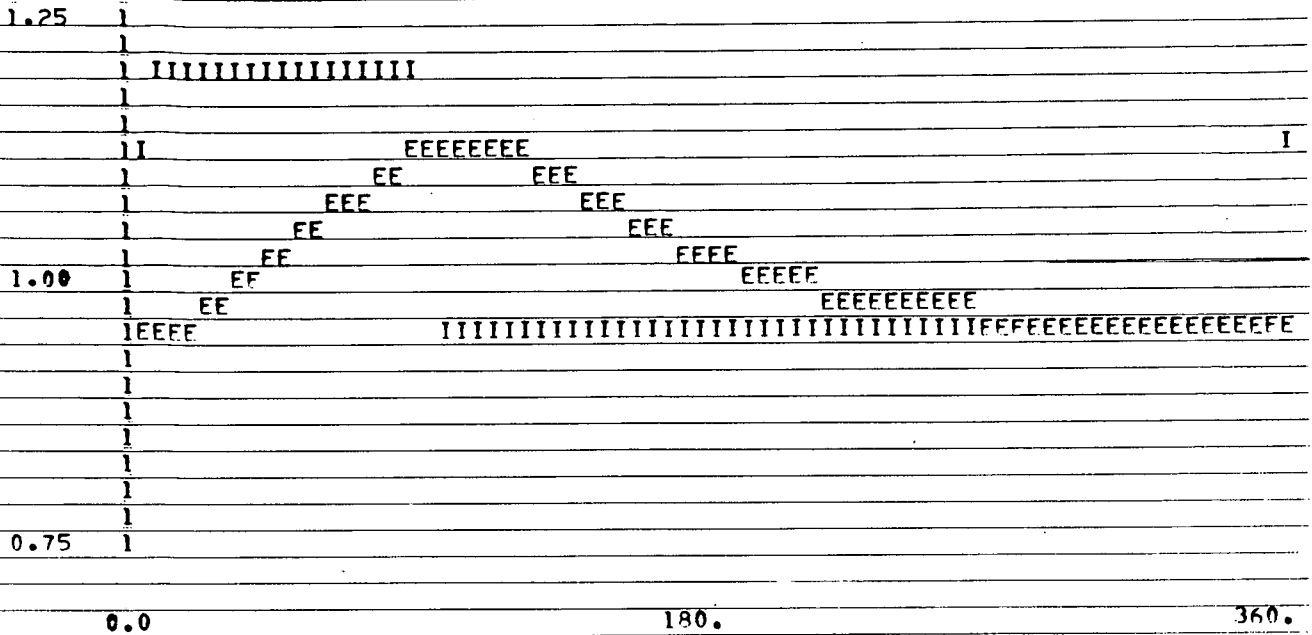
```
                              RPI/RPO  =INPUT=I
                              RP(EFF)/RPO=OUTPUT=E


 1.25   1
        1
        1 IIIIIIIIIIIIIIIII
        1
        1
        1I              EEEEEEEE                                                    I
        1              EE        EEE
        1            EEE            EEE
        1           EE              EEE
        1          EE              FFFF
 1.00   1        EF                     EEEEE
        1       EE                           EEEEEEEEEE
        1EEEE                    IIIIIIIIIIIIIIIIIIIIIIIIIIIIIIIIIIIIFEFEEEEEEEEEEEEEEEEEFE
        1
        1
        1
        1
        1
        1
        1
 0.75   1


      0.0                          180.                           360.


                    CIRCUMFERENTIAL POSITION . DEGREES
```

125

SYS ORDR	KC	TAU1	TAU2	LONG/SHORT PRINT OUT
2	.10000	3.50000	3.50000	2
1	2	.20000		

SINE WAVE INPUT
AMPLITUDE MULTIPLE/PEV NO.
    .20000   2.00000

OUTPUT DATA
PT AVG
    1.00000

TAU1	TAU2	KC
3.50000	3.50000	.10000

LOSS IN STALL PRESS RATIO	NORMALIZED LOSS
.06756	.33778

RPI/RPO =INPUT=I
RP(EFF)/RPO=OUTPUT=F
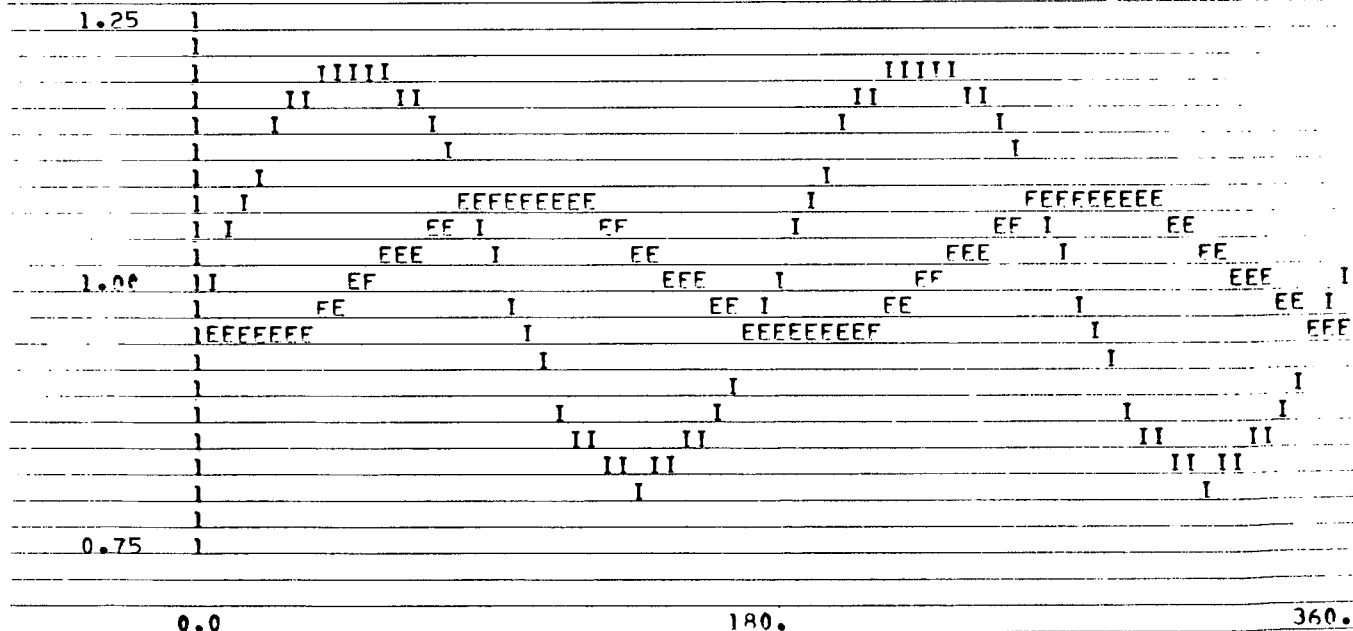
```
   1.25    I
           I
           I        IIIII                              IIIII
           I       II      II                        II      II
           I     I            I                      I            I
           I                   I                                 I
           I    I                                   I
           I   I              EEEEEEEEE             I              FEEEEEEEE
           I I             EE I        FF           I            EF I        EE
           I           EEE     I        EE                     FFF     I      FE
   1.00    II        EF                  EEE      I      FF          EEE
           I        FE          I          EE I        EE       I          EE I
           IEEEEEEE               I          EEEEEEEEF             I          FFF
           I                       I                                I            I
           I                        I         I                        I          I
           I                          II      II                        II      II
           I                           II II                             II II
           I                             I                                I
           I
   0.75    I

        0.0                            180.                            360.


                        CIRCUMFERENTIAL POSITION , DEGREES
```

126

SYS ORDR	KC	TAU1	TAU2	LONG/SHORT PRINT OUT
2	.10000	3.50000	3.50000	2

INPUT PT   THETA

1.00000	0	.90000	90.00000	1.00000	180.00000	1.05000	265.00000
1.20000	270.00000	1.05000	275.00000				

OUTPUT DATA
PT AVG
   .98960

TAU1	TAU2	KC
3.50000	3.50000	.10000

LOSS IN STALL PRESS RATIO	NORMALIZED LOSS
.04166	.46008

```
                              RPI/RPO  =INPUT=I
                              RP(EFF)/RPO=OUTPUT=F


   1.25    I
           I
           I
           I
           I
           I
           I                          IIIII
           I                 IIIII          IIIII
           I             IIII             EEEEEEEEEEEEEEEEEEEEEEEEE
           I   IIIII           EEEEEEEE        IIIII             EEEEEEE
   1.00    III     FEEEEEE                          IIIIII            EEEEEE              IIIII
           IEEEEEEE                                 IIIIIIIII       EEEEEEEEEEEEEEEEEE
           I                                            IIII  IIII
           I
           I
           I
           I
           I                                                        I
           I
   0.75    I


           0.0                                   180.                                  360.


                      CIRCUMFERENTIAL POSITION . DEGREES
```

APPENDIX F

Solutions of the Navier Stokes Equations for Vortex Flow

Definition of several vortex flow fields are developed below by solution of the Navier-Stokes Equations for both a steady and for a time dependent vortex. The choice of a vortex for use in describing turbulent flow will be made and the boundary conditions leading to this choice discussed.

Navier Stokes Equations of Motion: Using the cylindrical coordinate system shown below
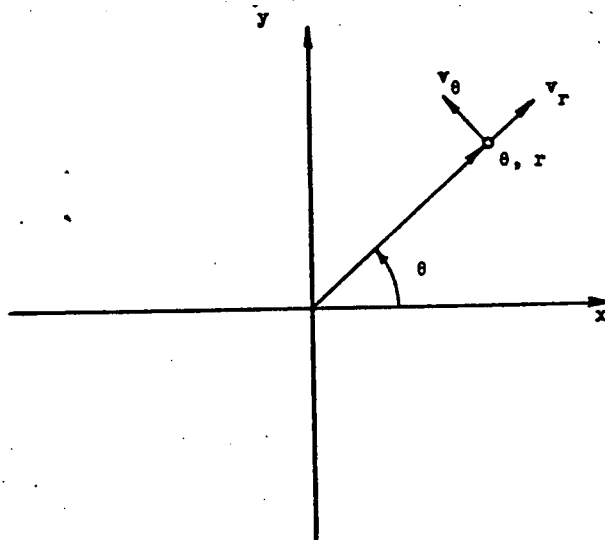
CYLINDRICAL COORDINATE SYSTEM

the equations of Motion of an incompressible viscous fluid in two dimensions are:

$$\frac{\partial v_r}{\partial t} + v_r \frac{\partial v_r}{\partial r} + \frac{v_\theta}{r} \frac{\partial v_r}{\partial \theta} - \frac{v_\theta^2}{r} = F_r - \frac{1}{\rho} \frac{\partial P}{\partial r} + \nu \left\{ \frac{\partial^2 v_r}{\partial r^2} + \frac{1}{r} \frac{\partial v_r}{\partial r} + \frac{1}{r^2} \left(\frac{\partial^2 v_r}{\partial \theta^2} - 2 \frac{\partial v_\theta}{\partial \theta} - v_r \right) \right\}$$

(F-1)

$$\frac{\partial v_\theta}{\partial t} + v_r \frac{\partial v_\theta}{\partial r} + \frac{v_\theta}{r} \frac{\partial r_\theta}{\partial \theta} + \frac{v_\theta v_r}{r} = F_r - \frac{1}{\rho} \frac{\partial P}{\partial \theta} + \nu \left\{ \frac{\partial^2 v_\theta}{\partial r^2} + \frac{1}{r} \frac{\partial v_\theta}{\partial r} + \frac{1}{r^2} \left(\frac{\partial^2 v_\theta}{\partial \theta^2} + 2 \frac{\partial v_r}{\partial \theta} - v_\theta \right) \right\}$$

(F-2)

Continuity:

$$\frac{\partial}{\partial r} (r v_r) + \frac{\partial v_\theta}{\partial \theta} = 0$$

(F-3)

For the vortex model, F_θ and F_r are zero and the pressure P and velocities v_r and v_θ are independent of θ. Further assume that no source or sink occurs

within the area enclosing the vortex, in which case $v_r = 0$. Equation (F-2) then reduces to the following:

$$\frac{\partial v_\theta}{\partial t} = \nu \left[\frac{\partial^2 v_\theta}{\partial r^2} + \frac{1}{r} \frac{\partial v_\theta}{\partial r} - \frac{1}{r} v_\theta \right] \qquad \text{(F-4)}$$

<u>Solution of the Navier Stokes Equations.</u> - There are several solutions of equation (F-4), each representing a different set of physical boundary conditions. Five of these solutions are discussed.

For a steady flow v_θ is independent of time and equation (F-4) reduces to the following:

$$\frac{\partial^2 v_\theta}{\partial r^2} + \frac{1}{r} \frac{\partial v_\theta}{\partial r} - \frac{1}{r^2} v_\theta = 0 \qquad \text{(F-5)}$$

The two solutions are:

    (a) For forced vortex (solid body rotation):

$$v_\theta = k_1 r \qquad \text{(F-6)}$$

        This is shown in Figure F-1.

    (b) For a Potential (free) vortex:

$$v_\theta = k_2/r \qquad \text{(F-7)}$$

        This is shown in Figure F-2.

A combination of equations F-6 and F-7 has been used to approximate a viscous flow model. Specifically, the following form results and is shown in Figure F-3.

$$v_\theta = \frac{kr}{1+r^2} \qquad \text{(F-8)}$$

This satisfies the Navier-Stokes equations when $r \ll 1$ or when $r \gg 1$; not, however, at $r = 1$ (see Figure F-4). Viscous effects cause non-recoverable losses. These losses dictate the vortex velocity and energy decrease with time. As a consequence a solution containing viscous dissipation must be time dependent and no steady state solution that fits the boundary conditions imposed by real flows can be found.

For unsteady flow, three basic solutions have been found. The first is as follows:

$$v_\theta = \frac{\Gamma_0}{2\pi r} \left\{ 1 - e^{-\frac{r^2}{4\nu t}} \right\} \qquad \text{(F-9)}$$

130
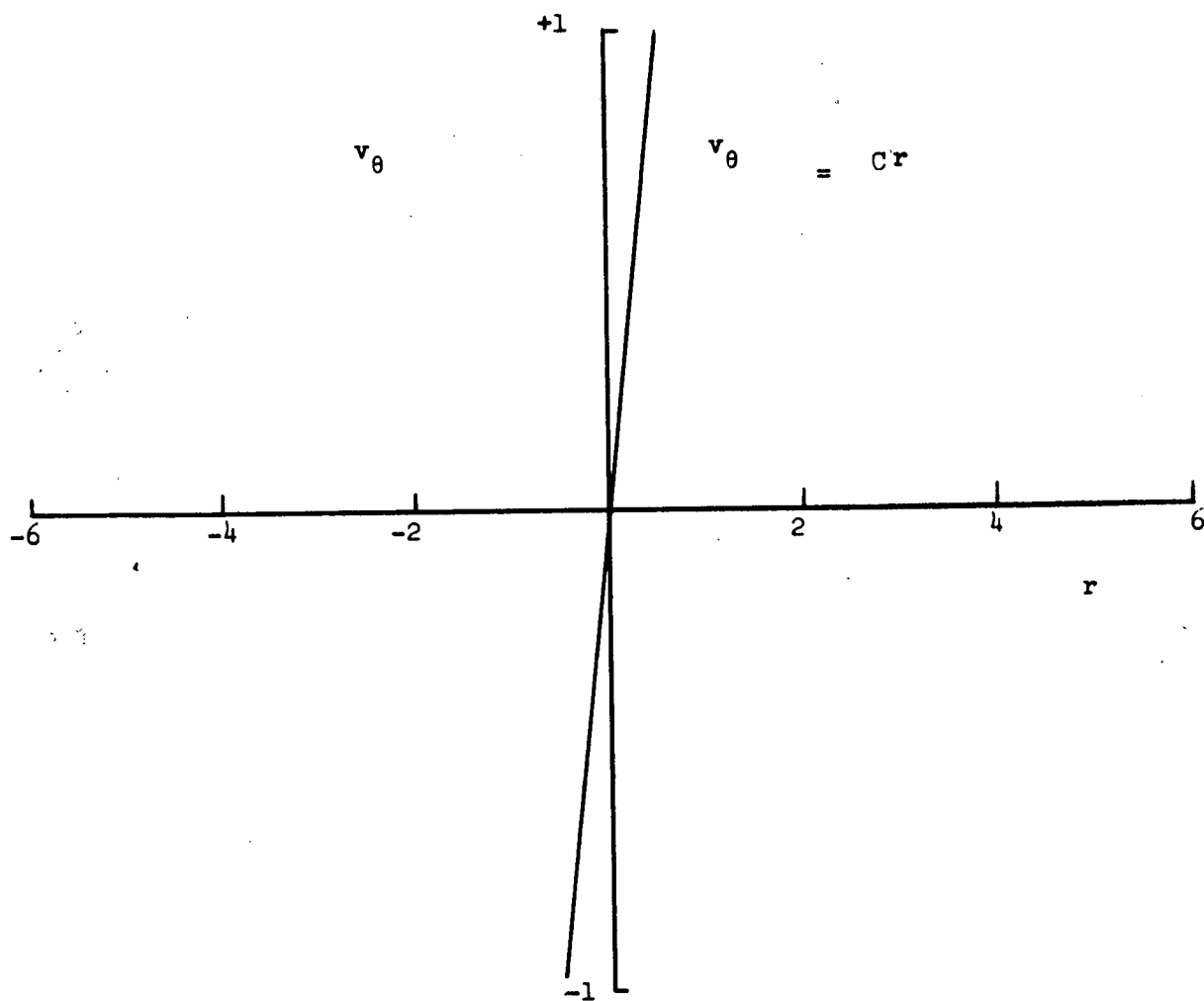
Figure F-1. Velocity Ratio of a Steady Forced Vortex
(Solid Body Rotation) --- Equation (F-6).
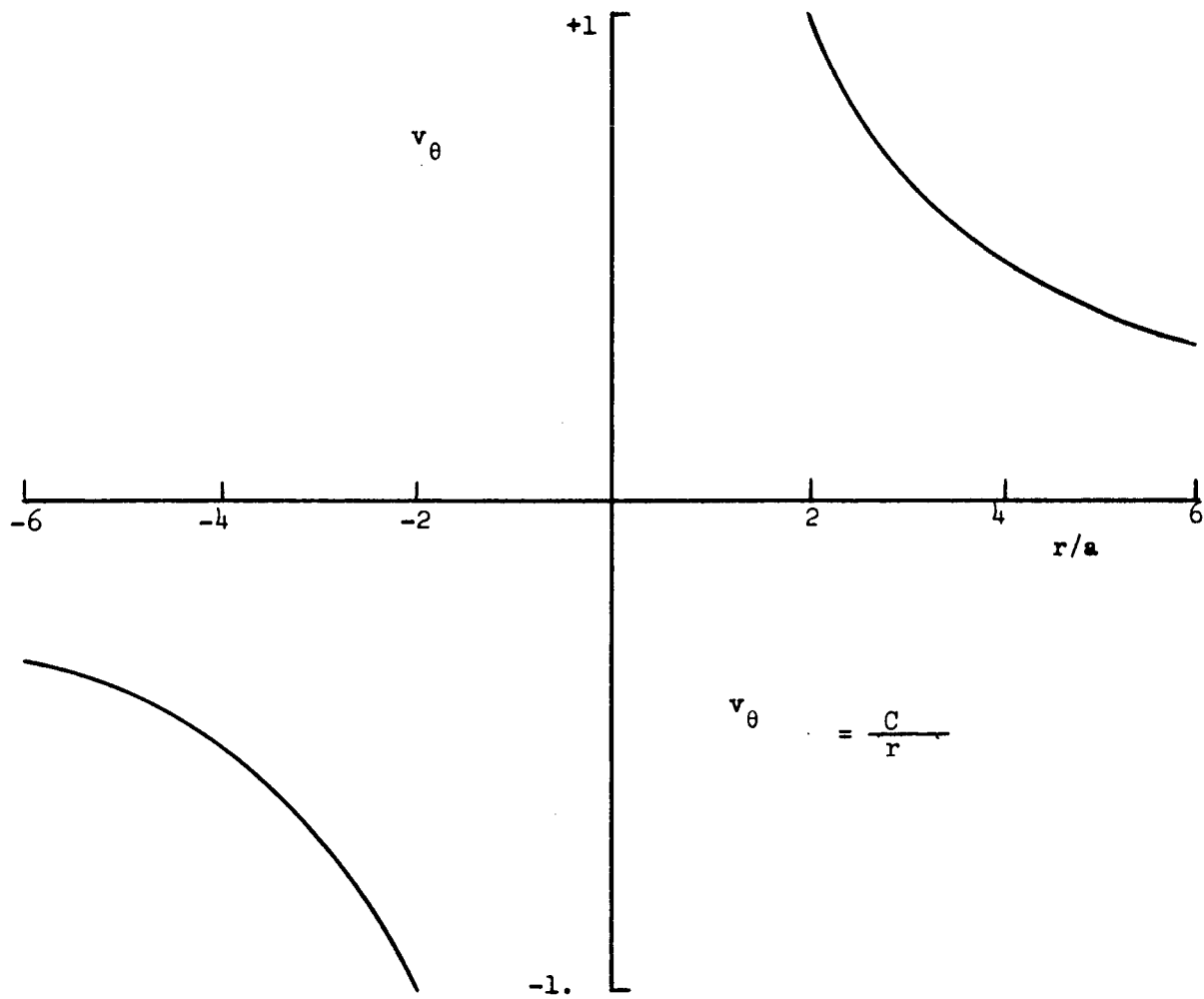
Figure F-2. Velocity Ratios of a Steady Potential
Vortex --- Equation (F-7).
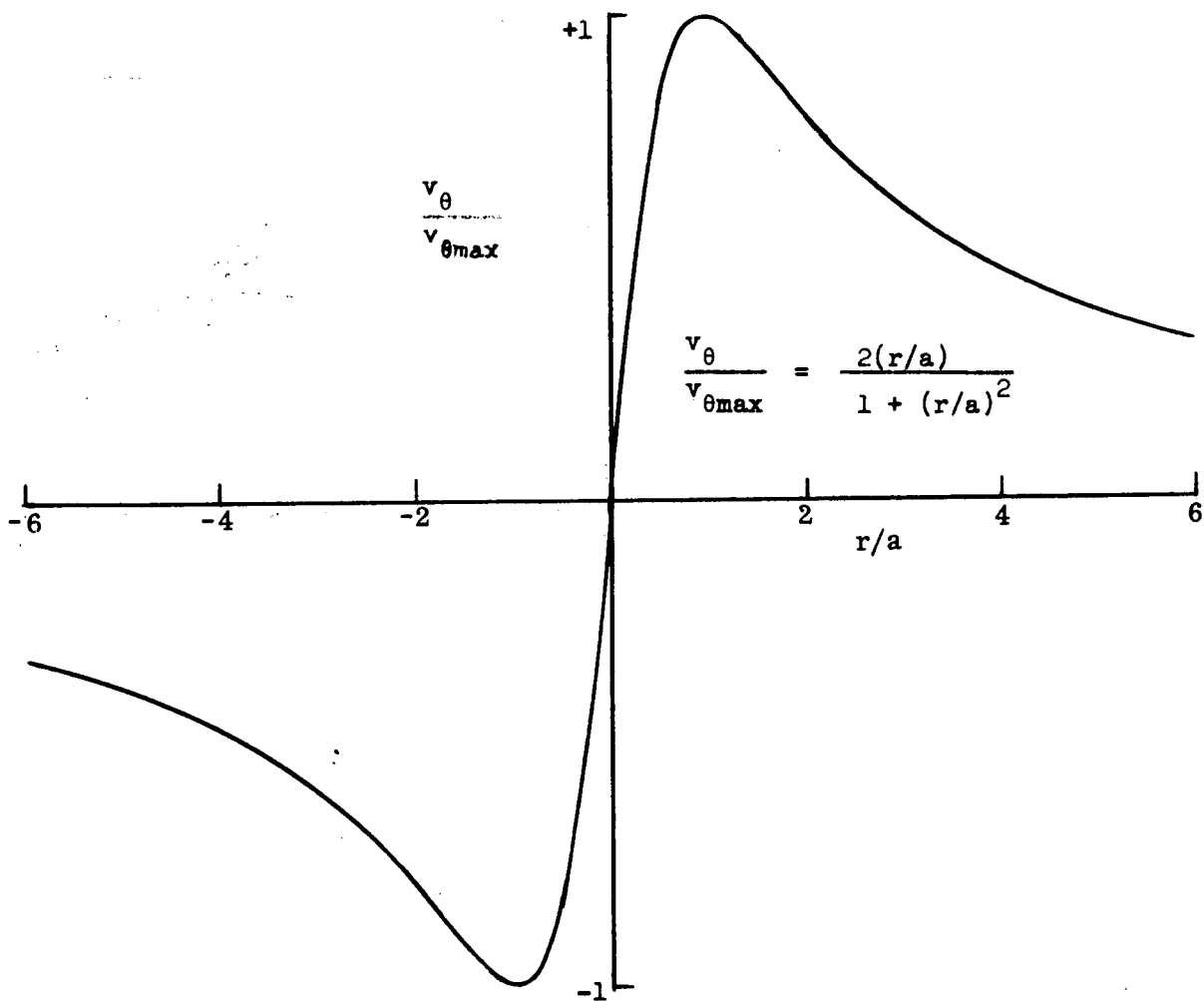
Figure F-3. Approximation to a Vortex Having a Forced Rotation
Near the Center and a Potential Motion at Large Radii ---
Equation (F-8).
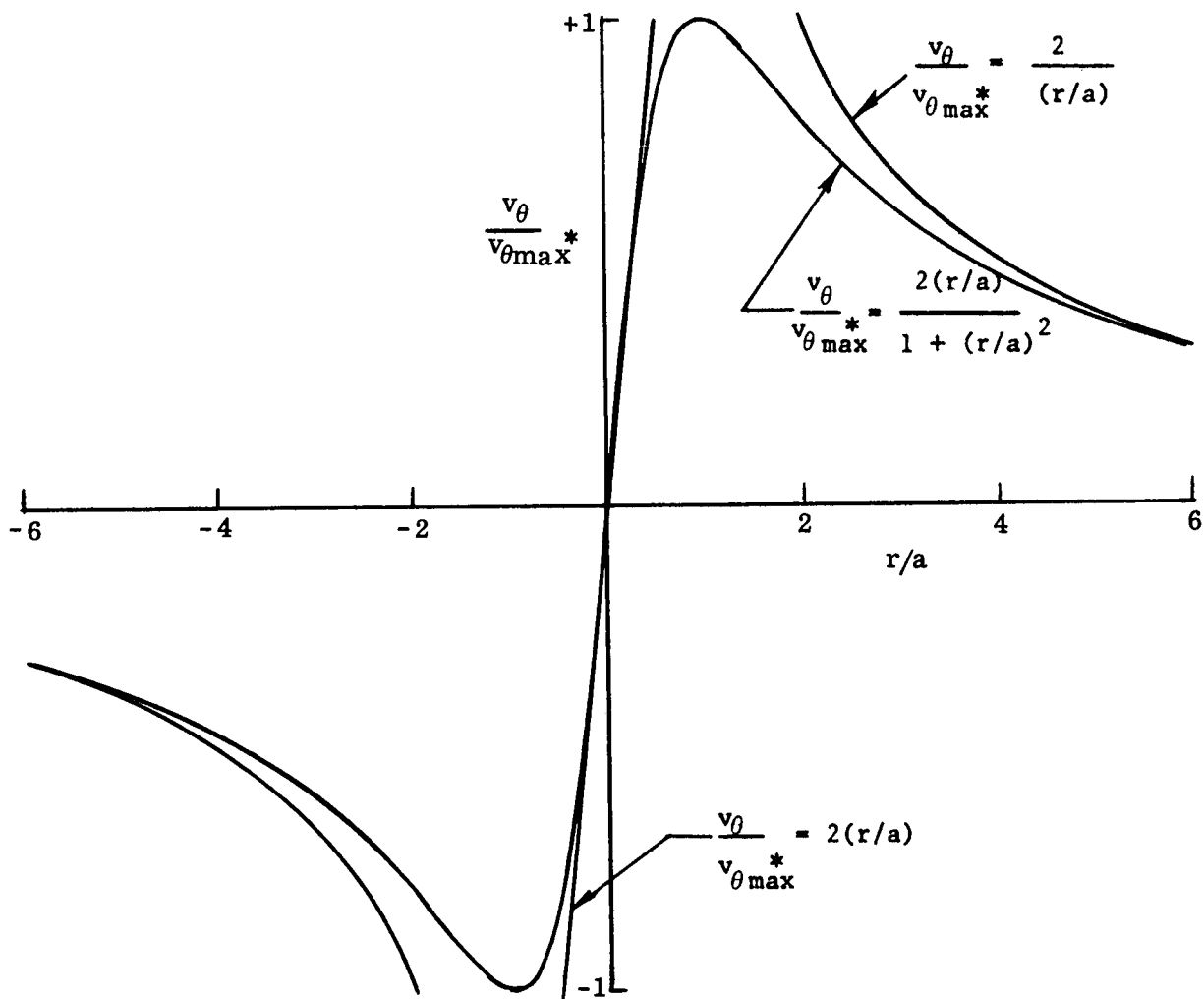
Figure F-4. Comparison of the Approximation with the Two Steady Solutions of the Navier-Stokes Equations.

$$\frac{v_\theta}{v_{\theta\,max}^*} = \frac{2}{(r/a)}$$

$$\frac{v_\theta}{v_{\theta\,max}^*} = \frac{2(r/a)}{1 + (r/a)^2}$$

$$\frac{v_\theta}{v_{\theta\,max}^*} = 2(r/a)$$

134

This represents a vortex that at zero time has a potential flow field. At t > 0, viscosity effects begin to cause the vortex to decay as shown in Figure F-5. The radius, r_o shown in Figure F-5 is that arbitrary radius having the velocity, v_θ, at time equal to zero. This solution is given, for example, in Reference 14 page 81.

A second solution exists for a vortex that is started impulsively at time t = 0, having a strength concentrated within a zero radius (a Delta function). At time t = 0 the influence of this line vortex spreads. The normalized shape of this vortex is shown in Figure F-6, and compared with the other vortex flow fields in Figure F-7. This particular solution is attributed to G. I. Taylor in Reference (15).

Its equation is given below:

$$v_\theta = B \frac{r}{t^2} e^{-\frac{r^2}{4\nu t}} \tag{F-10}$$

It will be assumed that this model most nearly represents the type of vortices in turbulent flow where the influence of a formed vortex is at first limited but increases radially with time. Reasons for this selection are discussed below in Appendix G.

A set of additional solutions to the Navier-Stokes equations can be found by the technique of separation of variables. These solutions are as follows:

$$v_\theta = e^{-\lambda^2 t} Z(u) \tag{F-11}$$

where: $Z(u) = J_1(u), J_{-1}(u), Y_1(u), H_1^1(u), H_2^1(u)$

$J_1(u)$ = Bessel Function of the first kind of order 1

$J_{-1}(u)$ = Bessel Function of the first kind of order -1

$Y_1(u)$ = Bessel Function of the second kind of order 1

$H_1^1(u)$ = Hankel Function of the first kind of order 1

$H_2^1(u)$ = Hankel Function of the second kind of order 1

$u^2 = (\lambda^2 r^2)/\nu$

These solutions however are oscillating with radius and as a result do not fit the boundary conditions of the problem at hand.

135
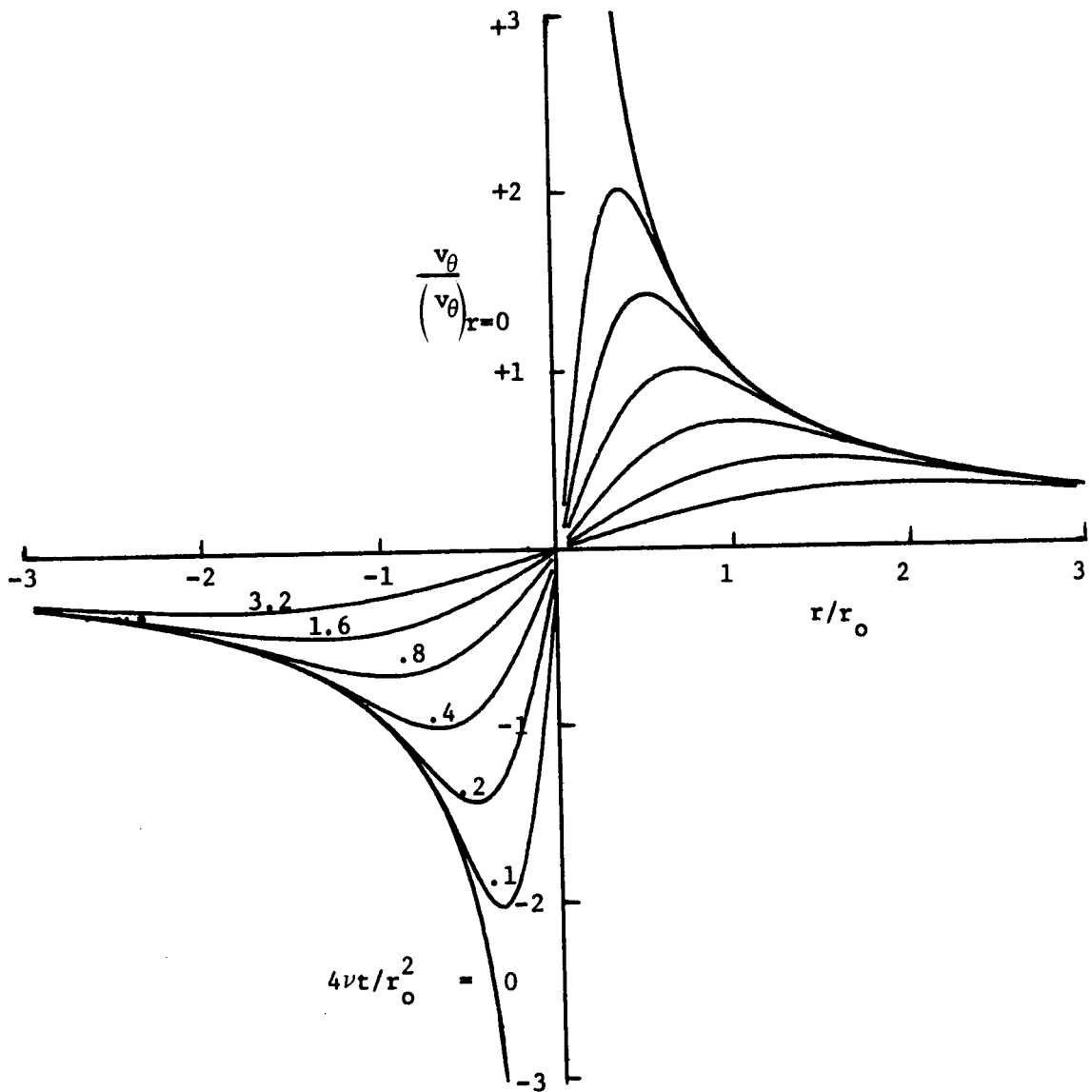
Figure F-5. Velocity Ratio for a Potential Vortex Allowed to Begin
Viscous Decay at Time Zero. --- Equation (F-9).
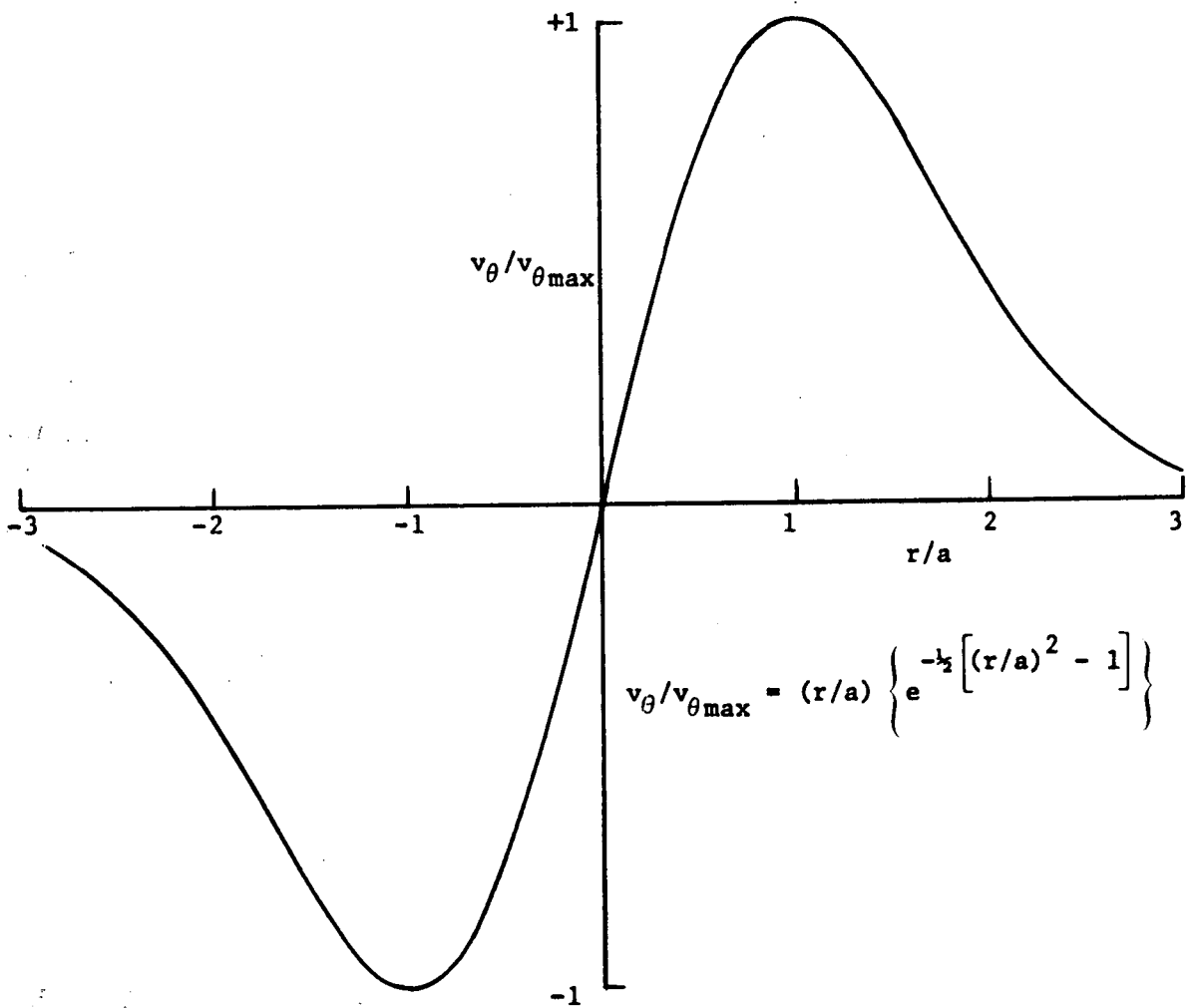
Figure F-6. Velocity Ratio of a Vortex Started Impulsively at Time Zero
--- Equation (F-10).

$$v_\theta/v_{\theta max} = (r/a) \left\{ e^{-\frac{1}{2}\left[(r/a)^2 - 1\right]} \right\}$$
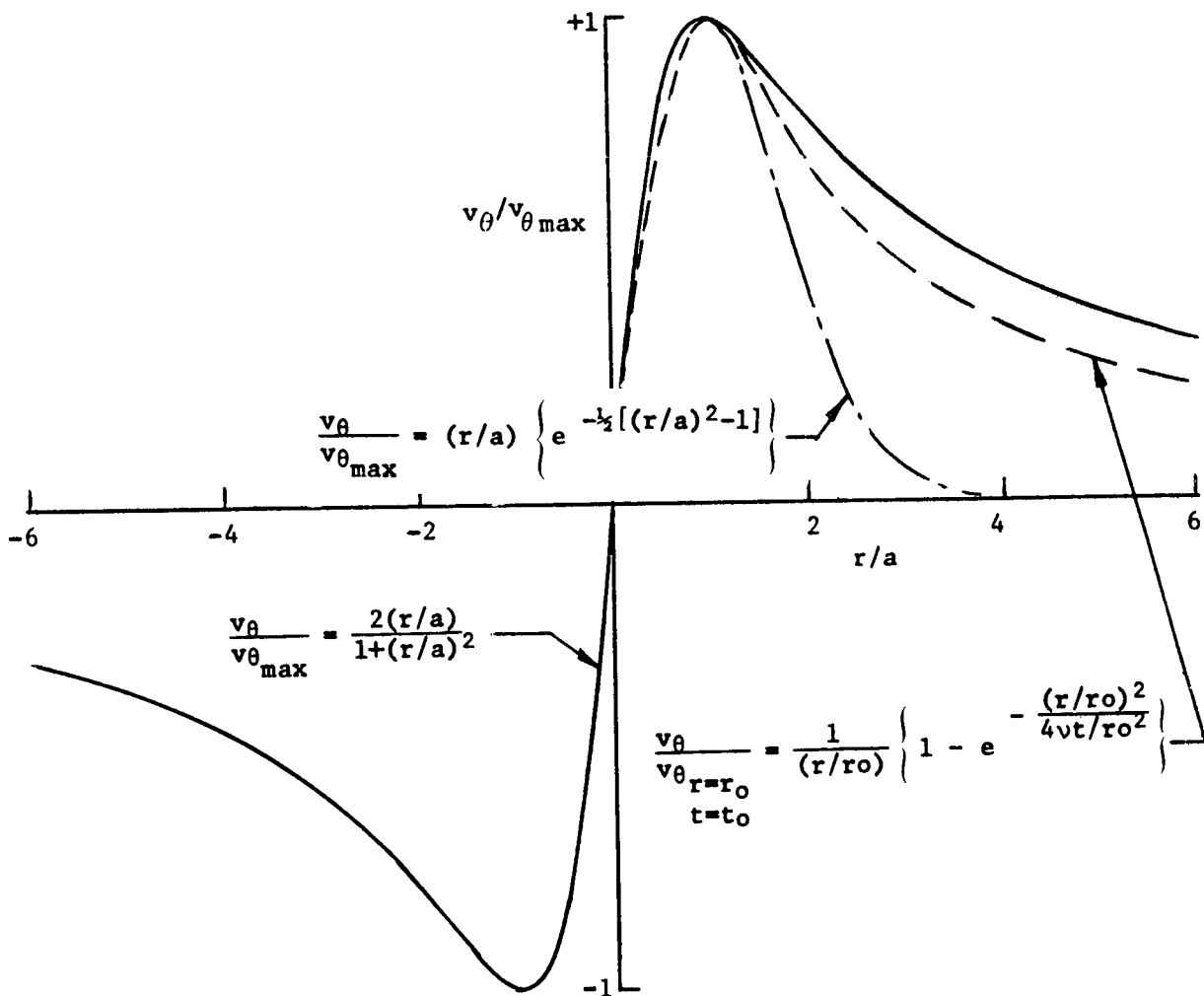
Figure F-7. A Comparison of the Vortex Velocity Ratio for Three Flow Fields Satisfying the Three Different Boundary Conditions.

The following equations appear as labels within the figure:

$$\frac{v_\theta}{v_{\theta_{max}}} = (r/a) \left\{ e^{-\frac{1}{2}[(r/a)^2-1]} \right\}$$

$$\frac{v_\theta}{v_{\theta_{max}}} = \frac{2(r/a)}{1+(r/a)^2}$$

$$\frac{v_\theta}{v_{\theta_{\substack{r=r_0 \\ t=t_0}}}} = \frac{1}{(r/r_0)} \left\{ 1 - e^{-\frac{(r/r_0)^2}{4\nu t/r_0^2}} \right\}$$

APPENDIX G

Boundary Conditions for Vortex Model

For the purposes of developing a fluid dynamic model of turbulent flow certain boundary conditions must be imposed on the vortex description that meet the physical conditions associated with the turbulent eddies. These are assumed to be as below:

(a) v_θ must be zero at a vortex radius of zero (viscous forces predominate).

(b) v_θ must be zero at a vortex radius of infinity.

(c) v_θ must be continuous between $0 \le r \le \infty$ and satisfy the equations of motion.

(d) The zone of influence of an eddy or vortex must be small at first, as when it first forms, and grow with time; as opposed to an eddy that is fully established at all radii, then proceeds to decay, i.e. the transfer of momentum is outward with time.

A summary of various vortex flows is given in Table G-1 along with a graphical representation of the vortex and its respective ability to meet the boundary conditions. The Figure numbers in the Table refer to Appendix F. As shown, only the vortex formed by the impulsive start meets all the required boundary conditions. For this reason it was chosen as a typical vortex in turbulent flow and will be used in further development of the fluid dynamic model of turbulent flow.

A word of caution, however, the vortex proposed assumes a laminar viscosity coefficient. Bear in mind that any given vortex may have smaller eddies forming in the core which in themselves may produce "turbulent" flow in which case decay would be governed by an eddy viscosity and occur an order of magnitude faster. This turbulence could also cause modification of the velocity profile. Because of the assumption to use a laminar viscosity coefficient or specifically a viscosity coefficient independent of both radius and time, and because of the assumed impulse start of the vortex, the option must remain open to select other vortex velocity fields subject to experimental verification.

DESCRIPTION	SATISFIES EQUATIONS OF MOTION STEADY	UNSTEADY	GOVERNING EQUATION	MEETS FOLLOWING BOUNDARY CONDITIONS $v_\theta = 0$ @ r=0	$v_\theta = 0$ @ r=∞	CONTINUOUS $0 \le r \le \pm\infty$	DIRECTION OF INFLUENCE OUTWARD WITH TIME	FIGURE NUMBER
Forced Vortex (Solid Body Rotation)	Yes	No	$v_\theta = k_1 r$	Yes	No	Yes	—	F-1
Free Vortex (Potential Flow)	Yes	No	$v_\theta = \kappa_2 / r$	No	Yes	Yes	—	F-2
Forced Vortex $r/a \ll 1$ Free Vortex $r/a \gg 1$	No	No	$\dfrac{v_\theta}{v_{\theta max}} = \dfrac{2(r/a)}{1+(r/a)^2}$	Yes	Yes	Yes	—	F-3
Potential Vortex @ $t \lessgtr 0$, Viscous Decay Beginning at $t = 0^+$	No	Yes	$\dfrac{v_\theta}{(v_\theta)_{\substack{r=0\\t=0}}} = \dfrac{1}{r/r_0}\left\{1 - e^{-\frac{(r/r_0)^2}{4\nu t/r_0^2}}\right\}$	Yes	Yes	Yes	Neutral	F-5
Impulse Vorticity @ $t = 0$. Propagation and Decay Beginning at $t = 0^+$	No	Yes	$\dfrac{v_\theta}{v_{\theta max}} = \dfrac{r}{a}\left\{e^{-\frac{1}{2}\left[\left(\frac{r}{a}\right)^2 - 1\right]}\right\}$	Yes	Yes	Yes	Yes	F-6
Vortex Velocity Oscillating With Radius	No	Yes	$v_\theta = Z_1(u)$ (See Equation 20)	Yes	Yes	Yes	Neutral	—

APPENDIX H

Details of the Selected Vortex Flow Field

A vortex flow field that satisfies the unsteady Navier-Stokes Equations and the proper boundary conditions was selected as representative of those eddies typical of inlet turbulent flow. This particular solution was first given by G. I. Taylor in 1918 and represents a vortex formed instantaneously in undisturbed flow. The influence of this impulse begins to propagate outward at $t = 0^+$. Table H-1 is presented in summary giving the velocity, angular momentum, vorticity, circulation, and static pressure distributions of the vortex along with the rates of decay of each parameter. Derivation of the characteristics and graphical representations follow.

Velocity. - The vortex flow field selected for detailed study is defined below:

$$v_\theta = B \frac{r}{t^2} e^{-\frac{r^2}{4\nu t}} \tag{H-1}$$

Where: v_θ = velocity in angular direction

B = constant

r = radius

t = time

ν = kinematic viscosity = μ/ρ

The radius, a, at which the velocity is a maximum can be determined by setting the derivative, $\partial v_\theta / \partial r$, equal to zero or

$$\frac{\partial v_\theta}{\partial r} = \frac{B}{t^2} e^{-\frac{r^2}{4\nu t}} - \frac{2Br^2}{4\nu t^3} e^{-\frac{r^2}{4\nu t}} = 0$$

Thus:

$$\frac{r^2}{2\nu t} = 1$$

or

$$r_{@v_\theta} = v_{\theta_{Max}} \equiv a = \sqrt{2\nu t} \tag{H-2}$$

Note that a grows at a rate proportional to, $t^{\frac{1}{2}}$. Normalizing the vortex radius by a, Equation H-1 becomes:

TABLE H-1

PROPERTIES OF A VORTEX STARTED BY IMPULSE AT TIME ZERO

PARAMETER	GOVERNING EQUATION	VORTEX RADIUS @ MAXIMUM VALUE	NORMALIZED EQUATION	LAW OF DECAY	RELATED FIGURES
Velocity	$v_\theta = B \dfrac{r}{t^2} e^{-\frac{r^2}{4\nu t}}$	$r = \sqrt{2\nu t} \equiv a$	$\dfrac{v_\theta}{v_{\theta_{max}}} = \dfrac{r}{a}\left\{ e^{-\frac{1}{2}\left(\left(\frac{r}{a}\right)^2 - 1\right)} \right\}$	$\dfrac{(v_{\theta_{max}})_t}{(v_{\theta_{max}})_{t_o}} = \dfrac{1}{(t/t_o)^{3/2}}$	H-1 & -5
Angular Momentum	$M_\omega = \pi \rho B (4\nu)^2$			$M_\omega \neq f(t)$	
Vorticity	$\Omega = e^{-\frac{r^2}{4\nu t}}\left(\dfrac{2B}{t^2} - \dfrac{Br^2}{2\nu t^3}\right)$	$r = 0$ $r = 2a$	$\dfrac{\Omega}{|\Omega|_{max}} = \left(\dfrac{1}{2}\left(\dfrac{r}{a}\right)^2 - 1\right) e^{-\frac{1}{2}\left(\frac{r}{a}\right)^2}$	$\dfrac{(\Omega_{max})_t}{(\Omega_{max})_{t_o}} = \dfrac{1}{(t/t_o)^2}$	H-1 & -5
Circulation	$\Gamma = 2\pi B \dfrac{r^2}{t^2} e^{-\frac{r^2}{4\nu t}}$	$r = \sqrt{2}\, a$	$\dfrac{\Gamma}{\Gamma_{max}} = \dfrac{1}{2}\left(\dfrac{r}{a}\right)^2 e^{-\left(\frac{1}{2}\left(\frac{r}{a}\right)^2 - 1\right)}$	$\dfrac{(\Gamma_{max})_t}{(\Gamma_{max})_{t_o}} - \dfrac{1}{t/t_o}$	H-3 & -5
Static Pressure	$P - P_o = -\rho B^2 \dfrac{\nu}{t^3} e^{-\frac{r^2}{2\nu t}}$	$r = 0$	$\dfrac{P_r - P_o}{P_{r=0} - P_o} = -e^{-\left(\frac{r}{a}\right)^2}$	$\dfrac{(P_{r=0})_t}{(P_{r=0})_{t_o}} = \dfrac{1}{(t/t_o)^3}$	H-4 & -5

$$v_\theta = \frac{\sqrt{2\nu}}{t^{3/2}} B \frac{r}{a} e^{-\frac{1}{2}\left(\frac{r}{a}\right)^2} \qquad (\text{H-3})$$

Normalizing v_θ by the maximum value, the velocity ratio is:

$$\frac{v_\theta}{(v_\theta)_{Max}} = \frac{r}{a} e^{-\frac{1}{2}\left[\left(\frac{r}{a}\right)^2-1\right]} \qquad (\text{H-4})$$

This is shown graphically (for a given time) in Figure H-1.

Vortex Angular Momentum. – The equation of moment of momentum (angular momentum) is as follows:

$$M_\omega = (\vec{V} \times \vec{r})dm \qquad (\text{H-5})$$

where the arrow denotes a vector quantity, "X" a cross (vector) product, and "dm" an elemental mass. In the cylindrical coordinate system

$$\vec{V} = v_\theta \, \vec{\theta}$$

$$\vec{r} = r \, \vec{r}$$

$$m = \rho \times \text{Volume}$$

$$dm = \rho r d\theta dr \text{ (unit depth)}$$

where $\vec{\theta}$ denotes the unit vector in the θ direction

$\vec{r}$ denotes the unit vector in the r direction

Therefore:

$$M_\omega = \int_0^\infty \int_0^{2\pi} v_\theta r \rho r d\theta dr$$
$$= 2\pi\rho \frac{B}{t^2} \int_0^\infty r^3 e^{-\frac{r^2}{4\nu t}} dr$$

To integrate let $\xi = r^2$

$$d\xi = 2rdr$$
$$dr = \frac{d\xi}{2\sqrt{\xi}}$$
$$r^3 = (r^2)^{3/2} = \xi^{3/2}$$
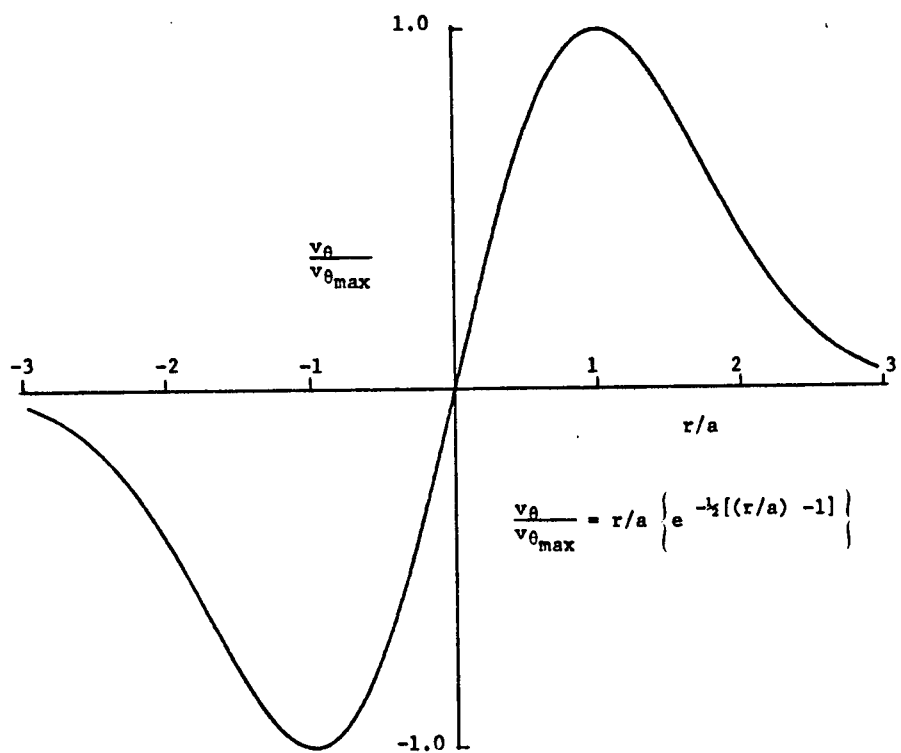
Figure H-1. Velocity Ratio of a Vortex Started Impulsively at Time Zero.

$$\frac{v_\theta}{v_{\theta_{max}}} = r/a \left\{ e^{-\frac{1}{2}[(r/a)^2 -1]} \right\}$$

Thus

$$M_\omega = \pi\rho\frac{B}{t^2}\int_0^\infty \xi \ e^{-\frac{\xi}{4\nu t}} \ d\xi$$

$$M_\omega = \pi\rho B(4\nu)^2 \qquad\qquad (H-6)$$

Note: The angular momentum is independent of time and hence is conserved. Because M_ω is conserved it would be a logical term in which to express the constant "B".

Thus:

$$B = \frac{M_\omega}{\pi\rho(4\nu)^2} \qquad\qquad (H-7)$$

Vorticity.- Vorticity is defined as:

$$\vec{\Omega} = \vec{\nabla} \times \vec{V}$$

$$\vec{\Omega} = \frac{1}{r} \vec{k} \left\{\frac{\partial}{\partial r} (rv_\theta)\right\}$$

$$= \frac{1}{r} \left\{\frac{\partial}{\partial r} (\frac{Br^2}{t^2} e^{-\frac{r^2}{4\nu t}})\right\} \vec{k}$$

$$\vec{\Omega} = e^{-\frac{r^2}{4\nu t}} \left\{\frac{2B}{t^2} - \frac{Br^2}{2\nu t^3}\right\} \vec{k} \qquad\qquad (H-8)$$

At a given time the maximum vorticity is found by setting the derivative of vorticity with respect to radius equal to zero. Thus:

$$\frac{\partial\Omega}{\partial r} = -\frac{2B}{t^2}\frac{2r}{4\nu t} e^{-\frac{r^2}{4\nu t}} - \frac{Br}{\nu t^2} e^{-\frac{r^2}{4\nu t}} + \frac{Br^3}{4\nu^2 t^4} e^{-\frac{r^2}{4\nu t}} = 0$$

$$r_{@\Omega = \Omega_{Max}} = 2a$$

$$r_{@\Omega = |\Omega|_{Max}} = 0 \qquad\qquad (H-9)$$

Substitute this radius in equation (H-8) the maximum vorticity is:

$$|\Omega|_{Max} = \frac{2B}{t^2} \qquad\qquad (H-10)$$

The maximum vorticity therefore decays proportional to $1/t^2$.

Substituting the radius at which the vorticity is maximum (Equation H-9) into the expression for vorticity (equation H-8) and using this maximum vorticity to normalize equation (H-10), the following becomes the normalized vorticity:

$$\frac{\Omega}{|\Omega|_{Max}} = (\tfrac{1}{2}(\tfrac{r}{a})^2 - 1)e^{-\tfrac{1}{2}(\tfrac{r}{a})^2} \qquad (H\text{-}11)$$

and is shown plotted in Figure H-2.

Circulation. - Vorticity is associated with a local elemental area. This vorticity can be different at each spatial location in the flow field. By multiplying each elemental area by its associated vorticity and summing the results over the total area, the circulation Γ will result. Thus:

$$\Gamma = \int_A \vec{\Omega} \cdot d\vec{A} = \oint \vec{V} \cdot d\vec{s} \qquad (H\text{-}12)$$

$$\vec{V} = v_\theta \vec{\theta}$$

$$d\vec{s} = rd\theta \ \vec{\theta}$$

$$\Gamma = \oint v_\theta rd\theta = B\int_0^{2\pi} \frac{r^2}{t^2} e^{-\frac{r^2}{4\nu t}} d\theta$$

$$\Gamma = 2\pi B \frac{r^2}{t^2} e^{-\frac{r^2}{4\nu t}} \qquad (H\text{-}13)$$

The circulation approaches zero at infinite radius indicating that the area associated with negative vorticity exactly balances the area weighted positive vorticity of Figure H-2. The maximum circulation can be found by setting the first derivative equal to zero.

$$\frac{\partial \Gamma}{\partial r}_{t \ = \ constant} = \frac{4\pi Br}{t^2} e^{-\frac{r^2}{4\nu t}} - \frac{Br^3}{\nu t^3} e^{-\frac{r^2}{4\nu t}} = 0$$

$$\frac{1}{t^2} - \frac{r^2}{4\nu t^3} = 0$$

$$r = \sqrt{4\nu t} = \sqrt{2} \ a \qquad (H\text{-}14)$$

Maximum circulation occurs at a radius $\sqrt{2} \ a$.

Normalizing the circulation by the maximum value results in the following:

$$\frac{\Gamma}{\Gamma_{Max}} = \frac{1}{2} (\tfrac{r}{a})^2 e^{-(\tfrac{1}{2}(\tfrac{r}{a})^2 - 1)} \qquad (H\text{-}15)$$

This is shown in Figure H-3.

146
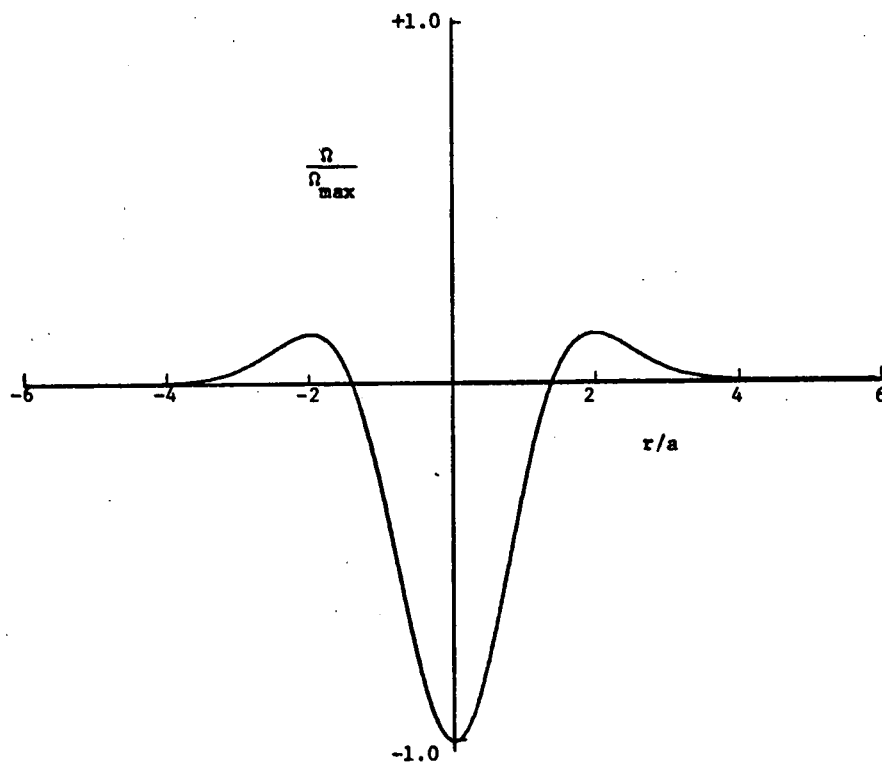
Figure H-2. Normalized (Vortex) Vorticity Distribution.
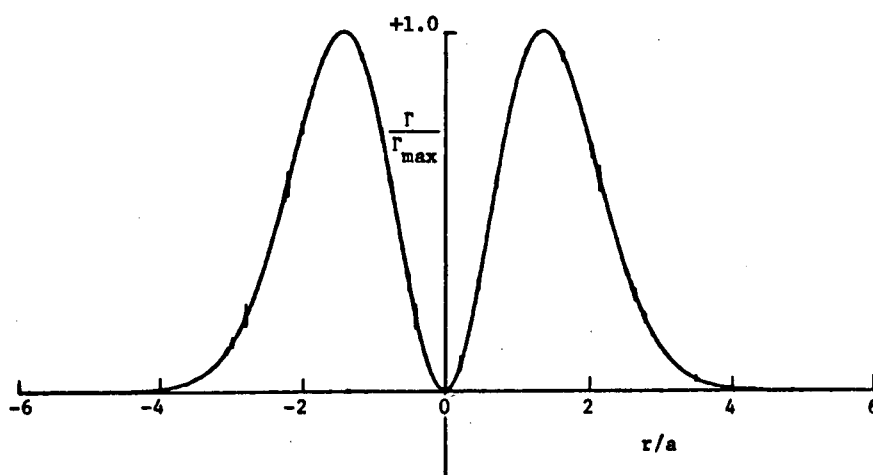
Figure H-3. Normalized Vortex Circulation.

147

Static Pressure. - By the assumptions made in developing the vortex, the momentum equation in the radial direction reduces to:

$$\frac{v_\theta^2}{r} = - \frac{1}{\rho} \frac{\partial P}{\partial r} \qquad \text{(H-16)}$$

Integration yields:

$$P_o - P_r = \Delta P = \int_r^\infty dp = \int_r^\infty \rho \frac{v_\theta^2}{r} \, dr = \rho \frac{B^2}{t^4} \int_r^\infty r e^{-\frac{r^2}{2\nu t}} \, dr$$

$$P_o - P_r = \rho \frac{B^2}{t^3} e^{-\frac{r^2}{2\nu t}} \qquad \text{(H-17)}$$

This static pressure difference can be normalized by the minimum static pressure, which occurs at r=0, to obtain the following dimensionless equation:

$$\frac{P_r - P_o}{P_{r=0}} = -e^{-\left(\frac{r}{a}\right)^2} \qquad \text{(H-18)}$$

The normalized static pressure ratio and velocity ratio are shown compared in Figure H-4.

Time of Origin of Vortices. - The vortex flow field defined herein began by an impulse function at time t = 0. In reality this is only an approximation to such vortex motion. Assuming the vortex motion (however the details of its beginning) can be represented by equation (H-2) the virtual origin can be defined at such time as the vortex radius "a" is zero. Thus:

$$a = \sqrt{2\nu t}$$

Conversely, given a vortex of radius a_o the time of origin must have been $t_o = \frac{a_o^2}{2\nu}$ seconds earlier.

The times involved with vortices having reasonable radii, i. e., a_o is greater than .003 meters, are so great that viscous decay for vortices formed in the inlet is virtually non-existent. To illustrate, the velocity will decay to a value 1/2 of a given value by the following:

$$\frac{v_{\theta t=t_2}}{v_{\theta t=t_1}} = \left(\frac{t_1}{t_2}\right)^{3/2}$$

$$t_2 = \left[\frac{v_{\theta t=t_1}}{v_{\theta t=t_2}}\right]^{2/3} t_1 = (2)^{2/3} t_1 = 1.6 t_1$$

148

VORTEX VELOCITY DISTRIBUTION
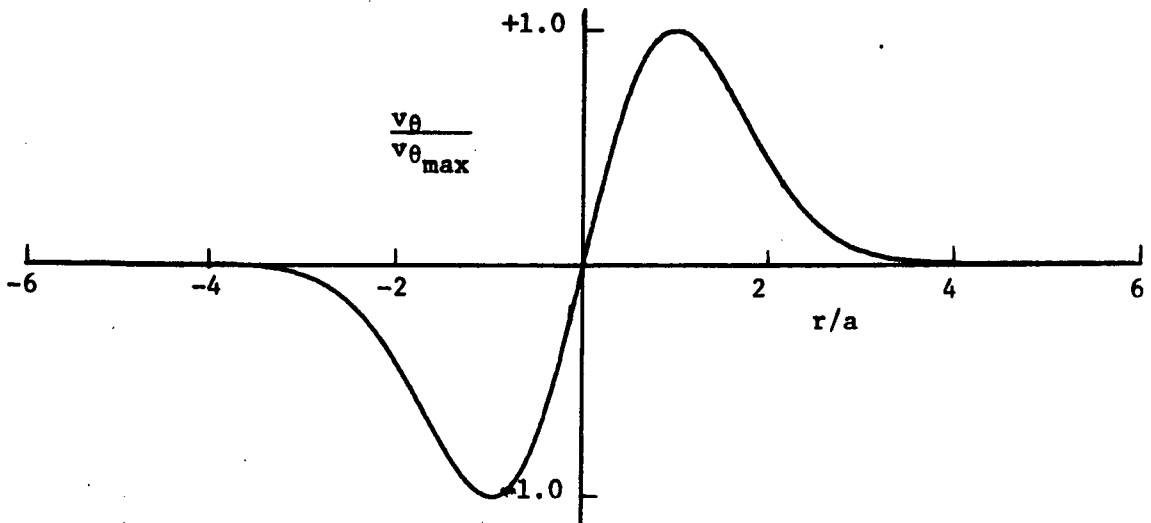
VORTEX STATIC PRESSURE DISTRIBUTION
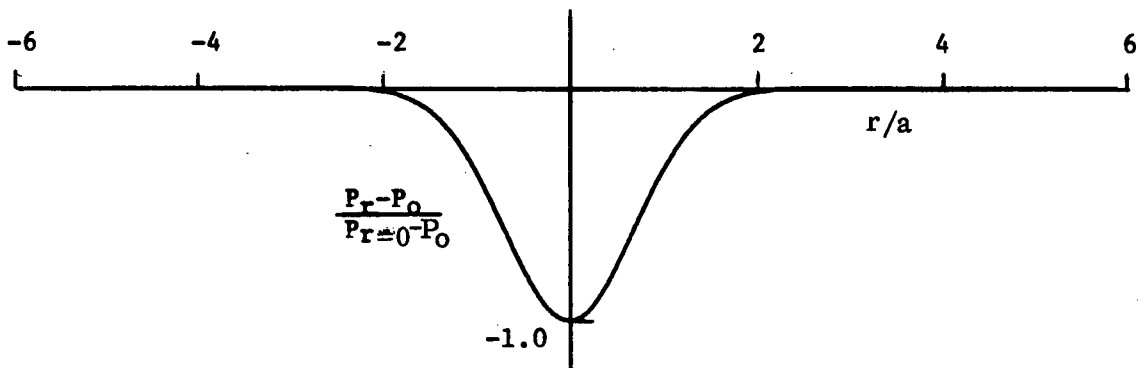
Figure H-4. Vortex Velocity and Static Pressure Distribution.
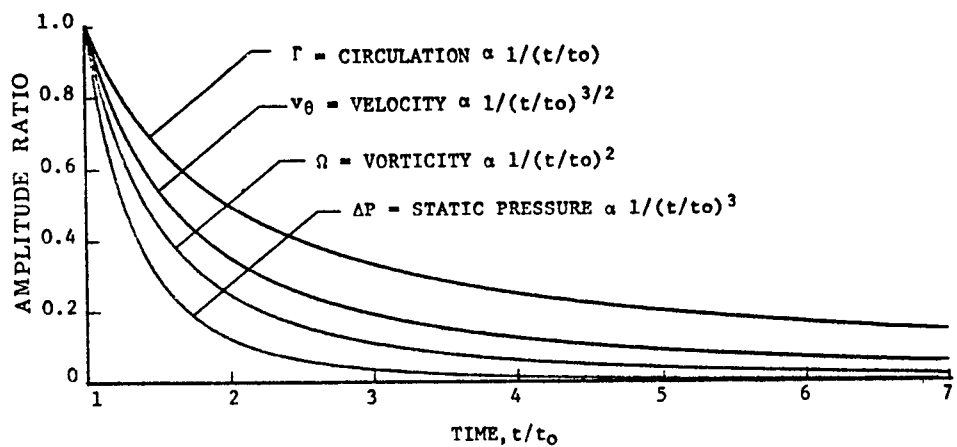
Figure H-5.   Rate of Decay for Vortex Flow Properties.

Assume: $a_1 = .3$ meters

$$t_1 = a_1^2 / 2\nu$$

$$t_2 = 1.6\, t_1 \text{ (from Figure H-5)} = 6250 \text{ seconds}$$

The residence time of this vortex in a 3 meters long inlet would be $\cong .02$ seconds. For this reason the assumption will be made that the vortex is essentially independent of time and defined as below:

$$v_\theta = B'' \left(\frac{r}{a}\right) e^{-\frac{1}{2}\left(\frac{r}{a}\right)^2}$$

where: $B'' = B' / t^{3/2}$

$B' = M\sqrt{2\nu} / (4\rho(4\nu)^2)$

$a = \sqrt{2\nu t}$

APPENDIX I

Total Pressure and Flow Angle of a Vortex Superimposed on a Local Flow

As a first step in developing the statistical model of turbulent flow the flow field of an isolated vortex was defined in the cylindrical coordinate system in Appendix F. In part A of the following discussion the vortex flow field will be converted to cartesian coordinates with the origin at the vortex center. In part B, the vortex is superimposed on axial flow in a channel and the flow properties of this moving vortex as measured by a probe fixed with the wall are determined by a transformation of coordinate systems.

A. <u>Single Vortex in Cartesian Coordinate System.</u> - The following is a description of the vortex flow field velocity components, flow angle, static pressure variation, and total pressure variation as seen in the cartesian coordinate system fixed at the vortex center. This coordinate system is sketched in Figure I-1. The circumferential angle, Θ, is measured counterclockwise from the positive x-axis. The vortex size, a, is the radius at which the maximum tangential velocity, $v_{\Theta max}$ occurs. These and other basic vortex relations to be used herein come from Appendix H.

Velocity Components -

The circumferential velocity is a function of the radius only and is given by

$$v_\theta = \frac{Br}{t^2} e^{-r^2/4\nu t} \tag{I-1}$$

where B is a constant dependent on the vortex strength (circulation)

ν is the kinematic viscosity

t is the time of origin, but is to be assumed constant because of the short period that the vortex is in the field of interest.

The maximum velocity occurs at the radius $r = a = \sqrt{2\nu t}$

$$v_{\theta max} = \frac{Ba}{t^2} e^{-\frac{a^2}{2a^2}} = \frac{Ba}{t^2} e^{-1/2} \tag{I-2}$$

PRECEDING PAGE BLANK NOT FILMED
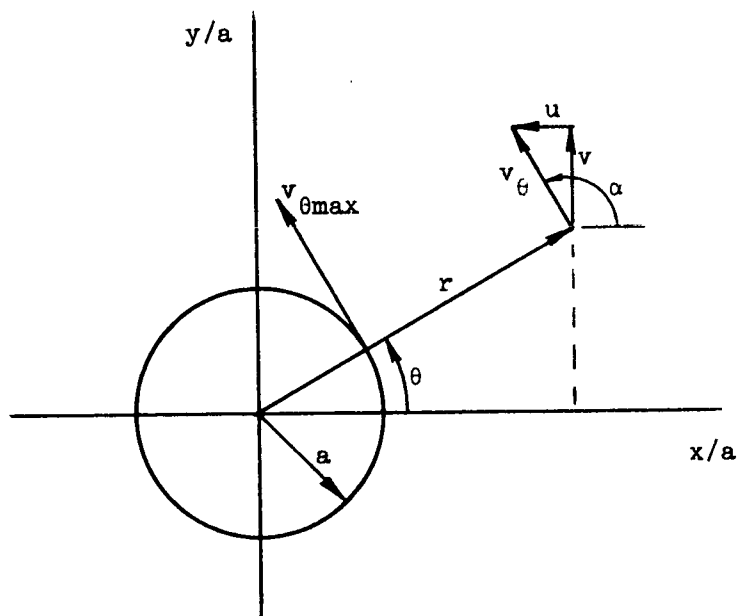
SYMBOLS:

a   Vortex size, $v_\theta = v_{\theta max}$ at $r = a$
θ   Circumferential angle, degrees
x/a Horizontal non-dimensional coordinate
y/a Vertical non-dimensional coordinate
v_θ Vortex tangential velocity
u Vortex horizontal velocity component
v   Vortex vertical velocity component
α   Flow angle
r   Radius from vortex center to flow field point

Figure I-1. Single Vortex Model in Cartesian Coordinate System.

154

So that in terms of the maximum velocity

$$\frac{v_\theta}{v_{\theta max}} = \frac{\frac{Br}{t^2} e^{-\left(\frac{r^2}{2a^2}\right)}}{\frac{Ba}{t^2} e^{-1/2}} = \left(\frac{r}{a}\right) e^{-1/2\,[(r/a)^2 - 1]} \qquad (I-3)$$

From the geometry of Figure I-1, the velocity components in the x and y directions are

$$u = -v_\theta \sin\theta$$
$$v = v_\theta \cos\theta \qquad (I-4)$$

The relation between the radius and the cartesian coordinates can be expressed as

$$\cos\theta = \frac{(x/a)}{(r/a)} \qquad \sin\theta = \frac{(y/a)}{(r/a)} \qquad (I-5)$$

Substituting equations (I-3) & (I-5) into (I-4) and using the relation $(r/a)^2 = (x/a)^2 + (y/a)^2$ yields

$$u = -v_{\theta max}\,(y/a)e^{-1/2\,[\,(x/a)^2 + (y/a)^2 - 1\,]} \qquad (I-6a)$$

$$v = v_{\theta max}\,(x/a)e^{-1/2\,[\,(x/a)^2 + (y/a)^2 - 1\,]} \qquad (I-6b)$$

Flow Angle: The local flow angle is always tangential. This is due to the fact that no radial velocity exists in the proposed vortex model. The flow angle as determined from the vertical and horizontal velocity components is:

$$\alpha = \arctan(v/u) = \arctan\left[\frac{v_{\theta max}\,\cos\theta}{-v_{\theta max}\,\sin\theta}\right] = \arctan\left[\frac{-1}{\frac{\sin\theta}{\cos\theta}}\right] \qquad (I-7)$$

$$\alpha = \arctan\left[\frac{-1}{\tan\theta}\right]$$

Static Pressure Variation: The absolute value of static pressure is required in order to later evaluate the total pressure. From Appendix H, the static pressure is

$$P_r - P_o = -\frac{\rho B^2 \nu}{t^3} e^{-r^2/2\nu t} \qquad (I-8)$$

155

where B, t, ν have been defined, see equation (I-1).

ρ is density
P$_\infty$ is the uniform "freestream" static pressure at infinity
P_r^0 is the static pressure at radius r from the vortex center

The maximum static pressure depression occurs at r = o, so

$$(P_r - P_o)_{max} = \frac{-\rho B^2 \nu}{t^3}$$

This equation can be written in the form

$$(P_r - P_o)_{max} = \frac{-\rho \nu t}{a^2} (Ba/t^2)^2 \tag{I-9}$$

By rearranging and squaring the expression for the maximum velocity, equation (I-2) yields

$$(Ba/t^2)^2 = v_{\theta max}^2 e \tag{I-10}$$

Substituting equation (I-10) into equation (I-9), together with the fact that

$\nu t = a^2/2$, yields

$$(P_r - P_o)_{max} = \frac{-\rho e}{2} v_{\theta max}^2 \tag{I-11}$$

The ratio of static pressure at any radius to the maximum static pressure depression is

$$\frac{P_r - P_o}{(P_r - P_o)_{max}} = \frac{-\dfrac{\rho B^2 \nu}{t^3} e^{-r^2/2\nu t}}{\dfrac{-\rho B^2 \nu}{t^3}} = e^{-(r/a)^2} \tag{I-12}$$

as given in Appendix H. Therefore, the absolute pressure at any radius is

$$P_r - P_o = (P_r - P_o)_{max} e^{-(r/a)^2} = -\frac{\rho}{e} v_{\theta max}^2 e^{[1 - (r/a)^2]} \tag{I-13}$$

Which, in terms of the cartesian coordinate system becomes

$$P_r = P_o - \frac{\rho}{2} v_{\theta max}^2 e^{[1 - (x/a)^2 - (y/a)^2]} \tag{I-14}$$

156

Vortex Total Pressure: The total pressure in the vortex flow field, as seen in the vortex coordinate system, is equal to the sum of the static pressure and the dynamic pressure. The total pressure is

$$P_T = P_r + \frac{\rho}{2} v_\theta^2 \tag{I-15}$$

where

P_r is defined by equation (I-14) and
v_θ is defined by equation (I-3)

So that the total pressure becomes

$$P_T = P_o - \frac{\rho}{2} v_{\theta max}^2 \, e^{[1-(r/a)^2]} + \frac{\rho}{2} v_{\theta max}^2 \, (r/a)^2 \, e^{[1-(r/a)^2]}$$

$$P_T = P_o + \frac{\rho}{2} [(x/a)^2 + (y/a)^2 - 1] \, v_{\theta max}^2 \, e^{[1 - (x/a)^2 - (y/a)^2]} \tag{I-16}$$

Velocity and pressure variations are shown in Figures I-2 and I-3. The results are plotted versus the dimensionless coordinate, X/a, for y/a = 0. The velocity distribution is maximum at x = a, is zero at x = 0, and diminishes to zero at large radii. The pressure distributions, both static and total, are shown as the ratio to the static pressure at infinity. The maximum static pressure depression occurs at r = 0. The total pressure reaches its maximum value at x/a ≅ 1.4, approaches the local static pressure at r = 0 (V = 0), and approaches the static pressure at infinity at large radii (V = 0).

B. **Single Vortex in a "Fixed" Coordinate System.** – The vortex flow field will now be defined in terms of a "fixed" coordinate system. The vortex model (and its coordinate system) are assumed to move at a constant axial velocity relative to a fixed channel as sketched below:
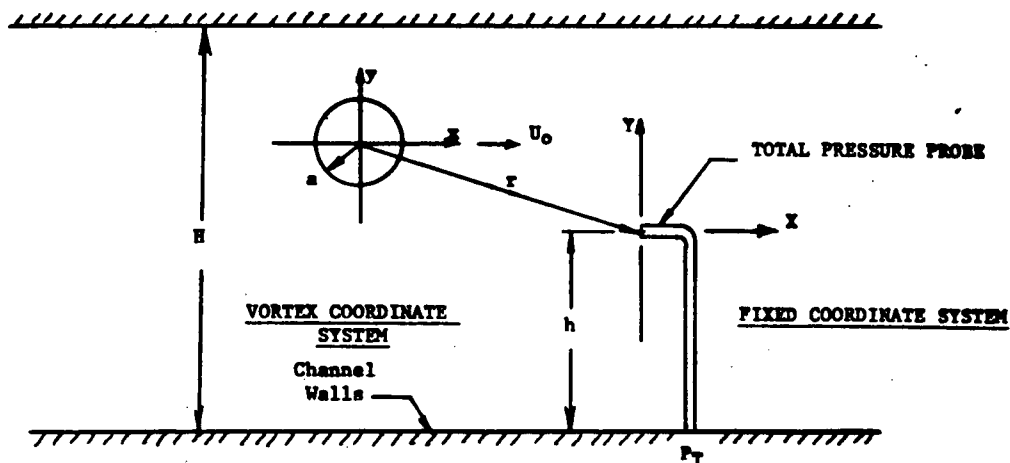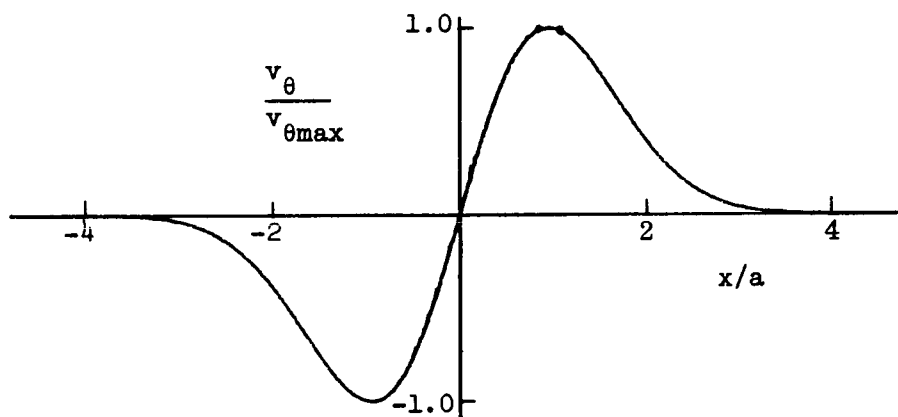
Figure I-2. Single Vortex Velocity Distribution
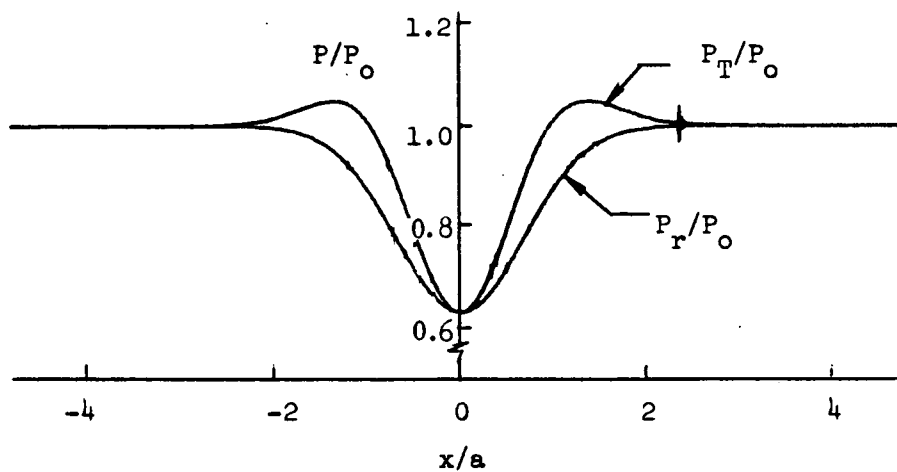
Figure I-3. Vortex Pressure Distributions.

158

In the vortex model coordinate system, the flow properties are the same as previously defined. In the "fixed" system, however, the uniform constant velocity must be added to the vortex velocity components. This yields different resultant velocity vectors and total pressures. In both cases, the static pressure at a point must be identical. (Properties of a flow field are independent of the coordinate system).

The fixed coordinate system is sketched in Figure I-4. The vortex and its coordinate system are assumed to move at constant velocity, U_o, which is defined as being parallel to the X-axis. The vortex system axes can be set parallel to the "fixed" system axes because the vortex flow field is dependent on radius only. The vortex flow field point of interest is the point which coincides with the "fixed" system origin. Therefore, the flow properties at the origin of the fixed coordinate system due to a vortex located at X, Y, can be obtained by applying the following transformation to the equations in the moving coordinate system.

$$X = -x \quad \text{and} \quad Y = -\dot{y} \tag{I-17}$$

The vertical coordinate remains constant, but the horizontal coordinate is a direct function of time

$$\Delta X = U_o \Delta t \tag{I-18}$$

Velocity Components. - The vortex flow field velocity components are determined by substituting (I-17) into (I-6), so that

$$u = v_{\theta_{max}} \left(\frac{Y}{a}\right) e^{-\frac{1}{2}[(X/a)^2 + (Y/a)^2 - 1]} \tag{I-19(a)}$$

$$v = -v_{\theta_{max}} (X/a) e^{-\frac{1}{2}[(X/a)^2 + (Y/a)^2 - 1]} \tag{I-19(b)}$$

And then adding the constant flow velocity, U_o

$$U = U_o + u$$

$$V = v$$

$$U = U_o + v_{\theta_{max}} (Y/a) e^{-\frac{1}{2}[(X/a)^2 + (Y/a)^2 - 1]} \tag{I-20(a)}$$

$$V = -v_{\theta_{max}} (X/a) e^{-\frac{1}{2}[(X/a)^2 + (Y/a)^2 - 1]} \tag{I-20(b)}$$

Flow Angle. - The flow angle at the "fixed" system origin is defined as the arc tangent of the ratio of vertical to horizontal velocity. It is measured counterclockwise from the positive X - axis. The expression is
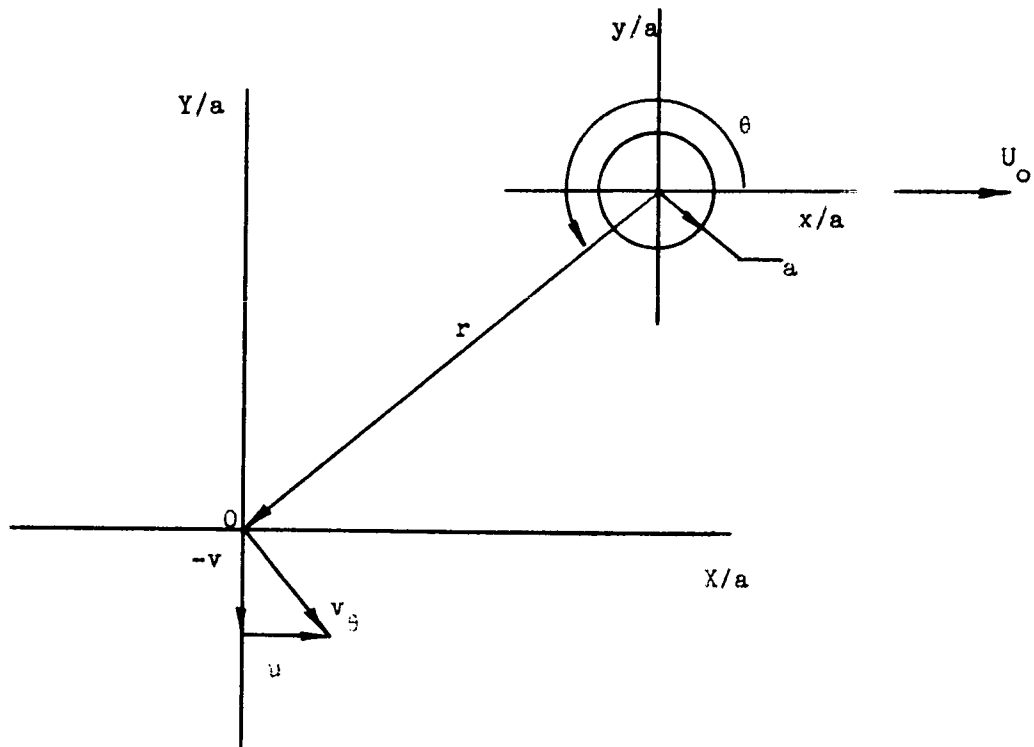
SYMBOLS:

U_o Flow field constant velocity

a   Vortex size, $v_\theta = v_{\theta max}$ at $r = a$

θ Circumferential angle in vortex system
x/a   Horizontal coordinate in vortex system
y/a   Vertical coordinate in vortex system
v   Tangential velocity
u   Vortex horizontal velocity component
v   Vortex vertical velocity component
α Flow angle
r   Radius from vortex center to fixed system center
X/a   Fixed system horizontal coordinate
Y/a   Fixed system vertical coordinate

Figure I-4.   Vortex Model in Fixed Coordinate System.

160

$$\alpha = \arctan (V/U)$$

$$\alpha = \arctan\left[\frac{-v_{\theta_{max}} (X/a)\ e^{-\frac{1}{2}[(X/a)^2+(Y/a)^2-1]}}{U_o + v_{\theta_{max}} (Y/a)\ e^{-\frac{1}{2}[(X/a)^2+(Y/a)^2-1]}}\right]$$

which after some rearranging

$$\alpha = \arctan\left[\frac{-(X/a)}{(Y/a)+\frac{U_o}{v_{\theta_{max}}}\ e^{-\frac{1}{2}[(x/a)^2+(Y/a)^2-1]}}\right]$$

Static Pressure. – The static pressure in the "fixed" system is identical to the static pressure in the vortex system at a given point. Therefore, in the "fixed" system, the static pressure is

$$P_r = P_o - \frac{\rho}{2} v_{\theta_{max}}^2\ e^{[1-(X/a)^2-(Y/a)^2]} \qquad (I-22)$$

Total Pressure in Fixed System. – The measured total pressure in the "fixed" system is the sum of the local static pressure and a corrected dynamic pressure. The correction is due to the fact that the local (at the origin) flow angle is not aligned to the "fixed" total pressure probe. The resulting relation is

$$P_T = P_r + \eta_R(\alpha)(\rho/2)W^2 \qquad (I-23)$$

where P_r is static pressure, equation I-22,

W   is the resultant velocity vector,

and $\eta_R(\alpha)$ is a recovery factor which is a function of the local flow angle

The resultant velocity vector is

$$W^2 = U^2 + V^2$$

$$W^2 = \left[(X/a)^2+(Y/a)^2\right]v_{\theta_{max}}^2\ e^{-[(X/a)^2+(Y/a)^2-1]}$$

$$+ U_o\left\{U_o+2v_{\theta_{max}} (Y/a)\ e^{-\frac{1}{2}[(X/a)^2+(Y/a)^2-1]}\right\} \qquad (I-24)$$

Substituting (I-22) and (I-24) in (I-23) and simplifying yields

$$P_T = P_o + \rho/2\ v_{\theta_{max}}^2\ e^{[1-(X/a)^2-(Y/a)^2]}\left\{\eta_R(\alpha)\left[(X/a)^2+(Y/a)^2\right]-1\right\}$$

$$+ \eta_R(\alpha)\ \rho/2\ U_o\left\{U_o+2v_{\theta_{max}} (Y/a)\ e^{-\frac{1}{2}[(Y/a)^2+(X/a)^2-1]}\right\} \qquad (I-25)$$

Velocity components, flow angle, and pressure distributions are presented in Figures I-5 through I-9. For this single vortex in a uniform constant velocity flow, the dynamic pressure recovery factor, $\eta_R(\alpha)$, is assumed to vary as the cosine squared function. The dynamic pressure recovery factor $\eta_R(\alpha)$ corrects for the probe characteristics which at angle of attack yield total pressure lower than the actual. This variation with angle of attack is illustrated in Figure I-10. For this example, the vortex is assumed to rotate counterclockwise. The ratio of constant velocity, U_o, to the maximum vortex tangential velocity, $v_{\theta max}$, is 1.2. The horizontal and vertical velocity components of the resultant velocity vector (vortex flow field superimposed on the constant flow velocity) are given in Figures I-5 and I-6. The coordinates (both X/a and Y/a) represent the distance from the "fixed" coordinate system origin, the sensing total pressure probe location to the center of the vortex flow field. The angle between the positive X-axis and the resultant velocity vector is given in Figure I-7. These flow angles follow directly from the velocity components and determine the dynamic pressure recovery factor. The static pressure distributions is presented as Figure I-8. It is basically dependent only on the distance from the vortex center. The total pressure distributions is presented in Figure I-9. Note that whereas the velocity component distribution are symmetric for negative and positive Y/a, the total pressure distribution is displaced downward. This is due to the static pressure distribution and to the angle of attack recovery factor being less than unity.
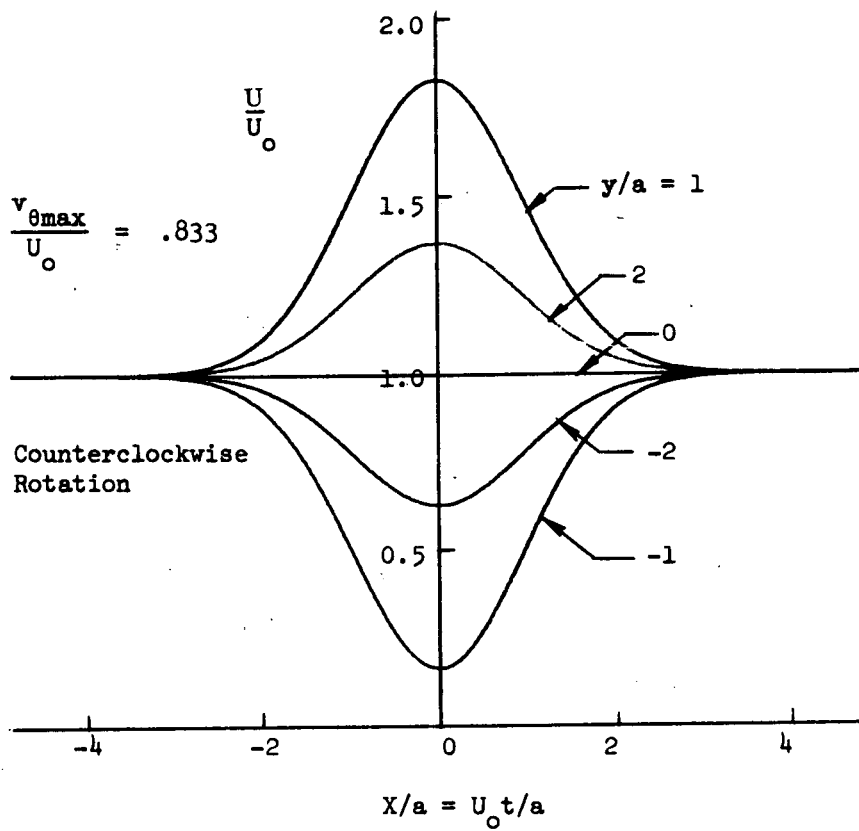
Figure I-5. Vortex Horizontal Velocity Component in Fixed System.
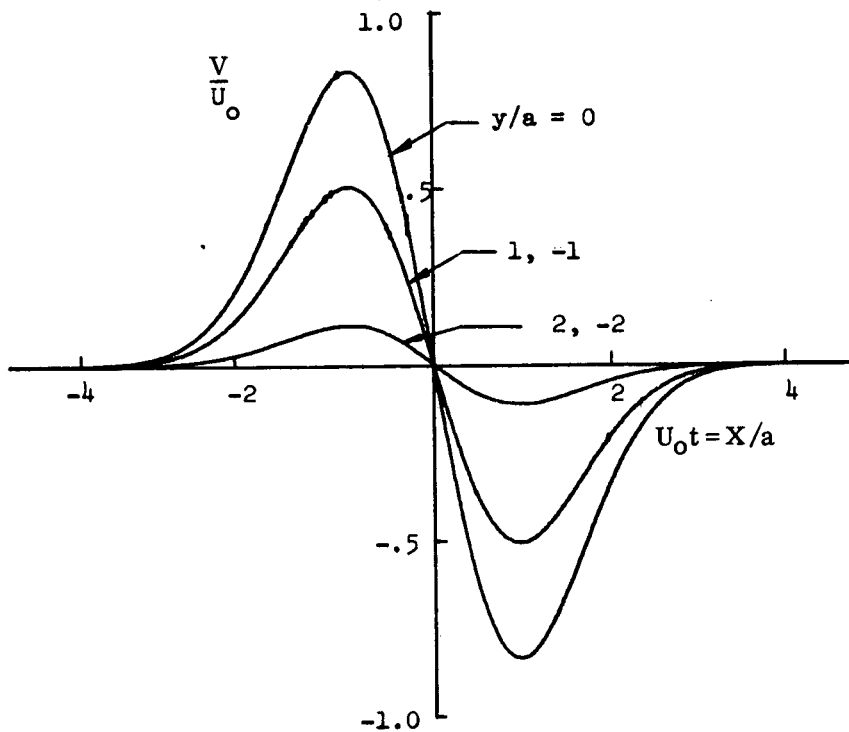
Figure I-6. Vortex Vertical Velocity Component in Fixed System.

163

60

40

20

Y/a = -1.0

0

1.0

-2.0

2.0

-2

-4

2

4

X/a = U$_o$t/a

FLOW ANGLE - α, DEG.

-20

Counterclockwise
Rotation

-40

$v_{\theta max}/U_o$ = .8333

-60
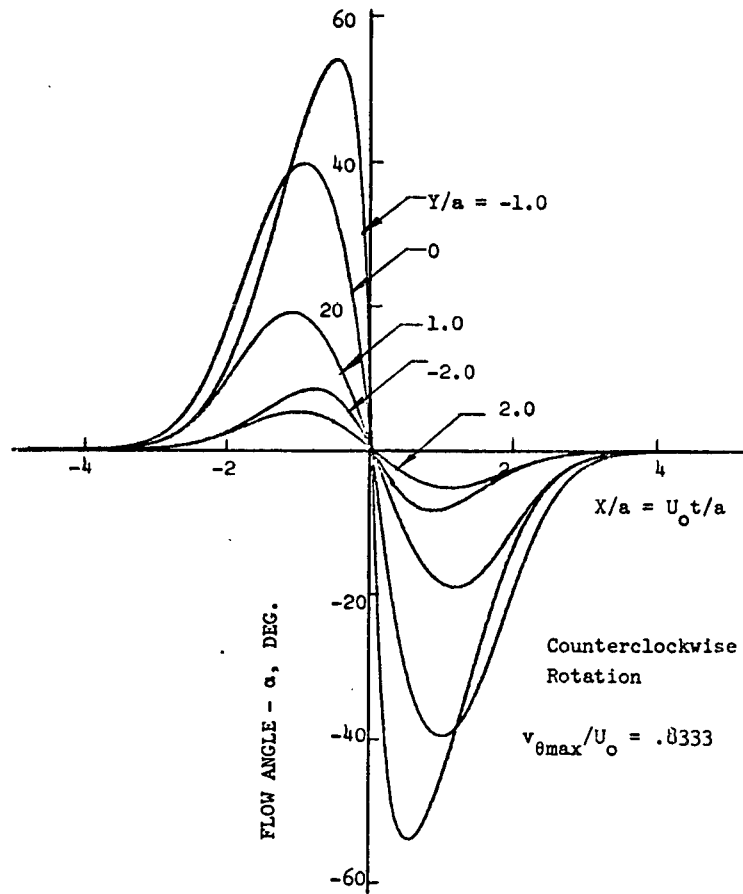
Figure I-7.   Flow Angle at Fixed System Origin

1.1

$\dfrac{P}{P_o}$

Y/a = -2, +2.0

-4

-2

2

4

X/a = U$_o$t/a

0.9

-1.0, +1.0

0.8

0

0.7

0.6
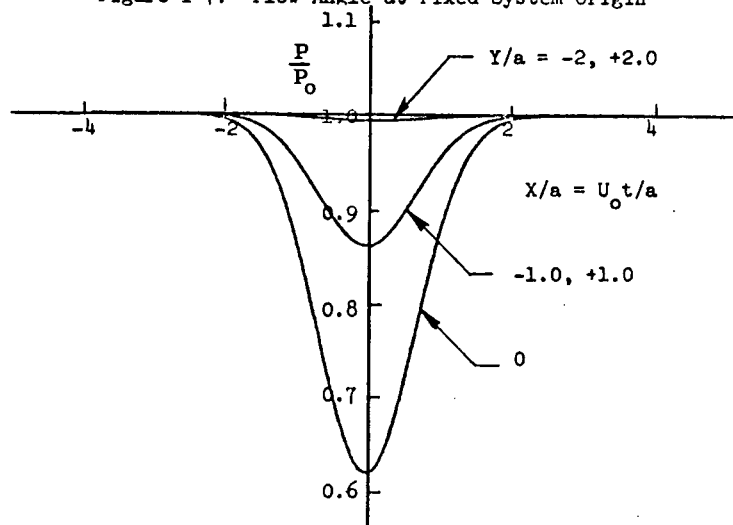
Figure I-8.   Vortex Static Pressure Distribution in Fixed System.
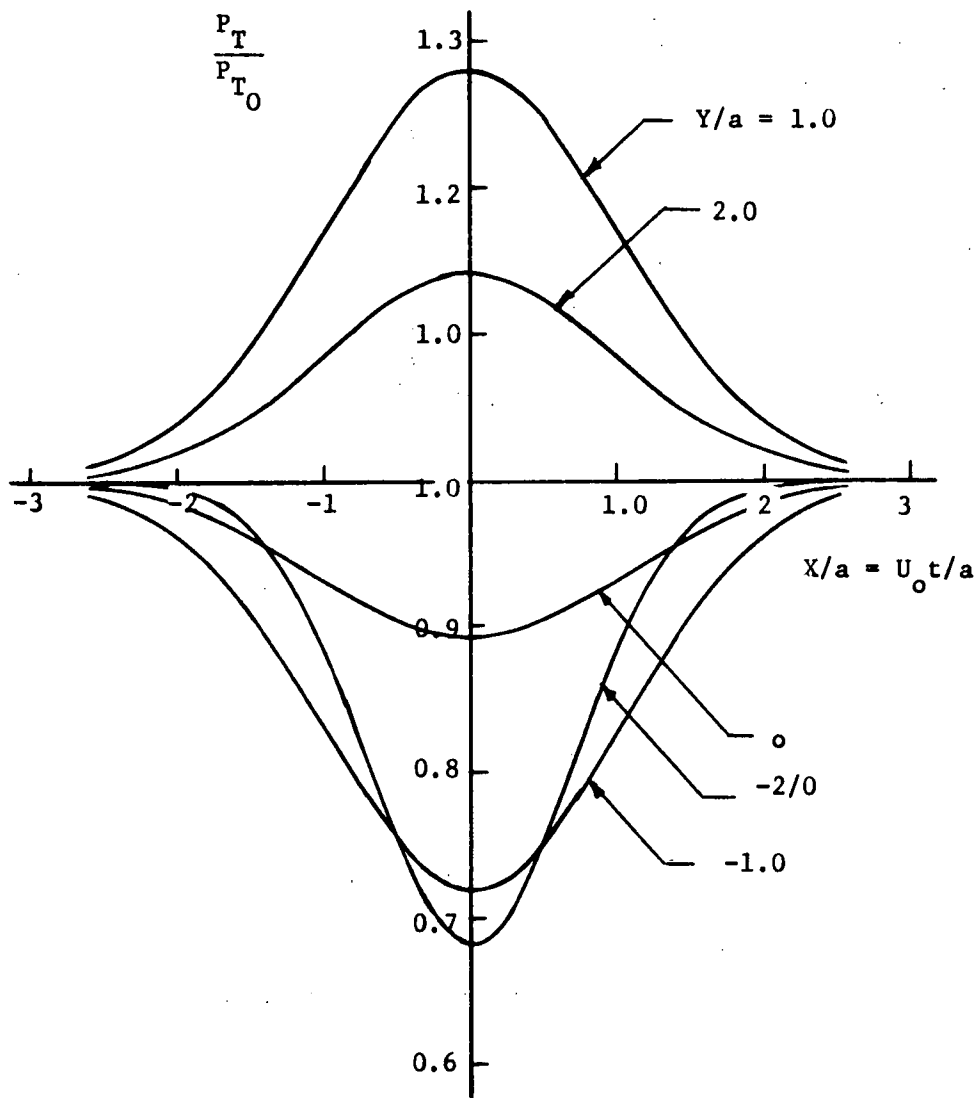
Figure I-9. Vortex Total Pressure Distribution in
Fixed System.
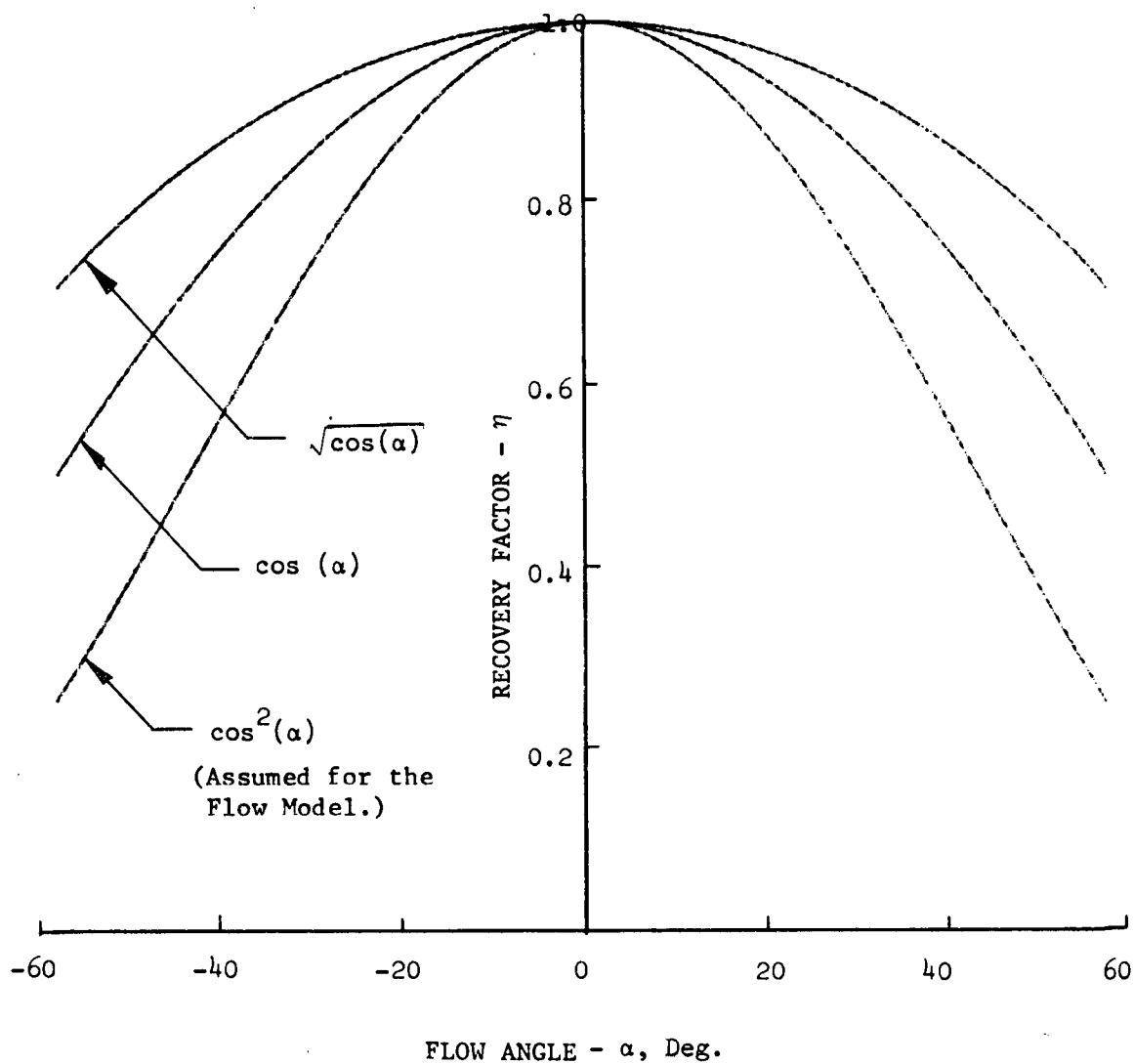
Figure I-10. Typical Dynamic Pressure Recovery Factor.

166

APPENDIX J

The Autocorrelation Function of a Random Signal
Composed of Several Independent Random Variables

     The autocorrelation function resulting from a stochastic process is found in functional form by statistical methods below. These developments are then applied to the vortex flow field and the autocorrelation function of the turbulence established.

     <u>Autocorrelation Function of a Stochastic Process</u>. - The objective of the following treatise is to establish the autocorrelation function of a resultant signal, $f(t)$, composed of wave forms $g(t)$ that occur randomly with time at an average rate of N per unit time (Poisson waves). Each waveform is specified by several variables that are random. Schematically;
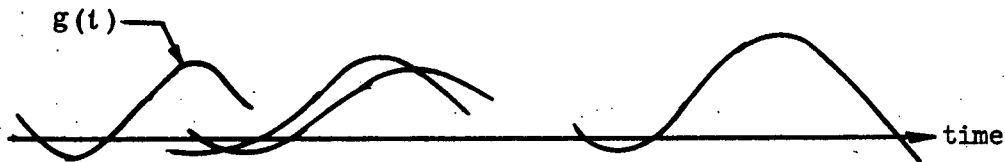
where $g(t)$ may be structured as below:

$$g(t) = f(a, v, y, n, t) \qquad (J-1)$$

167
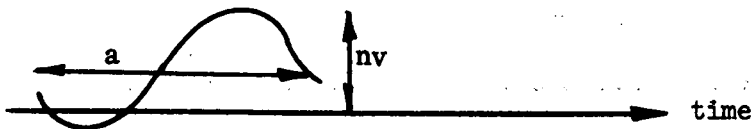
The waves $f(a, v, y, n)$ are identical for identical values of a, v, y and n.

The resultant signal, assuming the variables occur randomly, will be:
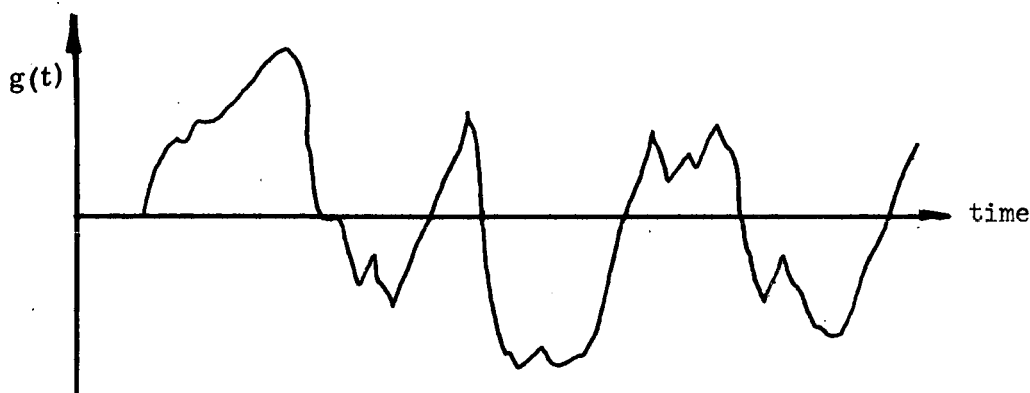
As a first step toward the development, assume the wave occurs randomly with time at a mean rate of n/second and has the waveform specified by only a single random variable, "a".
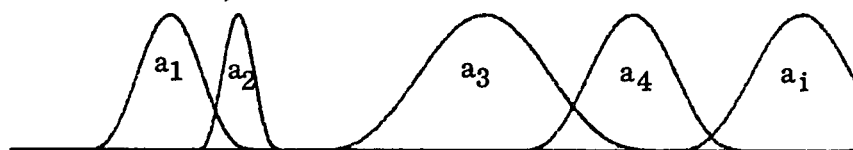
Where a_i is governed by its probability density function $P(a)$. This wave can also be considered as composed of various sets of identical waves, such as

Set 1

Set 2
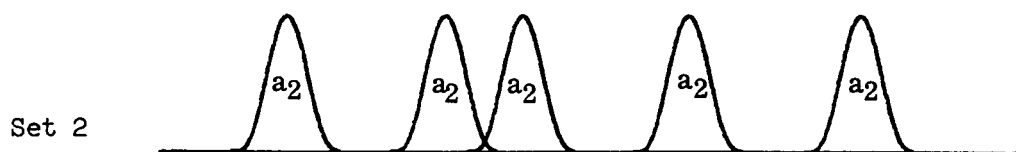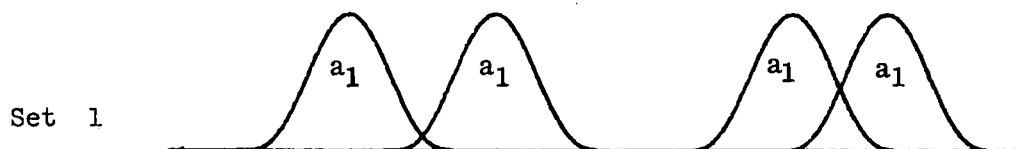
where the number of pulses n_1 of size a_1 and n_2 of size a_2, etc. is established by the probability density function $P(n_1)$ $P(a_1)$.

The autocorrelation function of pulses of size a_1, governed by a Poisson distribution having n_1 pulses per unit time is (see p 336-7 of Reference (16))

$$\bar{R}_{a_1} (\tau) = n_1 R_{a_1} (\tau) + \left(\overline{f_{a_1} (t)} \right)^2 \qquad (J-2)$$

where $R_{a_1}(\tau)$ is the autocorrelation function of a single wave.

Similarly, the autocorrelation function of pulses of size a_2 will be:

$$\bar{R}_{a_2} (\tau) = n_2 R_{a_2} (\tau) + \left(\overline{f_{a_2} (t)} \right)^2 \qquad (J-3)$$

Continuing the process, the overall autocorrelation function can be obtained by summing the above autocorrelations.

$$R_a (\tau) = \sum n_{a_i} R a_i (\tau) + [\sum p_{a_i} \overline{f_{a_i} (t)}]^2$$

$$= N \int_a P(a) R a (\tau) da + [\int_a P(a) \overline{f_a(t)} da]^2 \qquad (J-4)$$

Subtracting the D.C. component (which is independent of (τ)) from the autocorrelation function the following results.

$$R_a (\tau) = N \int_{L.L.}^{U.L.} P(a) R_a (\tau) da \qquad (J-5)$$

Extension to multi-variant signals

The typical wave is represented by the following general function $f(a, v, y, n)$ where a, v, y and n are independent random variables governed by their respective probability density functions:

$P(a)$
$P(v)$
$P(y)$
$P(n)$

Assume first v, y, and n are constant and only "a" varies. The resultant autocorrelation will be the same as given by Equation J-5.

$$R_a \ (\tau) \ = \ \{\textstyle\sum n_i \ R_{a_i} \ (\tau) + \text{constant}\} \ \begin{array}{l} v \\ y \\ n \end{array} \Bigg\} \quad \text{constant} \qquad\qquad \text{(J-6)}$$

or schematically
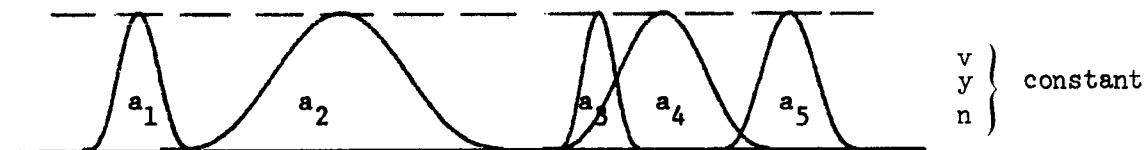
Now, for a given a_1, v will take on a random value illustrated schematically below:
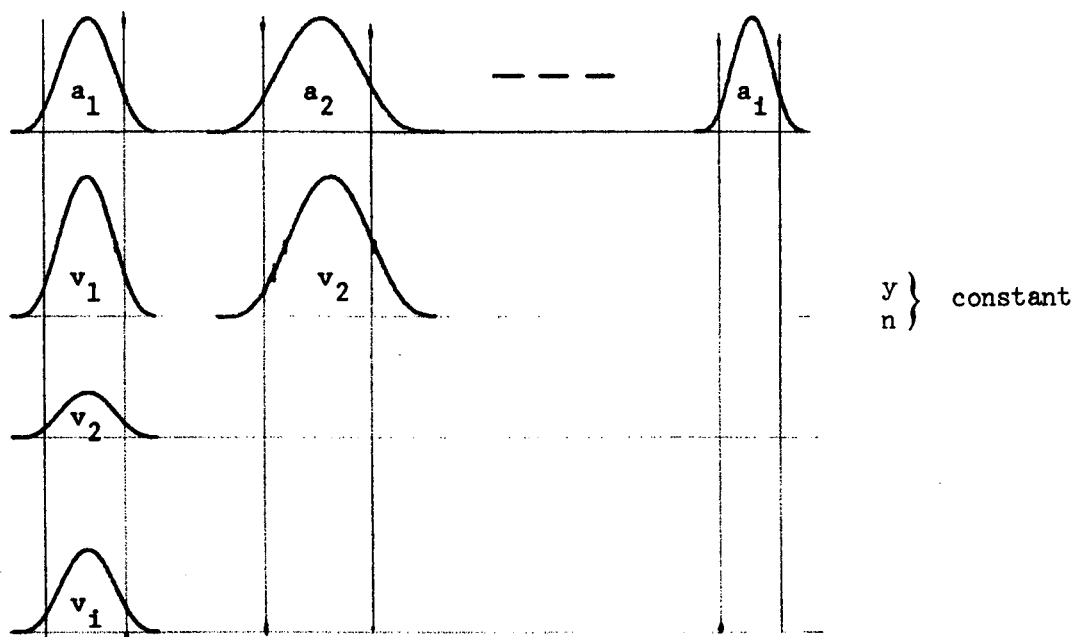
By Equation J-4 the autocorrelation of this signal of width a_1 and having random widths v_i as governed by a probability density will be:

$$R_{v_i} \ (\tau) \ \Big|_{a=a_1} \ = \ \textstyle\sum n_{v_i} \ R_{v_i} \ (\tau) \ \Big|_{a=a_1} \qquad\qquad \text{(J-7)}$$

170

There are n_{v_i} number of occurrences of this signal. Similarly for $a = a_2$:

$$R_{v_i}(\tau)\Big|_{a=a_2} = \sum n_{v_i} R_{v_i}(\tau)\Big|_{a=a_2} + \text{constant} \qquad (J-8)$$

with n_{a_2} occurrences of this signal. Continuing for $a = a_3$, $a_4 \ldots a_n$ the resultant autocorrelation function will be:

$$R_{av}(\tau) = n_{a_1} \sum n_{v_i} R_{v_i}(\tau)\Big|_{a=a_1} + n_{a_2} \sum n_{v_i} R_{v_i}(\tau)\Big|_{a=a_2}$$

$$+ \ldots \ldots n_{a_i} \sum n_{v_i} R_{v_i}(\tau)\Big|_{a=a_i} + \text{constant}$$

$$= \sum n_{a_i} \sum n_{v_i} R_{v_i}(\tau)\Big|_{a=a_i} + \text{constant} \qquad (J-9)$$

Continuing this same process allowing y and n to take on random values, the autocorrelation of the resultant signal will be:

$$R_{vayn}(\tau) = \sum n_{y_i} \sum n_{n_i} \sum n_{a_i} \sum n_{v_i} R_{v_i}(\tau) + \text{constant} \qquad (J-10)$$

For a continuous range of variables this will result in an integral form:

$$R_{vayn}(\tau) = N \int_n \int_y \int_v \int_a R(\tau)\, P(a)\, P(v)\, P(y)\, P(n)\, da\,dv\,dy\,dn \qquad (J-11)$$

$$+ \text{constant}$$

The constant is simply the mean of the resultant signal squared. Thus

$$\text{constant} = \overline{[\overline{f(t)}]}^2$$

If these positive pulses are added to a wave train of similar but negative pulses occurring at the same rate

$$R_{avyn} (\tau) = 2N \iiiint R(\tau) \; P(a) \; \underline{P(v)} \; P(y) \; P(n) \; da\,dv\,dy\,dn$$
$$+ f(t) \tag{J-12}$$

But since these negative pulses are equal in number and shape to the positive pulses and differ only in sign, $\overline{f(t)} = 0$. Then the following autocorrelation results for equally likely positive and negative pulses of total rate N

$$R_{avyn}(\tau) = N \iiiint R(\tau) \; P(a) \; P(v) \; P(y) \; P(n) \; da\,dv\,dy\,dn \tag{J-13}$$

Autocorrelation Function of the Total Pressures. - The model of turbulent inlet flow is hypothesized as being composed of a random distribution of vortices each having a specific size, strength, direction of rotation, and location. The total pressure fluctuation created by each vortex is given by Equation 39 of main text.

$$\frac{\Delta P_T}{q_o} = 2n(\frac{v_{\theta max}}{U_o}) \; (Y/a) \; e^{-\frac{1}{2}[(U_o t/a)^2 + (Y/a)^2 - 1]}$$
$$+ n^2 (\frac{v_{\theta max}}{U_o})^2 \left[(Y/a)^2 - 1 \right] e^{-[(U_o t/a)^2 + (Y/a)^2 - 1]} \tag{39}$$

For a specific vortex having a given set of properties (size, a; strength, $V_{\theta max}$; spin direction, n; and location, Y), Equation J-14 signifies a single time function. However, each vortex has a different set of properties. Therefore, the flow field is composed of a family of time functions. The autocorrelation function of the total pressure fluctuation composed of the random vortices flowing downstream with the flux of N per second is given by Equation J-13 with $P(a)$, $P(v)$, $P(y)$, and $P(n)$ being the probability density functions of the respective independent random variables, the autocorrelation function of the general wave $R(\tau)$ is found by means of the definition of autocorrelation function for discrete waves.

In Equation J-13, $P(a)$, $P(v)$, $P(y)$ and $P(n)$ are the probability density functions of the respective random variables as given by Equations J-14 through J-17. These density functions are in general described by a Beta probability density function.

172

This density function and its transformation are flexible and can be made to fit the boundary conditions of the respective random variables. See Appendix K for a detailed discussion of probability density functions. The respective vortex probability density functions are as follows:

a. Vortex Core size, a

$$P_{(a)} = \frac{k_a}{H} \left(\frac{a}{H}\right)^{m_a} \left(1 - \frac{a}{H}\right)^{n_a} \qquad \text{for } 0 \leq a \leq H \qquad \text{(J-14)}$$

b. Vortex Strength (Maximum tangential velocity),

$$P(v_{\theta_{max}}) = \frac{k_v}{U_o} \left(\frac{v_{\theta_{max}}}{U_o}\right)^{m_a} \left(1 - \frac{v_{\theta_{max}}}{U_o}\right)^{n_v} \qquad \text{for } 0 \leq v_{\theta_{max}} \leq U_o \quad \text{(J-15)}$$

c. Vortex Lateral Location, Y

$$P(Y) = \frac{1}{H} \qquad \text{for } -h \leq Y \leq H - h \qquad \text{(J-16)}$$

d. Vortex Spin Direction, n

$$P(n) = +1, -1 \qquad \text{(J-17)}$$

The autocorrelation function of the vortex flow field as measured at the total pressure probe is found by incorporating the total pressure wave (Equation 39), the definition of the autocorrelation for a descrete wave (Equation 41), and the density functions into Equation J-13. This is given by Equation J-18.

$$R_{\Delta P_T}(\tau) = 4Ne^{+1} \int n^2 \int_0^H \frac{k_a}{H} \left(\frac{a}{H}\right)^{m_a} \left(1 - \frac{a}{H}\right)^{n_a} \int_{-h}^{H-1} \frac{1}{H} \left(\frac{Y}{a}\right)^2 e^{-\left(\frac{Y}{a}\right)^2} \int_0^{U_o} \frac{k_v}{U_o} \left(\frac{v_{\theta m}}{U_o}\right)^{m_v+2}$$

$$\left(1 - \frac{v_{\theta m}}{U_o}\right)^{v_v} \int_{-\infty}^{\infty} e^{-[\frac{1}{2}\left(\frac{U_o}{a}\right)^2 (t^2 + (t+\tau)^2]} \, dt \, dv_{\theta m} \, dY \, da \, dn$$

$$4Ne^{+3/2} \int n^3 \int_0^H \frac{k_a}{H} \left(\frac{a}{H}\right)^{m_a} \left(1 - \frac{a}{H}\right)^{n_a} \int_{-h}^{H-h} \frac{1}{H}\left[\left(\frac{Y}{a}\right)^3 - \left(\frac{Y}{a}\right)\right]e^{-\frac{3}{2}\left(\frac{Y}{a}\right)^2} \int_0^{U_o} \frac{k_v}{U_o}\left(\frac{v_{\theta m}}{U_o}\right)^{m_v}$$

$$\left(1 - \frac{v_{\theta m}}{U_o}\right)^{n_v} \int_{-\infty}^{\infty} e^{-\left[\left(\frac{U_o}{a}\right)^2 (t^2 + \frac{(t+\tau)^2}{2}\right]} \, dt \, dv_{\theta m} \, dY \, da \, dn$$

$$Ne^{+2} \int n^4 \int_0^H \frac{k_a}{H}\left(\frac{a}{H}\right)^{m_a}\left(1 - \frac{a}{H}\right)^{n_a} \int_{-h}^{H-h} \frac{1}{H}\left[\left(\frac{Y}{a}\right)^2 - 1\right]^2 e^{-2\left(\frac{Y}{a}\right)^2} \int_0^{U_o} \frac{k_v}{U_o}\left(\frac{v_{\theta m}}{U_o}\right)^{m_v+4}$$

$$\left(1 - \frac{v_{\theta m}}{U_o}\right)^{n_v} \int_{-\infty}^{\infty} e^{-\left[\left(\frac{U_o}{a}\right)^2 (t^2 + (t+\tau)^2\right]} \, dt \, dv_{\theta m} \, dY \, da \, dn \tag{J-18}$$

This can be reduced as far as Equation J-19 in closed form. Integration with respect to the random variable, a, must be done by numerical techniques. A computer program was written to evaluate this integral.

$$R_{\Delta P_r}(\tau) = 8k_v k_a \left(\frac{NH}{U_o}\right) \left\{ \frac{n^2 (m_v + 2)! \, n_v!}{(m_v + n_v + 3)!} \left(\frac{e^{+1}}{2}\right) \int_0^1 [ERFC\,(\frac{U_o \tau}{a2})]\, e^{-\frac{\tau^2}{4}\left(\frac{U_o}{a}\right)^2} \right.$$

$$[\,(\frac{-h}{a})\, e^{-\left(\frac{-h}{a}\right)^2} - (\frac{H-h}{a})\, e^{-\left(\frac{H-h}{a}\right)^2} + ERF(h/a) + ERF(\frac{H-h}{a})]\, [(\frac{a}{H})^{m_a} (1 - \frac{a}{H})^{n_a}\, d(\frac{a}{H})]$$

$$+ \frac{n^2 e^{3/2}}{18} \sqrt{\frac{2}{3}}\, \frac{(m_v + 3)! \, n_v!}{(m_v + n_v + 4)!} \int_0^1 [e^{-\frac{3}{2}\left(\frac{H-h}{a}\right)^2}\left(1 - 3\,(\frac{H-h}{a})^2\right) - (1 - 3\,(\frac{-h}{a})^2)\, e^{-\frac{3}{2}\left(\frac{-h}{a}\right)^2}\,]$$

$$[ERFC\,(\frac{U_o}{a}\sqrt{\frac{2}{3}}\,\tau) + ERFC\,(\frac{U_o}{a}\, \frac{\tau}{\sqrt{6}})]\, e^{-\frac{\tau^2}{3}\left(\frac{U_o}{a}\right)^2}\, [(\frac{a}{H})^{m_a} (1 - \frac{a}{H})^{n_a}\, d(\frac{a}{H})]$$

$$+ \frac{n^2 e^{+2}}{4\sqrt{2}}\, \frac{(m_v + 4)! \, n_v!}{(m_v + n_v + 5)!} \int_0^1 ERFC\,(\frac{\tau}{\sqrt{2}}\,\frac{U_o}{a})\, e^{-\frac{\tau^2}{2}\left(\frac{U_o}{a}\right)^2}$$

$$[(\frac{1}{4}(\frac{-h}{a})^3 + \frac{5}{16}\,(\frac{-h}{a}))\, e^{-2\left(\frac{-h}{a}\right)^2} - \left(\frac{1}{4}(\frac{H-h}{a})^3 + \frac{5}{16}\,(\frac{H-h}{a})\right)\, e^{-2\left(\frac{H-h}{a}\right)^2} + \frac{11}{16\sqrt{2}}\,(ERF$$

$$\left. (\frac{h\sqrt{2}}{a}) + ERF\,(\frac{H-h}{a}\,\sqrt{2}))]\ \ [(\frac{a}{H})^{m_a} (1 - \frac{a}{H})^{n_a}\, d\,(\frac{a}{H})] \right\} \tag{J-19}$$

where

$$ERF(z) = \frac{2}{\sqrt{\pi}}\int_0^\infty e^{-\phi^2}\, d\phi$$

Numerical evaluation of this integral yields the normalized auto-correlation function as shown in Figure 27 of the main text.

175

APPENDIX K

Probability Density Functions

A physical interpretation and definition of the probability density function "f(x)" will be given below using the common Gaussian density function as an example. A summary of the more common density functions and their characteristics will then be given.

Transformation of the Beta distribution demonstrating the added flexibility that can be obtained by use of this technique will follow. Such flexibility is required to meet the wide range of density functions needed to fit the physical turbulence characteristics.

Probability Density Function.- The probability density function "f(x)" for random data describes the probability that the data will assume a value within some defined range for a single event or, as below, at any instant of time. Consider the following time history of the signal x(t) below:
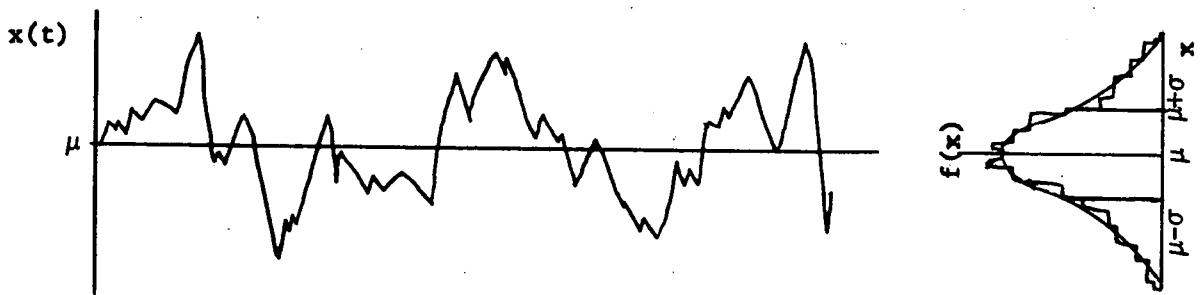
$$T_x = \sum_{i=1}^{n} \Delta t_i \qquad \text{Prob } [x < x(t) \le x + \Delta x] = \lim_{T \to \infty} \frac{T_x}{T} \qquad (K-1)$$

The probability that x(t) assumes a value within the range between x and $(x + \Delta x)$ may be obtained by taking the ratio of T_x/T when T_x is the total amount of time that x(t) falls inside the range $(x, x + \Delta x)$ during an observation time T. This ratio will approach an exact probability description as T approaches infinity. Often random data of this nature assumes a probability density approaching the bell shaped or Gaussian form as shown to the right of the above sketch. The mean value, μ of random data will be the average over the entire range. Thus:

$$\mu = \int_{l.l.}^{u.l.} x \; f(x) \; dx \qquad (K-2)$$

PRECEDING PAGE BLANK NOT FILMED

The mean square value, σ , is the squared value of x over the entire range. Thus:

$$\sigma^2 = \int_{l.l.}^{u.l.} x^2 f(x) \, dx \qquad (K\text{-}3)$$

The mean and mean square values are called the first and second moments respectively. In general the mth order moment is as follows:

$$\overline{\xi^m} = \int_{l.l.}^{u.l.} X^m f(x) \, dx \qquad (K\text{-}4)$$

A random variable is completely specified by definition of all its moments.

Examples of Probability Density Functions.- A summary of density functions is given in Table I along with a graphical representation. A typical source for these density functions is Reference 16. The characteristics of the functions are also given in the Table and will be significant when subsequently fitting the density function to the properties of the random vortex model.

It should be noted that all of these density functions are greatly limited in flexibility. Specifically the moments, and hence the shape of the respective density curves, are fixed (with the exception of the Beta Density).

As an example of experimental data consider the probability density function of the total pressure fluctuations measured in an inlet of Reference 12 and as shown in Figure K-1(a). The data obtained from test agrees closely with the Gaussian Density. However, at other conditions and measurement locations a skewed density has been measured in the same test. This is shown in Figure K-1(b). As evident, the Gaussian Density is not representative of this data.

The moments of the Beta Density can be changed by choice of the constants b and c (see Table K-1). The limit values of this function remain, however, at zero and unity. The flexibility of this density can be greatly increased by transformation as developed in the following section.

Transformation of the Beta Density Function.- The Beta Density Function is defined as:

$$f(x) = Ax^b(1-x)^c \quad \text{for} \quad 0 \le x \le 1 \qquad (K\text{-}5)$$

$$\text{where} \quad A = \frac{\Gamma(b+c+2)}{\Gamma(b+1)\,\Gamma(c+1)}$$

$$\text{and} \quad \Gamma = \text{Gamma Function}$$

178
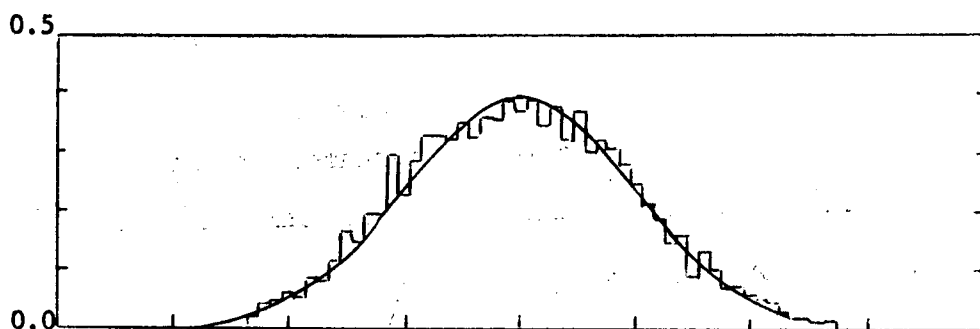
(a) Probe Location Near Midstream (225° Rake)
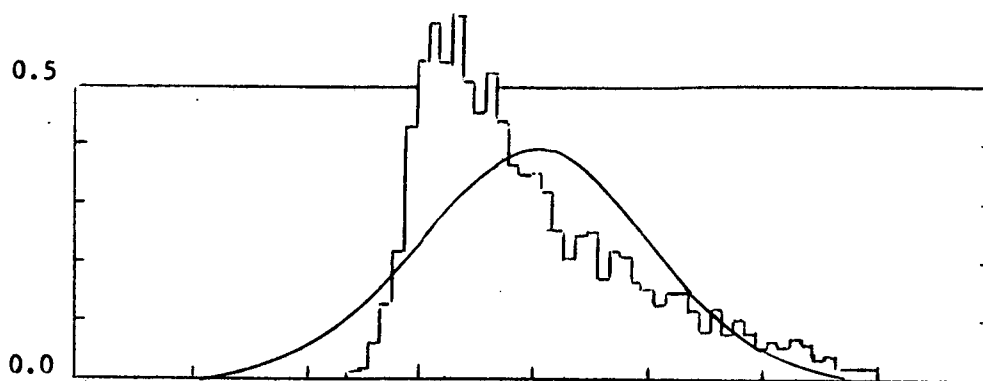
(b) Probe Location Near Midstream (315° Rake)

Figure K-1. Comparison of Probability Density Functions Obtained
from Inlet Turbulence Measurements with the Gaussian
Density Function. (Test Data from Reference 12,
page 321 and 326 respectively)

T A B L E   K-I

SUMMARY OF COMMON PROBABILITY DENSITY FUNCTIONS

DENSITY	EQUATION	FIGURE	RANGE LWR LIMIT	RANGE UPPR LIMIT	CAPABILITY TO VARY SHAPE
Gaussian	$f(x) = \dfrac{1}{\sigma\sqrt{2\pi}}\, e^{-(x-\eta)^2/2\sigma^2}$		$-\infty$	$+\infty$	None
Uniform	$f(x) = \dfrac{1}{x_2 - x_1}$		x_1	x_2	None
LaPlace	$f(x) = \dfrac{\alpha}{2}\, e^{-\alpha|x|}$		$-\infty$	$+\infty$	None
Cauchy	$f(x) = \dfrac{\alpha/\pi}{\alpha^2 + x^2}$		$-\infty$	$+\infty$	None
Rayleigh	$f(x) = \dfrac{x}{\alpha^2}\, e^{-x^2/2\alpha^2} U(x)$		0	$+\infty$	None
Maxwell	$f(x) = \dfrac{\sqrt{2}}{\alpha^3\sqrt{\pi}}\, x^2 e^{-x^2/2\alpha^2} U(x)$		0	$+\infty$	None
Beta	$f(x) = \begin{cases} A x^b (1-x)^c \\ 0 \end{cases}$		0	1	Limited

The Gamma function for integers is defined as

$$\Gamma(n) = (n-1)!$$

Therefore for integer values of b and c the mean value of f(x) is

$$\overline{f(x)} = \frac{b+1}{b+c+2}$$

For b = c = 2 the density function is as below:
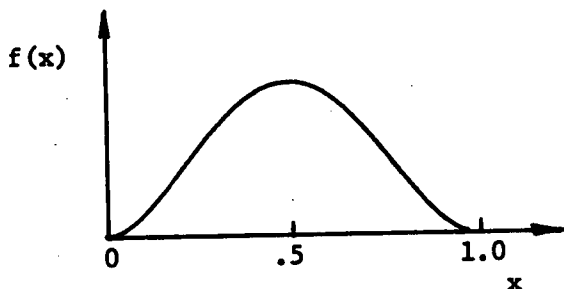
This can be skewed by choosing b ≠ c and for example with b = 2 and c = 3 the following density function results:
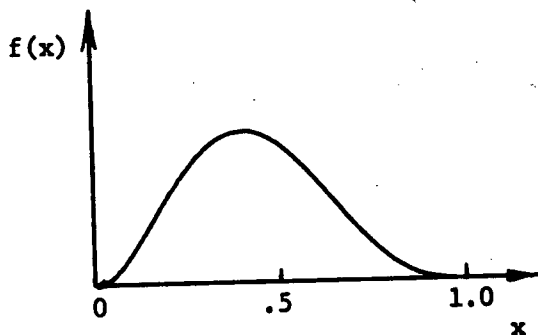
To increase the flexibility of this density function it will be transformed in two steps. First f(x) will be transformed linearly by y = dx. By use of the following transformation (see for example Reference 16, P   ):

$$f(y) = \left. \frac{f(x)}{\left| \frac{dy}{dx} \right|} \right|_{x=\frac{y}{d}} \tag{K-6}$$

The density function of y now becomes:

$$f(y) = \frac{A}{d} \left(\frac{y}{d} \right)^{b} \left(1 - \frac{y}{d} \right)^{c} \tag{K-7}$$

This function is shown below:
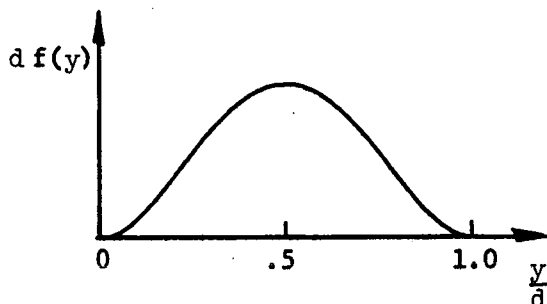
Secondly, transform by translating this distribution by its mean value $\bar{y}$, where:

$$\bar{y} = \int_0^d y \, f(y) \, dy$$

The required translation is:

$$Z = y - \bar{y}$$

This results in the following density:

$$f(z) = \frac{A}{d} \left(\frac{Z + \bar{y}}{d}\right)^b \left(1 - \frac{Z + \bar{y}}{d}\right)^c , \tag{K-8}$$

$$\text{where:} \quad A = \frac{\Gamma(b+c+2)}{\Gamma(b+1)\,\Gamma(c+1)}$$

$$\text{and} \quad \bar{y} = \frac{A}{d} \, \frac{\Gamma(b+2)\,\Gamma(c+1)}{\Gamma(b+c+3)}$$

$f(z)$ is sketched below:

182
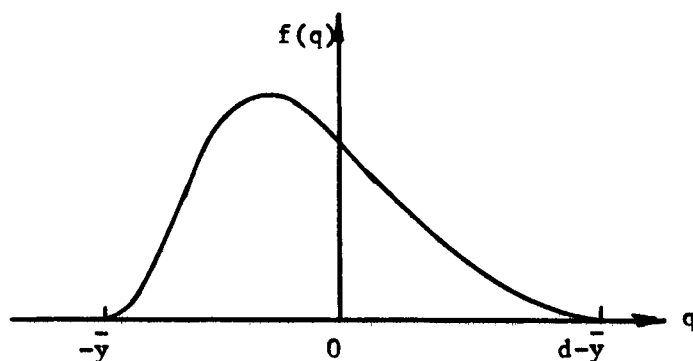
The first moment (mean) of this distribution is by reason of the translation, $z = y - \bar{y}$, equal to zero. The second moment, which is the mean square value is found by integration to be:

$$\sigma^2 = \bar{z}^2 = d^2 \left\{ \frac{(b+2)\ (b+1)}{(b+c+3)\ (b+c+2)} - [\frac{(b+1)}{b+c+2}]^2 \right\} \tag{K-9}$$

Normalizing the transformed density function by the root of the mean square value, σ, results in equation (K-10)

$$\sigma f(z) = \sigma \frac{A}{d} \ (\frac{\sigma}{d} \frac{z}{\sigma} + \frac{\bar{y}}{d})^b \ (1 - (\frac{\sigma}{d} \frac{\sigma}{d} \frac{z}{\sigma} + \frac{\bar{y}}{d}))^c \tag{K-10}$$

To illustrate the flexibility of the transformed Beta Density, equation (K-10) is shown graphically in Figure K-2 for various values of b and c, where $b \neq c$. Note the varying amounts of "skewness" that can be obtained. In Figure K-3, b is assumed equal to c which is equal to "n". Thus

$$b = c = n$$

This gives a symmetrical Density Function. For n = o, the uniform density is obtained; for n =   the Gaussian Density results, demonstrating the wide range of density functions that can be formed from this transformed Beta Density Function.

The transformed Beta density still has only the two constants b and c as variable to change the general shape of the density. As a result this density still falls short of fitting the data of Figure K-1(b). In an attempt to fit these data the following Hyper-Beta Density Function was developed.

Hyper-Beta Density Function. - Define a density function, similar to the Beta density as follows:

$$P(x) = D \ x^{nb} \ (1 - x^n)^c \quad \text{for } 0 \leq X \leq 1 \tag{K-11}$$

To establish D, it is known that the probability of a single event occurring somewhere in the region of interest is unity. Thus:

$$\int P(x) \ dx \equiv 1$$

The constant D is found to be,

$$D = \frac{n\Gamma\ (b+c+1+\frac{1}{n})}{\Gamma\ (b+\frac{1}{n})\ \Gamma\ (c+1)}$$

This density, which has lower and upper limits of zero and one respectively can be transformed as the Beta Density was transformed.

183

Such transformation leads to the following density:

$$\sigma P(z) = D\sigma^{1-nb}\left\{(\frac{z}{\sigma} + \frac{\mu}{\sigma})^{nb} \ (1 - \sigma^n \ (\frac{z}{\sigma} + \frac{\mu}{\sigma})^n)^c\right\}$$

where:

$$D = \frac{n\Gamma(b+c+1+\frac{1}{n})}{\Gamma(b+\frac{1}{n}) \ \Gamma(c+1)}$$

$$\sigma^2 = \frac{\Gamma(b+c+1+\frac{1}{n}) \ \Gamma(b+\frac{3}{n})}{\Gamma(b+c+1+\frac{3}{n}) \ \Gamma(b+\frac{1}{n})} - \mu^2$$

$$\mu = \frac{D}{n} \frac{\Gamma(b+\frac{2}{n}) \ \Gamma(c+1)}{\Gamma(b+c+1+\frac{2}{n})}$$

Comparison of this density for a set of constants b, c and n is shown in Figure K-4, again compared with the test data. Much better agreement is obtained because of the increased flexibility resulting from the additional constant, n, in the definition of the density function.
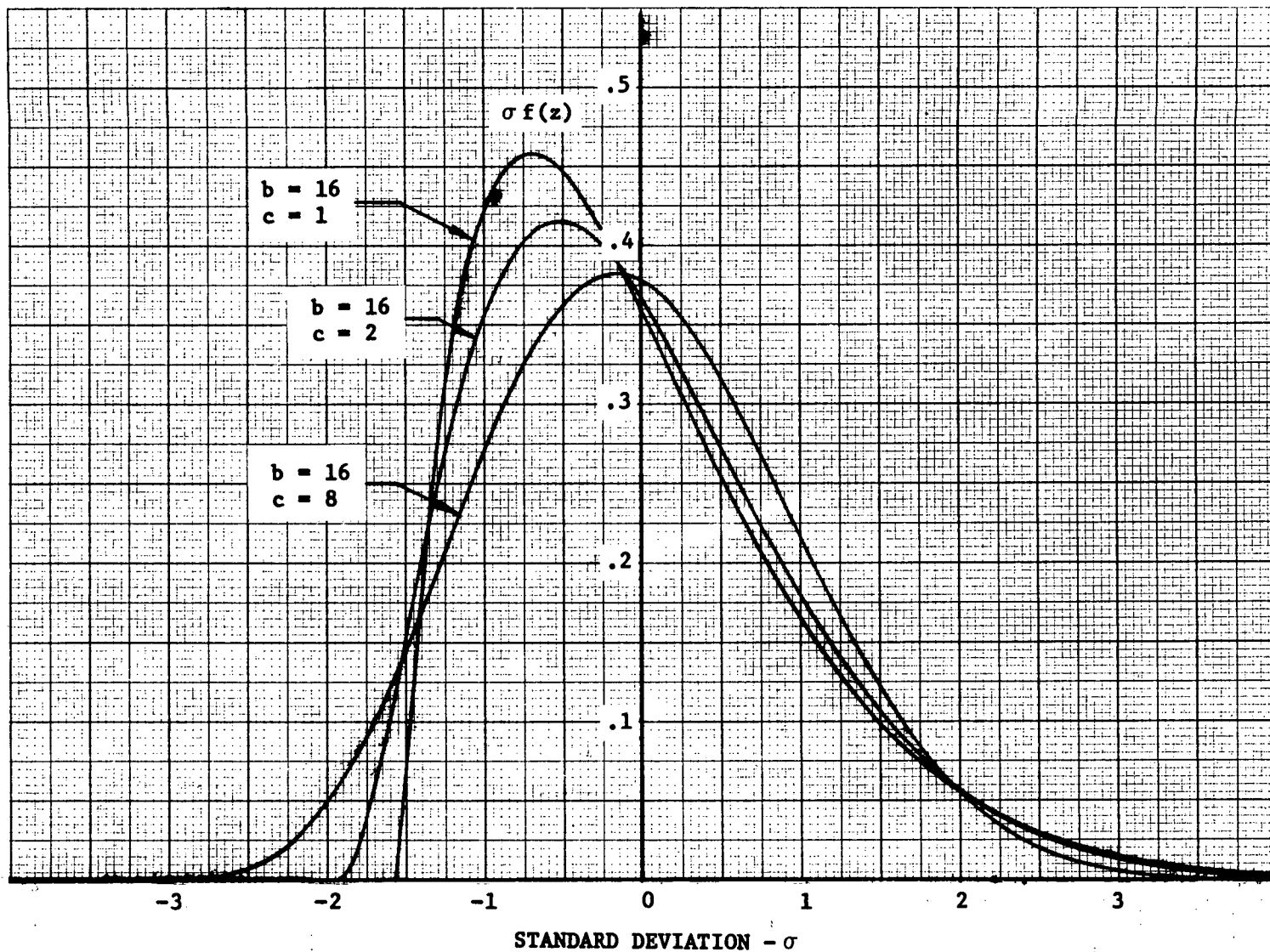
Figure K-2. Transformed Beta Density Function with $b \neq c$.
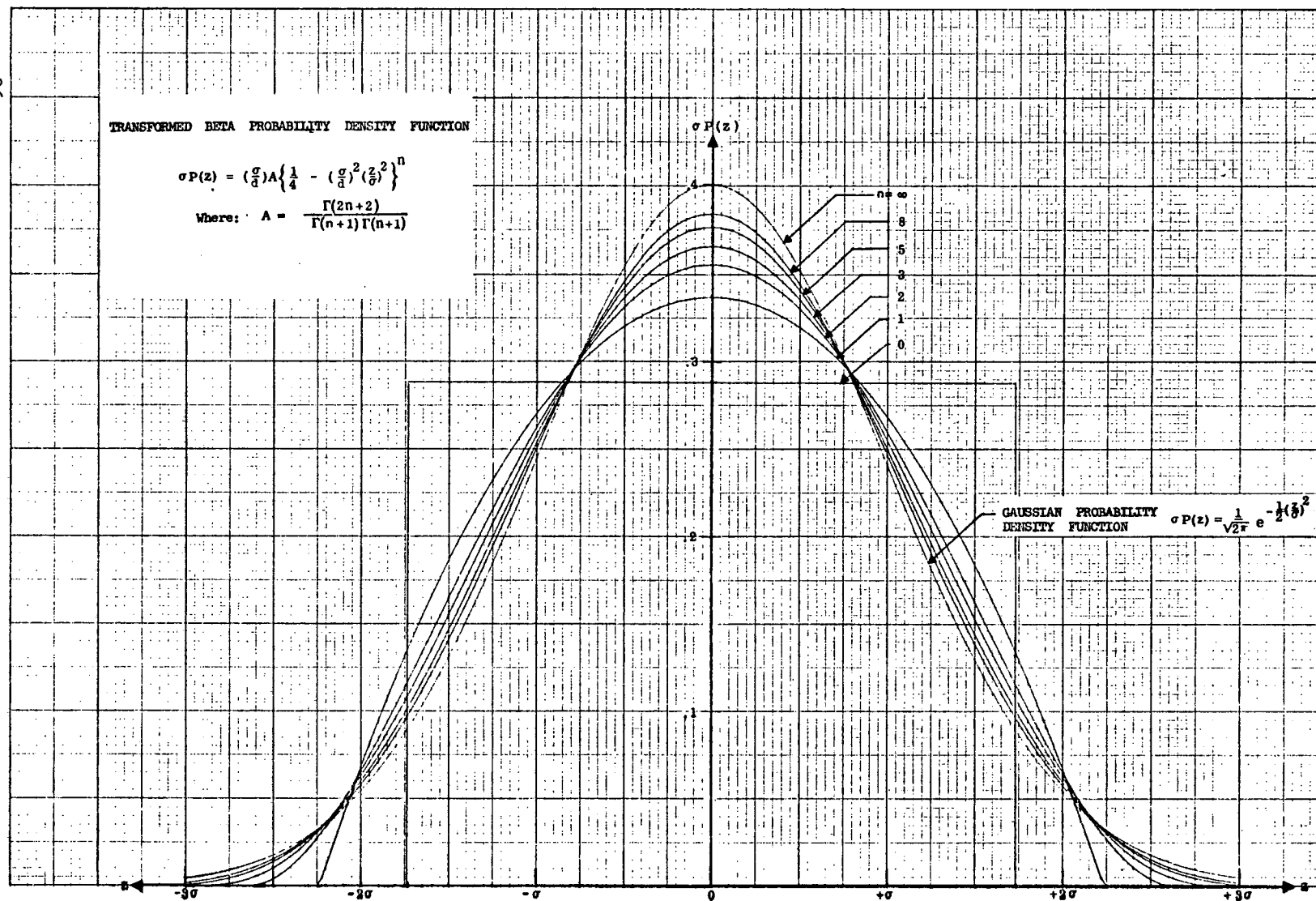
Figure K-3. Transformed Beta Density Function, b=c=n.

Comparison of this density for a set of constants b, c and n is shown in Figure K-4, again compared with the test data. Much better agreement is obtained because of the increased flexibility resulting from the additional constant, n, in the definition of the density function.
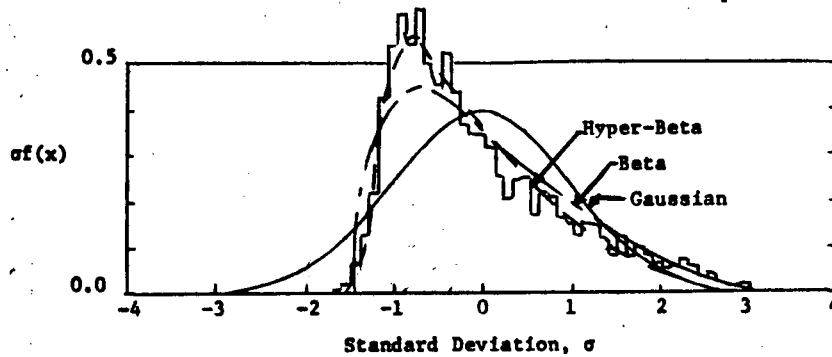
Figure K-4. Comparison of the Gaussian, Beta and Hyper-Beta Density Functions with Test Data of Reference . 12.

APPENDIX L

Velocity Correlations

The auto and cross-correlation functions of the velocity terms can also be computed by use of the statistical flow model. These correlations are commonly called the Reynold's stresses, $\overline{u^2}$, $\overline{v^2}$ and $\overline{uv}$. Such "stresses" produce a static pressure gradient which can also be obtained from the model. These correlations are developed below by application of the statistical techniques developed in Appendix J to the flow model.

Axial Velocity Correlation. - The mean square axial velocity correlation can be obtained from the vortex flow field model and the statistical model of turbulence by the method defined by Equation L-1.

$$\overline{u^2} = N \int_n \int_y \int_{v_{\theta m}} \int_a \int_t u(t)u(t) \; P(a) \; P(v_{\theta m}) \; P(Y) \; P(n) \; dt\,da\,dv_{\theta m}\,dY\,dn \tag{L-1}$$

Where the axial component of fluctuating velocity, $u(t)$, is Equation L-2:

$$u(t) = n v_{\theta m} \left(\frac{Y}{a}\right) e^{-\frac{1}{2}\left[\left(\frac{U_o t}{a}\right)^2 + \left(\frac{Y}{a}\right)^2 - 1\right]} \tag{L-2}$$

The respective vortex probability density functions are defined by Equations J-14, J-15, J-16, and J-17. Substitution of the probability density functions and the expression for $u(t)$ into Equation L-1 and division by U_o^2 yields the following integral:

$$\frac{\overline{u^2}}{U_o^2} = N e^{+1} \int n^2 \int_0^H \frac{k_a}{H}\left(\frac{a}{H}\right)^{m_a}\left(1 - \frac{a}{H}\right)^{n_a} \int_{-h}^{H-h} \frac{1}{H}\left(\frac{Y}{a}\right)^2 e^{-\left(\frac{Y}{a}\right)^2}$$

$$\int_o^{U_o} \frac{k_v}{U_o}\left(\frac{v_{\theta m}}{U_o}\right)^{m_v+2}\left(1 - \frac{v_{\theta m}}{U_o}\right)^{n_v} \int_{-\infty}^{\infty} e^{-\left(\frac{U_o t}{a}\right)^2} dt\,dv_{\theta m}\,dY\,da\,dn \tag{L-3}$$

Integration of this expression produces the desired mean square value of axial velocity fluctuation.

$$\frac{\overline{u^2}}{U_o^2} = n^2\left(\frac{NH}{U_o}\right)\frac{\pi}{2} e \frac{(m_v + 1)(m_v + 2)}{(m_v - n_v + 2)(m_v + n_v + 3)} \int_0^1 \left[\frac{-h}{a} e^{-(h/a)^2} - \right. \tag{L-4}$$

$$\left(\frac{H-h}{a}\right)e^{-\left(\frac{H-h}{a}\right)^2} + \text{ERF}\left(\frac{H-h}{a}\right) + \text{ERF}\left(\frac{h}{a}\right)\right] \left[k_a \left(\frac{a}{H}\right)^{m_a+2}\left(1 - \frac{a}{H}\right)^{n_a}\right] d\left(\frac{a}{H}\right)$$

189

The last integral must be solved by numerical integration techniques. The vertical velocity correlation can be solved in a similar manner.

Vertical Velocity Correlation. - The vertical component of fluctuating velocity, $v(t)$, is given by Equation L-1 and with the substitution $X = U_o t$ becomes:

$$v(t) = -nv_{\theta m} \left(\frac{U_o t}{a}\right) e^{-\frac{1}{2}\left[\left(\frac{U_o t}{a}\right)^2 + \left(\frac{Y}{a}\right)^2 - 1\right]} \qquad (L-5)$$

The mean square velocity will thus be:

$$\frac{\overline{v^2}}{U_o^2} = Ne^{+1} \int n^2 \int_0^H \frac{k_a}{H} \left(\frac{a}{H}\right)^{m_a} \left(1 - \frac{a}{H}\right)^{n_a} \int_{-h}^{H-h} \frac{1}{H} e^{-\left(\frac{Y}{a}\right)^2} \int_0^{U_o} \frac{k_v}{U_o} \left(\frac{v_{\theta m}}{U_o}\right)^{m_v + 2}$$

$$\left(1 - \frac{v_m}{U_o}\right)^{n_v} \int_{-\infty}^{\infty} \left(\frac{U_o t}{a}\right)^2 e^{-\left(\frac{U_o t}{a}\right)^2} dt \, dv_{\theta m} \, da \, dY \, dn \qquad (L-6)$$

Integration of this expression as far as possible in closed form yields the following equation:

$$\frac{\overline{v^2}}{U_o^2} = n^2 \left(\frac{NH}{U_o}\right) \frac{\pi}{2} e \frac{(m_v + 1)(m_v + 2)}{(m_v + n_v + 2)(m_v + n_v + 3)} \int_0^1 [ERF\left(\frac{H-h}{a}\right) +$$

$$ERF\left(\frac{h}{a}\right)] \, [k_a \left(\frac{a}{H}\right)^{m_a + 2} \left(1 - \frac{a}{H}\right)^{n_a}] \, d\left(\frac{a}{H}\right) \qquad (L-7)$$

Velocity Cross-correlation. - Combining the horizontal and vertical components yields:

$$uv = -n^2 v_{\theta m}^2 \left(\frac{Y}{a}\right) \left(\frac{U_o t}{a}\right) e^{-\left[\left(\frac{U_o t}{a}\right)^2 + \left(\frac{Y}{a}\right)^2 - 1\right]} \qquad (L-8)$$

190

The cross correlation is computed from the following integral equation:

$$\frac{\overline{uv}}{U_o^2} = Ne^{+1} \int n^2 \int_0^H \frac{k_a}{H} \left(\frac{a}{H}\right)^{m_a} \left(1 - \frac{a}{H}\right)^{n_a} \int_{-h}^{H-h} \frac{1}{H} \left(\frac{Y}{a}\right) e^{-\left(\frac{Y}{a}\right)^2}$$

$$\int_0^{U_o} \frac{k_v}{U_o} \left(\frac{v_{\theta m}}{U_o}\right)^{m_v+2} \left(1 - \frac{v_{\theta m}}{U_o}\right)^{n_v} \int_{-\infty}^{\infty} \left(\frac{U_o t}{a}\right) e^{-\left(\frac{U_o t}{a}\right)^2} dt\, dv_{\theta m}\, dY\, da\, dn$$

$$(L\text{-}9)$$

Integrating this expression as far as possible in closed form yields Equation L-10.

$$\frac{\overline{uv}}{U_o^2} = \frac{-n^2 e^{+1}}{2} \left(\frac{NH}{U_o}\right) \frac{(m_v + 1)(m_v + 2)}{(m_v + n_v + 2)(m_v + n_v + 3)} \int_0^1 \left[e^{-(h/a)^2} - e^{-\left(\frac{H-h}{a}\right)^2}\right]$$

$$\left[k_a \left(\frac{a}{H}\right)^{m_a+2} \left(1 - \frac{a}{H}\right)^{n_a}\right] d\left(\frac{a}{H}\right) \qquad (L\text{-}10)$$

Mean Velocity. - The mean value of the perturbation in axial velocity is found by use of Equation L-11.

$$\overline{u} = N \int_n \int_Y \int_{v_{\theta m}} \int_a \int_t \overline{u}(t)\ P(a)\ P(v_{\theta m})\ P(Y)\ P(n)\ dt\, dv_{\theta m}\, da\, dY\, dn \qquad (L\text{-}11)$$

Substitution of the axial velocity perturbation and density functions into Equation L-11 yields the time averaged or mean velocity:

$$\frac{\bar{u}}{U_o} = Ne^{+1/2} \int_n \int_0^H \frac{k_a}{H}(\frac{a}{H})^{m_a} (1 - \frac{a}{H})^{n_a} \int_{-h}^{H-h} (\frac{Y}{a}) e^{-\frac{1}{2}(\frac{Y}{a})^2}$$

$$\int_0^{U_o} \frac{k_v}{U_o} (\frac{v_{\theta m}}{U_o})^{m_v+1} (1 - \frac{v_{\theta m}}{U_o})^{n_v} \int_{-\infty}^{\infty} e^{-\frac{1}{2}(\frac{U_o t}{a})^2} dt dv_{\theta m} dY da dn$$

$$\text{(L-12)}$$

This can be simplified to Equation L-13.

$$\frac{\bar{u}}{U_o} = n(\frac{NH}{U_o}) \; 2\pi e \frac{(m_v + 1)}{(m_v + n_v + 2)} \int_0^1 [e^{-\frac{1}{2}(\frac{h}{a})^2} - e^{-\frac{1}{2}(\frac{H-h}{a})^2}]$$

$$[k_a (\frac{a}{H})^{m_a+2} (1 - \frac{a}{H})^{n_a}] \; d(\frac{a}{H}) \qquad \text{(L-13)}$$

The mean vertical velocity is found by similar methods.

$$\bar{v} = N \int_n \int_y \int_{v_{\theta m}} \int_a \int_t v(t) \; P(a) \; P(v_{\theta m}) \; P(Y) \; P(n) \; dt dv_{\theta m} da dY dn$$

After introducing the expression for the vertical velocity, this becomes:

$$\frac{\bar{v}}{U_o} = - Ne^{1/2} \int_n \int_0^H \frac{k_a}{H} (\frac{a}{H})^{m_a} (1 - \frac{a}{H})^{n_a} \int_{-h}^{H-h} \frac{1}{H} e^{-\frac{1}{2}(\frac{Y}{a})^2}$$

$$\int_0^{U_o} \frac{k_v}{U_o} (\frac{v_{\theta m}}{U_o})^{m_v+1} (1 - \frac{v_{\theta m}}{U_o})^{n_v} \int_{-\infty}^{\infty} (\frac{U_o t}{a}) e^{-\frac{1}{2}(\frac{U_o t}{a})^2} dt dv_{\theta m} dY da dn$$

$$\text{(L-14)}$$

192

And simplifies to:

$$\frac{\bar{v}}{U_o} = 0$$

Static Pressure. - A static pressure gradient can be supported by the Reynolds shear stresses. This can also be obtained by use of the turbulent flow model.

$$\frac{\Delta p}{\rho} = N \int_n \int_Y \int_{v_{\theta m}} \int_a \int_t \frac{n^2}{2} v_{\theta m}^2 \ e^{- [(\frac{U_o t}{a})^2 + (\frac{Y}{a})^2 - 1]}$$

$$P(a) \ P(v_{\theta m}) \ P(Y) \ P(n) \ dt dv_{\theta m} da dY dn \qquad \text{(L-16)}$$

Substitution of the density functions and integration yields:

$$\frac{\Delta p}{\rho} = n^2 (\frac{NH}{U_o}) \ e \ \pi \ U_o^2 (\frac{\bar{v}_{\theta m}}{U_o}) (\frac{m_v + 2}{m_v + n_v + 3})$$

$$\int_0^1 [ERF (\frac{H-h}{a}) + ERF (\frac{h}{a})] [k_a (\frac{a}{H})^{m_a + 2} (1 - \frac{a}{H})^{n_a}] \ d (\frac{a}{H}) \qquad \text{(L-17)}$$

The preceding velocity correlations and static pressure were evaluated by a numerical integration procedure for the probe location variation from h=o to h=H/2. The data are presented in Figure L-1, normalized by $\overline{u^2}$.

193
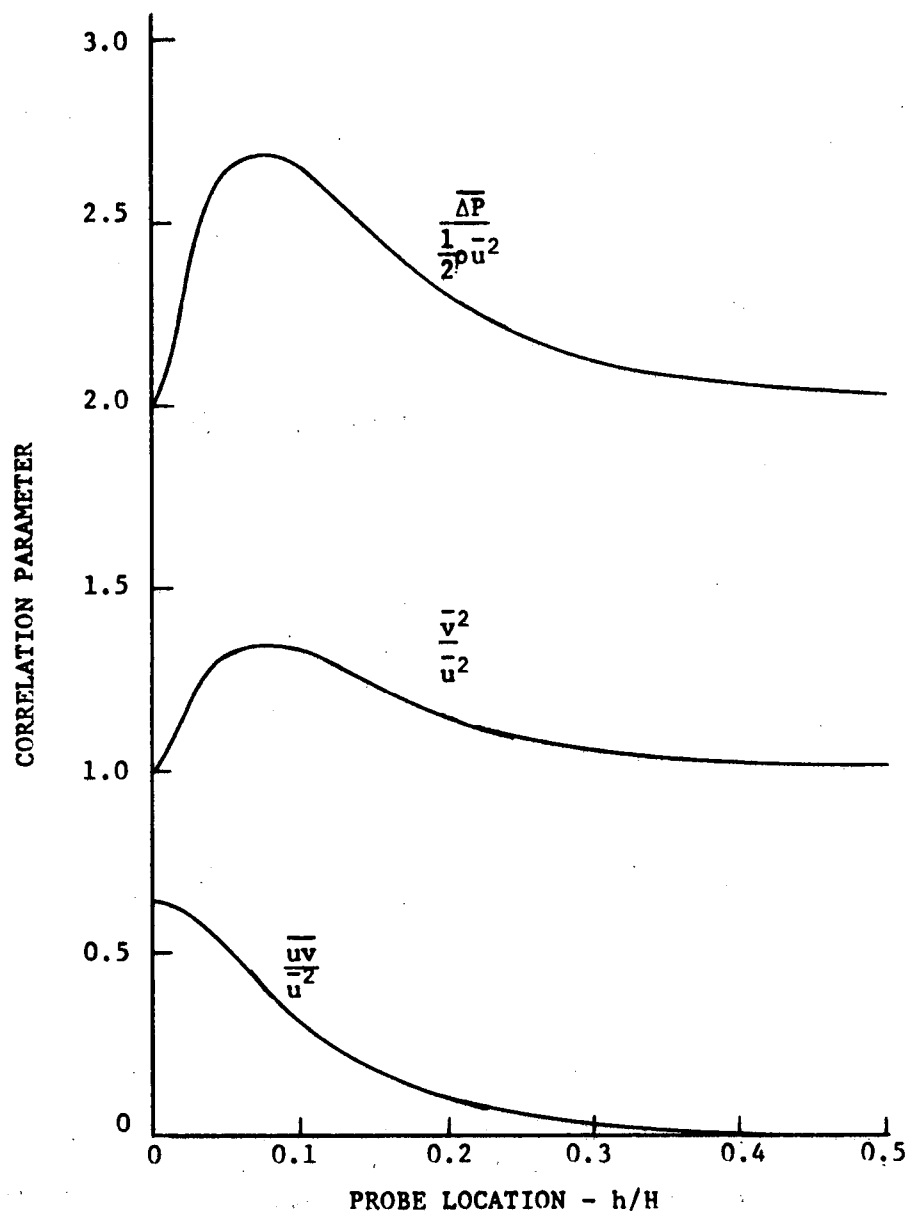
Figure L-1. Velocity Correlations (Reynolds Stresses) and Static Pressure Difference as Computed from the Turbulent Flow Model.

194

Evaluations. - With the assumption of the vortex rotational direction being equally probable plus or minus, and for the sensing probe in the center of the channel (h = H/2). The mean velocities and correlations can be found in closed form. These are:

$$\bar{u} = 0$$

$$\bar{v} = 0$$

$$\frac{\bar{u}^2}{U_o^2} = \frac{\bar{v}^2}{U_o^2} = \frac{\pi e}{2} \left(\frac{NH}{U_o}\right) \left(\frac{\bar{a}}{H}\right) \left(\frac{\bar{v}_{\theta m}}{U_o}\right) \frac{(m_v + 2)}{(m_v + n_v + 3)} \frac{(m_a + 2)}{(m_a + n_a + 3)} \qquad \text{(L-18)}$$

$$\frac{\overline{uv}}{U_o^2} = 0$$

$$\frac{\overline{\Delta P}}{1/2 \, \rho U_o^2} = 0$$

At h = 0 (at one wall) the static pressure simplifies to:

$$\frac{\overline{\Delta p}}{1/2 \, \rho U_o^2} = \pi e \left(\frac{NH}{U_o}\right) \left(\frac{\bar{a}}{H}\right) \left(\frac{\bar{v}_{\theta m}}{U_o}\right) \frac{(m_v + 2)}{(m_v + n_v + 3)} \frac{(m_a + 2)}{(m_a + n_a + 3)} \qquad \text{(L-19)}$$

A relationship between the velocity correlations (or Reynolds stresses as they are commonly called) and measurements taken by high response total pressure instrumentation can now be established by application of the turbulent flow model. An example is given in the next section.

Unsteady Total Pressure and Velocity Correlation. - The relationship
between the turbulent fluctuation in total pressure can now be related to the
fluctuations in velocity by use of the vortex flow model. This will link
total pressure and hot wire anermometer measurements. The mean square velocity
fluctuation was computed at the center of the duct in the preceding section.
This is:

$$\frac{\overline{u^2}}{U_o^2} = \frac{\pi e}{2} \left(\frac{NH}{U_o}\right) \left(\frac{\overline{a}}{H}\right) \left(\frac{\overline{v}_{\theta m}}{U_o}\right) \frac{(m_v + 2)}{(m_v + n_v + 3)} \frac{(m_a + 2)}{(m_a + n_a + 3)} \tag{L-18}$$

The mean square level of the total pressure fluctuations is given for
the center of the duct by Equation L-19.

$$\frac{\overline{\Delta p_T^2}}{q_o^2} = \pi e \left(\frac{NH}{U_o}\right) \left(\frac{\overline{a}}{H}\right) \left(\frac{\overline{v}_{\theta m}}{U_o}\right) \frac{(m_a + 2)}{(m_a + n_a + 3)} \left[\frac{2 (m_v + 2)}{(m_v + n_v + 3)} \right.$$

$$\left. + \frac{11e}{32} \frac{(m_v + 3)(m_v + 4)(m_v + 2)}{(m_v + n_v + 4)(m_v + n_v + 5)(m_v + n_v + 3)} \right. \tag{L-19}$$

The ratio of velocity fluctuation to total pressure fluctuation is
established from Equations L-18 and L-19.

$$\frac{\dfrac{\overline{u^2}}{U_o^2}}{\dfrac{\overline{\Delta p_T^2}}{q_o^2}} = \frac{1}{4 + \dfrac{11e (m_v + 3)(m_v + 5)}{16 (m_v + n_v + 4)(m_v + n_v + 5)}} \tag{L-20}$$

After appropriate simplification and for the velocity probability density func-
tion having the exponents $m_v = 4$ and $n_v = 14$ (Refer to Figure 26 for the
density functions), the ratio becomes:

$$\frac{\dfrac{\overline{u^2}}{U_o^2}}{\dfrac{\overline{\Delta p_T^2}}{q_o^2}} = \frac{1}{4 + \dfrac{11e (7)(8)}{16 (22)(23)}} = 0.238 \tag{L-21}$$

196

Results of Equation L20 , which has very little dependence on the exponents of the density functions (m_V, n_V), were shown graphically in Figure 31 of the main text for various levels of turbulence (ΔP_{TRMS}) and flow Mach numbers.

This result is significant. For the first time a relationship has been developed between turbulence as velocity fluctuations and turbulence as total pressure fluctuations. Previously, the relationship was obtained by assuming either sonic waves or a quasi-study analysis with a constant static pressure.

APPENDIX M

FLUID DYNAMIC MODEL OF TURBULENT FLOW - COMPUTER ROUTINE

A computer program was written to evaluate the statistical properties of turbulent flow by numerical integration of the equations described in the main text. These properties include the Power Spectral Density function, Auto-correlation function, and Root Mean Square value of the total pressure fluctuations. Also included are the velocity correlation terms, $\overline{u^2}$, $\overline{v^2}$, $\overline{uv}$, and the static pressure deviation, $\overline{\Delta P_S}$. A description of this computer program is the subject of this Appendix.

The program is a digital computer solution of the Fluid Dynamic Model of Turbulent Inlet Flow. The single vortex total pressure variations is combined with the vortex random properties of size, strength, location, and spin direction. The resultant equation is integrated with respect to the various random parameters and specified delay time (τ) to yield the autocorrelation function. This autocorrelation based on the deviation of the total pressure fluctuations from the mean is made non-dimensional by the uniform stream dynamic pressure ($q_0 = \frac{1}{2} \rho U_0^2$). The autocorrelation function is also computed normalized by the value at a delay (τ) of zero (the mean square level).

The Fourier transform of the normalized autocorrelation function is obtained by a numerical integration procedure. The result is the power spectral density (PSD) function of the total pressure fluctuations.

INPUT:

The input data card arrangement is shown in Figure 1. The input parameters are described below followed by a discussion of the Input default options.

PARAMETERS

UO	-	duct (engine face) flow uniform velocity - ft/sec
RHO	-	duct flow density - LBM/ft^3
HU	-	duct height (diameter) - in.
H	-	distance of sensing probe from lower duct wall - in.
DP	-	ratio of root mean square total pressure fluctuation to average total pressure - $\Delta P_T / \overline{P_T}$
MO	-	Mach Number
DTAU	-	delay time increment for computing autocorrelation function, normalized, DTAU = TAU * Uo/a
TAUL	-	limit value for computing autocorrelation function

MVD, NVD	-	vortex strength Beta probability density function (PDF) exponents
MAD, NAD	-	vortex size Beta PDF exponents
ANP, ANM	-	fraction of total vortices which have positive and negative, respectively, spin directions. Positive is counterclockwise; negative is clockwise rotation.
LINE	-	Key for printing the vortex core size and strength PDF's.
PN	-	Number of proportional parts per decade of the frequency that PSD is computed. $\Delta f = 10^{1/PN}$
FLM	-	Limiting value of frequency that PSD is computed. $1 \leqq f \leqq FLM \quad -HZ$

INPUT PARAMETER DEFAULT OPTIONS

IF Uo = 0, execution stops, use blank card to terminate.

IF Mo = 0, Mo defaults to 0.4

IF DP = 0, DP defaults to 0.02

IF TAUL = 0, TAUL defaults to 3.0

IF ANP = ANM = 0, set ANP = 0.5 & ANM = 0.5

IF MVD = NVD = 0 and MAD = MAD = 0, then previous core size and strength PDF's are used, but not printed.

IF MVD $\neq$ NVD and MAD $\neq$ NAD, then new core size and strength, PDF's are computed.

IF LINE = 0, the PDF's are not printed,
    LINE $\neq$ 0, the PDF's are printed.

IF DTAU = 0, autocorrelation and PSD will <u>not</u> be computed.

OUTPUT DESCRIPTION:

The output data are printed in four groups - Probability Density Functions, velocity correlations, autocorrelation function, and the power spectral density function. Each output data group will be discussed separately. In addition, the input data are printed with each output data group.

PROBABILITY DENSITY FUNCTIONS

KV	-	Beta PDF constant for vortex strength (velocity)
KA	-	Beta PDF constant for vortex size
VBAR	-	Mean vortex strength $(\overline{v\theta}_{max}/U_o)$
ABAR	-	Mean vortex core size $(\overline{a}/H)$
A/H	-	ratio of vortex core size to inlet duct height
A	-	vortex core size - in.

200

C-3

P(A)   -   probability of vortex having size A/H

VTM/Uo   -   ratio of vortex maximum velocity to local flow velocity ($v\theta_{max}/Uo$)

VTM   -   probability of vortices having strength VTM

VELOCITY CORRELATIONS

H/HU   -   total pressure probe location; h/H in model

H   -   absolute value of probe location - in.

UUBAR   -   mean square axial velocity fluctuation, normalized by local velocity square (Uo^2) and the term (NH/Uo).

VVBAR   -   mean square lateral velocity fluctuation, normalized by Uo^2 and (NH/Uo)

UVBAR   -   mean velocity cross correlation, normalized by Uo^2 and (NH/Uo).

UBAR/Uo   -   mean axial velocity fluctuation, normalized by Uo and (NH/Uo).

VBAR/Uo   -   mean lateral velocity fluctuation, normalized by Uo and (NH/Uo).

DP/Qo   -   mean static pressure fluctuation, normalized by dynamic pressure based on local flow ($qo = \frac{1}{2} \rho\, Uo^2$) and (NH/Uo).

DUUDY   -   gradient of mean square axial velocity fluctuation with respect to Y.

DVVDY   -   similar to DUUDY for mean square of lateral velocity

DUVDY   -   similar to DUUDY for velocity cross correlations

DUDY   -   similar to DUUDY for mean axial velocity

DVDY   -   similar to DUUDY for mean lateral velocity

DPBY   -   similar to DUUDY for mean static pressure

AUTOCORRELATION FUNCTIONS

ALUMP   -   intermediate results

ABAR/Uo   -   inverse of time delay normalizing factor

AK   -   number of vortices per unit time (N)

TAU*UO/A   -   normalized time delay

TAU   -   actual time delay, τ - sec

RXT   -   actual total pressure autocorrelation at time delay, τ

RXT/RXTO   -   total pressure autocorrelation normalized by value at $\tau = 0$

RUT   -   actual velocity autocorrelation at time delay, τ

RUT/RUTO   -   velocity autocorrelation normalized by value at $\tau = 0$.

POWER SPECTRAL DENSITY FUNCTION

F	-	frequency HZ (CPS)
FR	-	normalized frequency FR = F* ABAR/Uo
GXF	-	total pressure power spectral density at frequency, f
GXFR	-	normalized power spectral density at frequency, f or FR
RMS	-	integrated area under PSD curve
GUF	-	velocity power spectral density at frequency, f
GUFR	-	normalized power spectral density at frequency, f or FR

202

"BLANK CARD TERMINATES EXECUTION"

"REPEAT THREE DATA CARDS FOR ADDITIONAL CASES"

F10.5	F10.5		
PN	FLM		

I5	I5	I5	I5	F10.5	F10.5	I5
MVD	NVD	MAD	NAD	ANP	ANM	LINE

F10.5	F10.5	F10.5	F10.5	F10.5	F10.5	F10.5	F10.5
UO	RHO	HU	H	DP	MO	DTAU	TAUL

FIGURE M1 INPUT DATA DECK ARRANGEMENT.

203

```
      PROGRAM D4815(INPUT,OUTPUT,TAPE5=INPUT,TAPE6=OUTPUT)
C     AUTOCORELATION PROGRAM VERSION TWO BEGUN 11/30/1972         A  15
      REAL INTVA,INTVB,       INTVD,INTTA,INTTB,      INTTD,INTA,INTB,  A  20
     1INTC,INTD,INAA,INAB,     INAD,KV,KA                         A  30
      REAL INTYA,INTYB,       INTYD
      DIMENSION TR(100), RXTT(100), FUN(20) ,RUTT(100)
      COMMON   APAR,     AK,ALUMPA,      DA,     DT, DTAU,    H,     HU, A  60
     1      INTVA, INTVD,    KA,    KV,  LINE,     M,  MAD,   MV,   A  70
     2      MVD,    N,    NA,   NAD,   VV,   NVD,   RHO,    TL,   A  80
     3      UO, VRAR,    MA,  TAUL,   ANP,  ANM, ALUMP,   FUN,   A  90
     4      INTVB
      COMMON /DATA/ TR,RXTT,PN,FLM,TLM,NT,RUTT                    A 100
   10 FORMAT (1H1,20X,23HAUTOCORELATION PROGRAM//)                A 110
   20 FORMAT (8F10.5)                                             A 120
   30 FORMAT (14X,2HUO,5X,3HRHO,4X,2HHU,5X,1HH,5X3HDPT,4X,2HMO,3X,4HDTAU A 130
     1,2X,4HTAUL/10X,F7.1,F7.4,2F7.2,F6.3,F7.3,F6.3,F7.3)         A 140
   40 FORMAT (15X,F7.3,F8.4,F11.5,F9.5,F11.5,F9.5)                A 150
   50 FORMAT (/15X,8HTAU*UO/A,3X,3HTAU,7X,3HRXT,4X,8HPXT/RXTO,    A 160
     * 5X,3HPUT,4X,8HRUT/PUTO/)                                   A 165
   60 FORMAT (/12X,2HMV,3X,2HNV,6X,2HKV,5X,4HVRAR/9X,2I5,F9.0,F8.4//12X, A 170
     12HMA,3X,2HNA,6X,2HKA,5X,4HARAP,5X,2HN+,5X,2HN-/9X,2I5,F9.0,F8.4, A 180
     * 2F7.3)                                                     A 185
   70 FORMAT (4I5,2F10.5,2I5)                                     A 190
   80 FORMAT (/12X,5HALUMP,7X,7HARBAS/UO,7X,7H  AK   /10X,3E12.4) A 200
C     AWHOLE BUNCH OF CONSTANTS                                   A 210
      CA=2.0                                                      A 220
      CB=SQRT(2.0/3.0)                                            A 230
      CC=SQRT(2.0)                                                A 240
      CD=5.0/16.0                                                 A 250
      CE=11.0/(16.0*CC)                                           A 260
      CF=SQRT(6.0)                                                A 270
      ALUMPA=EXP(1.0)/CA                                          A 280
      ALUMPB=EXP(1.5)*CB/9.                                       A 290
      ALUMPD=EXP(2.0)/CC/4.0                                      A 300
   90 READ (5,20) UO,RHO,HU,H,DT,TL,DTAU,TAUL                     A 310
      IF (UO.EQ.0.0) STOP                                         A 320
      IF (TL.EQ.0) TL=0.4
      IF (DT.EQ.0.0) DT=0.02
      IF (TAUL.EQ.0) TAUL=3.0                                     A 340
      DDTAU=2.0*DTAU                                              A 350
      READ (5,70) MVD,NVD,MAD,NAD,ANP,ANM,LINE                    A 360
      IF (ANP.NE.0.0) GO TO 95                                    A 362
      IF (ANM.NE.0.0) GO TO 95                                    A 364
      ANP=0.5
      ANM=0.5
   95 READ (5,20) PN,FLM                                          A 370
      IF (MAD.EQ.0.AND.NAD.EQ.0) GO TO 100                        A 380
      GO TO 110                                                   A 390
  100 IF (MVD.EQ.0.AND.NAD.EQ.0) GO TO 120                        A 400
  110 CALL PROFLE                                                 A 410
  120 LINE=14                                                     A 420
C     LEADING CONSTAN  ALUMP                                      A 430
      ALUMP=8.0   *KA*HU/(12.0*UO)                                A 440
      CALL VELCOR                                                 A 450
      IF (DTAU.EQ.0.0) GO TO 90
```

204

```
              ALUMUA=AK    *KA*HU/(12.0*UO)*EXP(1.0)
              TLM=ABAR*HU/(12.0*UO)                                    A 460
              TLLM=1.0/(6.283185*FLM)                                  A 470
              TULM=TLLM/TLM                                            A 480
       60     CCC=10.0E-08                                             A 490
              DO 140 I=1,10                                            A 500
              IF (CCC-TULM) 130,150,150                                A 510
       130    CCC=10.0*CCC                                             A 520
       140    CONTINUE                                                 A 530
       65     150 DTU=0.1*CCC                                          A 540
              IF (DTU.GT.DTAU) DTU=DTAU                                A 550
              TU=0.0-DTU                                               A 560
              WRITE (6,10)                                             A 570
              WRITE (6,30) UO,RHO,HU,H,DT,TL,DTAU,TAUL                 A 580
       70     WRITE (6,60) MV,NV,KV,VBAP,MA,NA,KA,APAR,ANP,ANM         A 590
              WRITE (6,80) ALUMF,TLM,AK                                A 600
              WRITE (6,50)                                             A 610
              DO 240 ITU=1,1000                                        A 620
              IF (TU.GT.DTAU) GO TO 160                                A 630
       75     TU=TU+DTU                                                A 640
              IF (ITU.EQ.1) GO TO 170                                  A 650
              DTU=2.0*DTU                                              A 660
              GO TO 170                                                A 670
              160 IF (TU.LT.DDTAU) TU=DTAU                             A 680
       80     TU=TU+DTAU                                               A 690
              170 TR(ITU)=TU                                           A 700
              IF (TU.GT.TAUL) GO TO 250                                A 710
              TAU=TU*TLM                                               A 720
              TAU2=TAU*TAU                                             A 730
       85     AOH=0.0                                                  A 740
              J=0                                                      A 750
              FIA=0.0                                                  A 760
              FIP=0.0
              FID=0.0                                                  A 780
       90     FIIA=0.0                                                 A 790
              FIIB=0.0
              FIID=0.0                                                 A 810
              DO 20 I=1,20                                             A 820
              AOH=AOH+DA                                               A 830
       95     IF (AOH.GT.1.0) GO TO 210                                A 840
              A=AOH*HU                                                 A 850
              RAH=-H/A                                                 A 860
              RAH2=RAH*RAH                                             A 870
              RAHU=(HU-H)/A                                            A 880
       100    RAHU2=RAHU*RAHU                                          A 890
              PHIAL=-RAH                                               A 900
              PHIAH=RAHU                                               A 910
              KODE=1                                                   A 920
              CALL SUMMER (PHIAL,CINTAL,KODE)                          A 930
       105    CALL SUMMER (PHIAH,CINTAH,KODE)                          A 940
              INTYA=(RAH*EXP(-RAH2)-RAHU*EXP(-RAHU2)+CINTAL+CINTAH)     A 950
              INTYB=EXP(-1.5*RAHU2)*(1.0-3.0*RAHU2)-EXP(-1.5*RAH2)*(1.0-3.*RAH2)   A 960
              CHIL=-CC*RAH                                             A 970
              CHIH=CC*RAHU                                             A 980
       110    CALL SUMMER (CHIL,CINTDL,KODE)                           A 990
```

```
            CALL SUMMER (CHIH,CINTDH,KODE)                              A1000
            INTYD=EXP(-2.0*RAH2)*(RAH*RAH2/4.0+CD*RAH)-EXP(-2.C*RAHU2)*(RAHU*R  A1010
           1AHU2/4.0+CD*RAHU)+CE*(CINTDL+CINTDH)                        A1020
            FUNCA=FUN(I)                                                A1030
115         UOA=12.0*UO/A                                               A1040
            UOA2=UOA*UOA                                                A1050
            TAUA=TAU*TAU*UOA2/4.0                                       A1060
            TAUB=TAUA*4.0/3.0                                           A1070
            TAUD=TAU2*UOA2/2.                                           A1080
120         TA=EXP(-TAUA)                                              A1090
            TB=EXP(-TAUB)                                               A1100
            TD=EXP(-TAUD)                                               A1110
            T=0.0                                                       A1120
            PHI=UOA*TAU/2.0                                             A1130
125         PSI=UOA*TAU*CB                                             A1140
            OMEGA=UOA*TAU/CF                                            A1150
            CHI=UOA*TAU/CC                                              A1160
            KODE=2                                                      A1170
            CALL SUMMER (PHI,INTA,KODE)                                 A1180
130         CALL SUMMER (PSI,INTB,KODE)                                 A1190
            CALL SUMMER (OMEGA,INTC,KODE)                               A1200
            CALL SUMMER (CHI,INTD,KODE)                                 A1210
            INTTA=INTA*TA                                               A1220
            INTTB=TB*(INTB+INTC)                                        A1230
135         INTTD=INTD*TD                                              A1240
            PAA=FUNCA*INTTA*INTYA                                       A1250
            PAB=FUNCA*INTTB*INTYB                                       A1260
            PAD=FUNCA*INTTD*INTYD                                       A1270
            J=J+1                                                       A1280
140         GO TO (180,190), J                                         A1290
        180 FIA=FIA+PAA                                                A1300
            FIB=FIB+PAB                                                 A1310
            FID=FID+PAD                                                 A1320
            GO TO 200                                                   A1330
145     190 J=0                                                        A1340
            FIIA=FIIA+PAA                                               A1350
            FIIB=FIIB+PAB                                               A1360
            FIID=FIID+PAD                                               A1370
        200 CONTINUE                                                    A1380
150     210 CONTINUE                                                    A1390
            INAA=(PAA+4.0*FIA+2.C*FIIA)*DA/3.0                          A1400
            INAB=(PAB+4.0*FIB+2.)*FIIB)*DA/3.C                          A1410
            INAB=INAB*(ANP-ANM)
            INAD=(PAD+4.0*FID+2.C*FIID)*DA/3.0                          A1420
155         RXT=ALUMP*(ALUMPA*INAA*INTVA+ALUMPB*INAB*INTVB+ALUMPD*INAD*INTVD)  A1430
            RXT=RXT*AK
            RUT=ALUMUA*INAA*INTVA
            IF (ITU.NE.1) GO TO 220                                     A1440
            RXTO=RXT                                                    A1460
160         RUTO=RUT
        220 RXPT=RXT/RXTO                                               A1470
            RUPT=RUT/RUTO
            RXTT(ITU)=RXPT                                              A1480
            RUTT(ITU)=RUPT
165         LINE=LINE+1                                                A1490
```

```
              IF (LINE.LT.61) GO TO 230                              A1500
              WRITE (6,10)                                           A1510
              WRITE (6,50)                                           A1520
              LINE=6                                                 A1530
   170    230 WRITE (6,40) TU,TAU,RXT,RXRT,RUT,RURT                  A1540
              IF (RXRT.LT.0.001) GO TO 250                           A1550
          240 CONTINUE                                               A1560
          250 CONTINUE                                               A1570
              NT=ITU-1                                               A1580
   175        CALL FOWER                                             A1590
              GO TO 90                                               A1600
              END                                                    A1610-
```

```
208                    SUBROUTINE FACT (IS,SUM)                              B  10
                       SUM=1.0                                               B  20
                       DO 10 I=1,IS                                          B  30
                       SUM=I*SUM                                             B  40
       5            10 CONTINUE                                              B  50
                       RETURN                                                B  60
                       END                                                   B  70-
```

```
      SUBROUTINE KXBAR (M,N,K,XBAR)              C  10
      REAL K                                     C  20
      IS=M+N+1                                   C  30
      CALL FACT (M,SKM)                          C  40
5     CALL FACT (IS,SKNN)                        C  50
      CALL FACT (N,SKN)                          C  60
      K=SKNN/(SKM*SKN)                           C  70
      IS=IS+1                                    C  80
      SKNN=SKNN*IS                               C  90
10    SKM=SKM*(M+1)                              C 100
      XBAR=K*SKM*SKN/SKNN                        C 110
      RETURN                                     C 120
      END                                        C 130-
```

209

```
                    SUBROUTINE POWER                                         D   10
                    DIMENSION TR(100), RXTT(100), EE(100), EU(100), RUTT(100)
                    COMMON /DATA/ TR,RXTT,PN,FLM,TLM,NT,RUTT
             10 FORMAT (1H1,15X,19HPOWER SPECTRUM HACK/)                     D   40
      5      20 FORMAT (1H0,16X,1HF,9X,2HFP,9X,3HGXF,9X,4HGXFR,8X,3HRMS,     D   40
                *   9X,3HGUF,9X,4HGUFX/)                                     D   45
             30 FORMAT (10X,7E12.4)                                         D   60
             40 FORMAT (/12X,5H  PN  ,7X,7HABAR/UO,7X,7H FLIMIT/10X,3E12.4)  D   70
                    F=1.0/PN                                                D   80
      10        AMUL=10.0**F                                                D   90
                    WRITE (6,10)                                            D  100
                    IF (FLM.EQ.0.0) FLM=10.0E+06                            D  110
                    IF (PN.EQ.0.0) PN=1.0                                   D  120
                    WRITE (6,40) PN,TLM,FLM                                 D  130
      15        WRITE (6,20)                                                D  140
                    F=1.0                                                   D  150
                    EE(1)=0.0                                               D  160
                    EU(1)=0.0
                    DO 50 I=2,NT                                            D  170
      20        EE(I)=ALOG(RXTT(I))/TR(I)                                   D  180
                    EU(I)=ALOG(RUTT(I))/TR(I)
             50 CONTINUE                                                    D  190
                    RMS=0.0                                                 D  200
                    DO 140 I=1,100                                          D  210
      25        IF (I-2) 80,60,70                                           D  220
             60 F=AMUL                                                      D  230
                    GO TO 80                                                D  240
             70 F=F*AMUL                                                    D  250
             80 CONTINUE                                                    D  260
      30        IF (F.GT.FLM) GO TO 150                                     D  270
                    FR=F*TLM                                                D  280
                    ARG=2.0*3.14159*FR                                      D  290
                    TRCONS=1.0/FR                                          D  300
                    IF (TRCONS.GT.TR(NT)) GO TO 90                          D  310
      35        DT=0.1*TRCONS                                               D  320
                    GO TO 100                                               D  330
             90 DT=0.1*TR(NT)                                               D  340
            100 AN=TR(NT)/DT                                                D  350
                    N=AN+1                                                  D  360
      40        TA=TR(1)-DT                                                 D  370
                    GXF=0.0                                                 D  380
                    GUF=0.0
                    DO 120 J=1,N                                            D  390
                    TA=TA+DT                                                D  400
      45        CALL TBLUP1 (TR,EE,TA,EX,DEXDTR,NT)                         D  410
                    CALL TBLUP1 (TR,EU,TA,ER,DEADTR,NT)
                    RXT=EXP(EX*TA)
                    RUT=EXP(ER*TA)
                    IF (J.EQ.1) GO TO 110                                   D  430
      50        T=TA-0.5*DT                                                 D  440
                    ANF=COS(ARG*T)                                          D  450
                    GXF=GXF+(RXT+RXTL)*ANF*DT*2.0                           D  460
                    GUF=GUF+(RUT+RUTL)*ANF*DT*2.0
            110 RXTL=RXT                                                    D  470
      55        RUTL=RUT
```

```
              120 CONTINUE                                                    D 480
                  IF (I.EQ.1) GXFF=GXF                                        D 490
                  IF (I.EQ.1) GUFF=GUF
                  GXFR=GXF/GXFF                                               D 500
60                GUFR=GUF/GUFF
                  IF (I.EQ.1) GO TO 130                                       D 510
                  RMS=RMS+0.5*(GXF+GXFL)*(FR-FRL)                             D 520
              130 CONTINUE                                                    D 530
                  WRITE (6,30) F,FR,GXF,GXFR,RMS,GUF,GUFR                     D 540
65                GXFL=GXF                                                    D 550
                  FRL=FR                                                      D 560
              140 CONTINUE                                                    D 570
              150 CONTINUE                                                    D 580
                  RETURN                                                      D 590
70                END                                                        D 600-
```

211

```
                     SUBROUTINE PROFLE                              E  10
                     DIMENSION FUN(20)                              E  20
                     REAL INTVA,INTVD,KA,KV,INTVB                   E  30
                     COMMON  ABAR,     AK,ALUMPA,      DA,     DT,  DTAU,      H,    HU,    E  4C
        5            1        INTVA, INTVD,    KA,    KV,   LINE,     M,   MAD,    MV,    E  50
                     2        MVD,     N,    NA,  NAD,     NV,  NVD,   RHO,    TL,    E  60
                     3        UO,   VBAR,    MA,  TAUL,    ANF,   ANM, ALUMP,   FUN,    E  70
                     4        INTVB
                  10 FORMAT (1H1,20X,25HPROBABILITY DISTRIBUTIONS/)                    E  80
        1C        20 FORMAT (14X,2HUO,5X,3HRHO,4X,2HHU,5X,1HH,5X3HDPT,4X,2HMO,3X,4HDTAU E  90
                   1,2X,4HTAUL/10X,F7.1,F7.4,2F7.2,F6.3,F7.3,F6.3,F7.3)                E 100
                  30 FORMAT (/12X,2HMV,3X,2HNV,6X,2HKV,5X,4HVBAR/9X,2I5,F9.0,F8.4//12X, E 110
                   12HMA,3X,2HNA,6X,2HKA,5X,4HABAR,5X,2HN+,5X,2HN-/9X,2I5,F9.0,F8.4,    E 120
                   *   2F7.4)
        15        40 FORMAT (/11X,3HA/H,5X,1HA,5X,4HP(A),3X,5HVTM/UO,4X,3HVTM,4X,6HF(VT E 130
                   1M))                                                                E 140
                  50 FORMAT (8X,F6.2,F7.2,F8.4,F9.2,F8.2,F9.4)                         E 150
                     POA=0.0
                     MV=MVD                                                           E 160
        20           NV=NVD                                                           E 170
                     MA=MAD                                                           E 180
                     NA=NAD                                                           E 190
                     CALL KXBAR (MV,NV,KV,VBAR)                                        E 22C
                     CALL KXBAR (MA,NA,KA,ABAR)                                        E 23C
        25           NPRNT=LINE
                     IF (NPRNT.EQ.0) GO TO 51
                     WRITE (6,10)                                                     E 200
                     WRITE (6,20) UO,RHO,HU,H,DT,TL,DTAU,TAUL                          E 21C
                     WRITE (6,30) MV,NV,KV,VBAR,MA,NA,KA,ABAR,ANP,ANM                  E 240
        30           LINE=11                                                          E 380
                     WRITE (6,40)                                                     E 390
                  51 M=MA+2                                                           E 250
                     IS=MV+2                                                          E 260
                     VA1=(IS-1)*IS
        35           ISD=MV+NV+3                                                      E 290
                     VAD=(ISD-1)*ISD
                     INTVA=VA1    /VAD
                     VA1=VA1*(IS+1)                                                   E 320
                     VAD=VAD*(ISD+1)                                                  E 33C
        4C           INTVB=VA1    /VAD
                     VA1=VA1*(IS+2)                                                   E 350
                     VAD=VAD*(ISD+2)                                                  E 360
                     INTVD=VA1    /VAD
                     SV=KV                                                            E 400
        45           SA=KA                                                            E 410
                     DR=0.01                                                          E 42C
                     AR=0.0-DR                                                        E 430
                     AMAX=1.0                                                         E 440
                     N=0                                                              E 45C
        50           DO 100 I=1,101                                                   E 460
                     AR=AR+DR                                                         E 470
                     A=AR*HU                                                          E 48C
                     VTM=AR*UO                                                        E 490
                     IF (AR.NE.0.0) GO TO 50                                          E 500
        55           IF (MA.EQ.0) POA=SA                                              E 510
```

```
                    IF (MV.EQ.0) FOV=SV                                    E 520
                    GO TO 70                                               E 530
                 60 IF (AR.GT.1.0) GO TO 110                               E 540
                    FOV=SV*AR**MV*(1.0-AR)**NV                             E 550
     60             POA=SA*AR**MA*(1.0-AR)**NA                             E 560
                 70 AMAX=AMAX1(AMAX,POA)                                   E 570
                    IF (I.EQ.1) GO TO 80                                   E 580
                    RAT=POA/AMAX                                           E 590
                    IF (RAT.LT.0.0001) GO TO 80                            E 600
     65             N=N+1                                                  E 610
                 80 LINE=LINE+1                                            E 620
                    IF (NPRNT.EQ.0) GO TO 100                              E 630
                    IF (LINE.LT.61) GO TO 90                               E 640
                    WRITE (6,10)                                          E 650
     70             WRITE (6,40)                                           E 660
                    LINE=5                                                 E 670
                 90 WRITE (6,50) AR,A,POA,AR,VTM,POV                       E 680
                100 CONTINUE                                               E 690
                110 CONTINUE                                               E 700
     75             RETURN                                                 E 700
                    END                                                    E 710-
```

213

```
              SUBROUTINE SUMMER (X,ERF,KODE)                                  F  10
      C       NO. 70804 IN THE H-P PROGRAM BOOKLET
              DIMENSION XT( 30)
              DATA (J=1)                                                      F  30
  5           GO TO (10,30), J                                               F  40
           10 DO 20 K=1,30
              N=2*(K-1)+1                                                     F  60
              F=303.0/N                                                      F  70
           20 XT(K)=10.0**F                                                  F  80
 10           J=2                                                            F  90
              CHECK=0.00001                                                  F 100
           30 SUM=0.0                                                        F 110
              IF (X.LT.2.5) GO TO 40
              ERF=1.0                                                        F 130
 15           GO TO 70                                                       F 140
           40 D=1.0                                                          F 150
              AN=1.0                                                         F 160
              DO 50 I=1,30
              IF (X.GT.XT(I)) GO TO 60                                       F 180
 20           N=I-1                                                          F 190
              AN=2.0*AN                                                      F 200
              IF (N.EQ.0) AN=1.0                                             F 210
              ND=2*N+1                                                       F 220
              D=D*ND                                                         F 230
 25           XX=X**ND                                                       F 240
              TERM=AN*XX/D                                                   F 250
              IF (TERM.LT.CHECK) GO TO 60                                    F 260
              SUM=SUM+TERM                                                   F 270
              R=TERM/SUM
 30           IF (R.LT.CHECK) GO TO 60
           50 CONTINUE                                                       F 280
           60 CONTINUE                                                       F 290
              ERF=1.12838*EXP(-X*X)*SUM                                      F 300
           70 GO TO (90,80), KODE                                           F 310
 35        80 ERF=1.0-ERF                                                    F 320
           90 ERF=ERF/1.12838                                                F 330
              RETURN                                                         F 340
              END                                                           F 350-
```

```
              SUBROUTINE TBLUP1 (XT,YT,XA,YA,DYDX,NT)                    G  10
      C       TABLE LOOK UP SUBROUTINE                                   G  20
              DIMENSION XT(1),YT(1)                                      G  30
              DO 10 I=1,NT                                               G  40
              IF (XA-XT(I)) 20,20,10                                     G  50
           10 CONTINUE                                                   G  60
              I=NT                                                       G  70
           20 IF (I-1) 30,30,40                                          G  80
           30 I=2                                                        G  90
           40 I=I-1                                                      G 100
              DYDX=(YT(I+1)-YT(I))/(XT(I+1)-XT(I))                       G 110
              YA=YT(I)+(XA-XT(I))*DYDX                                   G 120
              RETURN                                                     G 130
              END                                                        G 140-
```

```
              SUBROUTINE VELCOR                                         H  10
              DIMENSION FUN(20)                                         H  20
              DIMENSION DU(25),DUU(25),DV(25),DVV(25),DUV(25),DFF(25)
              REAL INTVA,INTVD,KA,KV,INTVB                              H  30
              COMMON   ABAR,    AK,ALUMPA,   DA,     DT, DTAU,    H,    HU,   H  40
             1         INTVA, INTVD,    KA,   KV, LINE,     M,  MAD,   MV,   H  50
             2         MVD,    N,    NA,   NAD,    VV,  NVD,  RHO,   TL,   H  60
             3         UO,  VBAR,   MA,  TAUL,  ANP,ANM,    ALUMP,  FUN,   H  70
             4         INTVB
           10 FORMAT (1H1,20X,23H  VELOCITY CORRELATIONS//)            H  80
           20 FORMAT (14X,3HUO,5X,3HRHO,4X,2HHU,5X,1HH,5X3HDPT,4X,3HMO,3X,4HDTAU   H  90
             1,2X,4HTAUL/10X,F7.1,F7.4,2F7.2,F6.3,F7.3,F6.3,F7.3)            H 100
           30 FORMAT (/12X,2HMV,3X,2HNV,6X,2HKV,5X,4HVBAR/9X,3I5,F9.3,F8.4//12X,   H 110
             12HMA,3X,2HNA,6X,2HKA,5X,4HABAR,5X,2HN+,5X,2HN-/9X,2I5,F9.0,F8.4,     H 120
             *  2F7.4)
           40 FORMAT (5X,F10.2,F8.3,F9.5,5F9.5)                               H 130
           50 FORMAT (/11X,4HH/HU,5X,1HH,5X,5HUUBAR,4X,5HVVBAR,4X,5HUVBAR,2X,7HU   H 140
             1BAR/UO,2X,8HVBAR/UO ,1X,7H  DF/QO//)                            H 150
           60 FORMAT (1H0,15X,20H(U/UO)2/(DPT/QO)2 =  ,F7.4)                   H 160
           65 FORMAT (//11X,4HH/HU,5X,1HH, 6X,5HDUUDY,4X,5HDVVDY,4X,5HDUVDY,
             *  5X,4HDUDY,5X,4HDVDY,5X,4HDFDY/)
              EQUIVALENCE (DPTPTB,DT),  (AMO,TL)
              AMA=MA
              ANA=NA
              AMV=MV
              ANV=NV                                                    H 880
              FAT=KA*VBAR*(AMV+2.0)/(AMV+ANV+3.0)
              ALUMUU=2.405*FAT
              ALUMVV=2.405*FAT
              ALUMUV=-1.359*FAT
              ALUMU=4.13274*KA*VBAR*(ANP-ANM)
              ALUMV=3.29744*KA*VBAR*(ANP-AN )
              ALUMDP=4.81803*FAT
              AN=N                                                      H 210
              DA=AN/2000.0                                              H 220
              UUOPTO=1.0/(4.0+1.86882*(AMV+4.0)*(AMV+3.0)/((AMV+ANV+5.0)*(AMV+AN   H 890
             1V+4.0)))                                                  H 900
              DPTB=0.7*AMO*AMO/((1.0+0.2*AMO*AMO)**3.5)
              ANN=(DPTPTB/DPTB)**2
              UUO=UUOPTO*ANN
              ANHUO=UUO*2.0*(AMV+ANV+2.0)*(AMV+ANV+3.0)
             *   *(AMA+ANA+2.0)*(AMA+ANA+3. )/(8.53073*(AMV+1.0)*(AMV+2.0)
             *   *(AMA+1.0)*(AMA+2.0))
              AK=1.0
              WRITE (6,10)                                             H 260
              WRITE (6,20) UO,RHO,HU,H,DT,TL,DTAU,TAUL                 H 270
              WRITE (6,30) MV,NV,KV,VBAR,MA,NA,KA,ABAR,ANP,ANM         H 280
              WRITE (6,50)                                             H 290
              DHR=.05
              HR=0.0-DHR
              DO 120 I=1,2000
              HR=HR+DHR                                                H 310
              IF ( HR.GT.C.5.) GO TO 130                               H 315
              IT=I
              HI=HR*HU                                                 H 330
```

```
                         AOH=0.0                                                          H 340
                         J=0                                                              H 350
                         FIU=0.0
                         FIV=0.0
          60             FIP=0.0
                         FIUU=0.0                                                         H 360
                         FIVV=0.0                                                         H 370
                         FIUV=0.0                                                         H 380
                         FIIU=0.0
          65             FIIV=0.0
                         FIIP=0.0
                         FIIUU=0.0                                                        H 390
                         FIIVV=0.0                                                        H 400
                         FIIUV=0.0                                                        H 410
          70             DO 100 K=1,2000                                                  H 420
                         AOH=AOH+DA                                                       H 430
                         IF (AOH.GT.1.0) GO TO 110                                        H 440
                         A=AOH*HU                                                         H 450
                         RAH=-HI/A                                                        H 460
          75             RAH2=RAH*RAH                                                     H 470
                         RAHU=(HU-HI)/A                                                   H 480
                         RAHU2=RAHU*RAHU                                                  H 490
                         PHIAL=-RAH                                                       H 500
                         PHIAH=RAHU                                                       H 510
          80             SI=0.707*(HU-HI)/A
                         SII=0.707*HI/A
                         KODE=1                                                           H 520
                         CALL SUMMER (PHIAL,CINTAL,KODE)                                  H 530
                         CALL SUMMER (PHIAH,CINTAH,KODE)                                  H 540
          85             CALL SUMMER (SI,SIN,KODE)
                         CALL SUMMER (SII,SIIN,KODE)
                         IF (I.GT.1) GO TO 70                                             H 550
                         F2=AOH**M                                                        H 560
                         F3=(1.0-AOH)**NA                                                 H 570
          90             FUNCA=F2*F3                                                      H 580
                         FUN(K)=FUNCA                                                     H 590
                      70 FUNCA=FUN(K)                                                     H 600
                         PAU=FUNCA*(EXP(-.5*RAH2)-EXP(-.5*RAHU2))
                         PAV=FUNCA*(SIN+SIIN)
          95             PAUU=FUNCA*(RAH*EXP(-RAH2)-RAHU*EXP(-RAHU2)+CINTAL+CINTAH)        H 610
                         PAVV=FUNCA*(CINTAL+CINTAH)                                       H 620
                         PAUV=FUNCA*(EXP(-RAH2)-EXP(-RAHU2))                              H 630
                         PAP=PAVV
                         J=J+1                                                            H 640
          100            GO TO (80,90), J                                                H 650
                      80 FIUU=PAUU+FIUU                                                   H 660
                         FIVV=PAVV+FIVV                                                   H 670
                         FIUV=PAUV+FIUV                                                   H 680
                         FIU=FIU+PAU
          105            FIV=FIV+PAV
                         FIP=FIP+PAP
                         GO TO 100                                                        H 690
                      90 FIIUU=PAUU+FIIUU                                                 H 700
                         FIIVV=PAVV+FIIVV                                                 H 710
          110            FIIUV=PAUV+FIIUV                                                 H 720
```

217

```
                         FIIU=FIIU+PAU
                         FIIV=FIIV+PAV
                         FIIP=FIIP+PAP
                         J=0                                                        H 730
115              100 CONTINUE                                                       H 740
                 110 CONTINUE                                                       H 750
                         SINUU=(PAUU+4.0*FIUU+2.0*FIIUU)*DA/3.0                      H 760
                         SINVV=(PAVV+4.0*FIVV+2.0*FIIVV)*DA/3.0                      H 770
                         SINUV=(PAUV+4.0*FIUV+2.0*FIIUV)*DA/3.0                      H 780
120                      SINV=(PAV+4.0*FIV+2.0*FIIV)*DA/3.0
                         SINU=(PAU+4.0*FIU+2.0*FIIU)*DA/3.0
                         SINP=(PAP+4.0*FIP+2.0*FIIP)*DA/3.0
                         UBARR=ALUMU*SINU*AK
                         VBARR=ALUMV*SINV*AK
125                      DP=ALUMDP*SINP*AK
                         UUBAR=ALUMUU*SINUU*AK
                         VVBAR=ALUMVV*SINVV*AK
                         UVBAR=ALUMUV*SINUV*AK
         C               UVRUUB=UVBAP/UUBAR                                          H 820
130      C               UVBUVR=UVBAR/(SQRT(UUBAR)*SQRT(VVBAR))                      H 830
         C               VVRUUR=SQRT(VVBAR)/SQRT(UUBAR)                              H 840
         C               WRITE (6,40) HR,HI,UUBAR,VVBAR,UVBAR,UVRUUB,UVBUVR,VVRUUR   H 850
                         WRITE (6,40) HR,HI,UUBAR,VVBAR,UVBAR,UBARR,VBARR,DP
                         IF (I.EQ.1) GO TO 125
135                      DU(I)=(UBARR-UL)/(HI-YL)
                         DUU(I)=(UUBAR-UUL)/(HI-YL)
                         DV(I)=(VBARR-VL)/(HI-YL)
                         DVV(I)=(VVBAR-VVL)/(HI-YL)
                         DUV(I)=(UVBAR-UVL)/(HI-YL)
140                      DPP(I)=(DP-DPL)/(HI-YL)
                 125 YL=HI
                         UUL=UUBAR
                         VVL=VVBAR
                         UVL=UVBAR
145                      UL=UBARR
                         VL=VBARR
                         DPL=DP
                 120 CONTINUE                                                        H 860
                 130 WRITE (6,60) UUDETO                                             H 910
150                      AK=12.0*ANHUO*UO/HU
                         WRITE (6,65)
                         HR=0.0-DHR
                         DO 200 I=1,IT
                         HR=HR+DHR
155                      HI=HR*HU
                         WRITE (6,40) HR,HI,DUU(I),DVV(I),DUV(I),DU(I),DV(I),DPP(I)
                 200 CONTINUE
                         RETURN                                                      H 920
                         END                                                        H 930-
```

REFERENCES

1. Roberts; Plourde; Smakula: Insights Into Axial Compressor Response to Distortion. AIAA #68-565, 1968.

2. McAulay, J. E.: Effect of Dynamic Variations in Engine-Inlet Pressure on the Compressor System of a Twin-Spool Turbofan Engine. NASA TMX-2081, Sept. 1970.

3. Liiva, J.; Davenport, F. J.: Dynamic Stall of Airfoil Sections for High Speed Rotors. 24th Annual National Proceedings of the American Helicopter Association, Washington, D. C. (No. 206) May 8-10, 1968.

4. Alford, J. S.: Design Criteria for Turbomachinery Periodic Structures to Improve Tolerance to Inflow Distortion and Resonant Oscillatory Flows. SAE #690388, 1969.

5. Taylor, J. B.: Engine Compatibility Programs for the Supersonic Transport Propulsion System. AIAA #68-993, 1968.

6. Calogeros; Mehalic; Burstadt: Experimental Investigation of the Effect of Screen - Induced Total-Pressure Distortion on Turbojet Stall Margin. NASA TMX 2239, 1971.

7. Gostelow; Krabacher; Smith: Performance Comparisons of High Mach Number Compressor Rotor Blading. G. E./NASA CR-1256, December 1968.

8. Cotter, H. N.: Integration of Inlet and Engine - An Engine Man's Point of View. SAE Paper #680286, 1968.

9. Reid, C.: The Response of Axial Flow Compressors to Intake Flow Distortion. ASME #69-GT-29, 1969.

10. Hinze, J. O.: Turbulence. McGraw-Hill Book Co. Inc., New York, 1959.

11. Bendot, J. S.; Piersol, A. G.: Measurement and Analysis of Random Data. John Wiley and Sons, New York, 1966.

12. Martin; Beaulieu; Kostin: Analysis and Correlation of Inlet Unsteady Flow Data. NA-71-1146 prepared under Contract No. NAS-2-5916 for Ames Research Center, National Aeronautics and Space Administration.

13. Hill; Peterson: Mechanics and Thermodynamics of Propulsion (Page 254). Addison-Wesley Publishing Co., Inc., Dallas, 1965.

14. Schlicting, H: Boundary Layer Theory. McGraw-Hill Co., N. Y., 6th Edition, 1968.

15. British Advisory Committee for Aeronautics: R & M Number 598. December, 1918.

REFERENCES (Continued)

16. Lee, Y. W.: Statistical Theory of Communications. Wiley and Sons, Inc., 5th Printing, January 1966.

17. Papoulis: Probability, Random Variables and Stochastic Processes. McGraw-Hill Book Co., New York, 1965.

18. Bisplinghoff; Ashley; Halfman: Aeroelasticity. Addison - Wesley Publishing Co., Inc., Dallas, 1965.

19. Fung: The Theory of Aeroelasticity. John Wiley and Sons, Inc., 5th Printing January 1966.

20. Harper, P. W., and R. E. Flanigan: "The Effect of Rate of Change of Angle of Attack on the Maximum Lift of a Small Model", NACA TN 2061, March 1950.

21. Gadeberg, B. L.: "The Effect of Rate of Change of Angle of Attack on the Maximum Lift Coefficient of a Pursuit Airplane", NACA TN 2525, October, 1951.

22. Ericsson, L. E. and J. P. Reding: "Unsteady Airfoil Stall", NASA CR-66787, July 1969

23. Harper, P. W., and R. E. Flanigan: "Investigation of the Variation of Maximum Lift for a Pitching Airplane Model and Comparison with Flight Results", NACA TN 1734, October, 1948.

24. Shapiro, A. H.: Compressible Fluid Flow, Vol. I, The Ronald Press Co., 1953.